Measurement and Chemical Modeling of Calcium Sulfate Solubilities in Concentrated Chloride Media

by

Zhibao Li

Department of Mining, Metals and Materials Engineering
McGill University
Montreal, Quebec, Canada
June 2006

A Thesis submitted to the Office of Graduate and Postdoctoral Studies
in partial fulfillment of the requirements of the degree of
Doctor of Philosophy

© Zhibao Li, 2006

Library and
Archives Canada

Published Heritage
Branch

395 Wellington Street
Ottawa ON K1A 0N4
Canada

Bibliothèque et
Archives Canada

Direction du
Patrimoine de l'édition

395, rue Wellington
Ottawa ON K1A 0N4
Canada

Your file Votre référence
ISBN: 978-0-494-27814-7
Our file Notre référence
ISBN: 978-0-494-27814-7

NOTICE:
The author has granted a non-exclusive license allowing Library and Archives Canada to reproduce, publish, archive, preserve, conserve, communicate to the public by telecommunication or on the Internet, loan, distribute and sell theses worldwide, for commercial or non-commercial purposes, in microform, paper, electronic and/or any other formats.

The author retains copyright ownership and moral rights in this thesis. Neither the thesis nor substantial extracts from it may be printed or otherwise reproduced without the author's permission.

AVIS:
L'auteur a accordé une licence non exclusive permettant à la Bibliothèque et Archives Canada de reproduire, publier, archiver, sauvegarder, conserver, transmettre au public par télécommunication ou par l'Internet, prêter, distribuer et vendre des thèses partout dans le monde, à des fins commerciales ou autres, sur support microforme, papier, électronique et/ou autres formats.

L'auteur conserve la propriété du droit d'auteur et des droits moraux qui protège cette thèse. Ni la thèse ni des extraits substantiels de celle-ci ne doivent être imprimés ou autrement reproduits sans son autorisation.

In compliance with the Canadian Privacy Act some supporting forms may have been removed from this thesis.

While these forms may be included in the document page count, their removal does not represent any loss of content from the thesis.

Conformément à la loi canadienne sur la protection de la vie privée, quelques formulaires secondaires ont été enlevés de cette thèse.

Bien que ces formulaires aient inclus dans la pagination, il n'y aura aucun contenu manquant.

Canada

Abstract

Measurement and chemical modeling of $CaSO_4$ solubilities in HCl-containing mutil-component aqueous chloride solutions have been thoroughly investigated. Solubilities of calcium sulfate dihydrate, hemihydrate and anhydrite in concentrated HCl (up to 12 $mol\cdot dm^{-3}$), $CaCl_2$ (up to 3.5 $mol\cdot dm^{-3}$) and their mixed aqueous solutions were experimentally determined by using the classic isothermal dissolution method at the temperature range from (283 to 353) K. A self – consistent chemical model based on a single set of model parameters for all three $CaSO_4$ modifications was developed with the aid of OLI Systems software platform. This was accomplished via regression of experimental solubility data that led to the determination of new Bromley–Zemaitis model parameters for the Ca^{2+} – SO_4^{2-} and Ca^{2+} – HSO_4^- ion pairs. The model was successfully tested for the estimation of $CaSO_4$ solubilities in concentrated (up to 20 $mol\cdot kg^{-1}$) HCl–$CaCl_2$–H_2O systems up to 373 K. In addition this newly developed OLI–based chemical model was successfully applied to construct the $CaSO_4$ phase transition diagrams in the HCl-$CaCl_2$-H_2O system. The effect of various chloride salts (NaCl, $MgCl_2$, $FeCl_2$, $AlCl_3$ and $FeCl_3$) on the solubility of $CaSO_4$ phases in aqueous HCl or HCl + $CaCl_2$ solutions up to 353 K was further investigated by experiment and modeling. This led to the development of a truly global model of $CaSO_4$ solubility in the H + Na + Ca + Mg + Al + Fe(II) + Cl + SO_4 + H_2O system. The new model makes use of new Bromley – Zemaitis activity coefficient model parameters for many ion pairs consisting of cations (Na^+, Mg^{2+}, Fe^{2+}, and Al^{3+}) and anions (SO_4^-, HSO_4^-, and $Al(SO_4)_2^-$), as well as new empirical dissociation constant parameters for the species, $MgSO_4$(aq), $AlSO_4^+$, and $Al(SO_4)_2^-$. The new model was shown to successfully predict the solubility of calcium sulfate phases in multi-component systems not used in model parameterization.

Resume

La mesure et la modélisation chimique de la solubilité de $CaSO_4$ dans des solutions d'acide chlorhydrique de concentrations différentes ont été étudiées en détails. Les solubilités du sulfate de calcium dihydrate, semi- hydrate, et anhydrite dans l'acide chlorhydrique (concentrations pouvant aller jusqu'à 12 $mol.dm^{-3}$), le $CaCl_2$ (concentration maximum de 3.5 $mol.dm^{-3}$) et leurs solutions mixes furent déterminées expérimentalement en utilisant la méthode classique de dissolution à température constante dans l'intervalle [283-353] K. Un modèle chimique auto-cohérent, basé sur un simple ensemble de paramètres de modélisation pour les trois différents types de $CaSO_4$ fut développé à l'aide du système de logiciel OLI. Ce travail fut réalisé par la régression mathématique des données expérimentales de solubilités, ce qui a conduit à la détermination de nouveaux paramètres du modèle Bromley-Zemaitis pour les paires ioniques Ca^{2+} - SO_4^{2-} et Ca^{2+} - HSO_4^-. Le modèle fut testé avec succès sur l'estimation des solubilités de $CaSO_4$ dans les système concentrés (concentrations pouvant aller jusqu'à 20 $mol.kg^{-1}$) HCl-$CaCl_2$-H_2O, jusqu'à 373 K. De plus, ce nouveau modèle chimique basé sur OLI fut appliqué avec succès à la construction des diagrammes de transition de phases de $CaSO_4$ dans le system HCl-$CaCl_2$-H_2O. Les effets de divers sels chlorés ($NaCl$, $MgCl_2$, $FeCl_2$, $AlCl_3$ et $FeCl_3$) sur la solubilité des phases de $CaSO_4$ dans des solutions aqueuses HCl ou $HCl + CaCl_2$ jusqu'à 353 K furent également étudiés en détails par mesures expérimentales et modélisations. Ceci déboucha sur le développement d'un véritable modèle global pour la solubilité de $CaSO_4$ dans le system [H + Na + Ca + Mg + Al + Fe (II) +Cl + SO_4 + H_2O]. Ce nouveau modèle utilise de nouveaux paramètres pour le modèle des coefficients d'activité Bromley-Zemaitis pour plusieurs paires ioniques formées par les cations (Na^+, Mg^{2+}, Fe^{2+} et Al^{3+}) et les anions (SO_4^{2-}, HSO_4^- et $Al(SO_4)_2^-$). Il utilise également de nouveaux paramètres empiriques pour les constantes de dissociations des espèces $MgSO_{4(aq)}$, $AlSO_4^+$, et $Al(SO_4)_2^-$. Ce nouveau modèle prédit avec succès la solubilité des différentes phases de sulfate de calcium dans des systèmes complexes, non utilisés dans le paramétrage des modèles.

Foreword

As an alternative to the traditional thesis format, McGill University offers the option to Ph.D. candidates to use manuscript-based thesis format. The dissertation can consist of a collection of papers of which the student is an author or co-author. This thesis has in fact been prepared accordingly following this option.

This dissertation contains eight chapters, four of them (Chapters 3, 4, 5 and 6) are papers already published in refereed journals. It should be clearly stated that due to the manuscript-based format, i.e., whole chapters to be copies of papers, some minor duplication has inevitably occurred. Thus the introduction and experimental details section in Chapters 3, 4, 5 and 6 are to some extent common and each chapter starts with an abstract, which is a standard feature of all published papers.

Contributions of Authors

All papers have been submitted for publication with the supervisor, Dr. G. P. Demopoulos, as a co-author. Nevertheless, all of the work has been done by the author of this thesis, with the exception of the normal supervision and advice given by the supervisor.

The papers that form some chapters of this thesis are as follows.

Chapter 3: Li, Zhibao.; Demopoulos, G. P. Solubility of $CaSO_4$ Phases in Aqueous HCl + $CaCl_2$ Solutions from 283 K to 353 K. *J. Chem. Eng. Data* **2005**, 50, 1971.

Chapter 4: Li, Zhibao; Demopoulos, G. P. Development of an Improved Chemical Model for the Estimation of $CaSO_4$ Solubilities in the HCl-$CaCl_2$-H_2O System up to 100 °C. *Ind. Eng. Chem. Res.* **2006**, 45, 2914.

Chapter 5: Li, Zhibao; Demopoulos, G. P. Model-Based Construction of Calcium Sulfate Phase Transition Diagrams in the HCl - $CaCl_2$ - H_2O System between 0 and 100 °C. *Ind. Eng. Chem. Res.* **2006**, ASAP Article, Web Release Date: 19-May-2006.

Chapter 6: Li, Zhibao; Demopoulos, G. P. The Effect of NaCl, $MgCl_2$, $FeCl_2$, $FeCl_3$ and $AlCl_3$ on Solubility of $CaSO_4$ Phases in Aqueous HCl or HCl + $CaCl_2$ Solutions at 298 to 353 K. *J. Chem. Eng. Data* **2006**, 51, 569.

I hereby give copyright clearance for the inclusion of the above papers, of which I am a co-author, in the Ph.D. dissertation of Zhibao Li.

Signed by:_ Date: June 9, 2006

Dr. G. P. Demopoulos

Department of Mining, Metals and Materials Engineering

McGill University

Acknowledgements

I would like to thank my supervisor, Dr. George P. Demopoulos, for his advice, encouragement, and intellectual generosity.

I would also like to thank Jean-Fancois Le Berre for translating the abstract into French.

The support of Hatch, Noranda, Process Research Ortech, and NSERC (Natural Sciences and Engineering Research Council of Canada) is gratefully acknowledged.

Contents

Abstract......ii

Resume......iii

Forward......iv

Acknowledgements......vi

Chapter 1 Introduction

1.1 Background......1

1.2 Measurement and Modelling of $CaSO_4$ Solubility......2

1.3 Scope of This Work......3

1.4 Organization of the Thesis......4

1.5 Final Remarks......5

1.6 Literature Cited......6

Chapter 2 Literature Survey

2.1 Introduction......8

2.2 Solubilities of Calcium Sulfate......8

2.3 Previous Studies on Modeling $CaSO_4$ Solubilities......16

2.4 Introduction of OLI Software......21

2.5 Literature Cited......24

Chapter 3 Solubility of $CaSO_4$ Phases in Aqueous HCl + $CaCl_2$ Solutions from 283 K to 353 K

3.1 Abstract......28

3.2 Introduction......29

3.3 Experimental Section......30

    3.3.1 Chemicals......30

    3.3.2 Procedure......31

    3.3.3 Determination of Equilibration Time......32

    3.3.4 Reproducibility......34

3.4 Results and Discussion 35
3.4.1 Solubility of $CaSO_4{\cdot}2H_2O$ in HCl Solutions 35
3.4.2 Solubility of $CaSO_4{\cdot}2H_2O$ in $CaCl_2$ Solutions 42
3.4.3 Solubility of $CaSO_4{\cdot}2H_2O$ in Mixed HCl + $CaCl_2$ Solutions 44
3.4.4 Density Comparison with OLI Software 49
3.4.5 Solubility of $CaSO_4{\cdot}0.5H_2O$ 50
3.4.6 Solubility of $CaSO_4$ in HCl Solutions 54
3.4.7 Solubility of $CaSO_4$ in $CaCl_2$ Solutions 56
3.4.8 Solubility of $CaSO_4$ in Mixed HCl + $CaCl_2$ Solutions 59
3.4.9 Thermodynamic Interpretation..........61
3.5 Conclusions..........63
3.6 Literature Cited..........65

Chapter 4 Development of an Improved Chemical Model for the Estimation of $CaSO_4$ Solubilities in the HCl – $CaCl_2$ – H_2O System up to 100 °C

4.1 Abstract..........68
4.2 Introduction 69
4.3 Modeling Methodology..........73
4.3.1 Equilibrium Relationships and Data 73
4.3.2 Ion Activity Coefficient and Water Activity Relationships..........76
4.4 Results and Discussion 77
4.4.1 Solubility Estimation with Existing Model..........77
4.4.2 New Model Parameter Estimation..........80
4.4.3 Model Validation..........84
4.4.4 Model Calibration..........87
4.4.5 Speciation Calculations and Thermodynamic Interpretation..........89
4.4.6 Solubility Curve Interpretation..........92
4.5 Conclusions..........94
4.6 Literature Cited..........96

Chapter 5 Model-Based Construction of Calcium Sulfate Phase Transition Diagrams in the HCl - $CaCl_2$ - H_2O System between 0 and 100 °C

5.1 Abstract......100
5.2 Introduction......101
5.3 Theoretical Basis......103
5.4 Results and Discussion......106
  5.4.1 The $CaSO_4$ - H_2O System......106
  5.4.2 The $CaSO_4$ – HCl – $CaCl_2$ – H_2O System......107
  5.4.3 Validation of Phase Transition Diagram......121
5.5 Conclusions......123
5.6 Literature Cited......125

Chapter 6 The Effect of NaCl, $MgCl_2$, $FeCl_2$, $FeCl_3$ and $AlCl_3$ on Solubility of $CaSO_4$ Phases in Aqueous HCl or HCl + $CaCl_2$ Solutions at 298 to 353 K

6.1 Abstract......127
6.2 Introduction......128
6.3 Experimental Section......129
  6.3.1 Chemicals......129
  6.3.2 Procedure......129
6.4 Results and Discussion......130
  6.4.1 Solubility of $CaSO_4·2H_2O$ in HCl + NaCl Solutions......130
  6.4.2 Solubility of $CaSO_4·2H_2O$ and $CaSO_4$ in HCl + $MgCl_2$ Solutions.132
  6.4.3 Solubility of $CaSO_4·2H_2O$ in $AlCl_3$ Solutions......136
  6.4.4 Solubility of $CaSO_4·2H_2O$ in HCl + $AlCl_3$ Solutions......138
  6.4.5 Solubility of $CaSO_4·2H_2O$ in HCl + $FeCl_2$ or $FeCl_3$ Solutions......141
  6.4.6 Comparison of Solubility Data......144
  6.4.7 Solubility of $CaSO_4·2H_2O$ in HCl + Chloride Salts + $CaCl_2$ Solutions......147

6.4.8 Solubility of $CaSO_4 \cdot 0.5H_2O$ in HCl + Chloride Salts + $CaCl_2$ Solutions 148
6.4.9 Identification of Equilibrated Solids 150
6.5 Conclusions........152
6.6 Literature Cited........153

Chapter 7 A Speciation-Based Chemical Equilibrium Model of $CaSO_4$ Solubility in the H + Na + Ca + Mg + Al + Fe(II) + Cl + H_2O System

7.1 Abstract........155
7.2 Introduction 156
7.3 Chemical Equilibria 158
7.3.1 Dissolution Reaction of $CaSO_4$ 158
7.3.2 Speciation Reactions 159
7.4 Results and Discussion 161
7.4.1 Solubility Evaluation with OLI's Existing Model 161
7.4.2 Model Parameterization 165
7.4.3 Model Validation 171
7.4.4 Use of the Model 173
7.5 Conclusions........178
7.6 Literature Cited........179

Chapter 8 Synopsis

8.1 Conclusions 181
8.2 Claims to Originality........183
8.3 Suggestions for Future work 184

Appendix........185

List of Figures

2.1 Organization of OLI software..22

3.1 Solubility of calcium sulfate dihydrate in water and the density of the saturated solutions..34

3.2 Solubility of calcium sulfate dihydrate in hydrochloric acid solutions...............38

3.3 Comparison of the solubility of calcium sulfate as dihydrate in HCl solutions from different sources..39

3.4 SEM images of original gypsum and equilibrated solids 41

3.5 Solubility of calcium sulfate dihydrate in aqueous calcium chloride solutions 44

3.6 Solubility of calcium sulfate dihydrate in HCl(1 mol·dm^{-3}) + $CaCl_2$ solutions 48

3.7 Density of $CaSO_4$ saturated HCl + $CaCl_2$ mixed electrolyte solutions 49

3.8 Comparison of the solubility of $CaSO_4 \cdot 0.5H_2O$ modifications in concentrated HCl solutions 53

3.9 Solubility of β - hemihydrate in HCl + $CaCl_2$ mixed electrolyte solutions 53

3.10 SEM images of equilibrated solids 54

3.11 Solubility of calcium sulfate anhydrite in hydrochloric acid solutions 57

3.12 Solubility of calcium sulfate anhydrite in aqueous calcium chloride solutions 58

3.13 Solubility of calcium sulfate anhydrite in HCl + $CaCl_2$ mixed electrolyte solutions 61

4.1 Comparison of the solubility of calcium sulfate dihydrate in HCl solutions between experimental data and OLI's prediction..78

4.2 Comparison of the solubility of calcium sulfate dihydrate in mixed HCl(1 M)-$CaCl_2$ solutions between experimental data and OLI's prediction 79

4.3 Comparison of the solubility of calcium sulfate dihydrate in mixed HCl(5 M)-$CaCl_2$ solutions between experimental data and OLI's prediction 79

4.4 Comparison of the solubility of calcium sulfate anhydrite in mixed HCl solutions between experimental data and OLI's prediction 80

4.5 Dissociation constant of bisulfate as a function of temperature 82

4.6 Calculated pH at 323 K in 0.5 m H_2SO_4 solution 83

4.7 Comparison of regressed (solid lines) and experimental (symbols) solubility of calcium sulfate dihydrate in HCl solutions 83

4.8 Comparison of regressed (solid lines) and experimental (symbols) solubility of calcium sulfate dihydrate in mixed HCl(5 M)-$CaCl_2$ solutions 84

4.9 Comparison of predicted (solid lines) and literature (symbols) solubility of calcium sulfate hemihydrate in HCl solution 86

4.10 Comparison of predicted (solid lines) and experimental (symbols) solubility of calcium sulfate hemihydrate in mixed HCl-$CaCl_2$ solutions 86

4.11 Comparison of the solubility of calcium sulfate anhydrite in concentrated HCl solutions at 353 K 87

4.12 log K_{SP} vs T for calcium sulfate anhydrite..88

4.13 Comparison of the solubility of calcium sulfate anhydrite in concentrated HCl solutions at various temperatures 89

4.14 Sulfate speciation as a function of temperature for hemihydrate - saturated solution containing 5 m HCl............... 90

4.15 Sulfate speciation as a function of temperature for hemihydrate - saturated solution containing 5 m HCl and 1 m $CaCl_2$...91

4.16 Sulfate speciation at 298 K as a function of concentration for dihydrate - saturated HCl solution with 0.5 m $CaCl_2$...92

4.17 Calculated values of $\left(\gamma_{Ca^{2+}}\gamma_{SO_4^{2-}}a_{H_2O}^2\right)$ as a function of HCl concentration at 298 K 94

5.1 log K_{SP} of DH, HH and AH as a function of temperature...................................107

5.2 The intersection of the solubility curves of the three calcium sulfate phases in HCl solutions at 25 °C 109

5.3 Scaling tendency of DH, HH, and AH as a function of HCl concentration at 80 °C 110

5.4 The $CaSO_4$ phase transition diagram in pure HCl solutions........... 112

5.5 The $CaSO_4$ phase transition diagram in pure HCl-0.5 m $CaCl_2$ solutions 113

5.6 The $CaSO_4$ phase transition diagram in pure HCl-2 m $CaCl_2$ solutions 113

5.7 The $CaSO_4$ phase transition diagram in pure HCl-4 m $CaCl_2$ solutions 114

5.8 The $CaSO_4$ phase transition diagram of DH-AH and DH-HH in pure $CaCl_2$ solutions..117

5.9 The $CaSO_4$ phase transition diagram in $CaCl_2$-1m HCl solutions 117

5.10 The $CaSO_4$ phase transition diagram in $CaCl_2$-6m HCl solutions 118

5.11 Comparison of $CaSO_4$ phase transition diagram in HCl, $CaCl_2$ and mixed HCl-2m $CaCl_2$ solutions 118

5.12 Activity of water as a function of total Cl concentration in HCl, $CaCl_2$ and mixed HCl-2m $CaCl_2$ solutions at 25 °C..119

5.13 $CaSO_4$ phase transition temperature as function of the water activity in the HCl-$CaCl_2$-H_2O system 119

5.14 Region of metastability for DH and HH in $CaCl_2$-HCl Solutions at 40, 60, and 80 °C...120

5.15 The $CaSO_4$ phase transition diagram of DH-AH and DH-HH in HCl-$CaCl_2$ solutions at 20 °C 121

5.16 Comparison of DH-HH phase transition line between model prediction and experiment at 80 °C 123

6.1 Solubility of calcium sulfate dihydrate in HCl (0.5 mol·dm^{-3}) + NaCl solutions 132

6.2 Solubility of calcium sulfate dihydrate in HCl (0.5 mol·dm^{-3}) + $MgCl_2$ solutions 135

6.3 Solubility of calcium sulfate dihydrate in HCl (3 mol·dm^{-3}) + $MgCl_2$ solutions 135

6.4 Solubility of calcium sulfate anhydrite in HCl (3 mol·dm^{-3}) + $MgCl_2$ solutions at 353 K 136

6.5 Solubility of calcium sulfate dihydrate in $AlCl_3$ solutions 137

6.6 Comparison of dihydrate solubility in $MgCl_2$ and $AlCl_3$ solutions 138

6.7 Solubility of calcium sulfate dihydrate in HCl (0.5 mol·dm^{-3}) + $AlCl_3$ solutions..140

6.8 Solubility of calcium sulfate dihydrate in HCl (3 mol·dm^{-3}) + $AlCl_3$ solutions....140

6.9 Solubility of calcium sulfate dihydrate in HCl (0.5 mol·dm^{-3}) + $FeCl_2$ solutions..142

6.10 Solubility of calcium sulfate dihydrate in HCl (0.5 mol·dm^{-3}) + $FeCl_3$ solutions..143

6.11 Solubility of calcium sulfate dihydrate in HCl (3 mol·dm^{-3}) + $FeCl_3$ solutions....144

6.12 Comparison of dihydrate solubility in HCl (0.5 mol·dm^{-3}) + various chloride salts solutions versus total concentration of chloride at 323 K..............................145

6.13 Comparison of dihydrate solubility in HCl (0.5 mol·dm^{-3}) + various chloride salts solutions versus ionic strength at 323 K 145

6.14 Comparison of dihydrate solubility in HCl (3 mol·dm^{-3}) + various chloride salts solutions versus total concentration of chloride at 323 K 146

6.15 Comparison of dihydrate solubility in HCl (3 mol·dm^{-3}) + various chloride salts solutions versus ionic strength at 323 K 146

6.16 Solubility of calcium sulfate dihydrate in HCl (0.5 mol·dm^{-3}) + $MgCl_2$ (1 mol·dm^{-3}) + $CaCl_2$ solutions at 323 K 148

6.17 Solubility of calcium sulfate hemihydrate in HCl (6 mol·dm^{-3}) + $MgCl_2$ (1 mol·dm^{-3}) + $CaCl_2$ solutions at 333 K 150

7.1 Comparison of OLI predicted (lines) and experimental (symbols) solubility of calcium sulfate dihydrate in 0.5 mol·dm^{-3} HCl + NaCl solutions at 323 and 353 K 162

7.2 Comparison of OLI predicted (lines) and experimental (symbols) solubility of calcium sulfate dihydrate in 0.5 mol·dm^{-3} HCl + $MgCl_2$ solutions at various temperatures..163

7.3 Comparison of OLI predicted (lines) and experimental (symbols) solubility of calcium sulfate dihydrate in 0.5 mol·dm^{-3} HCl+$FeCl_2$ solutions at 323 and 353 K 163

7.4 Comparison of OLI predicted (lines) and experimental (symbols) solubility of calcium sulfate dihydrate in $AlCl_3$ solutions at various temperatures..................164

7.5 Comparison of OLI predicted (lines) and experimental (symbols) solubility of calcium sulfate dihydrate in 3 mol·dm^{-3} HCl + $AlCl_3$ solutions at 298 and 323 K 165

7.6 Comparison of new model's predictions (lines) with experimental (symbols) solubility data of calcium sulfate dihydrate in 0.5 mol·dm^{-3} HCl + NaCl solutions at 323 and 353 K...167

7.7 Comparison of new model's predictions (lines) with experimental (symbols) solubility data of calcium sulfate dihydrate in 0.5 mol·dm^{-3} HCl + $MgCl_2$ solutions at various temperatures 169

7.8 Comparison of new model's predictions (lines) with experimental (symbols) solubility data of calcium sulfate dihydrate in 0.5 mol·dm^{-3} HCl + $FeCl_2$ solutions at 323 and 353 K 169

7.9 Comparison of new model's predictions (lines) with experimental (symbols) solubility data of calcium sulfate dihydrate in $AlCl_3$ solutions at various temperatures 170

7.10 Comparison of new model's predictions (lines) with experimental (symbols) solubility data of calcium sulfate dihydrate in 3 mol·dm^{-3} HCl + $AlCl_3$ solutions at 298 and 323 K 171

7.11 Comparison of OLI and new model's predictions with experimental (symbols) solubility data of calcium sulfate dihydrate in HCl (0.5 mol·dm^{-3}) + $MgCl_2$ (1 mol·dm^{-3}) + $CaCl_2$ solutions at 323 K 172

7.12 Comparison of OLI and new model's predictions with experimental (symbols) solubility data of calcium sulfate anhydrite in 3 mol·dm^{-3} HCl + $MgCl_2$ solutions at 353 K 172

7.13 Comparison of new model's predictions (line) with experimental (symbols) solubility data of calcium sulfate hemihydrate in HCl (6 mol·dm^{-3}) + $MgCl_2$ (1 mol·dm^{-3}) + $CaCl_2$ solutions at 333 K 173

7.14 Effect of various chloride salts on the solubility of calcium sulfate dihydrate in 1 mol·dm^{-3} HCl solutions versus molal concentration at 323 K 175

7.15 Effect of various chloride salts on the solubility of calcium sulfate hemihydrate in 1 mol·dm^{-3} HCl solutions versus molal concentration at 323 K 175

7.16 Effect of various chloride salts on the solubility of calcium sulfate anhydrite in 1 mol·dm^{-3} HCl solutions versus molal concentration at 323 K 176

7.17 Effect of various chloride salts on the solubility of calcium sulfate dihydrate in 1 mol·dm^{-3} HCl solutions versus ionic strength at 323 K 176

7.18 Sulfate speciation as a function of ionic strength for dihydrate saturated solution containing 1m HCl + $MgCl_2$ at 323 K 177

7.19 Sulfate speciation as a function of ionic strength for dihydrate saturated solution containing 1m HCl + $AlCl_3$ at 323 K 177

List of Tables

2.1 Review of Literature on Solubilities of Calcium Sulfate and Its Hydrates in Water and Aqueous Electrolyte Solutions from 0 to 350 °C 9

3.1 Solubility of $CaSO_4$ (1) as Dihydrate in HCl(2) + H_2O(3) 36

3.2 XRD Characterization of the Equilibrated Solids 40

3.3 Solubility of $CaSO_4$ (1) as Dihydrate in $CaCl_2$ (2) + H_2O (3) 42

3.4 Solubility of $CaSO_4$ (1) as Dihydrate in 1 mol·dm^{-3} HCl (2) + $CaCl_2$ (3) + H_2O (4) 45

3.5 Solubility of $CaSO_4$ (1) as Dihydrate in 3 mol·dm^{-3} HCl (2) + $CaCl_2$ (3) + H_2O (4)..46

3.6 Solubility of $CaSO_4$ (1) as Dihydrate in 5 mol·dm^{-3} HCl (2) + $CaCl_2$ (3) + H_2O (4)..47

3.7 Solubility of $CaSO_4$ (1) as Hemihydrate in HCl(2) + H_2O(3)..........................51

3.8 Solubility of $CaSO_4$ (1) as Hemihydrate in HCl (2) + $CaCl_2$ (3) + H_2O (4)...........51

3.9 XRD Characterization of the Equilibrated Solids 52

3.10 Solubility of $CaSO_4$ (1) as Anhydrite in HCl(2) + H_2O(3) 55

3.11 Solubility of $CaSO_4$ (1) as Anhydrite in $CaCl_2$ (2) + H_2O (3) 57

3.12 Solubility of $CaSO_4$ (1) as Anhydrite in 3 mol·dm^{-3} HCl (2) + $CaCl_2$ (3) + H_2O (4) 59

3.13 Solubility of $CaSO_4$ (1) as Anhydrite in 6 mol·dm^{-3} HCl (2) - $CaCl_2$ (3) - H_2O (4) 60

4.1 Chemical Species and Their Speciation Reactions in the $CaSO_4$ – HCl – $CaCl_2$ – H_2O System 74

4.2 The Parameters for Species Whose Equilibrium Constant is Calculated with the Aid of Eq. (4.6) 75

4.3 The Parameters for Species Whose Equilibrium Constant is Calculated with the Aid of Eq. (4.6) 75

4.4 Newly Regressed Bromley-Zemaitis Model Parameters for Ca^{2-} - SO_4^{2-} and Ca^{2-} - HSO_4^- Interactions...84

5.1 Transition Temperatures between DH-AH and DH-HH in HCl Solutions of Fixed $CaCl_2$ Concentration 111

5.2 Transition Temperatures between DH-AH and DH-HH in Fixed HCl-$CaCl_2$ Solutions 115

5.3 Comparison of $CaSO_4$ Phase Transition in HCl-$CaCl_2$ Solutions between Model Prediction and Experiment...122

6.1 Solubility of $CaSO_4$ (1) as Dihydrate in 0.5 mol·dm^{-3} HCl (2) + NaCl (3) + H_2O (4)......131

6.2 Solubility of $CaSO_4$ (1) as Dihydrate in 0.5 mol·dm^{-3} HCl (2) + $MgCl_2$ (3) + H_2O (4)......133

6.3 Solubility of $CaSO_4$ (1) as Dihydrate in 3 mol·dm^{-3} HCl (2) + $MgCl_2$ (3) + H_2O (4)......133

6.4 Solubility of $CaSO_4$ (1) as Anhydrite in 3 mol·dm^{-3} HCl (2) + $MgCl_2$ (3) + H_2O (4)......134

6.5 Solubility of $CaSO_4$ (1) as Dihydrate in $AlCl_3$(2) + H_2O(3)......137

6.6 Solubility of $CaSO_4$ (1) as Dihydrate in 0.5 mol·dm^{-3} HCl (2) + $AlCl_3$ (3) + H_2O (4)......139

6.7 Solubility of $CaSO_4$ (1) as Dihydrate in 3 mol·dm^{-3} HCl (2) + $AlCl_3$ (3) + H_2O (4)......139

6.8 Solubility of $CaSO_4$ (1) as Dihydrate in 0.5 mol·dm^{-3} HCl (2) + $FeCl_2$ (3) + H_2O (4)......141

6.9 Solubility of $CaSO_4$ (1) as Dihydrate in 0.5 mol·dm^{-3} HCl (2) + $FeCl_3$ (3) + H_2O (4)......142

6.10 Solubility of $CaSO_4$ (1) as Dihydrate in 3 mol·dm^{-3} HCl (2) + $FeCl_3$ (3) + H_2O (4)......143

6.11 Solubility of $CaSO_4$ (1) as Dihydrate in 0.5 mol·dm^{-3} HCl (2) + 1 mol·dm^{-3} $MgCl_2$ (3) + $CaCl_2$ (4) + H_2O (5) at 323 K......147

6.12 Solubility of $CaSO_4$ (1) as Dihydrate in 0.5 mol·dm^{-3} HCl (2) + 0.5 mol·dm^{-3} Chloride Salts (3) + $CaCl_2$ (4) + H_2O (5) at 323 K......148

6.13 Solubility of $CaSO_4$ (1) as Hemihydrate in 6 mol·dm^{-3} HCl (2) + 1 mol·dm^{-3} $MgCl_2$ (3) + $CaCl_2$ (4) + H_2O (5) at 333 K......149

6.14 Solubility of $CaSO_4$ (1) as Hemihydrate in 6 mol·dm^{-3} HCl (2) + 0.2 mol·dm^{-3} $FeCl_2$ (3) + $CaCl_2$ (4) + H_2O (5) at 333 K......149

6.15 Solubility of $CaSO_4$ (1) as Hemihydrate in 6 mol·dm^{-3} HCl (2) + 0.1 mol·dm^{-3} Chloride Salts (3) + $CaCl_2$ (4) + H_2O (5) at 333 K......150

6.16 XRD Characterization of the Equilibrated Solids with Equilibrium Time......151

7.1 Retained Model Parameters (Eqs. (7.3) and (7.23)) from Previous Work......166

7.2 New Bromley-Zemaitis Parameters (Eq. (7.23)) Determined in This Work......168

7.3 New Eq. (7.3) Parameters Determined in This Work......168

A.1 Thermochemical Data for the Main Species in the H + Na + Ca + Mg + Al + Fe(II) + Cl + SO_4 + H_2O System......185

A.2 The HKF Parameters for the Main Species in the H + Na + Ca + Mg + Al + Fe(II) + Cl + SO_4 + H_2O System......186

Nomenclature

List of symbols

a	activity
a_{H_2O}	activity of water
A, B, C, D	Bromley model parameters, or adjustable parameters
AH	calcium sulfate anhydrite
DH	calcium sulfate dihydrate
G	Gibbs free energy, kJ·mol^{-1}
H	enthalpy, kJ·mol^{-1}
HH	calcium sulfate hemihydrate
I	the ionic strength, mol·kg^{-1}
K	equilibrium constant in terms of molality
K_{SP}	solubility product
m	molality, mol·kg^{-1}
M	molarity, mol·dm^{-3}
P	pressure, kPa
s	solubility, mol·kg^{-1}
S	supersaturation, the Dybye-Huckel limiting slope, entropy
T	temperature, K
t	time, h
Z	charge of the ionic species

Greek letters

γ	activity coefficient
β	Pitzer model parameter
ρ	density, g·cm^{-3}

Subscripts

aq	aqueous

eq	equilibrium
w	water
i, j	cation, anion

Chapter 1

Introduction

1.1 Background

A knowledge of the solubility and stability of calcium sulfate ($CaSO_4$) and its hydrates, dihydrate (DH: $CaSO_4{\cdot}2H_2O$), hemihydrate (HH: $CaSO_4{\cdot}0.5H_2O$), or anhydrite (AH: $CaSO_4$) in chloride media is of considerable practical importance and theoretical interest since calcium sulfate precipitation is often encountered in several aspects of aqueous processing of materials. One example is the low temperature regeneration of hydrochloric acid from spent calcium chloride by reaction with sulfuric acid. A process of this type – the subject of parallel investigations at McGill University (1, 2) may be associated with the concomitant production of marketable gypsum materials as is the case of the high value building material alpha-hemihydrate-the production of which by reaction between sulfuric acid (a major by-product of the non-ferrous metallurgical industry) and calcium chloride solution is described by Berrie and Woolley (3).

The leaching of complex sulphide concentrates with concentrated chloride media is another area where the solubilities of calcium sulfate are desirable for either to assess the potential for scale formation in process equipment or for the removal of sulfate (4). Similarly, in other chloride processes as the UGS process of QIT where titaniferous slag is upgraded as feedstock for pigment production via HCl leaching (5), or the Magnola process where $MgCl_2$ is produced from serpentinic material with HCl leaching (6) calcium sulfate removal may be included. Finally, the treatment of secondary materials such as EAF dust in chloride media (e.g. Terra Gaia process) (7) is another example where gypsum solubilities are of interest. The solubility and form (DH, HH, AH) of calcium sulfate depend on temperature and solution composition.

1.2 Measurement and Modelling of $CaSO_4$ Solubility

Optimization or analysis of precipitation processes is hindered in many cases because experimental solubilities for systems containing more than two components are difficult to obtain in the laboratory (8). However, practical industrial systems are normally multi-component systems in which numerous components may be involved. In the case of $CaSO_4$ material production through a reaction between sulfuric acid and spent calcium chloride solutions, the main constituents at least include three $CaSO_4$ modifications, HCl, $CaCl_2$ and other impurity or co-existing salts, such as NaCl, $MgCl_2$, $AlCl_3$, $FeCl_2$ and $FeCl_3$ (9). A literature review (9) revealed that there are much less experimentally determined solubilities for calcium sulfate in mixed electrolyte solutions than those in single electrolyte aqueous solutions, particularly at elevated temperatures. Actually, it is not cost-effective to measure the solubility data under all different practical conditions because of the large number of components and temperatures involved.

Supersaturation is the driving force in any precipitation operation, determining largely the outcome of the process (10). Considering a $CaSO_4$ supersaturated solution at elevated temperature, the hemihydrate may be precipitated according to the following reaction,

$$Ca^{2+} + SO_4^{2-} + 0.5H_2O = CaSO_4 \cdot 0.5H_2O \qquad (1.1)$$

The supersaturation for this reaction can be expressed in thermodynamically rigorous form as,

$$S = \frac{a_{Ca^{2+}} a_{SO_4^{2-}} a_{H_2O}^{0.5}}{a_{Ca^{2+},eq} a_{SO_4^{2-},eq} a_{H_2O,eq}^{0.5}} = \frac{a_{Ca^{2+}} a_{SO_4^{2-}} a_{H_2O}^{0.5}}{K_{sp,HH}} = \frac{m_{Ca^{2+}} \gamma_{Ca^{2+}} m_{SO_4^{2-}} \gamma_{SO_4^{2-}} a_{H_2O}^{0.5}}{K_{sp,HH}} \quad (1.2)$$

In order to calculate the supersaturation of calcium sulfate hemihydrate in electrolyte solution, the values for $K_{sp,\text{HH}}$, $\gamma_{Ca^{2+}}$, $\gamma_{SO_4^{2-}}$ and a_{H_2O} are required. The solubility product, $K_{sp,HH}$, can be obtained from solubility determination of calcium sulfate in solution, or from standard Gibbs free energy change for reaction (1.1). However, it is very difficult to experimentally determine $\gamma_{Ca^{2+}}$, $\gamma_{SO_4^{2-}}$ and a_{H_2O} values in supersaturated solutions. This hinders the determination of supersaturation deriving force and hence its use in precipitation research.

These problems mentioned above would be greatly overcome by developing a computer-based thermodynamic model capable of describing multi-component systems on the basis of simple binary or ternary solubility data.

1.3 Scope of this Work

The overall aim of the present research work is to experimentally determine the solubilities of three calcium sulfate phases (DH, HH, AH) in HCl, $CaCl_2$ and other metal chloride salts as well as their mixtures up to 80 °C and to develop methods to chemically model the solubility data and to establish the phase transition diagrams of calcium sulfate in chloride media with the help of OLI software (11). More specifically, the research objectives are as follows:

1. To set up a rapid isothermal dissolution method to determine the solubilities of sparingly soluble salts in solutions.

2. To determine the solubilities of calcium sulfate phases (DH, AH, and HH) in HCl, $CaCl_2$, and their mixed electrolyte solutions from 10 to 80 °C by the established method.

3. To determine the solubilities of calcium sulfate phases in other chloride salts, such as NaCl, $MgCl_2$, $FeCl_2$, $FeCl_3$, or $AlCl_3$, and their mixed electrolyte solutions at selected temperatures.

4. To use OLI software, namely, SteamAnalyzer and the Environmental Simulation Program to model the experimental solubility data in order to derive a single set of self –consistent model parameters for all three $CaSO_4$ modifications (DH, HH and AH).

5. To predict the solubilities of calcium sulfate hemihydrate at elevated temperatures and investigate the effect of electrolyte solution composition and temperature on solubility.

6. To establish the $CaSO_4$ phase transition diagrams as a function of temperature and HCl + $CaCl_2$ solution composition.

1.4 Organization of the Thesis

This thesis has been organized into a number of chapters in the following manner. Following this introduction, Chapter 2 gives literature survey of the subject-matter of the thesis which includes summary of extensive solubilities of calcium sulfate phases in various media, a review of basic thermodynamic aspects, and the introduction of OLI software. Chapter 3 - Experimental methodology is devoted to experimental equipment and procedures used. Chapter 3 also summarizes all experimentally determined solubility data for the $CaSO_4$+HCl+$CaCl_2$ system. Chapter 4 describes the modeling with the aid of OLI of the $CaSO_4$ solubility equilibria in HCl-$CaCl_2$ media. Chapter 5 deals with the establishment of phase transition diagrams while Chapters 6 and 7 describe the measurement and modeling of $CaSO_4$ solubilities in multi – component electrolyte systems.

1.5 Final Remarks

This thesis is composed of a number of chapters, some of which have already published in the course of the investigation. A small overlap in the introduction of the various chapters makes them understandable as separate papers or self – standing individual studies.

1.6 Literature Cited

(1) Girgin, S.; Demopoulos, G. P. Production of the High Value Material, Alpha-$CaSO_4$ Hemihydrate out of Spent $CaCl_2$ Solutions by Reaction with H_2SO_4. in *EPD Congress 2004*; Schlesinger, M. E. Ed.; TMS: Warendale, PA, USA, 2004, 627-639.

(2) Al-Othman, A.; Cheng, T. C.; Demopoulos, G. P. Regeneration of HCl and Production of Saleable Gypsum by Reaction of Spent $CaCl_2$ Leach Solutions with H_2SO_4. in *Proceedings of Fifth International Symposium on Waste Processing and Recycling in Mineral and Metallurgical Industries*; Rao, S. R. et al. Eds.; CIM: Montreal, Canada, 2004, 453-467.

(3) Berrie, J. S.; Woolley, G. E. Manufacture of Calcium Sulphate alpha Hemihydrate, *US Patent*, No. 4,120,737, Oct. 17, **1978**.

(4) Dutrizac, J. E. Sulphate Control in Chloride Leaching Processes. *Hydrometallurgy* **1989**, 23, 1.

(5) Borowiec, K.; Grau, A. E.; Gueguin, M.; Turgeon, J. F. Method to Upgrade Titania Slag and Resulting Product, *US Patent*, No. 5,830,420, Nov. 3, **1998**.

(6) Ficara, P.; Chin, E.; Walker, T.; Laroche, D.; Palumbo, E.; Celik, C.; Avedesian, M. Magnola: A Novel Commercial Process for the Primary Production of Magnesium, *CIM Bulletin* **1998**, 91, 75.

(7) McElroy, R. O.; Murray, W. Developments in the Terra Gaia Process for the Treatment of EAF Dust, *Iron Control in Hydrometallurgy*, J. E. Dutrizac and G. B. Harris, Eds., CIM, Montreal, Canada, **1996**, 505.

(8) Weare, J. H. Models of Mineral Solubility in Concentrated Brines with Application to Field Observations. *Thermodynamic Modeling of Geological Materials: Minerals, Fluids and Melts*; I.S.E. Carmichael and H.P. Eugster, Eds., Mineralogical Society of America: Washington, D.C., **1987**.

(9) Li, Zhibao and Demopoulos, G. P. $CaSO_4$ Solubilities in Concentrated Aqueous Chloride Solutions. *Chloride Metallurgy 2002: Practice and Theory of Chloride/Metal Interaction,* E. Peek and G. Van Weert, Eds., CIM, Montreal, Canada, **2002**, 561-574.

(10) Sohnel, O.; Garside, J. *Precipitation: Basic Principles and Industrial Application*; Butterworth-Heinemann: Oxford, 1995.

(11) *Aqueous System Modeling Course and Workshop*, OLI's manual, OLI System Inc. New Jersey, 2002.

Chapter 2

Literature Survey

2.1 Introduction

Calcium sulfate can exist in six solid phases: 3 anhydrites (AH), 2 hemihydrates (HH) and a dihydrate (DH) (1, 2). Much research work has been performed to determine the form of calcium sulfate in different media at different temperatures. Gypsum (dihydrate, $CaSO_4 \cdot 2H_2O$) is one of the more common minerals in sedimentary environments, which is the usual precipitating phase at ambient temperature whereas anhydrite ($CaSO_4$) and hemihydrate ($CaSO_4 \cdot 0.5H_2O$) are the species likely to precipitate at higher temperature. There are two forms of hemihydrate, that is, α-HH and β-HH. The latter known as Plaster of Paris has been used as building material for more than 100 years. However, α-HH has become important in recent years either as building material or dental material due to its excellent physical properties (3, 4). The design of aqueous – based process for the production of one or more of these $CaSO_4$ materials or simply precipitation of their possible (undesirable when it leads to scaling) formation in a process circuit calls for analysis/knowledge of their respective solubilities.

2.2 Solubilities of Calcium Sulfate

For over one century, the solubility of calcium sulfate phases in pure water or various electrolyte solutions has been investigated. The solutions include acids, such as, sulfuric acid, nitric acid, phosphoric acid, and hydrochloric acid as well as their mixed acids, or salts, such as, sodium chloride, calcium chloride, sodium sulfate, zinc sulfate and many other salts. The concentration of electrolytes ranges from 0 to saturation. The system temperature is up to 350 °C. A comprehensive list of sources relating to the solubilities of $CaSO_4$ phases is given in Table 2.1. Since this thesis is devoted to the investigation of solubilities and phase transition of various calcium sulfate phases in chloride media, the solubilities in these systems are reviewed in the following pages.

The earlier experimental data on the solubility of calcium sulfate in some chloride aqueous solutions has been reported in two useful handbooks. One is compiled by Linke and Seidell (5), the other by Silcock (6). There is a lot of work done on the solubility of calcium sulfate in sodium chloride systems. More recently, Raju and Atkinson (7) reviewed anhydrite and gypsum solubilities in water and sodium chloride aqueous solutions and summarized the data sources in a table. The authors also used fundamental thermodynamic relations to calculate the thermodynamic solubility product of anhydrite and gypsum.

Table 2.1. Review of Literature on Solubilities of Calcium Sulfate and Its Hydrates in Water and Aqueous Electrolyte Solutions from 0 to 350 °C

Systems		Solid	T / °C	Electrolyte medium range	Ref.
1	$CaSO_4·2H_2O$	DH	0 -107	H_2O	(5)
2	$CaSO_4·0.5H_2O$ $CaSO_4$	HH AH	0 -110 1 -110	H_2O	(5)
3	$CaSO_4·0.5H_2O$ $CaSO_4$	HH AH	100 - 200 100 - 220	H_2O	(5)
4	$CaSO_4$+H_2SO_4	unknown	25 25 43	H_2SO_4: 0.01-0.08 mol/L H_2SO_4: 0.0 - 292.02 g/L H_2SO_4: 0.0 - 292.02 g/L	(5)
5	$CaSO_4$+HCl	unknown	25 102	HCl: 0.0 - 80 g/L HCl: 0.0 - 60 g/L	(5)
6	$CaSO_4$+HCl	unknown	25	HCl: 0.01 - 0.08 mol/L	(5)
7	$CaSO_4·2H_2O$+HCl	DH	25	HCl: 3.56 - 26.73 wt %	(5)

8	$CaSO_4{\cdot}2H_2O+CaCl_2+HCl$	DH	20	HCl: 0.0 - 20.0 wt% $CaCl_2$: 0.0 - 25.0 wt%	(5)
9	$CaSO_4+CaCl_2$	unknown	25	$CaCl_2$: 0.16-38.91 wt %	(5)
10	$CaSO_4{\cdot}2H_2O+CaCl_2$	DH	55	$CaCl_2$: 8.23-42.5 wt%	(5)
	$CaSO_4{\cdot}0.5H_2O+CaCl_2$	HH	55	$CaCl_2$: 47.77-51.3 wt%	
11	$CaSO_4+HCl$	unknown	25	HCl: 0.37-2.92 wt%	(6)
12	$CaSO_4+CaCl_2$	unknown	25	$CaCl_2$: 0.0-367.85 g/L	(6)
			25	$CaCl_2$: 0.55-5.55 g/L	
13	$CaSO_4+CaCl_2$	AH	20	$CaCl_2$: 0.0-25.0 g/L	(6)
14	$CaSO_4+CaCl_2$	AH	110	$CaCl_2$: 0.0-50.45 wt%	(6)
15	$CaSO_4{\cdot}2H_2O+CaCl_2$	DH	16-22	$CaCl_2$: 0.1-40.0 wt%	(6)
16	$CaSO_4{\cdot}2H_2O+CaCl_2$	DH	25	$CaCl_2$: 0.0-38.91 wt%	(6)
17	$CaSO_4{\cdot}2H_2O+HCl$	DH	20	HCl: 0.548-3.65 wt%	(8)
		DH	30		
		DH	40		
		DH	50		
		DH	60		
		DH	70		
18	$CaSO_4{\cdot}0.5H_2O+HCl$	HH	100	HCl: 0.0-2.0 mol/L	(9)
19	$CaSO_4{\cdot}2H_2O+NaCl$	DH	0.5	NaCl: 0.0-6.1 mol/kg	(10)
		DH	5	NaCl: 0.0-3.9 mol/kg	
		DH	10	NaCl: 0.0-3.9 mol/kg	
		DH	15	NaCl: 0.0-3.9 mol/kg	
		DH	20	NaCl: 0.0-3.9 mol/kg	
		DH	25	NaCl: 0.0-6.1 mol/kg	
		DH	30	NaCl: 0.0-1.0 mol/kg	
		DH	40	NaCl: 0.0-1.0 mol/kg	
		DH	70	NaCl: 0.0-4.7 mol/kg	
		DH	80	NaCl: 0.0-3.0 mol/kg	
		DH	95	NaCl: 0.0-2.0 mol/kg	
		DH	110	NaCl: 0.0-5.1 mol/kg	
20	$CaSO_4{\cdot}2H_2O+NaCl$	DH	25	NaCl: 0.0-6.0 mol/kg	(11)
		DH	40	NaCl: 0.0-6.0 mol/kg	
		DH	60	NaCl: 0.0-6.0 mol/kg	
	$CaSO_4{\cdot}0.5H_2O+NaCl$	HH	100	NaCl: 0.0-6.0 mol/kg	
		HH	125	NaCl: 0.0-10.0 mol/kg	

	$CaSO_4$+NaCl	AH	100	NaCl: 0.0-6.0 mol/kg	
		AH	125	NaCl: 0.0-10.0 mol/kg	
		AH	150	NaCl: 0.0-10.0 mol/kg	
		AH	175	NaCl: 0.0-10.0 mol/kg	
		AH	200	NaCl: 0.0-10.0 mol/kg	
21	$CaSO_4$+NaCl	AH	25	NaCl: 0.0-5.24 mol/kg	(12)
		AH	30	NaCl: 0.0-5.55 mol/kg	
		AH	40	NaCl: 0.0-5.60 mol/kg	
		AH	50	NaCl: 0.0-6.30 mol/kg	
	$CaSO_4\cdot 2H_2O$+NaCl	DH	25	NaCl: 0.0-5.24 mol/kg	
		DH	30	NaCl: 0.0-5.55 mol/kg	
		DH	40	NaCl: 0.0-5.60 mol/kg	
		DH	50	NaCl: 0.0-5.87 mol/kg	
22	$CaSO_4\cdot 2H_2O$+NaCl	DH	65	NaCl: 3.0-6.16 mol/kg	(13)
	$CaSO_4$+NaCl	AH	65	NaCl: 3.0-6.00 mol/kg	
23	$CaSO_4\cdot 2H_2O+H_2SO_4$	DH	25	H_2SO_4: 0.0-4.6 mol/kg	(14)
		DH	30	H_2SO_4: 0.0-4.6 mol/kg	
		DH	40	H_2SO_4: 0.0-4.7 mol/kg	
		DH	60	H_2SO_4: 0.0-1.0 mol/kg	
	$CaSO_4\cdot 0.5H_2O+H_2SO_4$	HH	125	H_2SO_4: 0.0-0.89 mol/kg	
	$CaSO_4+H_2SO_4$	AH	150-350	H_2SO_4: 0.0-1.21 mol/kg	
24	$CaSO_4\cdot 2H_2O$+NaCl	DH	25	NaCl: 0.0-34.0 g/100g H_2O	(15)
		DH	35	NaCl: 0.0-30.0 g/100g H_2O	
	$CaSO_4\cdot 2H_2O$+NaCl with Na_2SO_4	DH	25	NaCl: 0.0-32.0 g/100g H_2O	
	$CaSO_4$+NaCl	AH	25	NaCl: 0.0-34.1 g/100g H_2O	
	$CaSO_4$+NaCl with Na_2SO_4	AH	25	NaCl: 0.0-35.5 g/100g H_2O	
25	$CaSO_4\cdot 2H_2O$+NaCl	DH	25	NaCl: 0.01-0.10 mol/L	(16)
	$CaSO_4\cdot 2H_2O+MgCl_2$	DH	25	$MgCl_2$: 0.005-0.05 mol/L	
	$CaSO_4\cdot 2H_2O+CaCl_2$	DH	25	$CaCl_2$: 0.005-0.05 mol/L	
	$CaSO_4\cdot 2H_2O+Na_2SO_4$	DH	25	Na_2SO_4: 0.0-0.05 mol/L	
	$CaSO_4\cdot 2H_2O$+MgSO4	DH	25	$MgSO_4$: 0.0-0.05 mol/L	

26	$CaSO_4\cdot2H_2O+Na_2SO_4+MgCl_2$	DH	40	Na_2SO_4: 0.0-2.0 mol/kg	(17)
				$MgCl_2$: 0.0-0.7 mol/kg	
27	$CaSO_4\cdot2H_2O+NaCl+MgCl_2$	DH	28	NaCl: 0.0-5.5 mol/kg	(18)
				$MgCl_2$: 0.0-0.325 mol/kg	
		DH	38	NaCl: 0.0-4.1 mol/kg	
				$MgCl_2$: 0.0-0.224 mol/kg	
		DH	50	NaCl: 0.0-4.36 mol/kg	
				$MgCl_2$: 0.0-0.208 mol/kg	
		DH	70	NaCl: 0.0-4.15 mol/kg	
				$MgCl_2$: 0.0-0.34 mol/kg	
		DH	90	NaCl: 0.0-1.57 mol/kg	
				$MgCl_2$: 0.0-0.207 mol/kg	
28	$CaSO_4\cdot2H_2O+Na_2SO_4+NaNO_3$	DH	25	Na_2SO_4: 0.0-0.598 mol/kg	(19)
				$NaNO_3$: 0.0-5.76 mol/kg	
	$CaSO_4\cdot2H_2O+Na_2SO_4+NaCl$	DH	25	Na_2SO_4: 0.0-0.559 mol/kg	
				NaCl: 0.0-5.91 mol/kg	
	$CaSO_4\cdot2H_2O+Li_2SO_4+LiNO_3$	DH	25	Li_2SO_4: 0.0-0.584 mol/kg	
				$LiNO_3$: 0.0-5.68 mol/kg	
	$CaSO_4\cdot2H_2O+Li_2SO_4+LiCl$	DH	25	Na_2SO_4: 0.0-0.317 mol/kg	
				LiCl: 0.0-5.85 mol/kg	
29	$CaSO_4\cdot2H_2O+H_2SO_4+H_3PO_4$	DH	20	H_2SO_4: 0.0-7.8 wt%	(20)
			50	H_3PO_4: 0.0-41.4 wt%	
			70		
30	$CaSO_4+ZnSO_4$	DH	25-100		(21)
		HH	100-150	Zn: 9.80-80.42 g/L	
		AH	150-200		
	$CaSO_4+MgSO_4$	DH	25-100		
		HH	100-150	Mg: 2.40-18.30 g/L	
		AH	150-200		
	$CaSO_4+CuSO_4$	DH	25-100	Cu: 4.96-58.84 g/L	
		HH	100-150		
		AH	150-200		
	$CaSO_4+CoSO_4$	DH	25-100	Co: 2.96-44.30 g/L	
		HH	100-150		
		AH	150-200		
31	$CaSO_4\cdot2H_2O+NaCl$	DH	40-100	All salts: 8-15 wt%	(22)
	$CaSO_4\cdot2H_2O+NH_4Cl$	DH	40-100		

	$CaSO_4 \cdot 2H_2O+NaNO_3$	DH	40-100		
	$CaSO_4 \cdot 2H_2O+NH_4NO_3$	DH	40-100		
	$CaSO_4 \cdot 2H_2O+CH_3COONH_4$	DH	40-100		
	$CaSO_4 \cdot 0.5H_2O+NaCl$	HH	60-100		
	$CaSO_4 \cdot 0.5H_2O+NH_4Cl$	HH	60-100		
	$CaSO_4 \cdot 0.5H_2O+NaNO_3$	HH	60-100		
	$CaSO_4 \cdot 0.5H_2O+NH_4NO_3$	HH	60-100		
	$CaSO_4 \cdot 0.5H_2O+CH_3COONH_4$	HH	60-100		
32	$CaSO_4 \cdot 2H_2O+HClO_4$	DH	25	$HClO_4$: 14.0-49.0 wt%	(23)
	$CaSO_4 \cdot 2H_2O+HBr$	DH	25	HBr: 16.5-39.1 wt%	
	$CaSO_4 \cdot 2H_2O+HCl$	DH	25	HCl: 9.15-35.80 wt%	
	$CaSO_4 \cdot 2H_2O+HNO_3$	DH	25	HNO_3: 14.0-49.0 wt%	
33	$CaSO_4 \cdot 2H_2O+H_3PO_4$	DH	0-90	H_3PO_4: 70 wt%	(24)
34	$CaSO_4 \cdot 0.5H_2O+H_3PO_4$	HH	80-110	P_2O_5: 55 wt%	(25, 26)
35	$CaSO_4+HCl$	DH	25	HCl: 35.8 wt %	(27)
		HH	25		
		AH	25		
36	$CaSO_4 \cdot 2H_2O+H_3PO_4$	DH	25	H_3PO_4: 1 mol/L	(28)
	$CaSO_4 \cdot 2H_2O+HNO_3$	DH	25	HNO_3: 8.01 mol/L	
37	$CaSO_4 \cdot 2H_2O\,_4+H_2SO_4+CuSO_4$	DH	25	H_2SO_4: 214 g/kg	(29)
			45	Cu: 61 g/L	
			50		
			60		
38	$CaSO_4 \cdot 2H_2O+MgCl_2$	DH	25	$MgCl_2$: 23.4 wt%	(30)
			40		
			50		
39	$CaSO_4 \cdot 2H_2O+H_2SO_4$ with $ZnSO_4$, $Fe_2(SO_4)_3$, $MgSO_4$, Na_2SO_4 and $(NH_4)_2SO_4$	DH	20-95	H_2SO_4: 2 mol/L	(31)
40	$CaSO_4 \cdot 0.5H_2O+H_2SO_4$	HH	100	H_2SO_4: 3.5 mol/kg	(32)

The solubility of calcium sulfate in hydrochloric acid aqueous solutions has been studied by many investigators, but mainly the studies dealt with the behavior of gypsum at low temperature and low electrolyte concentration. As early as in 1885, Zunge (5) published the solubility data of calcium sulfate in hydrochloric acid aqueous solutions with the concentration of up to 2.19 M without analyzing the solid phase. Gupta (8) studied the solubilities of gypsum in dilute hydrochloric acid solutions of concentration up to 1 m for temperatures from 20 to 70 °C. It was shown that the solubility of gypsum increases with temperature and concentration of hydrochloric acid. Ryss and Nilus (33) determined the solubility of calcium sulfate dihydrate in concentrated hydrochloric acid solutions from 1 to 10 m only at 25 °C. Experimental results show that solubility increases with the acid concentration initially, reaches a maximum value at about 2.5 m, then decreases with further increase of the acid concentration. Further explanation for the rise in the solubility of gypsum was not given in their paper. Kruchenko and Beremzhanov (27) investigated the solubility of gypsum, α -hemihydrate and γ -anhydrite in hydrochloric acid at 25 °C in the concentration range of 0.0-15 m. The results show that gypsum is the stable solid phase in the low acid concentration range while γ -anhydrite is stable in the high acid region. Later on, Kruchenko and Beremzhanov (34) reported their investigation into the solubility of gypsum in several monobasic inorganic acids (HCl, HNO_3, $HClO_4$, and HBr) and tried to provide the explanation why the solubility of gypsum in inorganic acid solutions passes through a maximum point by using salting-out and salting-in concepts. Further, they (23) reported the relation between the solubility of gypsum in inorganic acid solutions and the thermodynamic characteristics of anions of the acids. The solubility data of gypsum at 25 and 40 °C was reported in their work. The solubility of gypsum in aqueous solutions of $MgBr_2$, $MgCl_2$ and $Mg(NO_3)_2$ was determined by Kruchenko (30) to find the relationship of solubility to the activity of water and the thermodynamic characteristics of the hydration of the anions of the magnesium salts.

The solubility of calcium sulfate in hydrochloric acid mentioned above has been mainly reviewed at relatively low temperatures. Yasue *et al.* (9) investigated the effect of the supersaturation degree on crystal shape and modification of α -hemihydrate generated from the reaction of $CaCl_2$ and H_2SO_4. The solubility of α -hemihydrate in hydrochloric acid at 100 °C was determined and given in the form of a graph. At the range of acid concentration up to 2 M the solubility was found to increase with the increase of the acid concentration.

The solubility of calcium sulfate in calcium chloride aqueous solutions at 20 or 25 °C was investigated by Cameron and Seidell (5), Veldhulzeb (5), and Sveshnikova (35), but the equilibrium solid phase was not characterized. Sveshnikova published the solubility of gypsum in calcium chloride solutions at 25 or 55 °C while the solubility of calcium sulfate anhydrite in calcium chloride aqueous solutions was reported at 20 °C by Kuznetsov (36) and at 110 °C by Gromova (37). Sveshnikova gave a few data points of solubility of α -hemihydrate in calcium chloride solutions. All results show that the solubility value of calcium sulfate sharply decreases with the increase of concentration of calcium chloride.

Sukimoto *et al.* (38) investigated the effects of salts including NaCl, NH_4Cl, $NaNO_3$, NH_4NO_3 and CH_3COONH_4, on the formation of α -calcium sulfate hemihydrate in aqueous solutions at normal pressure. The solubility of both dihydrate and hemihydrate was measured from 40 °C to boiling point. The investigation provides a criterion to select a suitable salt to accelerate the formation of α -calcium sulfate hemihydrate.

There is much less solubility data for calcium sulfate in mixed electrolyte aqueous solutions in the literature compared with available data in single electrolyte aqueous solutions, particularly at temperature above 25 °C. However, in practice this solubility data is more useful. The solubilities of gypsum at 20 °C, in hydrochloric acid, in calcium chloride, and in their mixtures were given by Kuznetsov (36). In the mixed electrolyte solution, depressing effect of calcium chloride on solubility of gypsum prevails definitely over that of hydrochloric acid. This system is of particular significance in hydrochloric acid generation from spent calcium chloride by reaction with sulfuric acid. However, they did not report the solubility of calcium sulfate at elevated temperature. Ostroff and Metler (19) presented the solubility data of calcium sulfate dihydrate in the system NaCl + $MgCl_2$ + H_2O from 18 to 70 °C for sodium chloride molalities up to 5.5 and for the mixtures with magnesium chloride between 0.01 and 0.325 m. Their investigation showed that for the same concentration of magnesium chloride or sodium chloride, magnesium chloride causes a larger increase in the solubility of calcium sulfate.

2.3 Previous Studies on Modeling $CaSO_4$ Solubilities

Attempts to theoretically model calcium sulfate, $CaSO_4$, solubility in pure and multi-component aqueous solutions have been the topic of many studies. The chemical reaction representing the equilibrium between $CaSO_4$ hydrate and its ions is

$$CaSO_4{\cdot}nH_2O(s) = Ca^{2+} + SO_4^{2-} + nH_2O \qquad (2.1)$$

here n = 0, 0.5, and 2 corresponding to anhydrite, hemihydrate and dihydrate, respectively. The solubility product (thermodynamic equilibrium constant) takes the form

$$K_{SP}^{0} = (m_{Ca^{2+}}\gamma_{Ca^{2+}})(m_{SO_4^{2-}}\gamma_{SO_4^{2-}})(a_w)^n = (m_{Ca^{2+}})(m_{SO_4^{2-}})\gamma_{\pm(CaSO_4)}^{2}(a_w)^n \qquad (2.2)$$

where K_{SP}^{0} = the solubility product constant

m = the molal concentration of calcium and sulfate ions (mol·kg^{-1})

$\gamma_{\pm CaSO_4}$ = the mean activity coefficient of $CaSO_4$

a_w = the activity of water

So, the evaluation of solubility of calcium sulfate hydrates from solubility product (K_{SP}^{0}) requires the determination of the mean activity coefficient of $CaSO_4$($\gamma_{\pm CaSO_4}$) and the activity of water (a_w).

Marshall and Slusher (10) proposed a well-known empirical model based on an extended Debye-Huckel limiting-law expression. The practical solubility product was used without considering ionic association equilibria.

$$\log K_{sp}(practical) = \log K_{sp}^{0} + \frac{8SI^{1/2}}{1 + A_{sp}I^{1/2}} + B'I - C'I^2 \qquad (2.3)$$

where K_{sp} = the practical solubility product constant

I = the ionic strength

S = the Debye-Huckel limiting slope

A_{sp}, B', C' = adjustable parameters

This empirical model can give satisfactory solubility predictions (40) of dihydrate at 60 and 95 °C , hemihydrate and anhydrite at 100 to 200 °C in NaCl, KCl, Na_2SO_4, $CaCl_2$,

$MgCl_2$, $MgSO_4$ and some of their mixed solutions as well such as saline water at the concentration of less 6 m.

Zemaitis *et al.* (41) applied a theoretical thermodynamic method to calculate the solubility of calcium sulfate dihydrate in NaCl, $CaCl_2$ and HCl aqueous solutions to evaluate the various activity coefficient models, such as, Bromley's (41), Meissner's (41) and Pitzer's (41). In their calculations, complete dissociation was assumed for the $CaSO_4$ and other electrolytes. The results showed that interaction parameters based on the solubility data of gypsum in pure water were not very applicable when used in predicting the solubility of gypsum in multi-component electrolyte solutions. For the system containing $CaSO_4 + NaCl + H_2O$, inclusion of additional Pitzer higher order mixing parameters resulted in an improvement of solubility calculation.

Demopoulos *et al.* (42) used Meissner's method to successfully predict the solubility of gypsum for the chemical reaction system: $CaCl_2 + HCl + H_2SO_4 + H_2O$. The major difference from Zemaitis *et al.*'s method was that Demopoulos *et al.* introduced a new Meissner's parameter for $CaSO_4$ with the value of 0.108. Also excellent agreement between model prediction and experimental solubilities was obtained for gypsum in NaCl + H_2O at 25 °C.

Barba *et al.* (43) developed a thermodynamic model to describe the solubility of calcium sulfate dihydrate in salt water, which in itself is a multi-component aqueous solution. The model is based on the local compositions of the non-random two-liquid (NRTL) theory. The excess Gibbs free energy is assumed to be the sum of three terms, the first two related to long range forces between ions and the other to short range forces between all species:

$$G^E = G^E_{Debye-Huckel} + G^E_{Born} + G^{E*}_{NRTL} \qquad (2.4)$$

Using only binary parameters this relationship yields good agreement between the experimental and predicted values of calcium sulfate solubility in sea water and in natural and synthetic water at 25 °C. However, for multi-component solutions with high sodium chloride content, such as, $CaSO_4 \cdot 2H_2O + NaCl + Na_2SO_4 + H_2O$, the new binary parameters should be regressed to improve the calculation. In this case, the model becomes a partially data-fitting exercise.

Meijer *et al.* (44) developed a computer program to determine the driving force for calcium sulfate deposition from a supersaturated saline water solution of known composition. The solubility product for each calcium sulfate modification was calculated by a modified version of the model proposed by Marshall and Slusher (11). The activity of water and mean activity coefficient of calcium sulfate in saturated solution and in supersaturated solution were calculated from the ion specific interaction model developed by Pitzer (41). This ion-specific interaction model was employed by Harvie *et al.* (45) to predict mineral solubilities in natural waters.

Scrivner and Staples (46) developed a method by using the "speciation approach" with ECES computer program developed by OLI Systems. They listed three examples dealing with gypsum solubility in concentrated aqueous solutions at 25 °C. In the first system, addition of sodium chloride in water caused an increase of gypsum solubility due to an ionic strength effect. In the second solution, sodium chloride and sodium sulfate were added. The sulfate ion decreased the gypsum solubility by common ion effect. In the third solution, HCl was added. Complexing between hydrogen ion and the sulfate increased the solubility of calcium sulfate dihydrate. In the solubility calculations, the activity coefficient for $CaSO_4$ was estimated using Bromley's correlation at low ionic strength (41) and extrapolated to high ionic strength using Meissner's universal plot (41). So, this method is purely predictive with no parameter optimization or adjustment. The results from the first two systems yielded reasonable prediction with the mean deviation of 20 %. However, there was found a large discrepancy between experimental and predicted values in the case of HCl system since with the addition of HCl in water the solubility increased by a factor of 10. Moreover their model was tested only at 25 °C.

More recently, Raju and Atkinson (7) gave new coefficients required to calculate C_p^0, ΔH^0, ΔG^0, ΔS^0, and K_{SP} for the solubility equilibrium as a function of temperature. The transition temperature between anhydrite and gypsum was predicted by assuming the activity of water to be equal to 1. Their values for K_{SP} of anhydrite and gypsum are in good agreement with those of Marshall and Slusher (11). In the solubility check for anhydrite and gypsum in NaCl solution, the mean activity coefficient of $CaSO_4$ was calculated by modified Pitzer's equation which includes more 12 empirical parameters. There was no self - consistence and additional parameters for both anhydrite and gypsum had to be used in order to obtain good comparison with the experimental values.

The above review indicates that most of previous work focused on gypsum solubility at room temperature and on anhydrite solubility above 100 °C or on hemihydrate solubility just in seawater at high temperature. There is a lack of a model to simultaneously calculate the solubility of three solid phases of $CaSO_4$ in concentrated mixed acid-salt solutions by using a set of consistent model parameters, such as, same activity coefficient model parameters.

2.4 Introduction of OLI Software

In the present research work StreamAnalyzer 1.2 and ESP V-6.6.0.4 (The Environmental Simulation Program, V-6.6.0.4) (47) both available by OLI Systems are employed to evaluate and regress the calcium sulfate solubility data determined in the laboratory so to obtain new accurate (self – consistent and universal) model parameters. This work led to the building of an improved chemical model using the OLI platform for comprehensive description of solubility – phase equilibria of $CaSO_4$ in complex aqueous concentrated chloride solutions up to 100 °C.

The OLI software uses a speciation-based thermodynamic model to calculate speciation and chemical equilibria as well as phase equilibria for multi-component aqueous systems. The main components of OLI software include (a) Databank, (b) Chemistry model, (c) Generator and (d) OLI Engine. Their organization may be demonstrated as in Figure 2.1.

If the solubility product and mean activity coefficient of $CaSO_4$ as well as the activity of water in solutions are known, the solubility of $CaSO_4{\cdot}nH_2O$ can be calculated with the aid of Eq. (2.2). The standard state thermodynamic property of each species is required for the calculation of all chemical equilibrium constants. In OLI, the revised HKF equation (47) is applied extensively for such calculation. According to their equation the Gibbs free energy of formation ($\Delta\overline{G}^0$) is given by

$$\begin{aligned}
\Delta\overline{G}^0 &= \Delta\overline{G}^0_{f,p_r,T_r} + (\Delta\overline{G}^0_{P,T} - \Delta\overline{G}^0_{P_r,T_r})\\
&= \Delta\overline{G}^0_f - \overline{S}^0_{P_r,T_r}(T-T_r) - c_1(T\ln(\frac{T}{T_r}) - T + T_r)\\
&+ a_1(P-P_r) + a_2\ln(\frac{\Psi+P}{\Psi+P_r}) - c_2[((\frac{1}{T-\theta}) - (\frac{1}{T_r-\theta}))(\frac{\theta-T}{\theta}) - \frac{T}{\theta^2}\ln(\frac{T_r(T-\theta)}{T(T_r-\theta)})]
\end{aligned}$$

$$+\left(\frac{1}{T-\theta}\right)\left(a_3(P-P_r)+a_4\ln\left(\frac{\Psi+P}{\Psi+P_r}\right)\right)+\omega\left(\frac{1}{\varepsilon}-1\right)-\omega_{P_r,T_r}\left(\frac{1}{\varepsilon_{P_r,T_r}}-1\right)+\omega_{P_r,T_r}Y_{P_r,T_r}(T-T_r) \qquad (2.5)$$

$\Delta\overline{G}_f^0$ and $\overline{S}_{P_r,T_r}^0$ are the standard partial molal Gibbs free energy of formation and standard partial molal entropy at 298 K and 1 bar, a_1, a_2, a_3, a_4, c_1 and c_2 represent species-dependent non-solvation parameters, T_r, P_r, T and P are the reference temperature of 298.15 K, the reference pressure of 1 bar and the temperature and pressure of the system. ε stands for the dielectric constant of H_2O, Ψ and θ refer to solvation parameters equal to 2600 bars and 228 K, respectively.

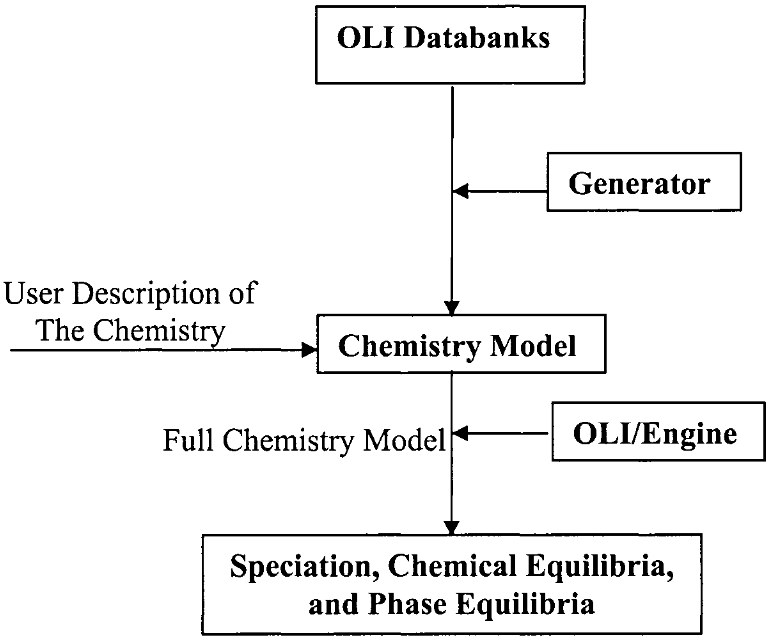

Figure 2.1. Organization of OLI software (47)

Alternatively when solubility data is available OLI may calculate a solubility product constant of solid phase by an empirical equation of the type expressed by

$$Log_{10}K_{SP} = A + \frac{B}{T} + CT + DT^2 \qquad (2.6)$$

In the above equation *A*, *B*, *C* and *D* are empirical parameters obtained via fitting to experimental solubility data.

The activity coefficient is estimated with the 9-parameters Bromley-Zemaitis equation (48) as follows:

$$Log\gamma_{\pm} = \frac{-A|Z_+Z_-|\sqrt{I}}{1+\sqrt{I}} + \frac{(0.06+0.6B)|Z_+Z_-|I}{(1+\frac{1.5}{|Z_+Z_-|I})^2} + BI + CI^2 + DI^3 \quad (2.7)$$

where $B=B_1+B_2T+B_3T^2$ is constant for ion interaction; *C* and *D* have the same form.

The ElectroChem program in ESP V-6.6.0.4 is run to obtain new OLI model parameters via regression of experimental data. For example, solubility data can be fixed as input and ElectroChem used to regress the thermodynamic model parameters, such as, Bromley-Zemaitis activity coefficient equation parameters.

2.5 Literature Cited

(1) Chong, T. H.; Sheikholeslami, R. Thermodynamics and Kinetics for Mixed Calcium Carbonate and Calcium Sulfate Precipitation. *Chem. Eng. Sci.* **2001**, 56, 5391.

(2) Hand, R. J. Calcium Sulphate Hydrates: a Review. *British Ceramic Trans.* **1997**, 96, 116.

(3) Ling, Y.; Demopoulos, G. P.; Giove, A.; Filippou, D. Technical Evaluation and Characterization of Alpha Calcium Sulphate Materials. *Gypsum and Fly Ash 2002*, Toronto, Canada, 2002, 6, 1-14.

(4) Ling, Y.; Demopoulos, G. P. Preparation of α-Calcium Sulfate Hemihydrate by Reaction of Sulfuric Acid with Lime. *Ind. Eng. Chem. Res.* **2005**, 44, 715.

(5) Linke, W. F.; Seidell, A. *Solubilities of Inorganic and Metal-Organic Compounds*; McGreger & Warner, American Chemical Society: Washington, D. C., USA, Vol. I, 1958, Vol.II, 1965.

(6) Silcock, H. L. *Solubilities of Inorganic and Organic Compounds, Vol. 3: Multicomponent Systems of Inorganic Substances*; Pergamon Press: Toronto, Canada, 1979.

(7) Raju, K. U. G.; Atkinson G. The Thermodynamics of "Scale" Mineral Solubilities. Calcium Sulfate in Aqueous NaCl. *J. Chem.Eng.Data* **1990**, 35, 361.

(8) Gupta, R. K. Solubility of Calcium Sulphate Dihydrate in Hydrochloric Acid Solutions. *J. Appl. Chem.* **1968**, 18, 49.

(9) Yasue, T.; Kojima, Y.; Kishimoto, Y.; Arai, Y. Preparation of α-Gypsum Hemihydrate and Control of Its Crystal Shape under Atmospheric Pressure, *Gypsum & Lime* (Japanese) **1992**, 239, 230.

(10) Marshall, W. L.; Slusher, R. Thermodynamics of Calcium Sulfate Dihydrate in Aqueous Sodium Chloride Solutions, 0-110 °C. *J. Phys. Chem.* **1966**, 70, 4015.

(11) Marshall, W. L.; Slusher, R.; Jones, E. V. Aqueous Systems at High Temperature. XIV. Solubility and Thermodynamic Relationships for $CaSO_4$ in NaCl-H_2O Solutions from 40 °C to 200 °C, 0 to 4 Molal NaCl. *J. Chem. Eng. Data* **1964**, 9, 187.

(12) Bock, E. On the Solubility of Anhydrous Calcium Sulphate and of Gypsum in Concentrated Solutions of Sodium Chloride at 25 °C, 30 °C, 40 °C, and 50 °C. *Can. J. Chem.* **1961**, 39, 1746.

(13) Glew, D. N.; Hames, D. A. Gypsum, Disodium Pentacalcium Sulfate, and Anhydrite Solubilities in Concentrated Sodium Chloride Solutions. *Can. J. Chem.* **1970**, 48, 3733.

(14) Marshall, W. L.; Jones, E. V. Second Dissociation Constant of Sulfuric Acid from 25 to 350 °C Evaluated from Solubilities of Calcium Sulfate in Sulfuric Acid Solutions. *J. Phys. Chem.* **1966**, 70, 4028.

(15) Madgin, W. M.; Swales, D. A. Solubilities in the System $CaSO_4$-NaCl-H_2O at 25 and 35 °C. *J. Appl. Chem.* **1956**, Nov., 482.

(16) Tanji, K. K. Solubility of Gypsum in Aqueous Electrolytes as Affected by Ion Association and Ionic Strengths up to 0.15 M and at 25 °C. *Environ. Sci. Technol.* **1969**, 3, 656.

(17) Barba, D.; Brandani, V.; Giacomo G. D. Solubility of Calcium Sulfate Dihydrate in the System Na_2SO_4-$MgCl_2$-H_2O. *J. Chem. Eng. Data*, **1984**, 29, 42.

(18) Ostroff, A. G.; Metler, A. V. Solubility of Calcium Sulfate Dihydrate in the System NaCl-$MgCl_2$-H_2O from 28 °C to 70 °C. *J. Chem. Eng. Data*, **1966**, 11, 346.

(19) Yeatts, L. B.; Marshall, W. L. Solubility of Calcium Sulfate Dihydrate and Association Equilibria in Several Aqueous Mixed Electrolyte Salt Systems at 25 °C. *J. Chem. Eng. Data*, **1972**, 17, 163.

(20) Calmanovici, C. E.; Gabas, N.; Laguerie, C. Solubility Measurements for Calcium Sulfate Dihydrate in Acid Solutions at 20, 50, and 70 °C. *J. Chem. Eng. Data*, **1993**, 38, 534.

(21) Umetsu, Y.; Mutalala, B. K.; Tozawa, K. Solubilities of $CaSO_4$ in Solutions of Zinc, Magnesium, Copper and Cobalt Sulfates over a Temperature Range of 25 to 200 °C. *Tohoku Daigaku Senko Seiren Kenkyusho Iho* **1989**, 45 (1), 13. (in Japanese).

(22) Sukimoto, S.; Hara, N.; Mukaiyama, H. Effects of Salts on the Formation of α-Calcium Sulfate Hemihydrates in Aqueous Salts Solution under the Atmospheric Pressure. *Gypsum & Lime* **1985**, 199, 363. (in Japanese)

(23) Kruchemko, V. P.; Beremzhanov, V. A. Relation of Gypsum Solubility in Inorganic Acid Solutions. *Rus. J. Inorg. Chem.* **1982**, 27(9), 2415.

(24) Zinyuk, R. Yu.; Pavlov, K. A.; Pavlova, T.A.; Kovalenko, L. V. Solubility and Stability of Gypsum in Aqueous Solutions of Citric and Phosphoric Acids. *Rus. J. Inorg. Chem.* **1997**, 70, 1570.

(25) Sullivan, J. M.; Kohler, J. J.; Grinstead, Jr. J. H. Solubility of α-Calcium Sulfate Hemihydrate in 40%, 45%, 50%, and 55% P_2O_5 Phosphoric Acid Solutions at 80, 90, 100, and 110 °C. *J. Chem. Eng. Data*, **1988**, 33, 367.

(26) Sullivan, J. M.; Kohler, J. J.; Grinstead, Jr. J. H. Effect of Aluminum, Iron, and Magnesium upon the Solubility of α-Calcium Sulfate Hemihydrate in 40%, 45%, 50%, and 55% P_2O_5 Phosphoric Acid Solutions at 80, 90, 100, and 110 °C: Correlations with Water Concentration. *J. Chem. Eng. Data*, **1991**, 36, 77.

(27) Kruchemko, V. P.; Beremzhanov, B. A. The Solubility of Salts in the Calcium Sulfate-Hydrochloric Acid-Water System at 25 °C. *Rus. J. Inorg. Chem.* **1976**, 21(1), 281.

(28) Zhang, Y.; Muhammed, M. Solubility of Calcium Sulfate Dihydrate in Nitric Acid Solutions Containing Calcium Nitrate and Phosphoric Acids. *J. Chem. Eng. Data*, **1989**, 34, 121.

(29) Mutalala, B. K.; Umetsu, Y.; Tozawa, K. Solubility of Calcium Sulfate in Acidic Copper Sulfate Solutions over the Temperature Range of 298 to 333 K. *Materials Trans. JIM* **1989**, 30, 394.

(30) Kruchemko, V. P. The Solubility of Gypsum in Aqueous Solutions of Magnesium Salts at 25, 40, and 50 °C. *Rus. J. Inorg. Chem.* **1985**, 30(6), 892.

(31) Dutrizac, J. E. Calcium Sulphate Solubilities in Simulated Zinc Processing Solutions. *Hydrometallurgy* **2002**, 65, 109.

(32) Ling, Yuanbing; Demopoulos, George P. Solubility of Calcium Sulfate Hydrates in (0 to 3.5) mol kg^{-1} Sulfuric Acid Solutions at 100 °C. *J. Chem. Eng. Data* **2004**, 49(5), 1263.

(33) Ryss, I. G.; Nilus, E. L. The Solubility of Calcium Sulfate in Hydrochloric Acid Solutions at 25 °C. *Zhurnal Obshchei Khimii* **1955**, 25, 1076.

(34) Kruchemko, V. P.; Beremzhanov, V. A. Solubility of Gypsum in Electrolyte Solutions. *Rus. J. Inorg. Chem.* **1980**, 25(11), 1689.

(35) Sveshnikova, V. N. Solubility Isotherms of the Systems $CaSO_4$-$CaCl_2$-H_2O at 25 °C and 55 °C and of $CaSO_4$-KCl-H_2O at 25 °C. *Izvest. Sektora Fiz.-Khim. Anal., Inst. Obshchei i Neorg. Khim., Akad. Nauk S.S.S.R.* **1949**, 17, 345.

(36) Kuznetsov, A. M. Solubility of Calcium Sulfate in the System Calcium Chloride-Hydrochloric Acid-Water. *J. Appl. Chem.* **1946**, 19, 1335 (in Russian).

(37) Gromova, E. T. The Solubility Isotherm at 110 ° for the System Na, CaCl, SO_4-H_2O**.** *Zh. Neorgan. Khim.* **1960**, 5, 2575.

(38) Sukimoto, S.; Hara, N.; Mukaiyama, H. Effects of Salts on the Formation of α-Calcium Sulfate Hemihydrates in Aqueous Salts Solution under the Atmospheric Pressure. *Gypsum & Lime* **1985**, 199, 363. (in Japanese)

(39) Ostroff, A. G.; Metler, A. V. Solubility of Calcium Sulfate Dihydrate in the System NaCl-$MgCl_2$-H_2O from 28 °C to 70 °C. *J. Chem. Eng. Data* **1966**, 11, 346.

(40) Marshall, W. L. and Slusher, R. Aqueous Systems at High Temperature: Solubility to 200^0C of Calcium Sulfate and Its Hydrates in Sea Water and Saline Water Concentrates, and Temperature-Concentration Limits. *J. Chem. Eng. Data* **1968**, 3, 83.

(41) Zemaitis, J. F.; Clark, D. M.; Rafal, M.; and Scrivner, N. C. *Handbook of Aqueous Electrolyte Thermodynamics Theory & Application*; AIChE: New York, 1986.

(42) Demopoulos, G. P.; Kondos, P.; Papangelakis, V. G. Prediction of Solubility in Chemical Compound Precipitation Systems. *Crystallization and Precipitation Symposium Proceedings*, G. L. Strathdee, M. O. Klein and L. A. Melis, Eds., Pergamon Press: Oxford, UK, 1987, 231-246.

(43) Barba, D.; Brandani, V.; and Giacomo, G. D. A Thermodynamic Model of $CaSO_4$ Solubility in Multicomponent Aqueous Solutions. *Chem. Eng. J.,* **1982**, 24, 191.

(44) Meijer, J. A. M.; Rosmalen, G. M. Solubilities and Supersaturations of Calcium Sulfate and Its Hydrates in Seawater. *Desalination* **1984**, 51, 255.

(45) Harvie, C. E.; Weare, J. H. The Prediction of Mineral Solubilities in Natural Waters: the Na-K-Mg-Ca-Cl-SO_4-H_2O System from Zero to High Concentration at 25 °C. *Geochim. Cosmochim. Acta* **1980**, 44, 981.

(46) Scrivner, N. C.; Staples, B. R. Equilibria in Aqueous Solutions: Industrial Applications, *Chemical Engineering Thermodynamics*; S. A. Newman, Ed., Ann Arbor Science: Ann Arbor, Mich., 1983.

(47) http://www.olisystems.com.

(48) *Aqueous System Modeling Course and Workshop*, OLI's manual, OLI Systems Inc., New Jersey, 2002.

Chapter 3

Solubility of $CaSO_4$ Phases in Aqueous HCl + $CaCl_2$ Solutions from 283 K to 353 K

3.1 Abstract

Solubilities of calcium sulfate dihydrate, hemihydrate and anhydrite in concentrated HCl, $CaCl_2$ and their mixed aqueous solutions were measured by using the classic isothermal dissolution method at the temperature range from (283 to 353) K. The concentration investigated for HCl is up to 12 $mol \cdot dm^{-3}$ and for $CaCl_2$ up to 3.5 $mol \cdot dm^{-3}$ at room temperature. The solubility of $CaSO_4$ phases in all cases investigated was found to increase with the temperature increment with the exception of anhydrite in $CaCl_2$ solutions. In pure HCl media, increasing the acid concentration in the range of (0.0 to 3) $mol \cdot dm^{-3}$ HCl, causes the solubility of $CaSO_4 \cdot 2H_2O$ (dihydrate: DH) or $CaSO_4$ (anhydrite: AH) to increase reaching a maximum value, and then decrease gradually with further increasing HCl concentration. In the concentrated range of (8 to 12) $mol \cdot dm^{-3}$ HCl, the solubility of $CaSO_4 \cdot 0.5H_2O$ (hemihydrate: HH) decreases with acid concentration. In HCl + $CaCl_2$ mixed media, the addition of $CaCl_2$ causes the solubility of all three phases to decrease due apparently to common ion effect.

3.2 Introduction

The solubility and phase equilibria of salts in electrolyte aqueous solutions play a significant role in the development, design, optimization and operation of precipitation processes (1-3). Precipitation is important in inorganic processing of materials but also in environmental protection, such as, wastewater treatment.

Solubility is essential to determine phase relationships in a system that includes unstable or metastable solid phases. In these cases, solubility determination becomes possible when equilibrium of unstable and metastable solids in solutions is reached before phase transformation occurs. One example is the solubility of calcium sulfate (4) that can be precipitated as dihydrate ($CaSO_4 \cdot 2H_2O$ - DH) at low temperature and hemihydrate ($CaSO_4 \cdot 0.5H_2O$ - HH) or anhydrite ($CaSO_4$ - AH) at elevated temperature in chloride media, such as the solutions containing HCl, $CaCl_2$, NaCl, $MgCl_2$, $AlCl_3$ or other chloride salts. These data are of considerable practical importance and theoretical significance in developing a new atmospheric process for the production of either dihydrate or the high value α - hemihydrate with simultaneous regeneration of hydrochloric acid from spent calcium chloride solutions by reaction with sulfuric acid (5, 6).

Solubility values of calcium sulfate in various aqueous chloride solutions are available in some compilations (7, 8). However, as we discussed in an earlier paper (9) most of the previous studies have been limited in reporting only the solubility of dihydrate in single acid or salt solutions at ambient temperature. There has been limited information on the influence of mixed electrolytes and no information on $CaSO_4$ solubility in concentrated chloride electrolytes at elevated temperatures.

Commercial software such as OLI Systems' StreamAnalyzer (OLI) (10), based on the thermodynamic model developed by Bromley and Zemaitis (11) can be employed to calculate the solubility of calcium sulfate dihydrate and anhydrite and even further to obtain the stability diagram. However, the accuracy of such software predictions strongly depends on the parameters stored in the databank, normally correlated from experimental data. Therefore, the applicability of the software is limited as their accuracy usually decreases with increasing component, concentration and temperature (9).

The above discussion indicates that there is still a need to systematically investigate the solubility of calcium sulfate and its hydrates in concentrated chloride electrolyte solutions, and this is done here for the system HCl + $CaCl_2$ + H_2O at over the temperature range (283 to 353) K. Additionally, the densities of the corresponding saturated solutions are reported. In a subsequent paper, a thermodynamic model for the system investigated in this work is described.

3.3 Experimental Section

A number of approaches (12,13) in the literature have been proposed to determine the solubility of salts in solutions, which can be categorized as either dissolution method or precipitation method. The dissolution method is considered to be more reliable and feasible since it avoids the complication of formation of intermediate phases that is commonly encountered in precipitation. In this work, the dissolution method was employed.

3.3.1 Chemicals

All substances, reagent grade, were directly used without further purification. All solutions used in this study were prepared by dissolving the following chemicals in de-ionized water (conductivity < 0.1 $\mu S \cdot cm^{-1}$): hydrochloric acid (mass fraction: (36.5 to 38.0) %) and calcium chloride dihydrate with high purity both from Fisher. Four solid substances were employed as the saturating solid phase: Gypsum from Alfa Aesar with 99 % purity, which contained trace anhydrite ($CaSO_4$), calcium sulfate hemihydrate (Plaster of Paris, also called β - hemihydrate) from Fisher, a commercial α - hemihydrate from Eastroc-BPB (14), which contained trace quantities of unknown additives and anhydrite from Alfa Aesar with 99 % purity.

3.3.2 Procedure

A typical experimental procedure can be described as follows. The 150 mL electrolyte aqueous solution of known composition was introduced to Erlenmeyer flasks, 250 mL volume, which were equipped with magnetic stirrer and capped with rubber stoppers. The flasks were then immersed in a temperature-controlled water bath, allowing the solution to stir continuously for about half an hour to establish the temperature equilibrium. The temperature was kept constant within ± 0.2 K. Then, excess solid (10-20 g of DH, HH or AH) was quickly added to the solutions in flasks, which were tightly capped again by using rubber stoppers to avoid loss of HCl vapor. The standard equilibration time used was 5 hours although other equilibration times were investigated as well as explained in the next section. After the solid-liquid equilibrium was attained, stirring was stopped to allow solids to settle. The supernatant solution was then withdrawn and immediately filtered by using 0.22 μm Whatman Puradisc™ syringe filters. The clear filtrate kept in water bath was taken by 10 mL glass pipette heated to bath temperature and diluted by de-ionized water in 1000 mL volumetric flask. The content of Ca or S was determined by inductively coupled plasma (ICP) analysis. The solubility (s) of calcium sulfate, expressed as g $CaSO_4$/L, was obtained from the Ca and S analysis. The saturated filtrate was also used to determine the density of saturated solutions at the experimental temperature by using 50 mL volumetric flask. The solid phase was filtered and washed each with water and acetone for 3 times. The washed solids were dried at 333 K for 24 hours and then subjected to XRD analysis by a Philips PW1710 diffractometer to determine whether the solid phase had been altered by phase transformation. Girgin and Demopoulos (5) have previously demonstrated that drying of DH or HH materials at 60 °C for 24 hours causes in itself no phase changes. Additionally, Scanning Electron Microscopy (SEM) image techniques were used for examination of the solid phases.

3.3.3 Determination of Equilibration Time

The equilibration time in solubility measurements normally varies from several hours to several days depending on the dissolution rate (15) of solid phase and the applied conditions. Power *et al.* (16,17) reported that the equilibrium of gypsum dissolution in pure water is reached within a minute, but the rate of phase transformation of gypsum to anhydrite above their transition temperature was reported to be extremely low. The analysis of the solid phase consistently indicated the presence of the dihydrate at all contact times studied for up to 222 hours. For the solubility determination of calcium sulfate dihydrate, Gupta (18) used 24 hours to attain the equilibrium between gypsum and hydrochloric acid solutions of less than 1 $mol \cdot kg^{-1}$ while 5 hours were used by Kruchenko and Beremzhanov (19). Rock (20) reported that the slurries were agitated for at least 48 hours during the measurement of gypsum and anhydrite solubilities in sodium chloride solution up to 323 K. The same interval was employed by Ostroff and

Metler (21) who investigated the dihydrate solubility in mixed NaCl + $MgCl_2$ solutions from (301 to 343) K.

For the determination of the solubility of calcium sulfate hemihydrate, in general much shorter equilibration times have been employed since hemihydrate is a metastable phase that experiences relatively fast transformation to gypsum at low temperature or anhydrite at elevated temperature. For example, β-hemihydrate which is unstable in pure water rapidly converts to gypsum at low temperature (7). In 1 $mol \cdot kg^{-1}$ sodium chloride, the same phenomenon occurs. Actually, it is very difficult to determine the solubility of hemihydrate at low temperature (17) within such a short time. However, hemihydrate at high temperature and high electrolyte concentration becomes less unstable so that there is enough time to attain solubility equilibrium. Kruchenko and Beremzhanov (19) determined the solubility of α-hemihydrate in concentrated HCl solutions at room temperature by equilibrating the solids for 5 hours. Sullivan *et al.* (22) found that the equilibrium between α-hemihydrate and phosphoric acid solutions at 353 K is established quite rapidly within about 3 minutes and there is no decrease in solubility over time intervals up to 70 hours, but 1 to 3 hours was used in their investigation. Similar procedure and time (1 hour) was used by Martynowicz *et al.* (23).

In the present study, the dissolution of calcium sulfate dihydrate in 1 $mol \cdot dm^{-1}$ HCl solution at room temperature was investigated as a function of time in order to select the appropriate equilibration time. The results of these kinetic experiments show that the solubility equilibrium between solid and liquid was established very rapidly within half an hour. However, in the experimental work a longer time of 5 hours for dihydrate and anhydrite and 1 hour for hemihydrate, respectively, was chosen to ensure achievement of solubility equilibrium. Longer times were not employed because of the possibility of conversion of the starting phases to other calcium sulfate hydrates.

3.3.4 Reproducibility

The solubility of calcium sulfate dihydrate in pure water has been investigated by many authors (7,8). Similar experiments were carried out by the authors to verify the reproducibility and accuracy of the adopted procedure in this work. The solubility comparison between experimental and literature values (7) is demonstrated in Figure 3.1. The uncertainty of the measured solubility values was within ± 0.031 g·dm^{-3} and relative deviation is 1.62 %. Three replicate measurements of dihydrate solubility in 1 mol·dm^{-3} HCl at ambient temperature were also carried out. The average deviation was ± 0.111 g·dm^{-3} with relative deviation of 0.77 %. Equally good accuracy was associated with the determined densities of calcium sulfate dihydrate saturated solutions as it can be deduced from the data in Figure 3.1. The measured densities were uncertain to ±0.001 g·cm^{-3}.

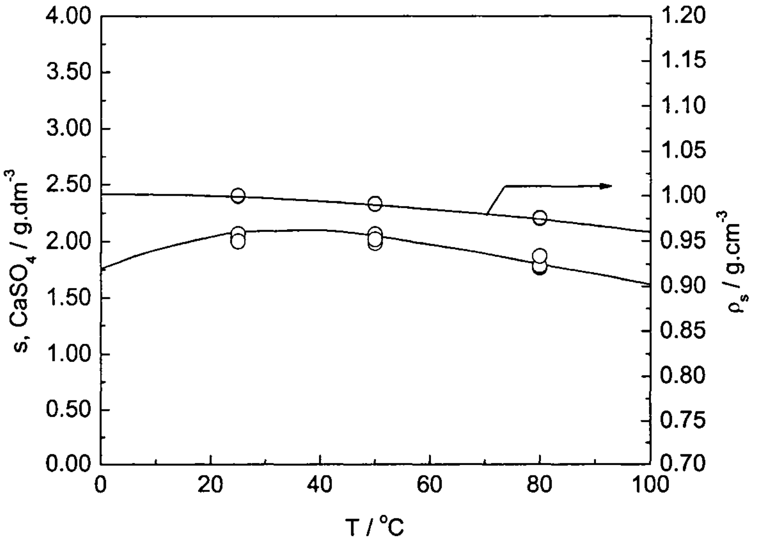

Figure 3.1. Solubility of calcium sulfate dihydrate in water and the density of the saturated solutions: — , Hulett and Allen;[7] ○, this work.

3.4 Results and Discussion

3.4.1 Solubility of $CaSO_4 \cdot 2H_2O$ in HCl Solutions

Calcium sulfate dihydrate solubilities in hydrochloric acid solution were measured at 283, 295, 313, 333 and 353 K. The investigated concentration of acid is from (0.0 to 5) mol·dm^{-3} at room temperature. The results of experimentally determined solubilities are summarized in Table 3.1 and graphically in Figure 3.2. In Table 3.1 the concentration of hydrochloric acid and calcium sulfate is expressed both in molarity (*M*/mol·dm^{-3}) and molality (*m*/mol·kg^{-1}) for convenient practical and thermodynamic reference. However, the concentration of HCl in molarity marked with M_2 is the initial concentration of the solution prepared at ambient temperature before introducing calcium sulfate dihydrate. The other quantities of acid and salts in different units express the solubility at the conditions of the system. In addition, the measured densities (required to convert solubility units from molarity to molality) for several saturated solution compositions are given in Table 3.1. OLI's StreamAnalyzer1.1 was used to convert the solubility units from molarity to molality when the experimental density of saturated solution was not available. Justification for the use of OLI in this context is given later in this paper (refer to Figure 3.7).

Figure 3.2 demonstrates that at constant temperature the solubility of calcium sulfate dihydrate in aqueous HCl solutions possesses two features. The solubility of dihydrate increases with increasing HCl concentration in the range of (0.0 to 3.0) mol·dm^{-3}. After passing a maximum, the solubility declines smoothly in the range of higher concentration of acid. In reference to temperature, the solubility increases systematically as the temperature increases from (283 to 353) K. Some of the data generated in this work is compared to the data available in literature (18,19) in Figure 3.3. There is good agreement of present data and earlier measurements.

Table 3.1. Solubility of $CaSO_4$ (1) as Dihydrate in HCl(2) + H_2O(3)(Equilibration Time: 5 Hours)

solution parameters			solubility as $CaSO_4$ in different units		
M_2 /mol·dm^{-3} ^{a}	m_2/mol·kg^{-1}	ρ_s /g·cm^{-3} ^{b}	C_1/g·dm^{-3}	M_1/mol·dm^{-3}	m_1/ mol·kg^{-1}
$T = 283$ K					
0.000	0.0000	1.002	1.928	0.0142	0.0142
0.200	0.2011	1.005	5.182	0.0381	0.0383
0.400	0.4034	1.013	7.218	0.0530	0.0535
0.600	0.6072	1.016	8.994	0.0661	0.0670
0.800	0.8123	1.019	10.492	0.0771	0.0786
1.000	1.0191	1.028	11.403	0.0838	0.0854
1.500	1.5431	1.037	13.062	0.0959	0.0990
2.000	2.0779	1.047	13.964	0.1026	0.1067
3.000	3.1828	1.064	13.926	0.1023	0.1087
4.000	4.3396	1.079	12.330	0.0906	0.0983
5.000	5.5524	1.094	10.726	0.0788	0.0874
$T = 295$ K					
0.000	0.0000		2.080	0.0153	0.0153
0.200	0.2010		6.755	0.0496	0.0500
0.400	0.4032		9.676	0.0711	0.0719
0.600	0.6067		11.854	0.0871	0.0885
0.800	0.8116		13.520	0.0993	0.1013
1.000	1.0182	1.027	14.573	0.1070	0.1096
1.200	1.2260		16.350	0.1201	0.1235
1.400	1.4360		16.574	0.1217	0.1257
1.600	1.6473		17.491	0.1285	0.1333
1.800	1.8601		18.391	0.1351	0.1407
2.000	2.0751	1.048	18.751	0.1377	0.1441
2.200	2.2919		18.901	0.1388	0.1458
2.400	2.5104		19.189	0.1409	0.1487
2.600	2.7311		19.135	0.1405	0.1489
2.800	2.9535		19.091	0.1402	0.1492
3.000	3.1782	1.066	18.975	0.1394	0.1489
3.200	3.4048		18.833	0.1383	0.1484
3.600	3.8651		17.752	0.1304	0.1411
4.000	4.3337	1.078	16.958	0.1246	0.1360
4.300	4.6908		16.496	0.1212	0.1332
4.600	5.0538		15.636	0.1148	0.1271
5.000	5.5456	1.092	14.770	0.1085	0.1211

$T = 313$ K					
0.000	0.0000		2.097	0.0154	0.0155
0.200	0.2009		7.811	0.0574	0.0581
0.400	0.4030		11.514	0.0846	0.0860
0.600	0.6062		14.425	0.1060	0.1083
0.800	0.8109		16.665	0.1224	0.1256
1.000	1.0170		18.687	0.1373	0.1415
1.200	1.2245		20.664	0.1518	0.1571
1.400	1.4338		21.846	0.1605	0.1668
1.600	1.6449		22.580	0.1658	0.1732
1.800	1.8574		23.446	0.1722	0.1806
2.000	2.0720		23.986	0.1762	0.1856
2.200	2.2881		24.675	0.1812	0.1917
2.400	2.5062		24.923	0.1831	0.1945
2.600	2.7263		25.124	0.1845	0.1969
2.800	2.9484		25.036	0.1839	0.1971
3.000	3.1725		25.087	0.1843	0.1983
3.600	3.8580		23.932	0.1758	0.1917
4.000	4.3258		23.059	0.1694	0.1864
4.300	4.6824		22.454	0.1649	0.1827
4.600	5.0448		21.496	0.1579	0.1761
5.000	5.5362		20.283	0.1490	0.1677
$T = 333$ K					
0.000	0.0000		1.971	0.0145	0.0147
0.200	0.2009		9.360	0.0688	0.0703
0.600	0.6055		18.541	0.1362	0.1405
1.000	1.0154		24.217	0.1779	0.1852
1.400	1.4312		28.096	0.2064	0.2168
2.000	2.0673		31.653	0.2325	0.2475
2.400	2.5004		32.692	0.2401	0.2580
2.600	2.7199		33.012	0.2425	0.2616
2.800	2.9411		33.324	0.2448	0.2653
3.000	3.1647		33.229	0.2441	0.2658
3.200	3.3897		33.671	0.2473	0.2705
3.600	3.8477		32.665	0.2399	0.2648
4.000	4.3142		31.779	0.2334	0.2600
4.300	4.6693		31.503	0.2314	0.2595
4.600	5.0310		30.335	0.2228	0.2516
5.000	5.5210		29.126	0.2139	0.2439
$T = 353$ K					
0.000	0.0000		1.801	0.0132	0.0136
0.200	0.2008		11.037	0.0811	0.0838
0.400	0.4023		16.898	0.1241	0.1290
0.800	0.8085		27.019	0.1985	0.2083
1.000	1.0134	1.016	30.756	0.2259	0.2377
1.200	1.2204		32.302	0.2373	0.2513

1.600	1.6378		37.129	0.2727	0.2915
2.000	2.0618	1.041	40.607	0.2983	0.3206
2.200	2.2761		42.190	0.3099	0.3359
2.600	2.7112		43.583	0.3201	0.3502
2.800	2.9312		44.364	0.3258	0.3582
3.000[c]	3.1541	1.054	44.126	0.3241	0.3578
4.000[c]	4.3008	1.071	41.898	0.3077	0.3456
5.000[c]	5.5060	1.084	37.788	0.2775	0.3184

[a] Initial concentration of solutions prepared at room temperature without calcium sulfate. [b] Experimental density of saturated solutions. [c] Equilibration time is 1 hour.

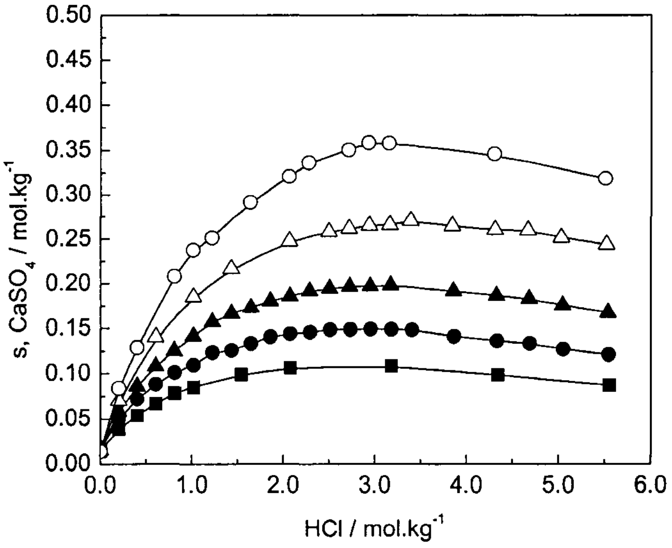

Figure 3.2. Solubility of calcium sulfate dihydrate in hydrochloric acid solutions: ■ ,283 K; ●, 295 K; ▲, 313 K; △, 333 K; ○, 353 K.

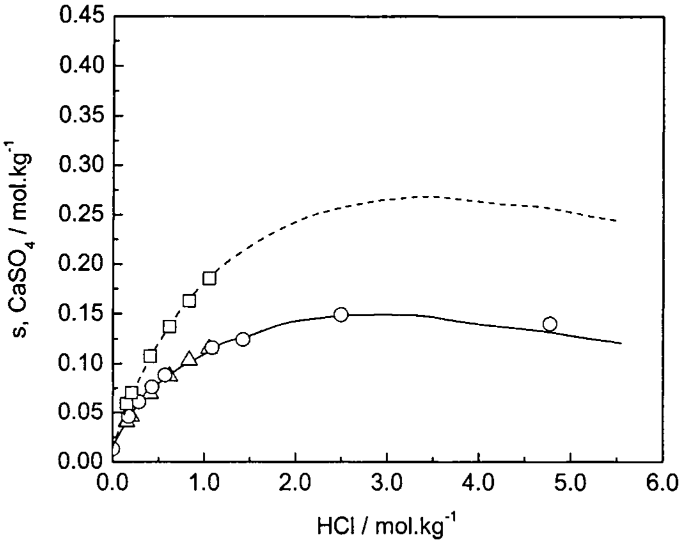

Figure 3.3. Comparison of the solubility of calcium sulfate as dihydrate in HCl solutions from different sources (lines, this work):△,Gupta(18) at 293 K;○, Kruchenko *et al.*(19) at 298 K; □, Gupta(18) at 333 K.

The XRD analysis of equilibrated solid phases showed the calcium sulfate dihydrate to be stable in HCl solutions with the concentration of (0.0 to 5.0) mol·dm^{-3} at temperatures below 333 K within 5 hours. However, at elevated temperature, such as at 353 K, and higher HCl concentration (more than 1 mol·dm^{-3}), the transformation from dihydrate to anhydrite is observed. For example, dihydrate in 5 mol·dm^{-3} HCl solutions at 353 K was completely converted to anhydrite within the time of 5 hours while in 1 mol·dm^{-3} HCl solution at 353 K no anhydrite was detected in equilibrated solids. The results of solids characterization by XRD are tabulated in Table 3.2. The equilibrated solids were examined by SEM. Typical SEM images are presented in Figure 3.4. It can be clearly seen that original crystals underwent ripening (compare Figure 3.4(a) and Figure 3.4(b)) with the small "dust" particles on the surface of the original gypsum crystals to have dissolved and crystallographic characteristics to have been "sharpened".

This is the case when the equilibrated solids are dihydrate (1 mol·dm^{-3} HCl, 353 K and 5 hours). However, the gypsum crystals were transformed to needle-shape anhydrite when the HCl concentration was 4 mol·dm^{-3} (see Figure 3.4(c)). The solubility data presented in Table 3.1 and Figure 3.2, though, is for DH in equilibration only, i.e. the data associated with conversion of DH to AH is excluded.

Table 3.2. XRD Characterization of the Equilibrated Solids (Starting Material is Dihydrate)

T/K	*M*/mol·dm^{-3}	Equilibration *t* /h	Equilibrated solid phase(s)[a]
333	4 (HCl)	1	DH
		2	DH
		3	DH+ trace AH
		4-5	DH+ minor AH
353	1 (HCl)	1-5	DH
353	3 (HCl)	5	DH+ minor AH
353	4 (HCl)	1	DH+ minor AH
		2	DH+ major AH
		3-5	AH
353	2 ($CaCl_2$)	5	DH+ trace HH
353	1 (HCl)+ 2 ($CaCl_2$)	5	DH+ minor AH
353	3 (HCl)+ <2 ($CaCl_2$)	5	DH+AH
353	3 (HCl)+ 2 ($CaCl_2$)	5	AH+HH
333	5 (HCl)+ 0.5 ($CaCl_2$)	5	DH
333	5 (HCl)+ 2 ($CaCl_2$)	5	AH+HH

[a] DH - $CaSO_4 \cdot 2H_2O$; HH - $CaSO_4 \cdot 0.5H_2O$; AH - $CaSO_4$.

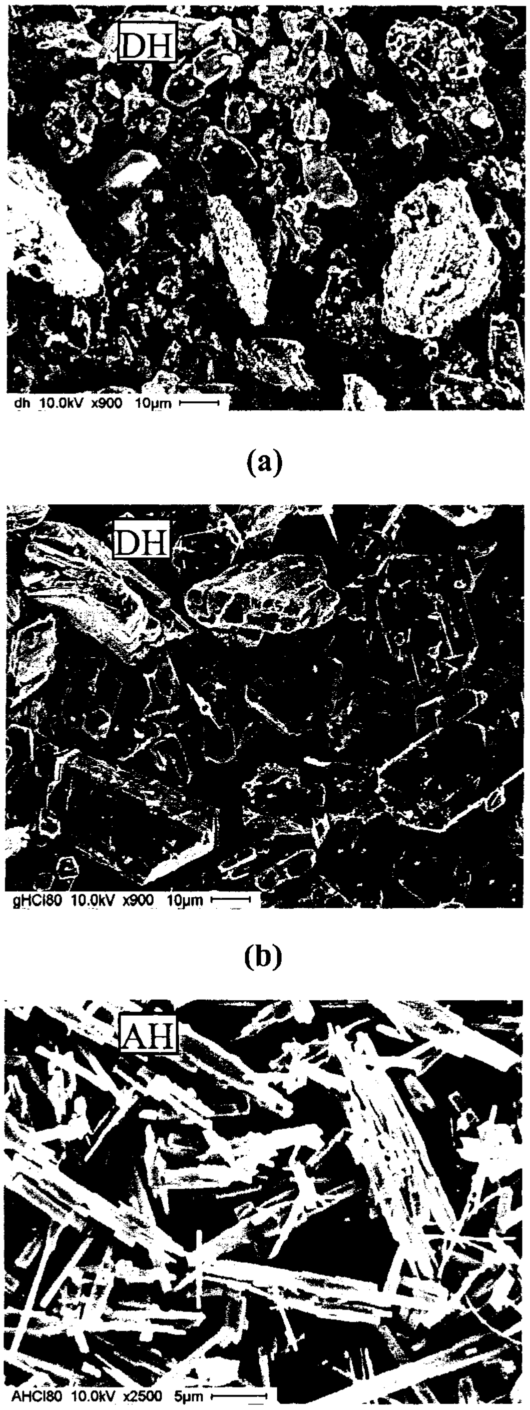

(a)

(b)

(c)

Figure 3.4. SEM images of original gypsum and equilibrated solids: (a) original gypsum from Alfa; (b) solids in 1 mol·dm^{-3} HCl at 353 K after 5 hours; (c) solids in 4 mol·dm^{-3} HCl at 353 K after 5 hours.

3.4.2 Solubility of $CaSO_4·2H_2O$ in $CaCl_2$ Solutions

Solubilities of calcium sulfate dihydrate (and saturated solution densities) at (295, 313, 333 and 353) K in calcium chloride solutions with concentrations up to 2 mol·dm^{-3} were determined by using the same procedure. The obtained experimental results are shown in Table 3.3 and Figure 3.5.

Figure 3.5 illustrates that the solubility of calcium sulfate dihydrate decreases with the concentration of $CaCl_2$. Initially, the solubility drops sharply, then continues to fall almost linearly with increasing concentration of $CaCl_2$. Common ion effect is responsible for this behavior. As also seen in Figure 3.5, the solubility slightly increases with increasing temperature. The XRD study in Table 3.2 shows that a trace of calcium sulfate hemihydrate was detected at 353 K; but otherwise the equilibrated solid phase remains gypsum.

Table 3.3. Solubility of $CaSO_4$ (1) as Dihydrate in $CaCl_2$ (2) + H_2O (3) (Equilibration Time: 5 Hours)

solution parameters			solubility as $CaSO_4$ in different units		
M_2 /mol·dm$^{-3\,a}$	m_2/mol·kg^{-1}	ρ_s /g·cm$^{-3\,b}$	C_1/g·dm^{-3}	M_1/mol·dm^{-3}	m_1/ mol·kg^{-1}
$T = 295$ K					
0.049	0.0498	1.002	1.353	0.0099	0.0099
0.099	0.0997	1.007	1.204	0.0088	0.0088
0.198	0.1998	1.016	1.127	0.0082	0.0083
0.297	0.3004	1.024	1.096	0.0080	0.0081
0.396	0.4013	1.033	1.031	0.0075	0.0076
0.496	0.5029	1.042	0.992	0.0072	0.0073
0.595	0.6048	1.050	0.963	0.0070	0.0071
0.694	0.7073	1.059	0.918	0.0067	0.0068
0.778	0.7943	1.066	0.863	0.0063	0.0064
0.972	0.9980	1.083	0.788	0.0057	0.0059
1.167	1.2038	1.099	0.700	0.0051	0.0053
1.361	1.4121	1.115	0.628	0.0046	0.0047
1.556	1.6231	1.131	0.527	0.0038	0.0040
1.750	1.8367	1.147	0.452	0.0033	0.0034
1.945	2.0532	1.163	0.388	0.0028	0.0030

$T = 313$ K					
0.049	0.0498	0.997	1.399	0.0102	0.0103
0.099	0.0997	1.002	1.296	0.0095	0.0096
0.198	0.1998	1.011	1.235	0.0090	0.0091
0.297	0.3004	1.019	1.197	0.0088	0.0089
0.396	0.4013	1.028	1.167	0.0085	0.0087
0.496	0.5029	1.037	1.118	0.0082	0.0083
0.595	0.6048	1.045	1.073	0.0078	0.0080
0.694	0.7073	1.054	1.030	0.0075	0.0077
0.778	0.7943	1.061	0.977	0.0071	0.0073
0.972	0.9979	1.077	0.905	0.0066	0.0068
1.167	1.2038	1.093	0.801	0.0058	0.0061
1.361	1.4121	1.109	0.715	0.0052	0.0054
1.556	1.6230	1.125	0.640	0.0047	0.0049
1.750	1.8366	1.141	0.554	0.0040	0.0043
1.945	2.0532	1.157	0.465	0.0034	0.0036
$T = 333$ K					
0.049	0.0498	0.989	1.360	0.0099	0.0101
0.099	0.0997	0.993	1.317	0.0096	0.0098
0.198	0.1998	1.002	1.271	0.0093	0.0095
0.297	0.3004	1.011	1.223	0.0089	0.0092
0.396	0.4013	1.019	1.219	0.0089	0.0091
0.496	0.5029	1.028	1.207	0.0088	0.0091
0.595	0.6047	1.036	1.171	0.0086	0.0088
0.694	0.7073	1.045	1.138	0.0083	0.0086
0.778	0.7943	1.052	1.107	0.0081	0.0084
0.972	0.9979	1.069	1.014	0.0074	0.0077
1.167	1.2037	1.086	0.953	0.0070	0.0073
1.361	1.4120	1.102	0.843	0.0061	0.0065
1.556	1.6230	1.118	0.765	0.0056	0.0059
1.750	1.8365	1.134	0.679	0.0049	0.0053
1.945	2.0531	1.150	0.594	0.0043	0.0046
$T = 353$ K					
0.049	0.0498	0.977	1.286	0.0094	0.0097
0.099	0.0997	0.982	1.270	0.0093	0.0096
0.198	0.1998	0.991	1.247	0.0091	0.0094
0.297	0.3004	0.999	1.305	0.0095	0.0099
0.396	0.4013	1.008	1.291	0.0094	0.0098
0.496	0.5029	1.017	1.262	0.0092	0.0096
0.595	0.6047	1.025	1.256	0.0092	0.0096
0.694	0.7073	1.034	1.250	0.0091	0.0095
0.778	0.7943	1.041	1.208	0.0088	0.0092
0.972	0.9978	1.058	1.156	0.0084	0.0089
1.167	1.2037	1.074	1.096	0.0080	0.0085
1.361	1.4120	1.091	0.998	0.0073	0.0077
1.556	1.6229	1.107	0.918	0.0067	0.0072

1.750	1.8365	1.123	0.845	0.0062	0.0066
1.945	2.0530	1.139	0.762	0.0056	0.0060

[a] Initial concentration of solutions prepared at room temperature without calcium sulfate. [b] Experimental density of saturated solutions.

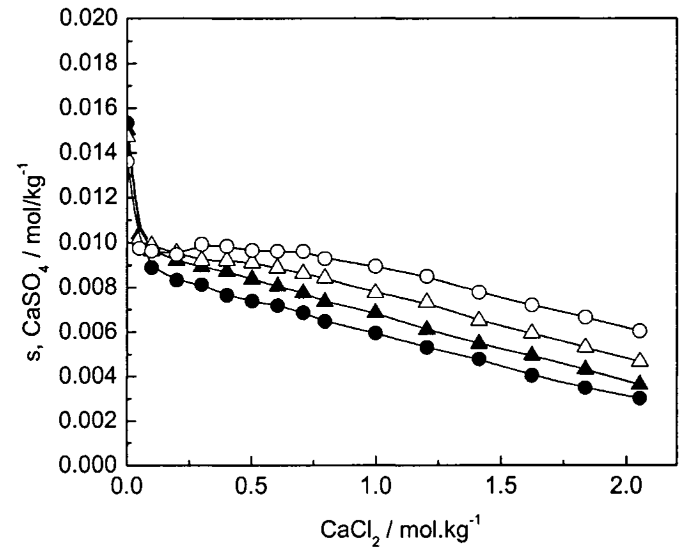

Figure 3.5. Solubility of calcium sulfate dihydrate in aqueous calcium chloride solutions: ●, 295 K; ▲, 313 K; △, 333 K; ○, 353 K.

3.4.3 Solubility of $CaSO_4 \cdot 2H_2O$ in Mixed HCl + $CaCl_2$ Solutions

The same approach was used to obtain the solubility of calcium sulfate dihydrate in HCl (1, 3, and 5 mol·dm^{-3}) + $CaCl_2$ mixed electrolyte solutions at (295, 313, 333 or 353) K. The results determined in this study are given in Tables 3.4-3.6 and graphically in Figure 3.6 for 1 mol·dm^{-3} HCl as an example.

The general behavior observed with all 3 acidic levels investigated is consistent showing an increase in solubility of $CaSO_4 \cdot 2H_2O$ with increasing temperature. The presence of $CaCl_2$ in the solutions makes the solubility fall sharply at the lower concentration of calcium chloride, then drop smoothly with increasing concentration. Once again the depressing effect of $CaCl_2$ on $CaSO_4$ solubility is attributed to the common ion effect. XRD analysis (see results in Table 3.2) showed the equilibrated solids in 1 mol·dm^{-3} HCl + $CaCl_2$ solutions at all temperatures after 5 hours to be predominantly dihydrate, but in higher HCl concentration (3 mol·dm^{-3}) solutions with $CaCl_2$ present (at 353 K) the equilibrated solids were a mixture of $CaSO_4$ dihydrate and hemihydrate after 5 hours equilibration. When the acid concentration was 5 mol·dm^{-3} (in mixed HCl + 2 mol·dm^{-3} $CaCl_2$ solution), the dihydrate was transformed completely to anhydrite and hemihydrate after 5 hours at 333 K. Once more the solubility data listed in Tables 3.4, 3.5 and 3.6 refer to DH equilibrated solids, i.e. tests associated with the complete conversion of DH to AH and/or HH within the prescribed 5 hour period were repeated at shorter equilibration time to ensure the integrity of DH.

Table 3.4. Solubility of $CaSO_4$ (1) as Dihydrate in 1 mol·dm^{-3} HCl (2) + $CaCl_2$ (3) + H_2O (4) (Equilibration Time: 5 Hours)

solution parameters				solubility as $CaSO_4$ in different units		
M_3/ mol.dm^{-3a}	m_2/ mol·kg^{-1}	m_3/ mol·kg^{-1}	ρ_s / g·cm$^{-3\ b}$	C_1/g·dm^{-3}	M_1/mol·dm^{-3}	m_1/ mol·kg^{-1}
			$T = 295$ K			
0.010	1.0186	0.0102	1.027	13.955	0.1025	0.1050
0.020	1.0190	0.0204	1.027	13.377	0.0983	0.1006
0.050	1.0201	0.0510	1.029	12.100	0.0889	0.0911
0.100	1.0218	0.1022	1.032	10.186	0.0748	0.0767
0.250	1.0266	0.2566	1.041	6.335	0.0465	0.0479
0.500	1.0338	0.5169	1.061	3.629	0.0267	0.0276
0.750	1.0411	0.7808	1.081	2.516	0.0185	0.0192
1.000	1.0487	1.0487	1.102	1.821	0.0134	0.0140
1.500	1.0648	1.5971	1.142	1.054	0.0077	0.0082
2.000	1.0825	2.1651	1.182	0.589	0.0043	0.0046
			$T = 313$ K			
0.010	1.0176	0.0102	1.024	17.678	0.1298	0.1338
0.020	1.0180	0.0204	1.025	17.066	0.1253	0.1292
0.050	1.0191	0.0510	1.026	15.568	0.1143	0.1179
0.100	1.0206	0.1021	1.029	14.177	0.1041	0.1075
0.250	1.0257	0.2564	1.038	9.411	0.0691	0.0715
0.500	1.0333	0.5167	1.056	5.489	0.0403	0.0419
0.750	1.0407	0.7805	1.076	3.877	0.0285	0.0298

1.000	1.0484	1.0484	1.096	2.802	0.0206	0.0217
1.500	1.0646	1.5969	1.136	1.680	0.0123	0.0132
2.000	1.0824	2.1648	1.175	0.994	0.0073	0.0079
			$T = 333$ K			
0.010	1.0158	0.0102	1.020	23.648	0.1737	0.1808
0.020	1.0162	0.0203	1.021	23.197	0.1704	0.1774
0.050	1.0174	0.0509	1.022	21.439	0.1575	0.1641
0.100	1.0191	0.1019	1.024	19.329	0.1420	0.1480
0.250	1.0243	0.2561	1.033	14.160	0.1040	0.1087
0.500	1.0323	0.5161	1.050	9.069	0.0666	0.0700
0.750	1.0400	0.7800	1.070	6.398	0.0470	0.0496
1.000	1.0478	1.0478	1.089	4.822	0.0354	0.0376
1.500	1.0642	1.5963	1.130	2.938	0.0216	0.0232
2.000	1.0822	2.1643	1.165	1.759	0.0129	0.0142
			$T = 353$ K			
0.010	1.0139	0.0101	1.014	30.302	0.2226	0.2347
0.020	1.0146	0.0203	1.014	28.566	0.2098	0.2212
0.050	1.0157	0.0508	1.015	27.366	0.2010	0.2121
0.100	1.0173	0.1017	1.018	25.396	0.1865	0.1970
0.250	1.0226	0.2557	1.026	19.776	0.1453	0.1537
0.500	1.0309	0.5154	1.042	13.658	0.1003	0.1067
0.750	1.0388	0.7791	1.061	10.169	0.0747	0.0798
1.000	1.0469	1.0469	1.080	7.807	0.0573	0.0617
1.500	1.0635	1.5953	1.120	4.978	0.0366	0.0398
2.000	1.0817	2.1634	1.159	3.155	0.0232	0.0256

[a] Initial concentration of solutions prepared at room temperature without calcium sulfate. [b] Experimental density of saturated solutions.

Table 3.5. Solubility of $CaSO_4$ (1) as Dihydrate in 3 mol·dm^{-3} HCl (2) + $CaCl_2$ (3) + H_2O (4) (Equilibration Time: 5 Hours)

solution parameters				solubility as $CaSO_4$ in different units		
M_3/ mol.dm^{-3a}	m_2/ mol·kg^{-1}	m_3/ mol·kg^{-1}	ρ_s/ g·cm$^{-3\,b}$	C_1/g·dm^{-3}	M_1/mol·dm^{-3}	m_1/ mol·kg^{-1}
			$T = 295$ K			
0.010	3.1807	0.0106	1.062	17.576	0.1291	0.1380
0.020	3.1822	0.0212	1.062	16.780	0.1233	0.1317
0.050	3.1870	0.0531	1.063	14.517	0.1066	0.1140
0.100	3.1935	0.1064	1.067	12.458	0.0915	0.0979
0.250	3.2112	0.2676	1.074	7.884	0.0579	0.0622
0.500	3.2389	0.5398	1.092	3.971	0.0292	0.0315
0.750	3.2655	0.8164	1.110	2.467	0.0181	0.0197
1.000	3.2929	1.0976	1.129	1.699	0.0125	0.0137
1.500	3.3514	1.6757	1.170	0.951	0.0070	0.0078
2.000	3.4155	2.2770	1.208	0.538	0.0040	0.0045
			$T = 313$ K			

0.010	3.1757	0.0106	1.060	22.958	0.1686	0.1814
0.020	3.1768	0.0212	1.061	22.520	0.1654	0.1780
0.050	3.1812	0.0530	1.061	20.805	0.1528	0.1647
0.100	3.1879	0.1063	1.064	18.423	0.1353	0.1459
0.250	3.2073	0.2673	1.071	11.968	0.0879	0.0951
0.500	3.2362	0.5394	1.087	6.736	0.0495	0.0539
0.750	3.2639	0.8160	1.107	4.116	0.0302	0.0331
1.000	3.2916	1.0972	1.124	3.041	0.0223	0.0247
1.500	3.3507	1.6753	1.162	1.678	0.0123	0.0139
2.000	3.4151	2.2767	1.200	0.949	0.0070	0.0080
			$T = 333$ K			
0.010	3.1676	0.0106	1.059	31.622	0.2323	0.2523
0.020	3.1684	0.0211	1.060	31.460	0.2311	0.2511
0.050	3.1735	0.0529	1.058	28.870	0.2120	0.2310
0.100	3.1808	0.1060	1.061	25.997	0.1909	0.2079
0.250	3.2004	0.2667	1.069	19.334	0.1420	0.1550
0.500	3.2317	0.5386	1.082	11.512	0.0846	0.0929
0.750	3.2603	0.8151	1.101	7.797	0.0573	0.0633
1.000	3.2889	1.0963	1.116	5.733	0.0421	0.0470
1.500	3.3492	1.6746	1.154	3.143	0.0231	0.0262
2.000	3.4140	2.2760	1.192	2.032	0.0149	0.0172

[a] Initial concentration of solutions prepared at room temperature without calcium sulfate. [b] Experimental density of saturated solutions.

Table 3.6. Solubility of $CaSO_4$ (1) as Dihydrate in 5 mol·dm^{-3} HCl (2) + $CaCl_2$ (3) + H_2O (4) (Equilibration Time: 5 Hours)

solution parameters				solubility as $CaSO_4$ in different units		
M_3/ mol.dm^{-3a}	m_2/ mol·kg^{-1}	m_3/ mol·kg^{-1}	ρ_s / g·cm$^{-3\,b}$	C_1/g·dm^{-3}	M_1/mol·dm^{-3}	m_1/ mol·kg^{-1}
			$T = 295$ K			
0.010	5.5513	0.0111	1.091	13.138	0.0965	0.1077
0.020	5.5541	0.0222	1.092	12.607	0.0926	0.1033
0.050	5.5621	0.0556	1.091	10.841	0.0796	0.0890
0.100	5.5746	0.1115	1.092	8.739	0.0642	0.0719
0.250	5.6095	0.2805	1.101	4.893	0.0359	0.0405
0.500	5.6625	0.5662	1.120	2.289	0.0168	0.0191
0.750	5.7148	0.8572	1.139	1.411	0.0104	0.0118
1.000	5.7693	1.1539	1.158	0.971	0.0071	0.0082
1.500	5.8869	1.7661	1.194	0.557	0.0041	0.0048
2.000	6.0169	2.4068	1.233	0.340	0.0025	0.0030
			$T = 313$ K			
0.010	5.5447	0.0111	1.087	17.040	0.1252	0.1407
0.020	5.5476	0.0222	1.087	16.453	0.1208	0.1359
0.050	5.5549	0.0555	1.089	15.164	0.1114	0.1253

0.100	5.5678	0.1114	1.089	12.751	0.0937	0.1057
0.250	5.6046	0.2802	1.097	7.744	0.0569	0.0645
0.500	5.6590	0.5659	1.114	4.321	0.0317	0.0362
0.750	5.7126	0.8569	1.132	2.622	0.0193	0.0222
1.000	5.7678	1.1536	1.151	1.800	0.0132	0.0153
1.500	5.8859	1.7658	1.188	1.064	0.0078	0.0092
2.000	6.0163	2.4065	1.225	0.678	0.0050	0.0060
$T = 333$ K						
0.010	5.5298	0.0111	1.084	25.751	0.1891	0.2149
0.020	5.5319	0.0221	1.085	25.626	0.1882	0.2139
0.050	5.5409	0.0554	1.086	23.316	0.1713	0.1946
0.100	5.5533	0.1111	1.086	21.223	0.1559	0.1778
0.250	5.5919	0.2796	1.094	15.127	0.1111	0.1271
0.500	5.6515	0.5652	1.106	8.554	0.0628	0.0725
0.750	5.7071	0.8561	1.124	5.746	0.0422	0.0491
1.000	5.7638	1.1528	1.137	4.007	0.0294	0.0347
1.500	5.8834	1.7650	1.177	2.398	0.0176	0.0211
2.000	6.0153	2.4061	1.212	1.150	0.0084	0.0103

---

[a] Initial concentration of solutions prepared at room temperature without calcium sulfate. [b] Experimental density of saturated solutions.

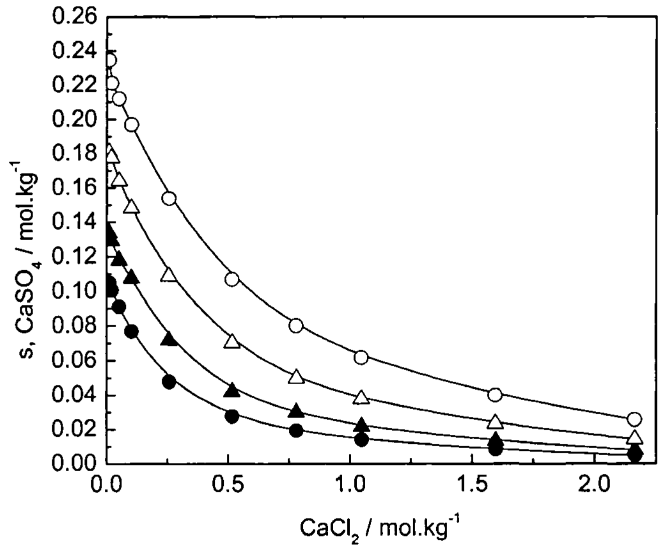

Figure 3.6. Solubility of calcium sulfate dihydrate in HCl(1 mol·dm^{-3}) + CaCl$_2$ solutions: ●, 295 K; ▲, 313 K; △, 333 K; ○, 353 K.

3.4.4 Density Comparison with OLI Software

The density of the saturated solutions is required to allow for unit conversion of solubility data from molarity to molality scale. For the $CaSO_4 \cdot 2H_2O + HCl + H_2O$ system (refer to Table 3.1), saturated solution densities were estimated using the StreamAnalyzer program of OLI only when experimental densities were not measured. This was done only after OLI proved reliable in estimating density data in this work. However, for the other systems all densities reported in Tables 3.3 – 3.8 and 3.10 – 3.13 are measured values. A measure of the accuracy of the OLI estimated density data can be obtained by referring to Figure 3.7 where a comparison is made with our experimentally determined density data. As it can be seen there is very good agreement between OLI predictions and experimental measurements for both single and mixed electrolytes (average relative deviation < 0.5 %)

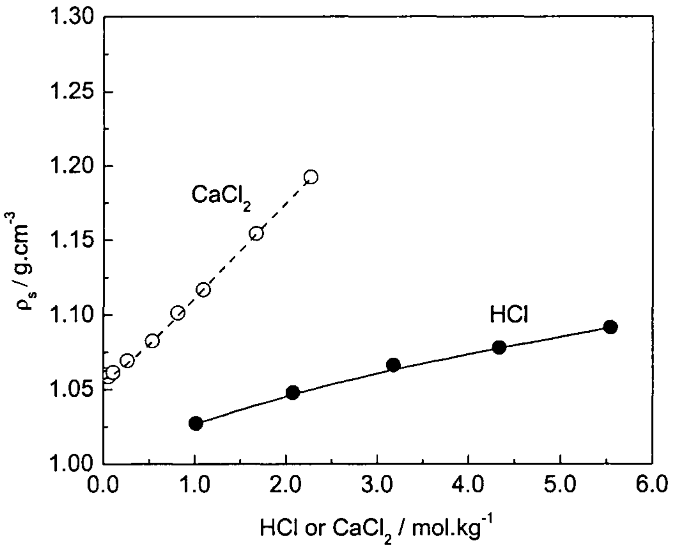

Figure 3.7. Density of $CaSO_4$ saturated $HCl + CaCl_2$ mixed electrolyte solutions (lines, OLI): ●, this work in HCl solutions at 295 K; ○, this work in HCl (3mol·dm^{-3}) + $CaCl_2$

3.4.5 Solubility of $CaSO_4 \cdot 0.5H_2O$

The measured results of the hemihydrate solubility in pure HCl solutions are given in Table 3.7 and presented in Figure 3.8. The solubility of hemihydrate decreases with increasing acid concentration (in the investigated range of 8.5 to 16 $mol \cdot kg^{-1}$) and increases with increasing temperature. The results in Figure 3.8 further show that there is no significant difference in solubility between α-hemihydrate and β-hemihydrate while our α-hemihydrate solubility is slightly higher than that reported in literature (19). Beta-hemihydrate is known (at least in H_2SO_4 solutions (29)) to be more soluble than α-hemihydrate. It is possible, therefore, in the context of the present work that the proximity in solubility between α-hemihydrate and β-hemihydrate to be due to the origin of the α-hemihydrate used here which was of industrial commercial grade. Impurities in the α-hemihydrate commercial product may be responsible for its somewhat elevated solubility. Table 3.8 and Figure 3.9 present the solubility of β-hemihydrate in HCl + $CaCl_2$ mixed solutions at 333 K and 353 K. Once again the apparent common-ion effect causes the solubility to decline sharply with increasing concentration of $CaCl_2$. The XRD analysis of the equilibrated solids for this system is summarized in Table 3.9. It can be observed that the presence of $CaCl_2$ in HCl suppressed the transformation of hemihydrate to anhydrite, hence making possible the determination of its solubility by this isothermal dissolution method. The solubility data reported in Tables 3.7 and 3.8 refer to HH as equilibrated phase only. The SEM micrographs of Figure 3.10 (a) and (b) indicate that the α- and β-calcium sulfate hemihydrate remained unaltered in concentrated 9 $mol \cdot dm^{-3}$ HCl solutions at 298 K (for 1 hour) while hemihydrate in 6 $mol \cdot dm^{-3}$ HCl at 353 K was converted to anhydrite (within the 1 hour equilibration time once more). As it can be deduced from Figure 3.10(c), however, when $CaCl_2$ is present in 6 mol·dm^{-3} HCl solution hemihydrate remains unaltered (within the 1 hour period) (compare Figure 3.10(a) to Figure 3.10(b)). The stability effect of $CaCl_2$ on HH is explored elsewhere for the elaboration of a method to produce the high value material α - hemihydrate (5).

Table 3.7. Solubility of $CaSO_4$ (1) as Hemihydrate in HCl(2) + H_2O(3)(Equilibration Time: 1 Hour)

solution parameters			solubility as $CaSO_4$ in different units		
M_2/mol·dm$^{-3\,a}$	m_2/mol·kg^{-1}	ρ_s/g·cm$^{-3\,b}$	C_1/g·dm^{-3}	M_1/mol·dm^{-3}	m_1/ mol·kg^{-1}
T = 298 K, Solid: α - hemihydrate					
8.000	9.6032	1.132	10.066	0.0739	0.0890
9.000	11.1046	1.140	6.970	0.0512	0.0634
10.000	12.6938	1.161	5.446	0.0400	0.0506
11.000	14.3767	1.168	4.496	0.0330	0.0433
12.000	16.1449	1.180	3.449	0.0253	0.0342
T = 298 K, Solid: β - hemihydrate					
8.000	9.6029	1.126	10.474	0.0769	0.0931
9.000	11.1042	1.141	7.430	0.0546	0.0676
10.000	12.6933	1.156	6.099	0.0448	0.0570
11.000	14.3768	1.167	4.385	0.0322	0.0422
12.000	16.1450	1.182	3.360	0.0247	0.0333
T = 323 K, Solid: β - hemihydrate					
7.000	8.5098	1.113	18.174	0.1335	0.1597
8.000	9.6008	1.118	13.879	0.1019	0.1247
9.000	11.1013	1.131	11.404	0.0838	0.1050
10.000	12.6908	1.146	9.066	0.0666	0.0856
11.000	14.3739	1.155	7.427	0.0546	0.0724
12.000	16.1412	1.165	6.909	0.0507	0.0696

[a] Initial concentration of solutions prepared at room temperature without calcium sulfate. [b] Experimental density of saturated solutions.

Table 3.8. Solubility of $CaSO_4$ (1) as Hemihydrate in HCl (2) + $CaCl_2$ (3) + H_2O (4) (Equilibration Time: 1 Hour)

solution parameters				solubility as $CaSO_4$ in different units		
M_3/ mol·dm^{-3a}	m_2/ mol·kg^{-1}	m_3/ mol·kg^{-1}	ρ_s/ g·cm$^{-3\,b}$	C_1/g·dm^{-3}	M_1/mol·dm^{-3}	m_1/ mol·kg^{-1}
T = 333 K, HCl = 6 M^a, Solid: β - hemihydrate						
0.050	6.8483	0.0571	1.099	21.833	0.1607	0.1874
0.100	6.8608	0.1143	1.105	19.700	0.1450	0.1687

0.250	6.9018	0.2876	1.110	13.191	0.0971	0.1136
0.500	6.9688	0.5807	1.126	7.196	0.0530	0.0624
1.000	7.1108	1.1851	1.157	2.719	0.0200	0.0241
1.500	7.2666	1.8167	1.193	1.392	0.0102	0.0126
2.000	7.4390	2.4797	1.231	0.861	0.0063	0.0079
2.500	7.6293	3.1789	1.264	0.546	0.0040	0.0051
3.000	7.8356	3.9178	1.292	0.494	0.0036	0.0048
3.500	8.0534	4.6978	1.334	0.407	0.0030	0.0040
$T = 353$ K, HCl = 3 M[a], Solid: β - hemihydrate						
0.050	3.1902	0.0532	1.064	42.85	0.3154	0.3463
0.100	3.1953	0.1065	1.065	40.54	0.2984	0.3286
0.250	3.2107	0.2676	1.074	32.71	0.2408	0.2651
0.500	3.2370	0.5395	1.082	22.97	0.1691	0.1880
1.000	3.2918	1.0973	1.117	11.10	0.0817	0.0917
1.500	3.3509	1.6754	1.153	5.82	0.0428	0.0488
2.000	3.4152	2.2768	1.183	3.44	0.0254	0.0295
2.500	3.4866	2.9055	1.221	1.96	0.0144	0.0171
3.000	3.5651	3.5651	1.253	1.34	0.0099	0.0120
3.500	3.6524	4.2612	1.295	1.01	0.0074	0.0092

[a] Initial concentration of solutions prepared at room temperature without calcium sulfate. [b] Experimental density of saturated solutions.

Table 3.9. XRD Characterization of the Equilibrated Solids (Starting Material is Hemihydrate)

T/K	M/mol·dm^{-3}	Equilibration t /h	Equilibrated solid phase(s)[a]
298	8 - 12 (HCl)	1	HH
323	7 - 12 (HCl)	1	HH
353	1 - 7 (HCl)	1	AH
333	0.0 -3 ($CaCl_2$)	1	HH+DH
	3.5 ($CaCl_2$)	1	HH
353	0.0 -2 ($CaCl_2$)	1	HH+DH
	2.5 - 3.5 ($CaCl_2$)	1	HH
333	3 (HCl)+ 0.0 – 2 ($CaCl_2$)	1	HH+DH
	3 (HCl)+ 2 – 3.5 ($CaCl_2$)	1	HH
353	3 (HCl)+ 0.05-0.1 ($CaCl_2$)	1	HH+ trace DH
	3 (HCl)+ 0.25 – 3.5 ($CaCl_2$)	1	HH
333	6 (HCl)+ 0.0-3.5 ($CaCl_2$)	1	HH

[a] DH - $CaSO_4 \cdot 2H_2O$; HH - $CaSO_4 \cdot 0.5H_2O$; AH - $CaSO_4$.

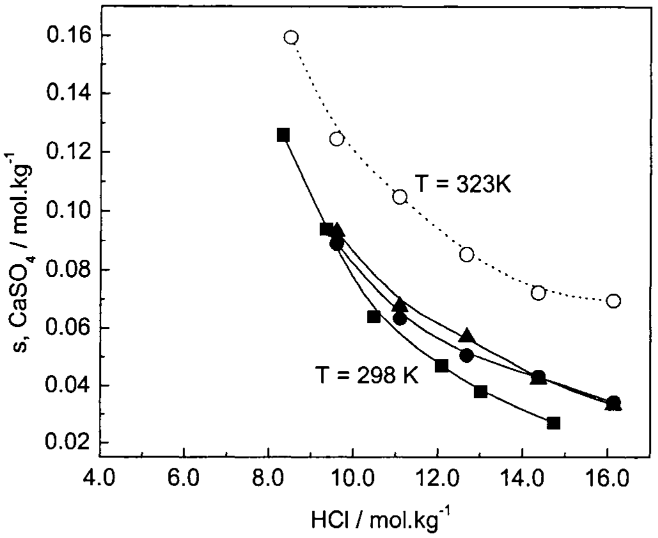

Figure 3.8. Comparison of the solubility of $CaSO_4 \cdot 0.5H_2O$ modifications in concentrated HCl solutions: ●, α – HH at 298 K; ▲, β – HH at 298 K; ○, β – HH at 323 K; ■Kruchenko *et al.*(19) at 298 K (α – HH).

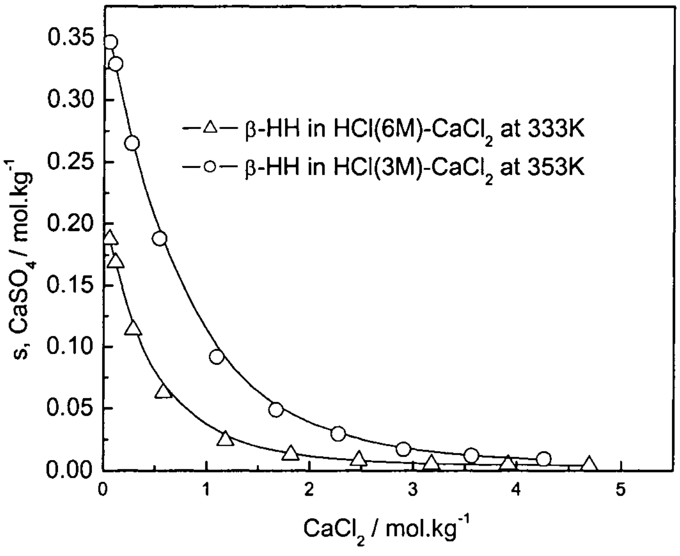

Figure 3.9. Solubility of β - hemihydrate in HCl + $CaCl_2$ mixed electrolyte solutions: △, 6 mol·dm^{-3} HCl + $CaCl_2$ at 333 K; ○, 3 mol·dm^{-3} HCl + $CaCl_2$ at 353 K.

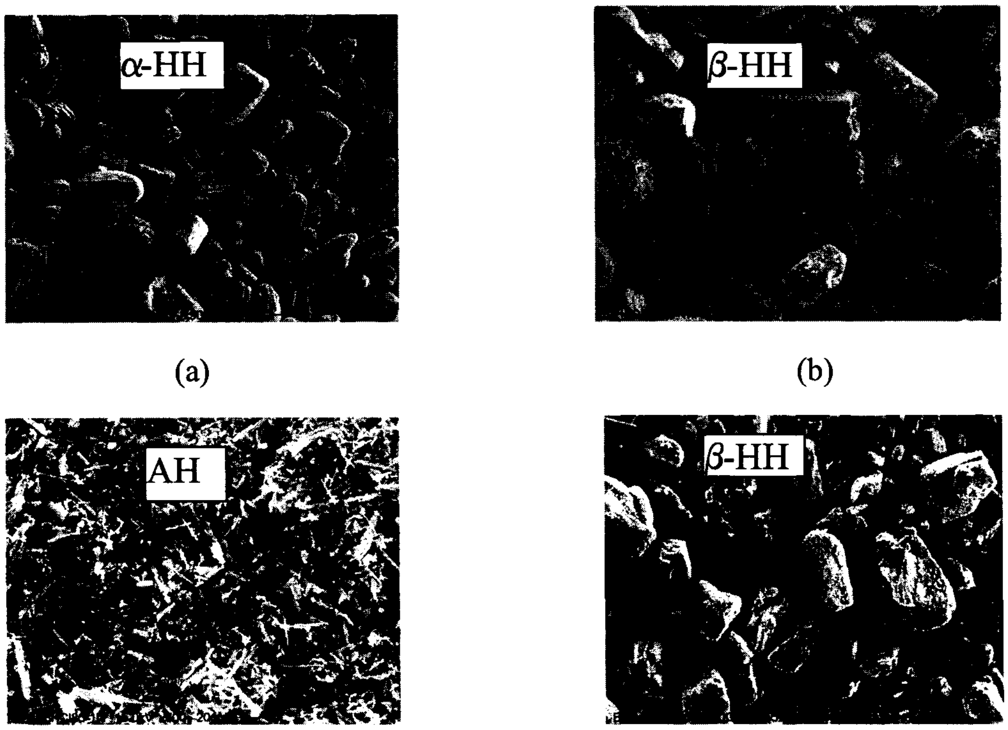

(a) (b) (c) (d)

Figure 3.10. SEM images of equilibrated solids (The starting material is α-or β hemihydrate): (a) solids (α - hemihydrate) in 9 mol·dm^{-3} HCl at 298 K after 1 hour; (b) solids (β - hemihydrate) in 9 mol·dm^{-3} HCl at 298 K after 1 hour; (c) solids in 6 mol·dm^{-3} HCl at 353 K after 1 hour; (d) solids in 0.1 mol·dm^{-3} $CaCl_2$-6 mol·dm^{-3} HCl solution at 333 K after 1 hour.

3.4.6 Solubility of $CaSO_4$ in HCl Solutions

Solubilities of calcium sulfate anhydrite in pure hydrochloric acid solutions were determined at (298, 313, 333 and 353) K. The investigated concentration of acid is from (0.0 to 6) mol·dm^{-3} at room temperature. The experimental results are presented in Table 3.10 and graphically in Figure 3.11.

It can be deduced by comparing Figure 3.11 to Figure 3.2 that the solubility of anhydrite in HCl aqueous solutions possesses similar features as dihydrate. The solubility of anhydrite increases with increasing the HCl concentration in the range of (0.0 to 3.0) mol·kg^{-3}. After passing a maximum, the solubility decreases sharply with further increasing HCl concentration. In reference to temperature, the solubility increases systematically as the temperature increases from (298 to 353) K. The solubility of anhydrite in HCl solutions at 25 °C was compared with experimental data from literature (19) as shown in Figure 3.11. The present experimental data is in good agreement with early measurements.

Table 3.10. Solubility of $CaSO_4$ (1) as Anhydrite in HCl(2) + H_2O(3)(Equilibration Time: 5 Hours)

solution parameters			solubility as $CaSO_4$ in different units		
M_2 /mol·dm$^{-3\ a}$	m_2/mol·kg^{-1}	ρ_s /g·cm$^{-3\ b}$	C_1/g·dm^{-3}	M_1/mol·dm^{-3}	m_1/ mol·kg^{-1}
		$T = 298$ K			
0.200	0.2014	1.008	8.723	0.0641	0.0646
0.500	0.5063	1.018	13.663	0.1003	0.1018
0.800	0.8147	1.025	16.647	0.1223	0.1247
1.000	1.0223	1.031	18.534	0.1361	0.1395
1.200	1.2315	1.034	19.685	0.1446	0.1488
1.500	1.5487	1.041	20.406	0.1499	0.1552
2.000	2.0859	1.049	20.997	0.1542	0.1614
2.500	2.6348	1.057	20.844	0.1531	0.1620
3.000	3.1956	1.064	19.740	0.1450	0.1550
3.500	3.7693	1.072	18.578	0.1365	0.1474
4.000	4.3559	1.077	16.791	0.1233	0.1347
4.500	4.9562	1.083	15.198	0.1116	0.1233
5.000	5.5710	1.090	12.987	0.0954	0.1066
5.500	6.2017	1.095	11.563	0.0849	0.0961
6.000	6.8478	1.103	9.953	0.0731	0.0836
		$T = 313$ K			
0.200	0.2014	1.003	7.623	0.0560	0.0566
0.500	0.5063	1.012	12.942	0.0951	0.0969
0.800	0.8147	1.021	16.326	0.1199	0.1229
1.000	1.0223	1.025	18.914	0.1389	0.1431
1.200	1.2315	1.030	19.638	0.1442	0.1492
1.500	1.5487	1.036	20.834	0.1530	0.1592
2.000	2.0859	1.045	21.645	0.1590	0.1671
2.500	2.6348	1.053	21.546	0.1583	0.1681
3.000	3.1956	1.060	20.956	0.1539	0.1654
3.500	3.7693	1.067	19.944	0.1465	0.1591
4.000	4.3559	1.073	18.184	0.1336	0.1467
4.500	4.9562	1.078	16.608	0.1220	0.1356
5.000	5.5710	1.084	14.712	0.1081	0.1215

5.500	6.2017	1.091	12.810	0.0941	0.1070
6.000	6.8478	1.098	11.217	0.0824	0.0948
$T = 333$ K					
0.200	0.2014	0.994	7.594	0.0558	0.0569
0.500	0.5063	1.003	13.085	0.0961	0.0988
0.800	0.8147	1.013	16.869	0.1239	0.1280
1.000	1.0223	1.019	18.860	0.1385	0.1437
1.200	1.2315	1.022	20.096	0.1476	0.1539
1.500	1.5487	1.028	21.574	0.1585	0.1663
2.000	2.0859	1.038	23.164	0.1701	0.1804
2.500	2.6348	1.046	23.739	0.1744	0.1869
3.000	3.1956	1.054	23.245	0.1707	0.1849
3.500	3.7693	1.059	22.039	0.1619	0.1775
4.000	4.3559	1.065	20.314	0.1492	0.1655
4.500	4.9562	1.072	18.333	0.1347	0.1508
5.000	5.5710	1.077	17.043	0.1252	0.1420
5.500	6.2017	1.084	14.994	0.1101	0.1263
6.000	6.8478	1.089	13.584	0.0998	0.1159
$T = 353$ K					
0.200	0.2014	0.985	7.319	0.0538	0.0554
0.500	0.5063	0.994	13.392	0.0984	0.1021
0.800	0.8147	1.003	17.280	0.1269	0.1325
1.000	1.0223	1.008	19.458	0.1429	0.1500
1.200	1.2315	1.013	20.972	0.1540	0.1621
1.500	1.5487	1.018	22.636	0.1663	0.1764
2.000	2.0859	1.028	24.529	0.1802	0.1931
2.500	2.6348	1.037	25.389	0.1865	0.2019
3.000	3.1956	1.045	25.120	0.1845	0.2019
3.500	3.7693	1.051	23.959	0.1760	0.1949
4.000	4.3559	1.057	22.692	0.1667	0.1867
4.500	4.9562	1.064	20.935	0.1538	0.1740
5.000	5.5710	1.071	19.169	0.1408	0.1610
5.500	6.2017	1.075	17.848	0.1311	0.1520
6.000	6.8478	1.081	15.636	0.1148	0.1347

[a] Initial concentration of solutions prepared at room temperature without calcium sulfate. [b] Experimental density of saturated solutions.

3.4.7 Solubility of $CaSO_4$ in $CaCl_2$ Solutions

The generated solubility data is tabulated in Table 3.11 and plotted in Figure 3.12. The solubility curves in Figure 3.12 illustrate that the solubility of calcium sulfate anhydrite sharply decreases with the addition of $CaCl_2$ due to common ion effect. In contrast to the behavior of calcium sulfate dihydrate the solubility of anhydrite in calcium chloride decreases with increasing temperature investigated. Interestingly, the anhydrite solubilities at the three temperatures approach a constant value at high $CaCl_2$ concentration.

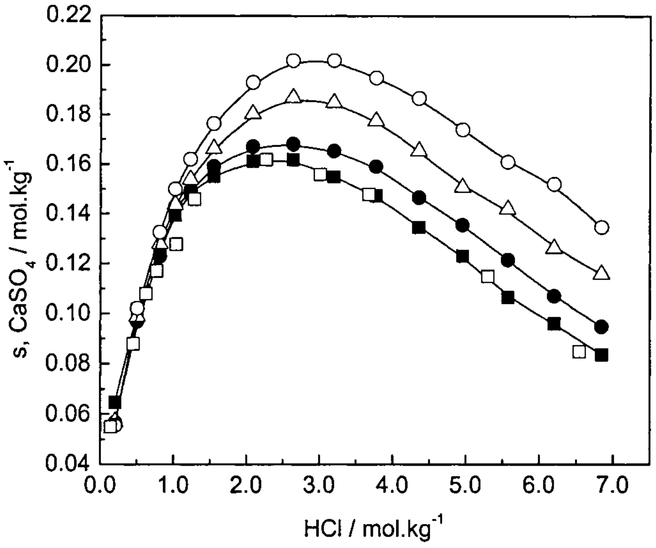

Figure 3.11. Solubility of calcium sulfate anhydrite in hydrochloric acid solutions: ■, 298 K; ●, 313 K; △, 333 K; ○, 353 K; □, Kruchenko *et al.*(19) at 298 K.

Table 3.11. Solubility of $CaSO_4$ (1) as Anhydrite in $CaCl_2$ (2) + H_2O (3)(Equilibration Time: 5 Hours)

solution parameters			solubility as $CaSO_4$ in different units		
M_2 /mol·dm^{-3} ^{a}	m_2/mol·kg^{-1}	ρ_s / g·cm^{-3} ^{b}	C_1/g·dm^{-3}	M_1/mol·dm^{-3}	m_1/ mol·kg^{-1}
		$T = 298$ K			
0.050	0.0502	1.004	2.149	0.0158	0.0158
0.100	0.1005	1.008	2.033	0.0149	0.0150
0.250	0.2521	1.022	1.858	0.0136	0.0137
0.500	0.5070	1.043	1.663	0.0122	0.0124
1.000	1.0269	1.085	1.298	0.0095	0.0098
1.500	1.5620	1.126	0.892	0.0066	0.0068
2.000	2.1148	1.165	0.574	0.0042	0.0045
2.500	2.6879	1.205	0.338	0.0025	0.0027
3.000	3.2841	1.243	0.188	0.0014	0.0015
3.500	3.9067	1.281	0.110	0.0008	0.0009
		$T = 323$ K			

0.050	0.0502	0.993	1.469	0.0108	0.0109
0.100	0.1005	0.998	1.391	0.0102	0.0104
0.250	0.2521	1.012	1.301	0.0096	0.0097
0.500	0.5070	1.033	1.224	0.0090	0.0092
1.000	1.0269	1.074	0.979	0.0072	0.0075
1.500	1.5620	1.116	0.712	0.0052	0.0055
2.000	2.1148	1.154	0.479	0.0035	0.0038
2.500	2.6879	1.193	0.303	0.0022	0.0024
3.000	3.2841	1.232	0.184	0.0013	0.0015
3.500	3.9067	1.271	0.104	0.0008	0.0009
T = 353 K					
0.050	0.0502	0.977	0.755	0.0055	0.0057
0.100	0.1005	0.982	0.756	0.0056	0.0057
0.250	0.2521	0.995	0.754	0.0055	0.0057
0.500	0.5070	1.017	0.761	0.0056	0.0058
1.000	1.0269	1.060	0.665	0.0049	0.0051
1.500	1.5620	1.099	0.507	0.0037	0.0040
2.000	2.1148	1.139	0.369	0.0027	0.0029
2.500	2.6879	1.177	0.248	0.0018	0.0020
3.000	3.2841	1.216	0.173	0.0013	0.0014
3.500	3.9067	1.254	0.107	0.0008	0.0009

[a] Initial concentration of solutions prepared at room temperature without calcium sulfate. [b] Experimental density of saturated solutions.

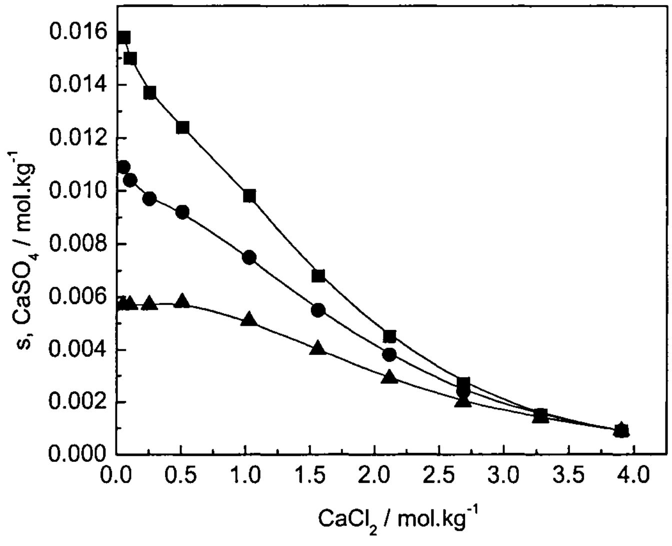

Figure 3.12. Solubility of calcium sulfate anhydrite in aqueous calcium chloride solutions: ■, 298 K; ● , 323 K; ▲ , 353 K.

3.4.8 Solubility of $CaSO_4$ in Mixed HCl + $CaCl_2$ Solutions

The solubility of calcium sulfate anhydrite in mixed HCl (3 and 6) mol·dm^{-3} + $CaCl_2$ solutions was obtained over the temperature range from (298 to 353) K. The determined experimental data is presented in Tables 3.12 and 3.13. The same data is shown also graphically in Figure 3.13.

It can be seen in Figure 3.13 that the solubility of anhydrite in both acidic concentrations slightly increases with increasing temperature. The addition of calcium chloride in saturated solution leads the solubility to decrease more sharply in 6 mol·dm^{-3} HCl concentration than in 3 mol·dm^{-3} HCl suggesting the HCl lowers water activity and results in decreasing solubility. The XRD analysis of equilibrated solids showed that there was no phase transformation of anhydrite in the course of 5 hours equilibration at the three temperatures investigated.

Table 3.12. Solubility of $CaSO_4$ (1) as Anhydrite in 3 mol·dm^{-3} HCl (2) + $CaCl_2$ (3) + H_2O (4) (Equilibration Time: 5 Hours)

solution parameters				solubility as $CaSO_4$ in different units		
M_3/ mol.dm^{-3a}	m_2/ mol·kg^{-1}	m_3/ mol·kg^{-1}	ρ_s/ g·cm$^{-3\,b}$	C_1/g·dm^{-3}	M_1/mol·dm^{-3}	m_1/ mol·kg^{-1}
			T = 298 K			
0.050	3.2002	0.0533	1.066	17.357	0.1275	0.1364
0.100	3.2048	0.1068	1.067	14.398	0.1058	0.1133
0.250	3.2184	0.2682	1.076	9.188	0.0675	0.0726
0.500	3.2425	0.5404	1.093	5.244	0.0385	0.0417
1.000	3.2945	1.0982	1.131	1.996	0.0147	0.0161
1.500	3.3523	1.6762	1.169	0.811	0.0060	0.0067
2.000	3.4161	2.2774	1.209	0.429	0.0031	0.0036
2.500	3.4872	2.9060	1.247	0.206	0.0015	0.0018
3.000	3.5655	3.5655	1.286	0.120	0.0009	0.0010
3.500	3.6527	4.2615	1.319	0.067	0.0005	0.0006
			T = 323 K			
0.050	3.2002	0.0533	1.057	19.973	0.1467	0.1588
0.100	3.2048	0.1068	1.060	17.124	0.1258	0.1361
0.250	3.2184	0.2682	1.067	11.175	0.0821	0.0891
0.500	3.2425	0.5404	1.083	6.348	0.0466	0.0510

1.000	3.2945	1.0982	1.120	2.646	0.0194	0.0216
1.500	3.3523	1.6762	1.157	1.221	0.0090	0.0102
2.000	3.4161	2.2774	1.196	0.648	0.0048	0.0055
2.500	3.4872	2.9060	1.234	0.323	0.0024	0.0028
3.000	3.5655	3.5655	1.271	0.196	0.0014	0.0017
3.500	3.6527	4.2615	1.305	0.118	0.0009	0.0011
			$T = 353$ K			
0.050	3.2002	0.0533	1.046	23.663	0.1738	0.1908
0.100	3.2048	0.1068	1.047	20.168	0.1481	0.1628
0.250	3.2184	0.2682	1.055	14.020	0.1030	0.1134
0.500	3.2425	0.5404	1.071	8.381	0.0616	0.0683
1.000	3.2945	1.0982	1.105	3.621	0.0266	0.0300
1.500	3.3523	1.6762	1.143	1.819	0.0134	0.0153
2.000	3.4161	2.2774	1.179	1.037	0.0076	0.0089
2.500	3.4872	2.9060	1.216	0.594	0.0044	0.0052
3.000	3.5655	3.5655	1.253	0.361	0.0027	0.0032
3.500	3.6527	4.2615	1.287	0.266	0.0020	0.0024

---

[a] Initial concentration of solutions prepared at room temperature without calcium sulfate. [b] Experimental density of saturated solutions.

Table 3.13. Solubility of $CaSO_4$ (1) as Anhydrite in 6 mol·dm^{-3} HCl (2) - $CaCl_2$ (3) - H_2O (4) (Equilibration Time: 5 Hours)

solution parameters				solubility as $CaSO_4$ in different units		
M_3/ mol.dm^{-3a}	m_2/ mol·kg^{-1}	m_3/ mol·kg^{-1}	ρ_s / g·cm$^{-3\,b}$	C_1/g·dm^{-3}	M_1/mol·dm^{-3}	m_1/ mol·kg^{-1}
			$T = 298$ K			
0.050	6.8599	0.0572	1.103	7.863	0.0578	0.0663
0.100	6.8713	0.1145	1.106	6.966	0.0512	0.0588
0.250	6.9089	0.2879	1.116	2.635	0.0194	0.0223
0.500	6.9727	0.5811	1.133	1.092	0.0080	0.0093
1.000	7.1124	1.1854	1.174	0.372	0.0027	0.0032
1.500	7.2674	1.8169	1.212	0.154	0.0011	0.0014
2.000	7.4396	2.4799	1.249	0.086	0.0006	0.0008
2.500	7.6297	3.1790	1.286	0.050	0.0004	0.0005
3.000	7.8360	3.9180	1.318	0.035	0.0003	0.0003
3.500	8.0537	4.6980	1.353	0.029	0.0002	0.0003
			$T = 323$ K			
0.050	6.8599	0.0572	1.094	10.228	0.0751	0.0871
0.100	6.8713	0.1145	1.097	8.460	0.0621	0.0721
0.250	6.9089	0.2879	1.105	4.214	0.0310	0.0361
0.500	6.9727	0.5811	1.125	1.900	0.0140	0.0164
1.000	7.1124	1.1854	1.164	0.601	0.0044	0.0053
1.500	7.2674	1.8169	1.197	0.281	0.0021	0.0025
2.000	7.4396	2.4799	1.236	0.165	0.0012	0.0015
2.500	7.6297	3.1790	1.271	0.114	0.0008	0.0011
3.000	7.8360	3.9180	1.302	0.085	0.0006	0.0008

3.500	8.0537	4.6980	1.336	0.076	0.0006	0.0008
			$T = 353$ K			
0.050	6.8599	0.0572	1.081	13.710	0.1007	0.1185
0.100	6.8713	0.1145	1.084	11.426	0.0839	0.0988
0.250	6.9089	0.2879	1.090	6.636	0.0487	0.0577
0.500	6.9727	0.5811	1.107	3.125	0.0230	0.0274
1.000	7.1124	1.1854	1.147	1.245	0.0091	0.0111
1.500	7.2674	1.8169	1.181	0.638	0.0047	0.0058
2.000	7.4396	2.4799	1.216	0.415	0.0031	0.0039
2.500	7.6297	3.1790	1.251	0.282	0.0021	0.0027

[a] Initial concentration of solutions prepared at room temperature without calcium sulfate. [b] Experimental density of saturated solutions.

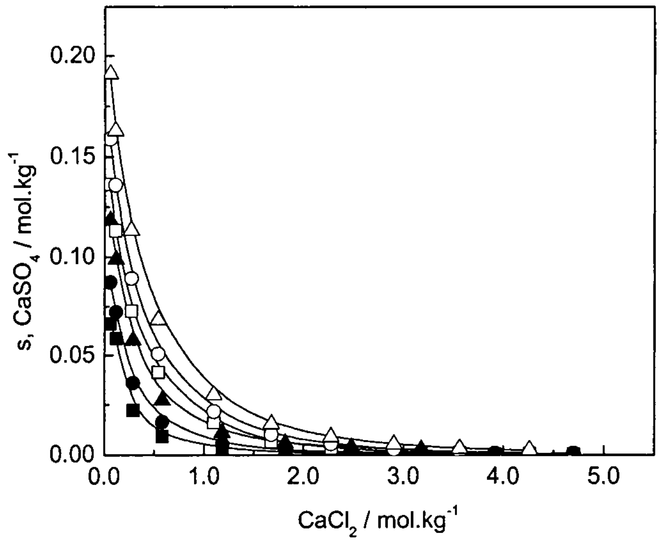

Figure 3.13. Solubility of calcium sulfate anhydrite in HCl + $CaCl_2$ mixed electrolyte solutions (solid points, 6 mol·dm^{-3}; empty points, 3 mol·dm^{-3}): ■, □, 298 K; ●, ○, 323 K; ▲, △, 353 K.

3.4.9 Thermodynamic Interpretation

The observed behavior of $CaSO_4$ solubility in the current study may be explained by considering the various equilibria, such as, solid-liquid and chemical solution (speciation) involved in the system. The solubility equilibrium for $CaSO_4$ solids in electrolyte aqueous solutions is expressed as follows (24).

$$CaSO_4{\cdot}nH_2O \leftrightarrow Ca^{2+} + SO_4^{2-} + nH_2O \qquad (3.1)$$

where n is 2, 0.5 or 0 corresponding to DH, HH and AH, respectively. The thermodynamic solubility product for gypsum is given by

$$K_{sp} = a_{Ca^{2+}} a_{SO_4^{2-}} a_{H_2O}^2 = \left(m_{Ca^{2+}} \gamma_{Ca^{2+}}\right)\left(m_{SO_4^{2-}} \gamma_{SO_4^{2-}}\right) a_{H_2O}^2 \qquad (3.2)$$

where $m_{Ca^{2+}}$ and $m_{SO_4^{2-}}$ are the molal concentrations of cation Ca^{2+} and anion SO_4^{2-} in solution. $\gamma_{Ca^{2+}}$ and $\gamma_{SO_4^{2-}}$ are the ion activity coefficients, and a_{H_2O} is the activity of water in solution. In contrast to the solubility in pure water, the solubility of gypsum in acidic HCl solution is complicated because of the bisulfate (HSO_4^-) ion formation. The dissociation equilibrium is expressed as

$$HSO_4^- \leftrightarrow H^+ + SO_4^{2-} \qquad (3.3)$$

The thermodynamic equilibrium constant of reaction (3.3) is described as

$$K_2 = \frac{(m_{H^+} \gamma_{H^+})(m_{SO_4^{2-}} \gamma_{SO_4^{2-}})}{m_{HSO_4^-} \gamma_{HSO_4^-}} \qquad (3.4)$$

where K_2, the second dissociation constant of H_2SO_4, has been investigated by numerous authors (25-27), and $m_{HSO_4^-}$ and $\gamma_{HSO_4^-}$ are the molal concentration and activity coefficient of HSO_4^- ion.

In the system $CaSO_4 \cdot 2H_2O(s) + HCl + H_2O$, the solubility of gypsum, s, is expressed by the molal concentration of Ca^{2+} ion or the summation of all the sulfur-bearing species:

$$s = m_{Ca^{2+}} = m_{SO_4^{2-}} + m_{HSO_4^-} \qquad (3.5)$$

Substituting eqs (3.2) and (3.4) to eq (3.5) yields the following relationship,

$$s = \frac{1}{a_{H_2O}} \left(\frac{K_{sp}}{\gamma_{Ca^{2+}}} \right)^{1/2} \left(\frac{1}{\gamma_{SO_4^{2-}}} + \frac{1}{K_2} \frac{\gamma_{H^+}}{\gamma_{HSO_4^-}} m_{H^+} \right)^{1/2} \qquad (3.6)$$

eq.(3.6) indicates qualitatively that the solubility of gypsum increases with increasing acid concentration at the range of less than 3 M HCl as shown in Figure 3.2. At this range the formation of bisulfate apparently contributes to the solubility increase. In the concentrated acid (> 3 mol·dm^{-3}) solutions, however, the opposite effect on the solubility of gypsum has been observed since apparently the activity of water and ion activity coefficients become to have more influence on the solubility.

Similarly, the effect of calcium chloride in the system $CaSO_4 \cdot 2H_2O(s) + HCl + CaCl_2 + H_2O$, may be qualitatively explained by referring to eq.(3.7):

$$s = \frac{K_{sp}}{\gamma_{Ca^{2+}} a_{H_2O}^2} \left(\frac{1}{\gamma_{SO_4^{2-}}} + \frac{1}{K_2} \frac{m_{H^+} \gamma_{H^+}}{\gamma_{HSO_4^-}} \right) \frac{1}{m_{Ca^{2+}}} \qquad (3.7)$$

It can be seen in eq.(3.7) that at fixed HCl concentration the solubility of gypsum decreases consistently with the concentration of calcium chloride, such as, as shown in Figure 3.5. A comprehensive thermodynamic model developed and described elsewhere (28) provides quantitative explanation for the obtained solubility behaviour.

3.5 Conclusions

The solubility of calcium sulfate dihydrate, hemihydrate and anhydrite in HCl and $CaCl_2$ or their mixed electrolyte solutions has been measured for a wide range of conditions up to 12 mol·dm^{-3} HCl, 3 mol·dm^{-3} $CaCl_2$ and (283 to 353) K. The solubility of all calcium sulfate modifications in chloride solutions increases monotonically with increasing systems temperature except for AH in $CaCl_2$ solutions. The solubility of dihydrate or anhydrite in HCl solution increases with the acid concentration up to around (2.5 to 3.0) mol·dm^{-3} HCl. It decreases gradually above this value. The solubility of calcium sulfate hemihydrate in HCl solution with more than 8 mol·dm^{-3} concentration decreases with increasing acid concentration, and both α or β hemihydrate forms have close solubility values. The addition of $CaCl_2$ in acid solution makes the solubility of all $CaSO_4$ modifications to decrease sharply due to the common ion effect. The behavior of solubility of calcium sulfate was partially explained by thermodynamic interpretation considering the various equilibria in solutions. The formation of HSO_4^- ion in acidic solution was thought to be responsible for the solubility increase. XRD results and SEM micrographs indicate that the gypsum and hemihydrate crystals are unstable at elevated temperatures and high HCl concentration converting to anhydrite within a short period of time (< 5 hours). The presence of $CaCl_2$ was found to suppress this transformation of hemihydrate to anhydrite.

Acknowledgement

The support of Hatch, Noranda, Process Research Ortech and NSERC (Natural Sciences and Engineering Research Council of Canada) is gratefully acknowledged.

3.6 Literature Cited

(1) Sohnel, O.; Garside, J. *Precipitation: Basic Principles and Industrial Application*; Butterworth Heinemann: Oxford, 1995.

(2) Mullin, J. W. *Crystallization*; Butterworth-Heinemann: Oxford, 2001.

(3) Myerson, A. S. *Handbook of Industrial Crystallization*; Butterworth-Heinemann: Oxford, 2002.

(4) Dutrizac, J.E. Calcium Sulfate Solubilities in Simulated Zinc Processing Solutions. *Hydrometallurgy* **2002**, 65, 109-135.

(5) Girgin, S.; Demopoulos, G. P. Production of the High Value Material, Alpha-$CaSO_4$ Hemihydrate out of Spent $CaCl_2$ Solutions by Reaction with H_2SO_4. in *EPD Congress 2004*; Schlesinger, M. E. Ed.; TMS: Warendale, PA, USA, 2004, 627-639.

(6) Al-Othman, A.; Cheng, T. C.; Demopoulos, G. P. Regeneration of HCl and Production of Saleable Gypsum by Reaction of Spent $CaCl_2$ Leach Solutions with H_2SO_4. in *Proceedings of Fifth International Symposium on Waste Processing and Recycling in Mineral and Metallurgical Industries*; Rao, S. R. *et al.* Eds.; CIM: Montreal, Canada, 2004, 453-467.

(7) Linke, W. F.; Seidell, A. *Solubilities of Inorganic and Metal-Organic Compounds*; American Chemical Society: Washington, DC, 1965.

(8) Silcock, H. L. *Solubilities of Inorganic and Organic Compounds, Vol.3: Multicomponent Systems of Inorganic Substances*; Pergamon Press: Toronto, 1979.

(9) Li, Z.; Demopoulos, G. P. $CaSO_4$ Solubilities in Concentrated Aqueous Chloride Solutions. In *Chloride Metallurgy 2002: International Conference on Practice and Theory of Chloride/Metal Interaction, 32nd Annual Hydrometallurgy Meeting*; Peek, E., Van Weert, G. Eds; CIM: Montreal, 2002, 561-574.

(10) *Aqueous System Modeling Course and Workshop*, OLI's manual, OLI System Inc. New Jersey, 2002.

(11) Zemaitis, J. F.; Clark, D. M.; Rafal, M.; Scrivner, N. C. *Handbook of Aqueous Electrolyte Thermodynamics: Theory & Application*; AIChE: New York, 1986.

(12) Nyvlt, J. *Solid-Liquid-Phase Equilibrium*; Publishing House of the Czechoslovak: Praha, 1977.

(13) Zhang, L.; Gui, Q.; Lu, X.; Wang, Y.; Shi, J. Lu, B. C. Y. Measurement of Solid-Liquid Equilibria by a Flow-Cloud-Point Method. *J. Chem. Eng. Data* **1998**, 43, 32-37.

(14) Ling, Yuanbing; Demopoulos, G. P. Giove, A.; Filippou, D. Technical Evaluation and Characterization of alpha Calcium sulfate Materials. In *Gypsum and Fly Ash 2002, 7th International Science and Technology Conference and Short Course*; Toronto, 2002, 6, 1-14.

(15) Lucas, A.; Rodriguez, L.; Sanchez, P.; Carmona, M.; Romero, P. Lobato, J. Comparative Study of the Solubility of the Crystalline Layered Silicates α-$Na_2Si_2O_5$ and δ-$Na_2Si_2O_5$ and the Amorphous Silicate $Na_2Si_2O_5$. *Ind. Eng. Chem. Res.* **2004**, 43, 1472-1477.

(16) Power, W. H.; Fabuss B. M.; Satterfield, C. N. Transient Solubilities in the Calcium Sulfate –Water System. *J. Chem. Eng. Data* **1964**, 9, 437-442.

(17) Power, W. H.; Fabuss B. M.; Satterfield, C. N. Transient Solute Concentrations and Phase Changes of Calcium Sulfate in Aqueous Sodium Chloride. *J. Chem. Eng. Data* 1966, 11, 149-154.

(18) Gupta, R. K. Solubility of Calcium Sulphate Dihydrate in Hydrochloric Acid Solutions. *J. Appl. Chem.* **1968**, 18, 49-51.

(19) Kruchenko, V. P.; Beremzhanov, V. A. The Solubilities of the Salts in the Calcium Sulphate-Hydrochloric Acid-Water System at 25 °C. *Russ. J. Inorg. Chem.* **1976**, 21, 281-282.

(20) Rock, E. On the Solubility of Anhydrous Calcium Sulphate and Gypsum in Concentrated Solutions of Sodium Chloride. *Can. J. Chem.* **1961**, 39, 1746-1751.

(21) Ostroff, A. G.; Metler, A. V. Solubility of Calcium Sulfate Dihydrate in the System NaCl-$MgCl_2$-H_2O from 28 ° to 70 °C. *J. Chem. Eng. Data* **1966**, 11, 346-350.

(22) Sullivan, J. M.; Kohler, J. J.; Grinstead, Jr. J. H. Solubility of α-Calcium Sulfate Hemihydrate in 40, 45, 50, and 55% P_2O_5 Phosphoric Acid Solutions at 80, 90, 100, and 110 °C. *J. Chem. Eng. Data* **1988**, 33, 367-370

(23) Martynowicz, E. T. M. J.; Witkamp, G. J.; Rosmalen, G. M. The Effect of Aluminium Fluoride on the Formation of Calcium Sulfate Hydrates. *Hydrometallurgy* **1996**, 41, 171-186.

(24) Marshall, W. L.; Slusher, R. Thermodynamics of Calcium Sulfate Dihydrate in Aqueous Sodium Chloride Solutions, 0-110 °C. *J. Phys. Chem.* **1966**, 70, 4015-4027.

(25) Marshall, W. L.; Jones, E. V. Second Dissociation Constant of Sulfuric Acid from 25 to 350 °C Evaluated from Solubilities of Calcium Sulfate in Sulfuric Acid Solutions. *J. Phys. Chem.* **1966**, 70, 4028-4044.

(26) Filippou, D.; Demopoulos, G. P.; Papangelakis, V. G. Hydrogen Ion Activities and Species Distribution in Mixed Metal Sulfate Aqueous Systems. *AIChE J.* **1995**, 41, 171-184.

(27) Dickson, A. G.; Wesolowski, D. J.; Palmer, D. A.; Mesmer, R. E. Dissociation Constant of Bisulfate Ion in Aqueous Sodium Chloride Solutions to 250 °C. *J. Phys. Chem.* **1990**, 94, 7978-7985.

(28) Li, Z.; Demopoulos, G. P. Modelling of Phase Transformations and Equilibria of Calcium Sulfate Hydrates in Concentrated Aqueous Chloride Solutions Using the OLI Software. In *COM 2005: International Conference on Computational Analysis in Hydrometallurgy, 35th Annual Hydrometallurgy Meeting*; CIM: Montreal, 2005, 387-404.

(29) Zdanovskii, A. B.; Vlasov, G. A. Solubility of the Various Modifications of Calcium Sulphate in H_2SO_4 Solutions at 25 °C. *Russ. J. Inorg. Chem.* **1968**, 13, 1415-1418.

Chapter 4

Development of an Improved Chemical Model for the Estimation of $CaSO_4$ Solubilities in the HCl – $CaCl_2$ – H_2O System up to 100 °C

4.1 Abstract

A self – consistent chemical model based on a single set of model parameters for all three $CaSO_4$ modifications, namely dihydrate, hemihydrate and anhydrite was developed and described in this work. The model was successfully tested for the estimation of $CaSO_4$ solubilities in concentrated (up to 20 molal) mixed $HCl–CaCl_2–H_2O$ systems up to 100 °C. The new model makes use of OLI Systems software platform. Via regression of experimental solubility data new Bromley–Zemaitis model parameters were determined for the Ca^{2+} – SO_4^{2-} and Ca^{2+} – HSO_4^- ion pairs. Moreover, for the first time the new model incorporates data for hemihydrate modification ($CaSO_4·0.5H_2O$). After validation the model was calibrated by determining new temperature–dependent parameters of the solubility product constants of hemihydrate and anhydrite. With the aid of the newly developed model the bell – shaped solubility curves for dihydrate and anhydrite as a function of HCl concentration were successfully explained on the basis of the bisulfate ion formation and ion – activity coefficient.

4.2 Introduction

Prediction or estimation of the solubilities of calcium sulfate ($CaSO_4$) and its various modifications, dihydrate (DH: $CaSO_4 \cdot 2H_2O$), hemihydrate (HH: $CaSO_4 \cdot 0.5H_2O$) and anhydrite (AH: $CaSO_4$) in hot and highly concentrated chloride solutions is an important requirement in developing, designing and optimizing various industrial processes in which calcium sulfate precipitation (1) may be involved. Reliable estimation of $CaSO_4$ solubilities can prove invaluable in predicting $CaSO_4$ scale formation (2) or in determining and controlling supersaturation in a crystallization process (3). A new process currently under development in which estimation of $CaSO_4$ solubilities is a requirement involves the regeneration of hydrochloric acid (up to 6 M strength) from spent $CaCl_2$ brine solutions (up to 4 M strength) by reaction with concentrated H_2SO_4 under atmospheric pressure (4):

$$CaCl_2\,(aq) + H_2SO_4\,(aq) + xH_2O \leftrightarrow CaSO_4 \cdot xH_2O\,(s) + 2HCl(aq) \qquad (4.1)$$

The process may be controlled to produce dihydrate ($x = 2$) or hemihydrate ($x = 0.5$), the alpha variety of which is a high value material (5).

Experimental determination of $CaSO_4$ solubilities in a particular system of interest is of course an option but this is a time-consuming enterprise not to mention that it is not feasible to test all possible combinations of conditions. Development and validation of a chemical model capable of providing reliable estimation of $CaSO_4$ solubilities in concentrated and multi-component electrolyte solutions is preferred instead.

Chemical modeling works have been undertaken to either develop empirical or theoretical solubility models for calcium sulfate in pure or multi-component electrolyte aqueous solutions with variable degrees of success in the past. Marshall and his associates (6-8) proposed an empirical model based on the extended Debye-Huckel limiting-law expression to correlate the solubility of calcium sulfate in seawater and concentrated brines. This empirical model can give satisfactory solubility estimation of dihydrate, hemihydrate and anhydrite in electrolytes, such as NaCl, Na_2SO_4, and $MgSO_4$, and their mixed solutions, as well as saline water. However, their model takes into account only the total dissolved solids (TDS) and not the individual ions hence is not applicable to acidic media (in which the HSO_4^- dominates) as is the HCl – $CaCl_2$ system investigated in this work. As a consequence, the same calcium sulfate solubility is predicted in the presence of both chloride and nitrate salts, while the experimental data show a remarkable difference in the two cases (9). Finally, according to Barba *et al.*'s, Marshall's model becomes unsatisfactory when used for solutions with a high sulfate/magnesium ratio.

Barba *et al.* (9,10) developed a thermodynamic model to describe the solubility of calcium sulfate in salt water, that is, relatively dilute but consisting of several components. The model is based on the local compositions of the non-random two-liquid (NRTL) theory. Using only binary parameters their model yields good agreement between the experimental and predicted values of calcium sulfate dihydrate solubility in seawater and in natural and synthetic water at 298 K. However, for concentrated multi-component solutions with high sodium chloride content new binary parameters should be regressed to improve the calculation. Moreover, it cannot be used at elevated temperatures because of the omission to consider hemihydrate.

The ion specific interaction approach originally proposed by Pitzer (11) was employed to model the solubility of $CaSO_4$ in electrolyte solutions. Thus, Harvie *et al.*

(12), using Pitzer's framework, developed a chemical model for predicting mineral solubilities in brines from zero to high ionic strength ($I > 20$ m) at 298 K. In their modeling the single electrolyte parameters were taken from the Pitzer parameterization while the third virial coefficient mixing parameters were chosen by fitting ternary common ion solubility data. The calculated solubility of gypsum in NaCl solution was in good agreement with experiment. Pitzer's equations were also used by Meijer and Rosmalen (13) who proposed a computer program to calculate the solubility and supersaturation of $CaSO_4$ in seawater this time extending the calculations to elevated temperatures (up to 100 °C).

Zemaitis *et al.* (14) evaluated the various activity coefficient models, such as, Bromley, Meissner and Pitzer, by calculating the solubility of calcium sulfate dihydrate in NaCl, $CaCl_2$ and HCl aqueous solutions. Their results showed that interaction parameters based on the solubility data of gypsum in pure water cannot be used in predicting the solubility of gypsum in multi-component electrolyte solutions. Demopoulos *et al.* (15) used Meissner's method to predict the solubility of gypsum in the concentrated (up to saturation) NaCl – H_2O system with satisfactory results. The major difference with reference to Zemaitis *et al.*'s work was that they made use of a new Meissner's parameter for $CaSO_4$ with the value of 0.108.

All $CaSO_4$ solubility modeling works described above are based on the assumption of complete electrolyte dissociation, i.e. they adopt a non-speciation approach (16) which is normally accurate for simple electrolyte systems or limited to vapor – liquid – equilibria (VLE) type phase equilibrium calculations only (17). However, formation of solution complexes occurs in most concentrated aqueous electrolyte systems (with the exception perhaps of single univalent metal chlorides), hence a speciation – based approach becomes the preferred one in thermodynamic modeling (18,19).

The speciation modeling approach was used by Scrivner and Staples (16) to model the solubility of gypsum in NaCl, mixed NaCl and Na_2SO_4, and HCl aqueous solutions with the aid of the ECES computer program developed by OLI Systems. The activity coefficient for $CaSO_4$ was estimated using Bromley's correlation (20) at low ionic strength and Meissner's universal plot (14) at high ionic strength. Reasonable results were obtained for the NaCl and NaCl - Na_2SO_4 systems but not for the HCl system. More recently, Raju and Atkinson (2) used a modified Pitzer equation to calculate the solubility of both gypsum and anhydrite in NaCl solutions with good agreement. However, the model, they developed, was not self – consistent as two separate sets of model parameters (12 in total for each phase) were used for gypsum and anhydrite. Moreover, the model was not demonstrated to apply to mixed electrolyte systems or HCl media.

Another thermodynamic model based on the speciation approach that potentially can be used for the estimation of $CaSO_4$ solubilities in concentrated and hot $CaCl_2$ – HCl media is the one that forms the basis of OLI Systems (21). Activity coefficient estimation in this model is done via the Bromley – Zemaitis equation (20, 22). Preliminary estimations of $CaSO_4$ dihydrate solubilities using OLI's StreamAnalyzer software package (version 1.1) and comparison with experimental data generated by the authors yielded poor results (23), not to mention OLI's inability to deal with calcium sulfate hemihydrate phase(s). Given, however, the attractiveness of the speciation-based modeling approach that characterizes the OLI platform and the user-friendly interface of it, further work was undertaken with the purpose of improving OLI's solubility estimation capability via determination and validation of new model parameters. For the determination of the new model parameters the experimental solubility data recently generated for all three $CaSO_4$ modifications (DH, HH and AH) (24) in $CaCl_2$ – HCl media from 10 to 80 °C were used along with OLI's regression module ESP V-6.6.0.6. (25) With this regression an internally self – consistent model making use of a single set of model parameters was developed good for solubility estimation of all three $CaSO_4$ modifications, namely DH, HH and AH.

4.3 Modeling Methodology

4.3.1 Equilibrium Relationships and Data

The solubility equilibrium of $CaSO_4$ in electrolyte solutions can be described by the following dissolution reaction

$$CaSO_4{\cdot}nH_2O(s) \leftrightarrow Ca^{2+}(aq) + SO_4^{2-}(aq) + nH_2O(l) \tag{4.2}$$

where n is 0, 0.5 and 2 respectively for anhydrite (AH), hemihydrate (HH) and dihydrate (DH). The thermodynamic equilibrium constant, K_{SP}, for $CaSO_4$ solids takes the form,

$$K_{SP} = a_{Ca^{2+}} a_{SO_4^{2-}} a_{H_2O}^{n} = \left(m_{Ca^{2+}} \gamma_{Ca^{2+}}\right)\left(m_{SO_4^{2-}} \gamma_{SO_4^{2-}}\right) a_{H_2O}^{n} \tag{4.3}$$

where $m_{Ca^{2+}}$ and $m_{SO_4^{2-}}$ are the molal concentrations of cation Ca^{2+} and anion SO_4^{2-} in solution, $\gamma_{Ca^{2+}}$ and $\gamma_{SO_4^{2-}}$ are the ion activity coefficients, and a_{H_2O} is the activity of water. The experimental $CaSO_4$ solubility, s (expressed in mol·kg^{-1}) in pure water is simply $s = m_{Ca^{2+}} = m_{SO_4^{2-}}$, but in mixed $CaCl_2$ – HCl media the solubility becomes $s = \sum m_{\text{"}SO_4\text{"}}$, i.e. s is taken as the sum of all "SO_4"-containing species. This explains why the speciation modeling approach makes sense in this context. Table 4.1 provides a list with all species and their dissociation reactions considered in this system. As an example, the second dissociation of H_2SO_4 is as follows

$$HSO_4^- = H^+ + SO_4^{2-} \tag{4.4}$$

Table 4.1. Chemical Species and Their Speciation Reactions in the $CaSO_4$ – HCl – $CaCl_2$ – H_2O System

species	dissociation reaction
H_2O	$H_2O = H^+ + OH^-$
$CaCl_2$ (aq)	$CaCl_2$ (aq) = $CaCl^+ + Cl^-$
$CaCl^+$	$CaCl^+ = Ca^{2+} + Cl^-$
$CaOH^+$	$CaOH^+ = Ca^{2+} + OH^-$
HCl (aq)	HCl (aq) = $H^+ + Cl^-$
H_2SO_4 (aq)	H_2SO_4 (aq) = $H^+ + HSO_4^-$
HSO_4^-	$HSO_4^- = H^+ + SO_4^{2-}$
$CaSO_4$ (aq)	$CaSO_4$ (aq) = $Ca^{2+} + SO_4^{2-}$
$CaSO_4$(s)(AH)	$CaSO_4(s) = Ca^{2+} + SO_4^{2-}$
$CaSO_4 \cdot 0.5H_2O$(s)(HH)	$CaSO_4 \cdot 0.5H_2O(s) = Ca^{2+} + SO_4^{2-} + 0.5H_2O$
$CaSO_4 \cdot 2H_2O$(s)(DH)	$CaSO_4 \cdot 2H_2O(s) = Ca^{2+} + SO_4^{2-} + 2H_2O$

The thermodynamic equilibrium constant for this reaction is

$$K_{HSO_4^-} = \frac{(m_{H^+}\gamma_{H^+})(m_{SO_4^{2-}}\gamma_{SO_4^{2-}})}{m_{HSO_4^-}\gamma_{HSO_4^-}} \tag{4.5}$$

Determination of the concentration of the various chemical species calls for setting up and solving N number of equations equal to the number of unknown species (29). Of these N equations M corresponds to the chemical equilibrium equations (such as 4.3 and 4.5), N-M-1 are mass balance equations and one is the charge balance equation.

For the calculation of the constants of aqueous speciation equilibria (e.g. $K_{HSO_4^-}$) the standard – state thermodynamic parameters of each aqueous species are required. In the OLI software (25) two alternative methods are used to accomplish this task. The first method makes use of the revised HKF equation of state originally proposed by Helgeson and co-workers (26,30-33) while the second method makes use of an empirical equation of the form

$$Log_{10}K = A + \frac{B}{T} + CT + DT^2 \tag{4.6}$$

The above equation may be applied to either solubility product constants or to dissociation constants of solution complexes. *A*, *B*, *C* and *D* are empirical parameters obtained via fitting to experimental solubility data. Table 4.2 lists the species whose *K* (solubility product or dissociation constants) is calculated by OLI with the aid of Eq.(4.6). Table 4.3 lists the thermodynamic data of the relating species used by OLI to calculate equilibrium constants with the aid of the HKF equation.

Table 4.2. The Parameters for Species Whose Equilibrium Constant is Calculated with the Aid of Eq. (4.6) [a]

Species	*A*	*B*	*C*	*D*
$CaCl_2$(aq)	-46.242	14154.1	0.0408507	0.0
$CaCl^+$	2.40192	1871.39	-0.0136144	0.0
CaSO4(aq)	34.31792	-4403.012	-0.0884494	5.89741×10^{-5}
H_2SO_4(aq)	13.9312	-704.65	-0.002916	-3.24087×10^{-6}
HCl(aq)	32.1499	-1328.3	-0.10083	9.66894×10^{-5}
$CaSO_4$(s) (AH)	19.12274	-3066.119	-0.04785357	1.20537×10^{-5}
$CaSO_4\cdot2H_2O$(s) (DH)	40.11184	-5481.185	-0.115199	9.1384×10^{-5}

[a] The data is from OLI's databank.

Table 4.3. Thermochemical Data[26] Used by OLI in Calculating Equilibrium Constants with the HKF Method

species	$\Delta\bar{G}^0_{f,25}$ (kJ/mol)	$\Delta\bar{H}^0_{f,25}$ (kJ/mol)	$\bar{S}^0_{f,25}$ (J/K/mol)	$C^0_{P,25}$ (J/K/mol)
H^+	0	0	0	0
OH^-	-157.29	-230.0	-10.7	-137.19
H_2O[27]	-237.18	-285.85	69.95	75.35

SO_4^{2-}	-744.46	-909.6	18.83	-269.37
HSO_4^-	-755.76	-889.1	125.52	22.18
Ca^{2+}	-552.79	-543.083	-56.48	-31.50
$CaOH^-$[28]	-717.138	-764.417	-14.4683	89.45
Cl^-	-131.29	-167.08	56.735	-123.177

4.3.2 Ion Activity Coefficient and Water Activity Relationships

It is clear from Eqs. (4.3) and (4.5) that determination of $CaSO_4$ solubility or abundance of solution species necessitates knowledge of the relevant ion activity coefficients and activity of water. There are different kinds of coefficient models that may be used in this context (21,22). The Bromley-Zemaitis activity coefficient model (21,25) developed by Bromley (20) and empirically modified by Zemaitis (22) is employed in the OLI software. This model has been successfully used for highly concentrated electrolytes (up to 30 molal) and elevated temperature (up to 473 K) (25), hence it is appropriate for the present system that is up to 20 molal and 373 K.

The Bromley-Zemaitis activity coefficient model for the case of cation i in a multi-component electrolyte solution is expressed by Eq. (4.7)

$$\log\gamma_i = \frac{-AZ_i^2\sqrt{I}}{1+\sqrt{I}} + \sum_j \left[\frac{(0.06+0.6B_{ij})|Z_iZ_j|}{\left(1+\frac{1.5I}{|Z_iZ_j|}\right)^2} + B_{ij} + C_{ij}I + D_{ij}I^2 \right] \left(\frac{|Z_i|+|Z_j|}{2}\right)^2 m_j \qquad (4.7)$$

where j indicates all anions in solution; A is the Debye-Huckel parameter; I is the ionic strength of the solution; B, C, and D are temperature - dependent empirical coefficients; Z_i and Z_j are the cation and anion charges, respectively; $B_{ij} = B_{1ij} + B_{2ij}T + B_{3ij}T^2$ and T is the temperature in °C; the other coefficients C and D have similar temperature dependence forms. For the activity coefficient of an anion, subscript i stands for that anion and subscript j then represents all cations in the solution. Each ion-pair is described with this 9-parameter equation. The 9 parameters are determined via regression of electrolyte solution properties such as osmotic coefficient data or solubility data.

In the case of neutral aqueous species, e.g. $CaSO_4^0$, the B-Z model (Eq.(4.7)) cannot be used. In this case the expression proposed by Pitzer (25) is used to obtain the activity coefficient,

$$ln\gamma_{aq} = 2\beta_{0(m-m)} + 2\beta_{1(m-s)}m_s \tag{4.8}$$

where $\beta_{0(m-m)}$ is the adjustable parameter for molecule-molecule interactions; $\beta_{1(m-s)}$ represents the adjustable parameter for molecule-ion interactions; and m_s is the concentration of the neutral species.

Finally for the activity of water in a multi-component system the formulation proposed by Meissner and Kusik (34) is adopted in OLI's thermodynamic framework.

$$\log(a_w)_{mix} = \sum_i \sum_j X_i Y_j \log(a_w^0)_{ij} \tag{4.9}$$

where (a_w^0) is the hypothetical water activity of pure electrolyte ij, i is an odd number for all cations and j an even number for all anions, $X_i = I_i/I_c$ represents cationic fraction and $Y_j = I_j/I_a$ anionic fraction, respectively.

4.4 Results and Discussion

4.4.1 Solubility Estimation with Existing Model

The accuracy of OLI's existing model (available as software package StreamAnalyzer 1.2) in estimating $CaSO_4$ solubilities in HCl-$CaCl_2$ aqueous solutions was first evaluated by comparing OLI's prediction to experimental data generated by the authors (24)[1]. Both sets of data (model predictions and experimental) are plotted in Figure 4.1 for the case of the solubility of calcium sulfate dihydrate in 0.0 - 5.5 m HCl solutions in the 283 K-353 K temperature range. As it can be seen a significant deviation of OLI prediction from experiments is observed at the concentrated HCl range this being enlarged at elevated temperature. Figures 4.2 and 4.3 provide further comparison between OLI solubility prediction and experiment in the case of DH solubility in mixed HCl-$CaCl_2$ solutions. While the comparison is satisfactory at low acid concentration the deviation becomes significant at higher HCl concentrations. For example, the average relative deviation is 11 %, 25 % and 34 % as the HCl concentration increases from 1 to 3 to 5 M HCl, respectively.

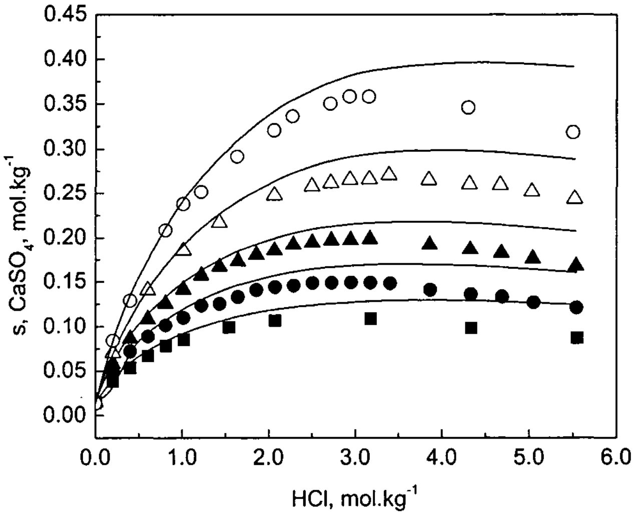

Figure 4.1. Comparison of the solubility of calcium sulfate dihydrate in HCl solutions between experimental data[24] and OLI's prediction (lines): ■, 283 K; ●, 295 K; ▲, 313 K; △, 333 K; ○, 353 K.

---

[1] See Chapter 3.

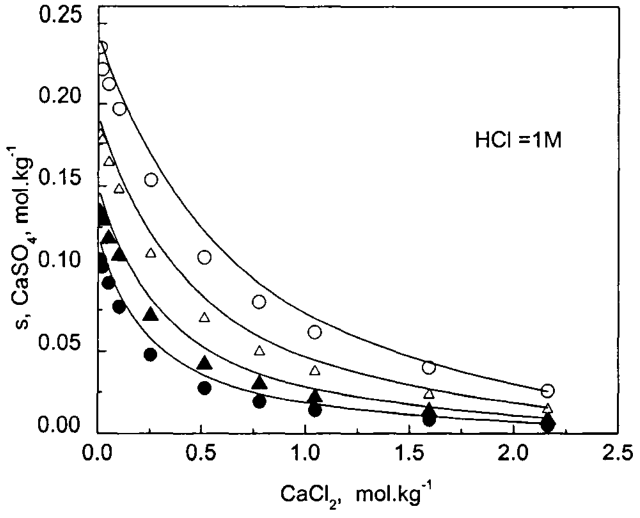

Figure 4.2. Comparison of the solubility of calcium sulfate dihydrate in mixed HCl(1 M)-$CaCl_2$ solutions between experimental data[24] and OLI's prediction (lines): ●, 295 K; ▲, 313 K; △, 333 K; ○, 353 K.

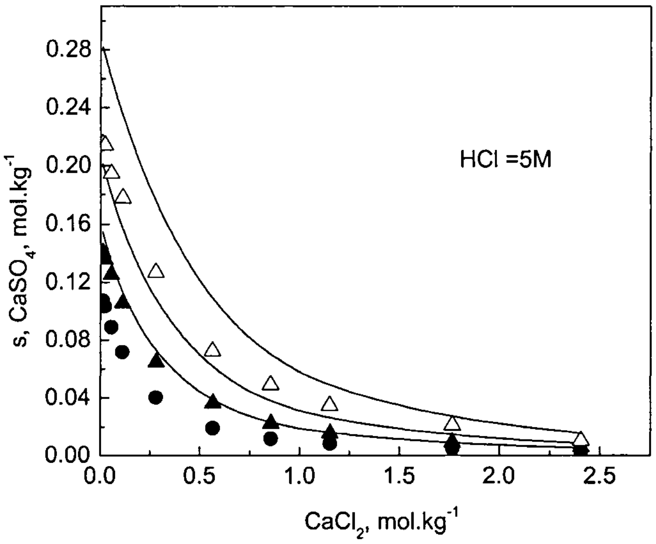

Figure 4.3. Comparison of the solubility of calcium sulfate dihydrate in mixed HCl(5 M)-$CaCl_2$ solutions between experimental data[24] and OLI's prediction (lines): ●, 295 K; ▲, 313 K; △, 333 K.

Similarly with DH, OLI yielded relatively large deviation when the solubility of anhydrite in HCl was estimated (Figure 4.4). The relative deviation is 10 %, 16 %, 22 %, and 25 % at 298 K, 313 K, 333 K and 353 K, respectively. The accuracy of OLI predictions strongly depend on the availability of experimental data on the basis of which the model is built. There is limited solubility data available in literature for calcium sulfate anhydrite in concentrated HCl solutions hence the observed large deviation. Finally as mentioned earlier no estimation of hemihydrate solubility is possible with the current OLI model.

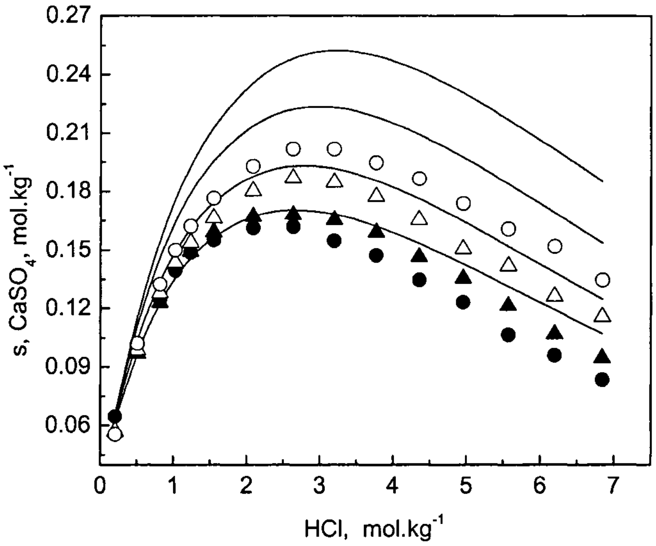

Figure 4.4. Comparison of the solubility of calcium sulfate anhydrite in mixed HCl solutions between experimental data[24] and OLI's prediction (lines): ●, 298 K; ▲, 313 K; △, 333 K; ○, 353 K.

4.4.2 New Model Parameter Estimation

With the purpose of improving the OLI System's prediction capability when it comes to $CaSO_4$ solubilities in HCl – $CaCl_2$ media, new model parameters were determined via regression of experimental data recently produced by the authors (24). In this regression, the model parameters are obtained by minimizing the sum of squared deviations between the experimental and calculated values of solubility of $CaSO_4$. In particular the parameters of two model equations were scrutinized and modified (when necessary): the Bromley-Zemaitis activity coefficient model parameters in Eq.(4.7) and the empirical parameters in equilibrium constant relationship, Eq. (4.6). The main aqueous species or ions that are present in the system of $CaSO_4$-HCl-$CaCl_2$-H_2O are two cations (H^+, Ca^{2+}) and three anions (Cl^-, SO_4^{2-} and HSO_4^-) as listed in Table 4.1. According to the Bromley-Zemaitis model (Eq.(4.7)) in order to calculate the activity coefficient of each ion (and the activity of water), we have to know 6 pairs of ion interaction parameters. Among the 6 possible ion pairs only the Bromley-Zemaitis parameters for two pairs, namely Ca^{2+}- SO_4^{2-} and Ca^{2+}- HSO_4^- were regressed with the model parameters with all other ion – pairs kept the same as in OLI's default databank. These ion pairs were selected because they were intuitively thought to directly impact on the solubility of $CaSO_4$.

The new Bromley-Zemaitis interaction parameters for these two ion – pairs were determined by regressing the DH experimental solubility data published elsewhere (24). Best fit was obtained when the dissociation constant of the HSO_4^- ion was expressed with the aid of Eq. (4.6) and not by the HKF method as done in original version of OLI. The adopted equation for the dissociation constant of HSO_4^- is given below

$$Log_{10}K_{HSO_4^-} = -66.6422 + \frac{7402.28}{T} + 0.200352T - 2.20974\times10^{-4}T^2 \qquad (4.10)$$

It is considered important to evaluate the validity of the adopted Eq. (4.10) by comparing the temperature dependency of the dissociation constant of HSO_4^- calculated with it to the values calculated by OLI's HKF method (25) and other values reported in literature (7,35,36). This is done in Figure 4.5. As it can be observed, Eq. (4.10) gives marginally lower values of $-\log K_{HSO_4^-}$ than the HKF method of OLI (25) but within the range of values reported in literature. The validity of Eq.(4.10) was further tested by calculating and comparing the pH for the 0.5m H_2SO_4 – H_2O system from 10 to 100 °C with that calculated by OLI. Figure 4.6 shows that the pH values by both methods are very close.

It is not surprising that the bisulfate ion plays a central role in this system as it was qualitatively discussed elsewhere (24). The critical role of HSO_4^- in affecting the solubility of $CaSO_4$ phases explains the failure of earlier efforts (16) in modeling solubility equilibria in strong HCl- containing solutions. The new Bromley-Zemaitis model parameters obtained via the regression of the DH solubility data (Figures 4.7 and 4.8) are tabulated in Table 4.4. The total average relative deviation between DH experimental data and new OLI model obtained by regression model is 2.7 %.

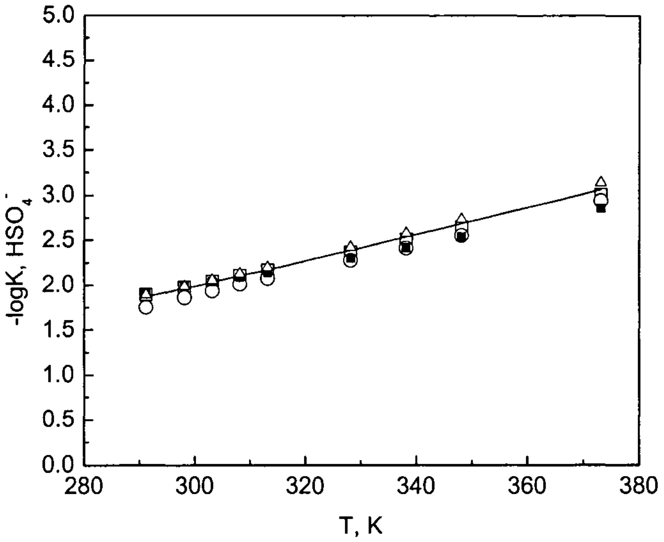

Figure 4.5. Dissociation constant of bisulfate as a function of temperature (line: Dickson *et al.*[35]): □, OLI(HKF);[25] ○, this work; ■, Marshall *et al.*;[7] △, Hovey *et al.*.[36]

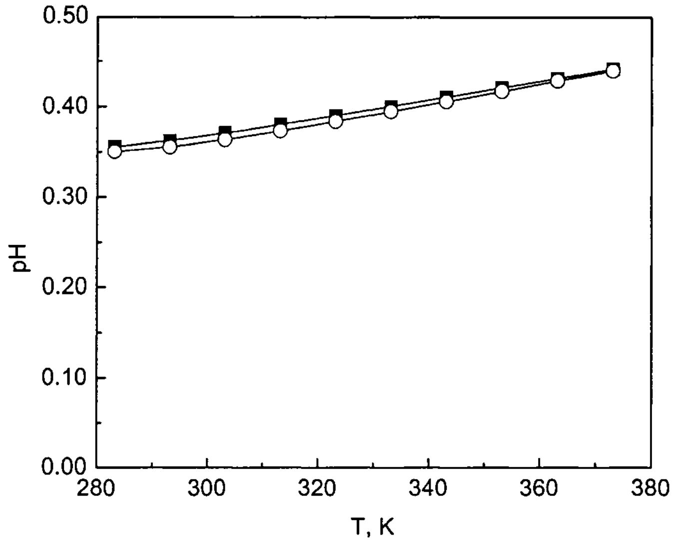

Figure 4.6. Calculated pH at 323 K in 0.5 m H_2SO_4 solution: ○, this work; ■, OLI.

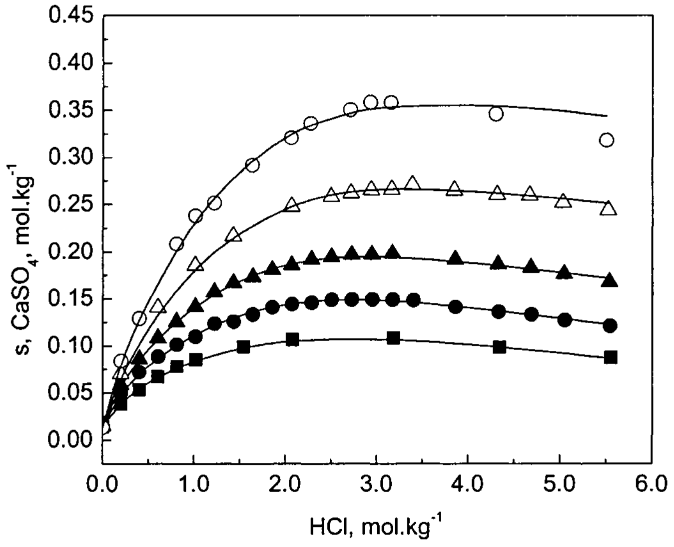

Figure 4.7. Comparison of regressed (solid lines) and experimental[24] (symbols) solubility of calcium sulfate dihydrate in HCl solutions: ■, 283 K; ●, 295 K; ▲, 313 K; △, 333 K; ○, 353 K.

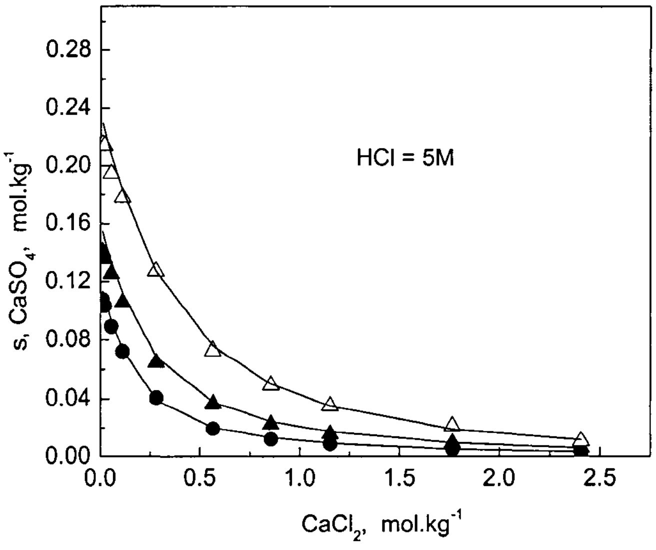

Figure 4.8. Comparison of regressed (solid lines) and experimental[24] (symbols) solubility of calcium sulfate dihydrate in mixed HCl(5 M)-$CaCl_2$ solutions: ●, 295 K; ▲, 313 K; △, 333 K.

Table 4.4. Newly Regressed Bromley-Zemaitis Model Parameters for Ca^{2+} - SO_4^{2-} and Ca^{2+} - HSO_4^- Interactions

parameters	Ca^{2-} - SO_4^{2-}	Ca^{2-} - HSO_4^-
B_1	-0.246708	-0.0816875
B_2	0.0035632	3.96067×10^{-4}
B_3	-5.12319×10^{-5}	1.65505×10^{-5}
C_1	0.0731743	0.00617896
C_2	-0.00107027	6.64883×10^{-4}
C_3	1.15506×10^{-5}	-1.07042×10^{-5}
D_1	0.010482	0.00149402
D_2	-2.91146×10^{-5}	-8.87896×10^{-5}
D_3	1.28589×10^{-6}	1.05082×10^{-6}

4.4.3 Model Validation

Having successfully modeled the solubility data of calcium sulfate dihydrate in HCl-$CaCl_2$ solutions, we proceeded to test the new model in the case of hemihydrate and anhydrite solubilities. Towards this end a new databank was created, called "OLI-

McGill", in which the newly obtained Bromley-Zemaitis parameters shown in Table 4.4 and the new parameters of the dissociation equilibrium constant of bisulfate ion (Eq.(4.10)) were added. In order to calculate the solubility of hemihydrate, the solubility product of hemihydrate is required. This is not available in the current OLI databank. Initially the solubility data (37) of calcium sulfate hemihydrate in pure water at various temperatures was used to obtain the hemihydrate solubility product parameters (refer to Eq.(4.6)):

$$Log_{10}K_{HH} = -65.7208 - \frac{7758.18}{T} - 0.199782T + 1.77968 \times 10^{-5}T^2 \qquad (4.11)$$

With the aid of Eq.(4.11) and the new model parameters (Table 4.4 and Eq.(4.10)) the solubility of hemihydrate was calculated using StreamAnalyzer 1.2. A comparison of experimental and predicted HH solubility values is presented in Figures 4.9 and 4.10. Figure 4.9 shows the excellent agreement between literature (38) and predicted solubility of α-calcium sulfate hemihydrate in pure HCl solutions at 373 K. Equally good agreement is seen between experimental data and model predictions in Figures 4.9 and 4.10. All of these results serve as validation of the newly developed model since it proved capable in making good solubility predictions for a $CaSO_4$ phase (hemihydrate) other than the one (dihydrate) used to determine the model parameters in a range of conditions outside the regression zone, i.e. T > 353 K and [HCl] > 6 M. The new model was further validated by comparing its predictions to anhydrite solubility data (24) (Figure 4.11). Predictions are now much better than the ones obtained with the current version (1.2) of OLI's StreamAnalyzer.

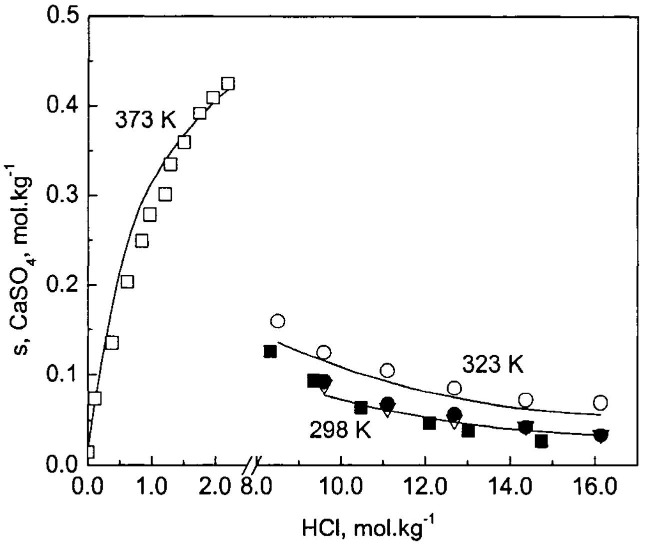

Figure 4.9. Comparison of predicted (solid lines) and literature (symbols) solubility of calcium sulfate hemihydrate in HCl solutions: ■, HH at 298 K;[39] ●, *β*-HH at 298 K;[24] ▿, *α*-HH at 298 K;[24] ○, *β*-HH at 323 K;[24] □, *α*-HH at 373 K.[38]

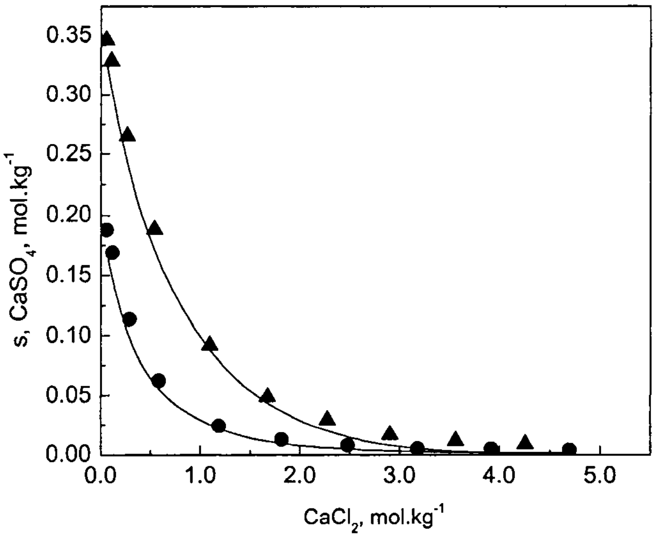

Figure 4.10. Comparison of predicted (solid lines) and experimental[24] (symbols) solubility of calcium sulfate hemihydrate in mixed HCl-CaCl$_2$ solutions: ●, in 6M HCl at 333 K; ▲, in 3M HCl at 353 K.

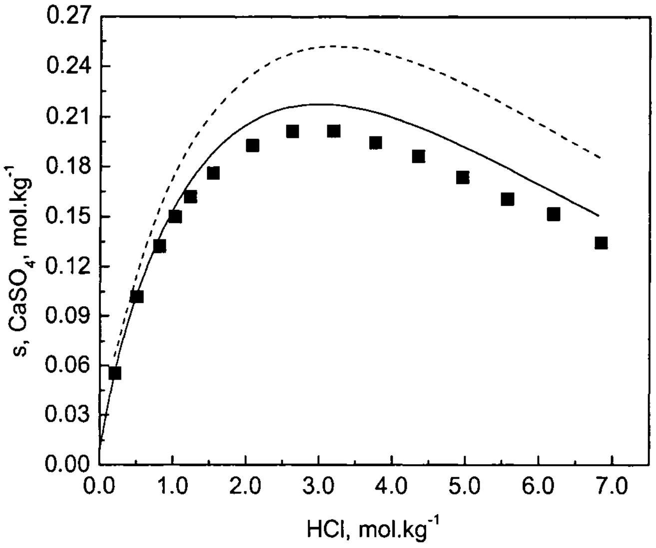

Figure 4.11. Comparison of the solubility of calcium sulfate anhydrite in concentrated HCl solutions at 353 K: ---, predicted by OLI; —, predicted by OLI equipped with new model parameters (Table 4.4 and Eq.(4.10)); ■, experimental data.[24]

4.4.4 Model Calibration

The developed model was subjected to calibration by retaining the new set of Bromley-Zemaitis parameters that were obtained by regression of the dihydrate solubility data (Table 4.4), but this time slightly adjusting the K_{SP} equation parameters (Eq.(4.6)) for hemihydrate and anhydrite. The Eq. (4.6) parameters were recalculated by performing regression using the HH and AH solubility data generated by the authors (24) instead of using the AH default values in OLI's databank or the parameters obtained from the regression of HH solubility data in water (Eq.(4.11)).

As a result of this regression-calibration work the following two solubility product equations were derived for hemihydrate and anhydrite respectively:

$$Log_{10}K_{SP(HH)} = 34.4739 - \frac{4939.1}{T} - 0.0870353T + 4.59692\times10^{-5}T^2 \qquad (4.12)$$

$$(0 < T < 100\ ^\circ\mathrm{C})$$

$$Log_{10}K_{SP(AH)} = -85.601 + \frac{8775.05}{T} + 0.261521T - 2.93598\times10^{-4}T^2 \qquad (4.13)$$

$$(20 < T < 100\ ^\circ\mathrm{C})$$

The solubility product constant (K_{SP}) values for anhydrite, obtained with Eq.(4.13) at various temperatures are shown in Figure 4.12. In the same figure, the K_{SP} values reported by Ling and Demopoulos (40), Raju and Atkinson (2), Marshall and Slusher (8), Langmuir and Melchior (41) and values stored in OLI databank are also plotted for comparison. OLI's values are lower than ours at lower temperatures and higher than ours at higher temperatures. The values obtained in this work are in very good agreement with those of Raju and Atkinson (2) and good agreement overall with those of Langmuir and Melchior. The data reported in other sources as shown in Figure 4.12 are consistently higher than ours.

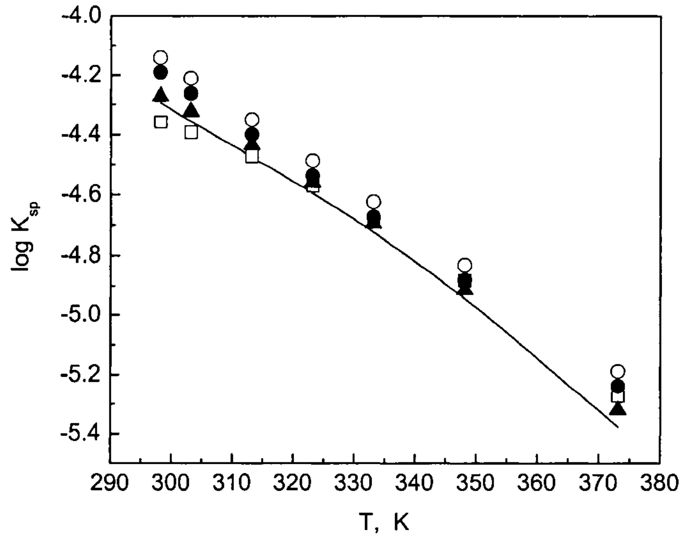

Figure 4.12. log K_{SP} vs T for calcium sulfate anhydrite. —, this work; □, OLI; ○, Ling and Demopoulos;[40] △, Raju and Atkinson;[2] ●, Marshall and Slusher;[8] ▲, Langmuir and Melchior.[41]

The new solubility product parameters for hemihydrate and anhydrite shown in Eqs. (4.12) and (4.13) were finally retained along the set of new Bromley-Zemaitis model parameters (Table 4.4) and Eq.(4.10) to formulate the improved OLI-McGill model for the estimation of $CaSO_4$ solubilities in mixed HCl-$CaCl_2$ media in the temperature range up to 100 °C. The excellent agreement of calibrated model's predictions with experimental data is exemplified with the data plotted in Figure 4.13. The relative deviation from experimental data as described in Figure 4.13 is only 1.48 %.

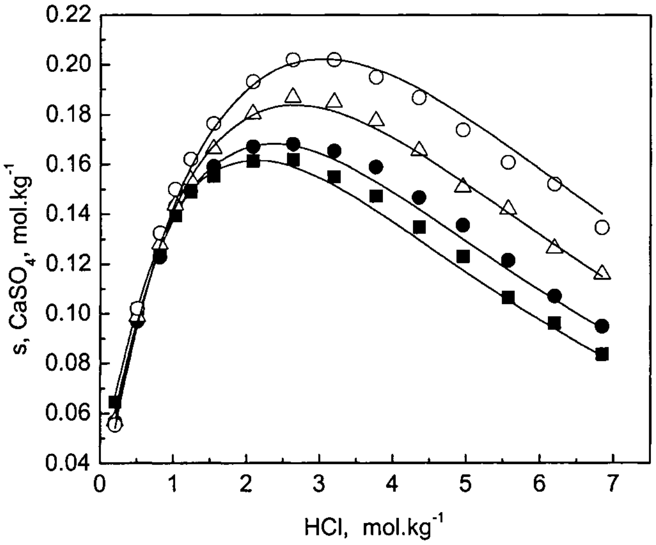

Figure 4.13. Comparison of the solubility of calcium sulfate anhydrite in concentrated HCl solutions at various temperatures: — , predicted by OLI equipped with new model parameters (Table 4.4 and Eqs.(4.10) and (4.13)); ■ , 298 K; ● , 313 K; △ , 333 K; ○ , 353 K.

4.4.5 Speciation Calculations and Thermodynamic Interpretation

OLI's StreamAnalyzer 1.2 equipped with the new model parameters developed in this work was used to study and to analyze concentration and temperature effects on species distribution as well as in interpreting the observed $CaSO_4$ solubility behavior in the $CaSO_4$-HCl-$CaCl_2$-H_2O system.

Temperature Effects: Figure 4.14 shows the relative concentration of sulfate species, $CaSO_{4(aq)}$, HSO_4^-, and SO_4^{2-} in HH - saturated 5 m HCl solutions as a function of temperature. In this case the solubility of hemihydrate is equal to the total concentration of these sulfate species in the solution. It is obvious that the relative concentration of HSO_4^- increases with increasing temperature, indicating an increase in ion association degree. Simultaneously, the concentration of ion, SO_4^{2-}, decreases with temperature. The relative concentration of HSO_4^-, and SO_4^{2-} are 81 % and 17 % at 303 K, but 98 % and 0.7 % at 353 K, respectively. The $CaSO_{4(aq)}$ is present in less than 4 % of total sulfate concentration.

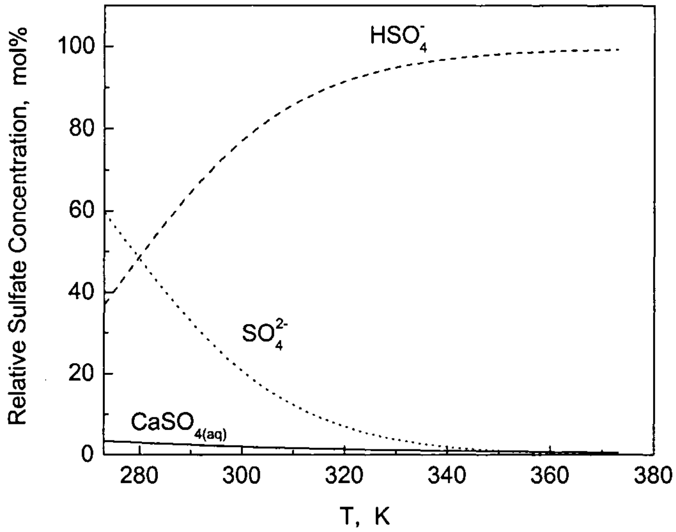

Figure 4.14. Sulfate speciation as a function of temperature for hemihydrate - saturated solution containing 5 m HCl.

In the case of $CaCl_2$ addition to the HCl solution the distribution of species present in HH - saturated solution changes. Figure 4.15 shows the speciation calculation for HH - saturated 5 m HCl and 1 m $CaCl_2$ solution. The neutral species, $CaSO_{4(aq)}$, becomes important in this case at the expense of the SO_4^{2-} species which is negligible. Bisulfate ion formation is once more favored with temperature elevation (88 % at 303 K vs 97 % at 353 K).

Concentration Effects: The relative concentration of sulfate species in the system containing $CaSO_4 \cdot 2H_2O$-HCl-$CaCl_2$-H_2O as a function of HCl concentration is shown in Figure 4.16 for the case of 0.5 m $CaCl_2$. It can be seen that the relative concentration of HSO_4^- firstly increase sharply with HCl concentration, then decreases after passing a maximum, while the relative concentration of SO_4^{2-} consistently decreases. However, the relative concentration of $CaSO_{4(aq)}$ consistently increases with increasing HCl concentration from 3.3 % at 2 m HCl to 37.5 % at 10 m HCl. This behavior indicates that in the presence of $CaCl_2$ we cannot neglect the contribution of $CaSO_{4(aq)}$ to the solubility.

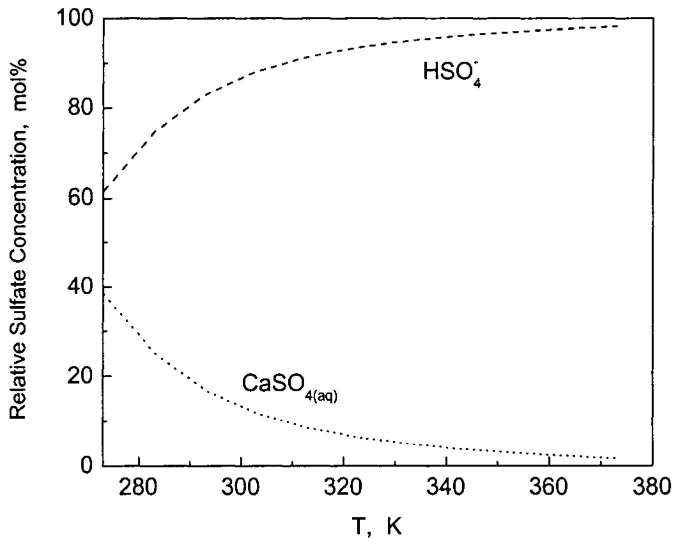

Figure 4.15. Sulfate speciation as a function of temperature for hemihydrate - saturated solution containing 5 m HCl and 1 m $CaCl_2$.

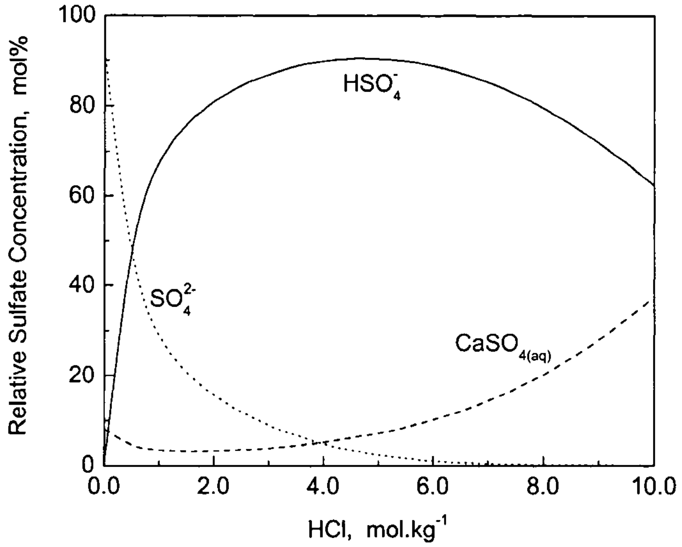

Figure 4.16. Sulfate speciation at 298 K as a function of concentration for dihydrate - saturated HCl solution with 0.5 m $CaCl_2$.

4.4.6 Solubility Curve Interpretation

As observed in Figure 4.7, the solubility of calcium sulfate dihydrate (as well as that of anhydrite – see Figure 4.13) in HCl solutions firstly increases with HCl concentration and then decreases with further addition of HCl. The increase in the solubility can be explained by bisulfate formation. However, the explanation of decrease in the solubility in concentrated HCl solution is attributed to activity coefficient and water activity changes as is shown below. The gypsum (dihydrate) solubility in chloride media is equal to the total concentration of sulfate - bearing species in the gypsum - saturated solution, which is controlled by the following main dissociation equilibria:

$$CaSO_4{\cdot}2H_2O = Ca^{2+} + SO_4^{2-} + 2H_2O \qquad (4.14)$$

$$HSO_4^- = SO_4^{2-} + H^+ \qquad (4.4)$$

According to the thermodynamic definition (Eq.(4.3)), the solubility product constant is given by

$$\begin{aligned} K_{sp} &= a_{Ca^{2+}} a_{SO_4^{2-}} a_{H_2O}^2 = \left(m_{Ca^{2+}} \gamma_{Ca^{2+}}\right)\left(m_{SO_4^{2-}} \gamma_{SO_4^{2-}}\right) a_{H_2O}^2 \\ &= m_{Ca^{2+}} m_{SO_4^{2-}} \left(\gamma_{Ca^{2+}} \gamma_{SO_4^{2-}} a_{H_2O}^2\right) \end{aligned} \tag{4.15}$$

By defining B=$\left(\gamma_{Ca^{2+}} \gamma_{SO_4^{2-}} a_{H_2O}^2\right)$, and plotting its value (as calculated with the aid of the newly developed model) as a function of HCl concentration at 298 K the curve in Figure 4.17 is obtained. As it can be seen the value of B term sharply decreases with addition of HCl acid reaching a minimum (at around 2 – 3 m), then gradually increases with further increasing HCl concentration. The minimum corresponds to the maximum of gypsum solubility (see Figure 4.7). This behavior mirrors the shape of solubility curve, and can be explained as following. The increase of B term's value in the HCl concentration region results in the decrease of $m_{SO_4^{2-}}$ controlled by Eq.(4.15), which in turn results in a decrease in the concentration of HSO_4^- controlled by Eq.(4.4). The total decrease in concentration of both HSO_4^- and SO_4^{2-} ($s = m_{SO_4^{2-}} + m_{HSO_4^-}$) means a decrease of gypsum solubility in high HCl concentration solutions.

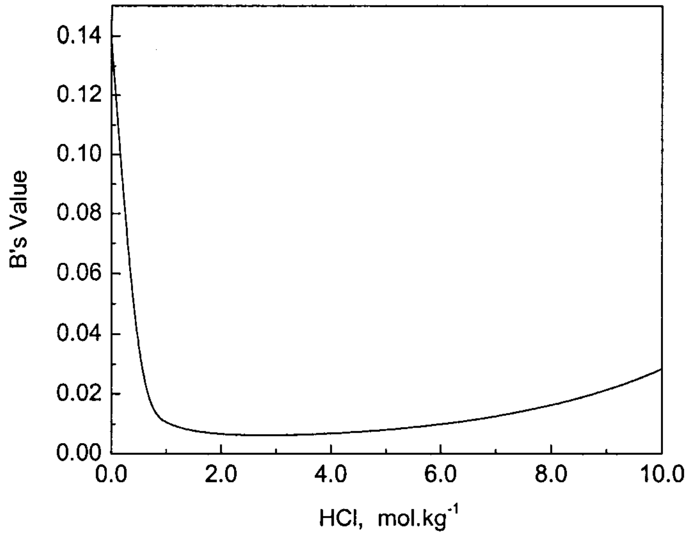

Figure 4.17. Calculated values of $\left(\gamma_{Ca^{2+}}\gamma_{SO_4^{2-}}a_{H_2O}^2\right)$ as a function of HCl concentration at 298 K.

4.5 Conclusions

OLI System's StreamAnalyzer software was employed "as is" to the estimation of $CaSO_4$ solubilities in concentrated HCl-$CaCl_2$ solutions up to 100 °C with limited success. The source of deviation of OLI's prediction from experiment was traced to be the Bromley-Zemaitis model parameters for Ca^{2+}-SO_4^{2-} and Ca^{2+}-HSO_4^- ion pairs as well as the dissociation constant of HSO_4^-. A new set of model parameters was determined by fitting experimental data generated by the authors for the system $CaSO_4{\cdot}2H_2O$-HCl-$CaCl_2$-H_2O. The new model parameters yielded a highly improved model capable of predicting the solubility not only of dihydrate but also hemihydrate and anhydrite. Finally the new model was calibrated by determining new empirical parameters for the solubility product constants of hemihydrate and anhydrite. The modeling results indicate that the speciation-based thermodynamic model forming the basis of OLI's StreamAnalyzer after the improvements made to it in this work is a good tool to describe $CaSO_4$ solubility behavior and calculate solution speciation. With the aid of the model the solubility curve for dihydrate (or anhydrite) as a function of HCl concentration (increasing solubility up to 3 m HCl and subsequent decrease) was successfully explained by this modeling work on the basis of the formation of HSO_4^- and ion activity coefficient changes.

Acknowledgement

The support of Hatch, Noranda, Process Research Ortech and NSERC (Natural Sciences and Engineering Research Council of Canada) is gratefully acknowledged.

4.6 Literature Cited

(1) Sohnel, O.; Garside, J. *Precipitation: Basic Principles and Industrial Application*; Butterworth-Heinemann: Oxford, 1995.

(2) Raju, K. U. G.; Atkinson G. The Thermodynamics of "Scale" Mineral Solubilities. 3. Calcium Sulfate in Aqueous NaCl. *J. Chem. Eng. Data* **1990**, 35, 361.

(3) Mohan, R.; Myerson, A. S. Growth Kinetics: a Thermodynamics Approach. *Chem. Eng. Sci.* **2002**, 57, 4277.

(4) Al-Othman, A.; Cheng, T. C.; Demopoulos, G. P. Regeneration of HCl and Production of Saleable Gypsum by Reaction of Spent $CaCl_2$ Leach Solutions with H_2SO_4. in *Proceedings of Fifth International Symposium on Waste Processing and Recycling in Mineral and Metallurgical Industries*; Rao, S. R. *et al.* Eds.; CIM: Montreal, Canada, 2004, 453-467.

(5) Girgin, S.; Demopoulos, G. P. Production of the High Value Material, Alpha-$CaSO_4$ Hemihydrate out of Spent $CaCl_2$ Solutions by Reaction with H_2SO_4. in *EPD Congress 2004*; Schlesinger, M. E. Ed.; TMS: Warrendale, Pa, 2004, 627-639.

(6) Marshall, W. L.; Slusher, R.; Jones, E. V. Aqueous Systems at High Temperature. XIV. Solubility and Thermodynamic Relationships for $CaSO_4$ in NaCl-H_2O Solutions from 40 °C to 200 °C, 0 to 4 Molal NaCl. *J. Chem. Eng. Data* **1964**, 9, 187.

(7) Marshall, W. L.; Slusher, R. Thermodynamics of Calcium Sulfate Dihydrate in Aqueous Sodium Chloride Solutions, 0-110 °C. *J. Phys. Chem.* **1966**, 70, 4015.

(8) Marshall, W. L.; Slusher, R. Aqueous Systems at High Temperature. Solubility to 200 °C of Calcium Sulfate and Its hydrates in Seawater and Saline Water Concentrates, and Temperature-Concentration Limits. *J. Chem. Eng. Data* **1968**, 13, 83.

(9) Barba, D.; Brandani, V.; Giacomo G. D. A Thermodynamic Model of $CaSO_4$ Solubility in Multicomponent Aqueous Solutions. *Chem. Eng. J.* **1982**, 24, 191.

(10) Barba, D.; Brandani, V.; Giacomo G. D. Solubility of Calcium Sulfate Dihydrate in the System Na_2SO_4-$MgCl_2$-H_2O. *J. Chem. Eng. Data* **1984**, 29, 42.

(11) Pitzer, K. S. *Activity coefficients in Electrolyte Solution*; CRC Press: Boca Raton, Fl, 1991.

(12) Harvie, C. E.; Weare, J. H. The Prediction of Mineral Solubilities in Natural Waters: the Na-K-Mg-Ca-Cl-SO_4-H_2O System from Zero to High Concentration at 25 °C. *Geochim. Cosmochim. Acta* **1980**, 44, 981.

(13) Meijer, J. A. M.; Rosmalen, G. M. Solubilities and Supersaturations of Calcium Sulfate and Its Hydrates in Seawater. *Desalination* **1984**, 51, 255.

(14) Zemaitis, J. F.; Clark, D. M.; Rafal, M.; Scrivner, N. C. *Handbook of Aqueous Electrolyte Thermodynamics: Theory & Application*; AIChE: New York, 1986.

(15) Demopoulos, G. P.; Kondos, P.; Papangelakis, V. G. Prediction of Solubility in Chemical Compound Precipitation Systems. *Cryst. Precip., Proc. Int. Symp.*; Strathdee, G. L. *et al.* Eds; Pergamon: Oxford, 1987, 231.

(16) Scrivner, N. C.; Staples, B. R. Equilibria in Aqueous Solutions: Industrial Application. *Chemical Engineering Thermodynamics*, Newman, S. A. Ed; Ann Arbor Science: Ann Arbor Mich., 1983, 349.

(17) Anderko, A.; Wang, Peiming; Rafal, M. Electrolyte Solutions: from Thermodynamic and Transport Property Models to the Simulation of Industrial Processes. *Fluid Phase Equilib.* **2002**,194-197, 123.

(18) Chen, C. C.; Mathias, P. M. Applied Thermodynamics for Process Modeling. *AIChE J.* **2002**, 48, 194.

(19) Prausnitz, J. M.; Tavares, F. W. Thermodynamics of Fluid-Phase Equilibria for Standard Chemical Engineering Operations. *AIChE J.* **2004**, 50, 739.

(20) Bromley, L. A. J. Thermodynamic Properties of Strong Electrolytes in Aqueous Solutions, *AIChE J.* **1973**, 19, 313.

(21) Rafal, M.; Berthold, J. W.; Scrivner, N. C.; Grise, S. L. Models for Electrolyte Solutions, in *Models for Thermodynamic and Phase Equilibria Calculations*, Sandler, S. I. (Ed.), Marcell Dekker: New York, 1994.

(22) Zemaitis, J. F. Predicting Vapor-Liquid-Equilibria in Multicomponent Aqueous Solutions of Electrolytes, in *Thermodynamics of Aqueous Systems with Industrial Applications;* Newman, S. A. et al (Eds.), American Chemical Society: Washington, DC, 1980, 227.

(23) Li, Z.; Demopoulos, G. P. $CaSO_4$ Solubilities in Concentrated Aqueous Chloride Solutions. In *Chloride Metallurgy 2002: International Conference on Practice and Theory of Chloride/Metal Interaction, 32nd Annual Hydrometallurgy Meeting*; Peek, E., Van Weert, G. Eds; CIM: Montreal, 2002, 561.

(24) Li, Z.; Demopoulos, G. P. Solubility of $CaSO_4$ Phases in Aqueous HCl + $CaCl_2$ Solutions from 283 K to 353 K. *J. Chem. Eng. Data* **2005**, 50, 1971.

(25) *Aqueous System Modeling Course and Workshop*, OLI's manual, OLI Systems Inc., NJ, 2002.

(26) Shock, E. L.; Helgeson, H. C. Calculation of the Thermodynamic and Transport Properties of Aqueous Species at High Pressures and Temperatures: Correlation

Algorithms for Ionic Species and Equation of State Predictions to 5 kb and 1000 °C. *Geochim. Cosmochim. Acta* **1988**, 52, 2009.

(27) Gurvich, L. V.; Veyts, I. V.; Alcock, C. B. *Thermodynamic Properties of Individual Substances*; 4th ed., Hemisphere Publishing Corporation: 1989, Vol.1 (Part 1, 2).

(28) Glushko, V. P. Medvedev, V. A. *et al. Thermal Constants of Compounds*; Academy of Sciences: USSR, 1979, Vol.9 (Part 1).

(29) Anderson, G. M.; Crerar, D. A. *Thermodynamics in Geochemistry the Equilibrium Model*; Oxford University Press: New York, 1993.

(30) Helgeson, H. C.; Kirkham, D. H.; Flowers, G. C. Theoretical Prediction of the Thermodynamic Behavior of Aqueous Electrolytes at High Pressures and Temperatures: IV. Calculation of Activity Coefficients, Osmotic Coefficients, and Apparent Molal and Standard and Relative Partial Molal Properties to 600 °C and 5 kb. *Amer. J. Sci.* **1981**, 281, 1249.

(31) Tanger, J. C., IV; Helgeson, H. C. Calculation of the Thermodynamic and Transport Properties of Aqueous Species at High Pressures and Temperatures: Revised Equations of State for the Standard Partial Molal Properties of Ions and Electrolytes. *Amer. J. Sci.* **1988**, 288, 19.

(32) Shock, E. L.; Helgeson, H. C.; Sverjensky D. A. Calculation of the Thermodynamic and Transport Properties of Aqueous Species at High Pressures and Temperatures: Standard Partial Molal Properties of Inorganic Neutral Species. *Geochim. Cosmochim. Acta* **1989**, 53, 2157.

(33) Shock, E. L.; Sassani, D. C.; Willis M.; Sverjensky D. A. Inorganic Species in Geologic Fluids: Correlations among Standard Molal Thermodynamic Properties of Aqueous Ions and Hydroxide Complexes. *Geochim. Cosmochim. Acta* **1997**, 61, 907.

(34) Meissner, H. P.; Kusik, C. L. Aqueous Solutions of Two or More Strong Electrolytes: Vapor Pressure and Solubilities. *Ind. Eng. Chem. Process Des. Develop.* **1973**, 12, 205.

(35) Dickson, A. G.; Wesolowski, D. J.; Palmer, D. A.; Mesmer, R. E. Dissociation Constant of Bisulfate Ion in Aqueous Sodium Chloride Solutions to 250 °C. *J. Phys. Chem.* **1990**, 94, 7978.

(36) Hovey, J. K.; Hepler, L. G. Thermodynamics of Sulphuric Acid: Apparent and Partial Molar Heat Capacities and Volumes of Aqueous HSO_4^- from 10-50 °C and Calculation of the Second Dissociation Constant to 350 °C. *J. Chem. Soc. Faraday Trans.* **1990**, 86(16), 2831.

(37) Zdanovskii, A. B.; Spiridonov, F. P. Polytherm for the Solubilities of Various Forms of $CaSO_4.xH_2O$ in Water between 0 and 100 °C. *J. Applied Chem.*(USSR) **1967**, 12, 1101.

(38) Yasue, T.; Kojima, Y.; Kishimoto, Y.; Arai, Y. Preparation of α-Gypsum Hemihydrate and Control of Its Crystal Shape under Atmospheric Pressure. *Gypsum & Lime* (Japan) **1992**, 239, 230.

(39) Kruchenko, V. P.; Beremzhanov, B. A. The Solubility of Salts in the Calcium Sulfate-Hydrochloric Acid-Water System at 25 °C. *Russ. J. Inorg. Chem.* **1976**, 21(1), 281.

(40) Ling, Yuanbing; Demopoulos, George P. Phase Transformation Relationships in the $CaSO_4$-H_2SO_4-H_2O System. *EPD Congress 2004*; Schlesinger, M. E. Ed.; TMS: Warrendale, Pa, 2004, 477.

(41) Langmuir, D.; Melchior, D. The Geochemistry of Calcium, Strontium, Barium and Radium Sulfates and in Some Deep Brines from the Palo Duro Basin, Texas. *Geochim. Cosmochim. Acta* **1985**, 49, 2423.

Chapter 5

Model-Based Construction of Calcium Sulfate Phase Transition Diagrams in the HCl - $CaCl_2$ - H_2O System between 0 and 100 °C

5.1 Abstract

Phase transition diagrams of three $CaSO_4$ phases, namely dihydrate, hemihydrate and anhydrate, in the HCl-$CaCl_2$-H_2O system are successfully constructed making use of a recently developed OLI–based chemical model. After initial validation of the model by comparison to experimentally determined $CaSO_4$-phase transition points in H_2O or pure HCl solutions, the phase transition border between dihydrate and anhydrite, and dihydrate and hemihydrate was obtained by calculating the solution supersaturation (or scaling tendency according to OLI). The constructed phase transition diagrams show three main regions, namely region I, II and III. In region I, dihydrate is stable, while anhydrite is stable in regions II and III. Dihydrate is metastable in region II while hemihydrate is metastable in region III. An increase in HCl and/or $CaCl_2$ concentration causes the metastable region of HH to expand at the expense of DH. This has as result the lowering of the corresponding transition temperatures. The phase transition diagram at 80 °C was experimentally validated reasonably well.

5.2. Introduction

Formation of $CaSO_4$ and its hydrates (namely dihydrate (DH), hemihydrate (HH), and anhydrite (AH)) is encountered frequently in aqueous chemical processes either in the form of scale on equipment or as precipitates. An important industrial practice where knowledge on the formation of $CaSO_4$ phases is desirable is the processing of minerals and metals in concentrated acidic chloride solutions (1).

A recent study completed in our laboratory dealt with the measurement (2)[1] and the modeling (3)[2] of $CaSO_4$ solubilities in the $HCl - CaCl_2 - H_2O$ system up to 100 °C. During the experimental part of the study (2) that involved equilibration of the three $CaSO_4$ modifications (DH, HH and AH) in various solutions and temperatures phase transition from one phase to the other was observed. It was decided with the aid of the recently developed chemical solution model (3) to construct $CaSO_4$ phase transition diagrams for the $HCl - CaCl_2 - H_2O$ system that can be conveniently used during the design or optimization studies of aqueous chloride processing of minerals and/or metals.

A review of literature reveals that a study of $CaSO_4$ phase transitions has been previously focused on the $CaSO_4 - H_2O$ system, and to less extend to the $H_3PO_4 - H_2O$ system with only occasioned reference to other electrolyte systems like the $H_2SO_4 - H_2O$ system (4) or some chloride electrolytes. Thus, Van't Hoff *et al.*(5), as early as in 1903, studied the $CaSO_4 - H_2O$ system and reported that the transition temperature between calcium sulfate dihydrate and anhydrite is 63.5 °C while the transition point of dihydrate into hemihydrate lies at 107.2 °C. Later on, Hardie (6) reported the gypsum – anhydrite transition temperature to be 58 °C rather than 63.5 °C. His results were supported by Raju

---

[1] See Chapter 3. [2] See Chapter 4.

and Atkinson's study (7) and that of Ling and Demopoulos (4). The above studies arrived to the determined transition temperature via thermodynamic calculations. But the transition temperature can also be determined via solubility measurements. The transition temperature is the one at which the solubilities of two phases are equal. Thus according to the solubility studies of Hill (8), Bock (9) and Power *et al.* (10) the DH – AH transition temperature in water is only 40 °C. More recently Innorta at al. (11) determined through their own solubility measurements, this transition point to be 49.5 °C. No explanation for the difference between their data and previous measurements was offered. On the other hand, the transition temperature for DH – HH in water was determined by Partridge and White (12) on the basis of solubility measurements to be 98 °C and not 107.2 °C as earlier Van't Hoff *et al.* had suggested.

From an industrial point of view the transition temperatures of the various $CaSO_4$ phases in electrolyte solutions as opposed to pure water are required. The only phase transition diagram in electrolyte solutions is the one published by Dahlgren (13) for the $H_3PO_4 - H_2O$ system. According to this work the respective transition temperatures for DH-AH and DH-HH decrease with increasing electrolyte concentration. Thus, $T_{tran.,DH/AH}$ was found to decrease from 40 °C in water down to 0 °C at 38 wt% P_2O_5 while $T_{tran.,DH/HH}$ decreases from 104 °C down to 67 °C at 38 wt% P_2O_5. The Dahlgren diagram has been widely used by those conducting research relating to phosphoric acid production (14). Currently, no similar phase transition diagram is available for concentrated aqueous chloride solutions but only some limited data. Thus, Bock (9) and Kruchenko and Beremzhanov (15) appear to be the only investigators to have reported on the transition of $CaSO_4$ phases in NaCl and HCl aqueous solutions respectively. Bock (9) investigated the effect of NaCl on the transition temperature for dihydrate – anhydrite by determining their solubilities at various temperatures. He found that this transition point is shifted progressively to lower temperatures with increasing NaCl concentration. Kruchenko and Beremzhanov on the other hand determined the HCl concentrations at which both transition points lie at 25 °C. The transition for dihydrate – anhydrite at 25 °C was found to take place in 11.5 wt% HCl solution while the transition point for dihydrate – hemihydrate was attained in 24.5 wt % HCl solution. Given the scarcity of information of $CaSO_4$ phase transition in various composition of HCl and $CaCl_2$ solutions above 25 °C, the purpose of the present work is to construct a similar to Dahlgren diagram for the industrially important system of $CaSO_4$ - HCl – $CaCl_2$ – H_2O (16) between 0 to 100 °C.

5.3. Theoretical Basis

$CaSO_4$ may crystallize in three modifications, namely, dihydrate, hemihydrate and anhydrite. The dissolution of the three solid phases in aqueous solution is expressed as follows:

$$CaSO_4 \cdot 2H_2O(s)(DH) = Ca^{2+} + SO_4^{2-} + 2H_2O \tag{5.1}$$

$$CaSO_4 \cdot 0.5H_2O(s)(HH) = Ca^{2+} + SO_4^{2-} + 0.5H_2O \tag{5.2}$$

$$CaSO_4(s)(AH) = Ca^{2+} + SO_4^{2-} \tag{5.3}$$

The respective equilibrium constants for reactions 5.1 to 5.3, that is, solubility product constants, are:

$$K_{SP,DH} = a_{Ca^{2+}} a_{SO_4^{2-}} a_{H_2O}^2 \tag{5.4}$$

$$K_{SP,HH} = a_{Ca^{2+}} a_{SO_4^{2-}} a_{H_2O}^{0.5} \tag{5.5}$$

$$K_{SP,AH} = a_{Ca^{2+}} a_{SO_4^{2-}} \tag{5.6}$$

There are two possible phase transformation reactions between DH - AH and DH - HH as follows:

$$CaSO_4{\cdot}2H_2O(s)(DH) = CaSO_4(s)(AH) + 2H_2O \qquad (5.7)$$

$$CaSO_4{\cdot}2H_2O(s)(DH) = CaSO_4{\cdot}0.5H_2O(s)(HH) + 1.5H_2O \qquad (5.8)$$

Their thermodynamic equilibrium constants, that relate to phase transition equilibrium conditions, are obtained by rearranging Eqs. (5.4)-(5.6):

$$K_{DH-AH} = \frac{K_{SP,DH}}{K_{SP,AH}} = a_{H_2O}^{2} \qquad (5.9)$$

$$K_{DH-HH} = \frac{K_{SP,DH}}{K_{SP,HH}} = a_{H_2O}^{1.5} \qquad (5.10)$$

Eqs. (5.9) and (5.10) indicate that the phase transition temperatures between DH – AH and DH – HH in aqueous solutions are determined by the water activity which in turn depends on the composition of solution and the system temperature. Hence, the temperature of $CaSO_4$ phase transition is expected to vary with the concentration of electrolyte in solution.

For ionic crystal precipitation, such as, $CaSO_4$ precipitation (refer to reactions (5.1) to (5.3)), the solution needs to be supersaturated in terms of the respective phases. Supersaturation or rather the saturation ratio, of dihydrate, hemihydrate and anhydrite can be expressed by invoking their solubility product, K_{SP} (17):

$$S_{DH} = \frac{a_{Ca^{2+}} a_{SO_4^{2-}} a_{H_2O}^{2}}{K_{SP,DH}} \qquad (5.11)$$

$$S_{HH} = \frac{a_{Ca^{2+}} a_{SO_4^{2-}} a_{H_2O}^{0.5}}{K_{SP,HH}} \qquad (5.12)$$

$$S_{AH} = \frac{a_{Ca^{2+}} a_{SO_4^{2-}}}{K_{SP,AH}} \quad (5.13)$$

Combination of Eqs. (5.11), (5.12) and (5.13) enables the saturation ratios for the three $CaSO_4$ phases to be related (18):

$$\ln S_{DH} = \ln S_{AH} + \ln \frac{K_{SP,AH}}{K_{SP,DH}} + 2 \ln a_{H_2O} \quad (5.14)$$

$$\ln S_{HH} = \ln S_{AH} + \ln \frac{K_{SP,AH}}{K_{SP,HH}} + 0.5 \ln a_{H_2O} \quad (5.15)$$

We should mention that the supersaturation expressed by Eqs. (5.11) - (5.13) is called scaling tendency (ST) in OLI software (19). The latter constitutes the platform of the chemical model used in this work. If supersaturation (S), or scaling tendency (ST), is less than 1, the solution is undersaturated while the solution is supersaturated when scaling tendency (ST) is greater than 1. At saturation, the scaling tendency is equal to 1.

Phase transition diagrams are constructed in this work for the system $CaSO_4$ - HCl - $CaCl_2$ - H_2O making use of a recently developed OLI-based chemical model (3). This model makes use of a new self – consistent set of Bromley – Zemaitis model parameters determined by fitting experimental solubility data generated by the authors (2). The model was successfully calibrated and validated proving capable in predicting the solubility of all three $CaSO_4$ phases, namely, dihydrate, hemihydrate and anhydrite (3), hence making an excellent tool to undertake the work described in this paper.

5.4. Results and Discussion

5.4.1 The $CaSO_4$ - H_2O System

Because the solubility of the three $CaSO_4$ modifications in pure water is very low, the activity of water in $CaSO_4$ – saturated water is practically equal to 1. The phase transition equilibrium constants between DH-AH and DH-HH (i.e. Eqs. (5.9) and (5.10)) are simplified thus to:

$$K_{DH-AH} = \frac{K_{SP,DH}}{K_{SP,AH}} = 1 \tag{5.16}$$

$$K_{DH-HH} = \frac{K_{SP,DH}}{K_{SP,HH}} = 1 \tag{5.17}$$

Eq. (5.16) shows that at transition point the values of solubility product of both DH and AH are equal. This equality is used as the basis for the estimation of the respective transition points. According to our modeling work (3) the dependency of solubility product constants of the $CaSO_4$ modifications on temperature is expressed by the following equations:

$$Log_{10}K_{SP(DH)} = 40.11184 - \frac{5481.185}{T} - 0.115199T + 9.1384 \times 10^{-5}T^2 \tag{5.18}$$

$$Log_{10}K_{SP(HH)} = 34.4739 - \frac{4939.1}{T} - 0.0870353T + 4.59692 \times 10^{-5}T^2 \tag{5.19}$$

$$Log_{10}K_{SP(AH)} = -85.601 + \frac{8775.05}{T} + 0.261521T - 2.93598 \times 10^{-4}T^2 \tag{5.20}$$

where T is in degree K. The above equations were derived via regression of solubility data. Eq.(5.18) is available in OLI's databank while Eqs. (5.19) and (5.20) were derived by the authors as described elsewhere (3). Eqs. (5.18) to (5.20) are plotted in Figure 5.1

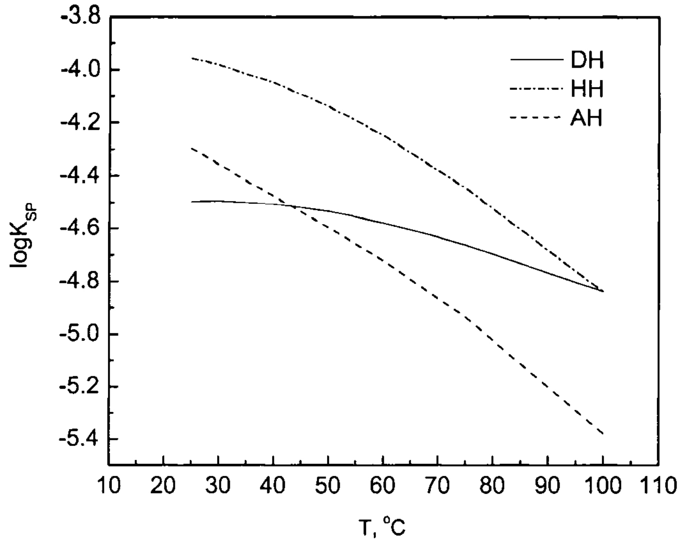

Figure 5.1. log K_{SP} of DH, HH and AH as a function of temperature.

It can be seen from Figure 5.1 that the $K_{SP,DH}$ curve intersects with $K_{SP,AH}$ curve at 43 °C at which the phase transition between DH and AH occurs in pure water. This value lies between the values of 40 °C reported by Hill (8), Bock (9) and Power *et al.* (10) and 49.5 °C reported by Innorta at al. (11). On the other hand, the intersection of $K_{SP,DH}$ and $K_{SP,HH}$ lines corresponding to transition point between DH and HH is at 100 °C which is close to 98 °C of Partridge *et al.* (12), but clearly lower than Dahlgren's 104 °C or Van't Hoff et al's 107 °C.

5.4.2 The $CaSO_4 - HCl - CaCl_2 - H_2O$ System

In concentrated HCl and $CaCl_2$ solutions, the water activity can strongly deviate from 1 due to the strong non-ideality of solution (20). The phase transition temperature between $CaSO_4$ modifications is expected, thus to vary with the concentration of acid and salt. The phase transition equilibria between DH-AH and DH-HH can be determined with the aid of Eqs.(5.9) and (5.10) or on the basis of phase solubilities as the latter rely on experimental rather than thermodynamic grounds. At transition point, where the equilibrium between two phases exists, the solubility of one phase is equal to that of the other (9). Consequently, it is possible from the intersection of the solubility curves of the two phases to obtain the phase transition point and further establish the phase transition diagram. As an example, the intersections of the solubility curves for DH, HH and AH in HCl solutions at 25 °C is demonstrated in Figure 5.2 (15). It can be seen from Figure 5.2 that the intersection of dihydrate and anhydrite curves corresponds to the concentration of 3.8 m, while the phase transition point between DH and HH corresponds to the concentration of 8.8 m HCl at 25 °C.

Analyzing solubility data like those plotted in Figure 5.2 can lead to determination of the transition points from the intersection of the respective solubility curves. However, this is not practical as on one hand the available solubility data is limited while on the other hand the intersection points are difficult to obtain when solubility curves intersect at very small angles. This problem can be easily overcome if the transition points are determined using a solubilities-based thermodynamic model as the one developed by the authors (3). Before this model is used to construct the phase transition diagrams it is important to test the validity of its prediction by estimating the solubilities of DH, HH and AH in HCl solutions at 25 °C. The model predicted solubility curves are also plotted in Figure 5.2 along with the experimental data points taken from Kruchenko's work (15). It can be clearly seen that the model and experimental data is in reasonable agreement for all three $CaSO_4$ phases. Moreover, the transition points determined from the intersection of the model predicted solubility curves are 4.1 m and

9.7 m comparing well with the experimentally determined ones of 3.8 m and 8.8 m for DH – AH and DH – HH respectively.

In the remaining of the work the transition points are determined by calculating the variation of scaling tendency (ST) or supersaturation in terms of solution composition or temperature of the system. The ST of the three $CaSO_4$ modifications is given by Eqs. (5.11)-(5.13). The variation of scaling tendency of DH, HH and AH with HCl concentration at 80 °C is shown in Figure 5.3. It can be seen from Figure 5.3 that the transition between dihydrate and hemihydrate takes place in the concentration of 4.93 m HCl. Consequently, using this method the boundaries of phase transition DH – HH and also DH – AH in HCl - $CaCl_2$ solutions are determined and a series of phase transition diagrams are constructed.

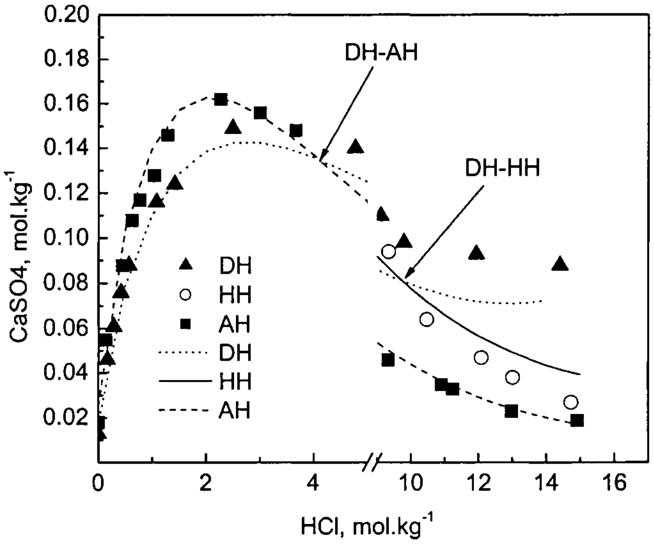

Figure 5.2. The intersection of the solubility curves of the three calcium sulfate phases in HCl solutions at 25 °C. Curves: model predictions; dots: experimental data from ref. (15).

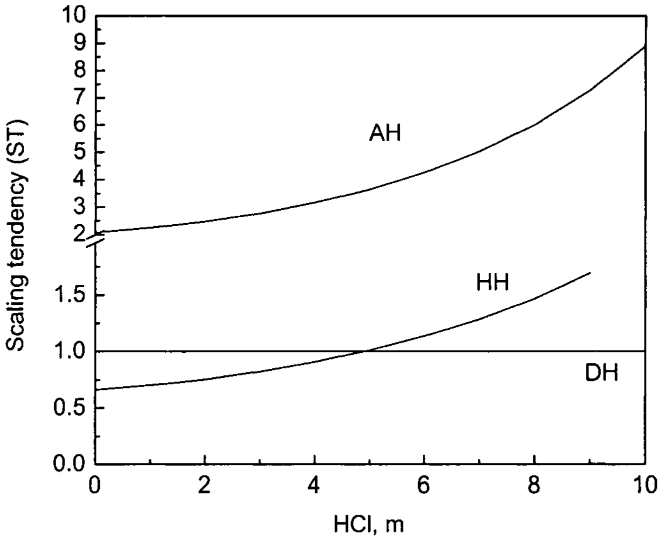

Figure 5.3. Scaling tendency of DH, HH, and AH as a function of HCl concentration at 80 °C.

Concentration Effects: The transition temperatures between DH-AH and DH-HH at fixed $CaCl_2$ concentration as a function of HCl concentration were calculated and presented in Table 5.1 and Figures 5.4-5.7. Figure 5.4 describes the stable zones for dihydrate and anhydrite and metastable zones for dihydrate and hemihydrate for the $CaSO_4$–HCl–H_2O system. In region I, calcium sulfate dihydrate is the stable phase, but anhydrite is the stable phase in regions II and III. Dihydrate is metastable in region II while hemihydrate is metastable in region III. It is clear that with increasing HCl concentration the transition temperature for both DH-AH and DH-HH decreases as it would be expected from the decrease of water activity with electrolyte concentration (20).

The effect of $CaCl_2$ on the $T_{trans.}$ – C_{HCl} of $CaSO_4$ phase diagram is illustrated in Figures 5.5-5.7 at 0.5, 2, and 4 m $CaCl_2$ concentration level respectively. Comparison of the diagram of Figure 5.4 with those in Figure 5.5 to 5.7 shows that the addition of $CaCl_2$ causes regions I and II to shrink.

Table 5.1. Transition Temperatures between DH-AH and DH-HH in HCl Solutions of Fixed $CaCl_2$ Concentration

DH-AH		DH-HH	
$CaCl_2$=0.0 m		$CaCl_2$=0.0 m	
HCl (m)	T (°C)	HCl (m)	T (°C)
8.77	0.0	10.47	0.0
6.88	10.0	10.24	10.0
5.04	20.0	9.93	20.0
3.13	30.0	9.53	30.0
0.89	40.0	9.01	40.0
0.02	43.0	8.35	50.0
0.00	43.1	7.49	60.0
		6.38	70.0
		4.93	80.0
		3.01	90.0
		1.74	95.0
		0.78	98.0
		0.00	100.0
$CaCl_2$=0.5 m		$CaCl_2$=0.5 m	
HCl (m)	T (°C)	HCl (m)	T (°C)
8.05	0.0	9.75	0.0
7.11	5.0	9.52	10.0
6.18	10.0	9.21	20.0
5.28	15.0	8.82	30.0
4.37	20.0	8.31	40.0
3.45	25.0	7.66	50.0
2.49	30.0	6.83	60.0
1.45	35.0	5.74	70.0
0.23	40.0	4.31	80.0
0.00	40.8	2.39	90.0
		1.12	95.0
		0.15	98.0
		0.00	98.4
$CaCl_2$= 2.0 m		$CaCl_2$= 2.0 m	
HCl (m)	T (°C)	HCl (m)	T (°C)
5.63	0.0	7.35	0.0
4.67	5.0	7.10	10.0
3.75	10.0	6.78	20.0
2.84	15.0	6.38	30.0
1.94	20.0	5.87	40.0
1.03	25.0	5.22	50.0
0.08	30.0	4.40	60.0
0.00	30.5	3.34	70.0
		1.96	80.0
		1.10	85.0
		0.10	90.0

		0.00	90.5
$CaCl_2$=3.0 m		$CaCl_2$=3.0 m	
HCl (m)	T (°C)	HCl (m)	T (°C)
3.92	0.0	5.66	0.0
2.95	5.0	5.39	10.0
2.02	10.0	5.06	20.0
1.11	15.0	4.64	30.0
0.21	20.0	4.11	40.0
0.00	21.2	3.45	50.0
		2.63	60.0
		1.57	70.0
		0.93	75.0
		0.00	81.2
$CaCl_2$= 4.0 m		$CaCl_2$= 4.0 m	
HCl (m)	T (°C)	HCl (m)	T (°C)
2.15	0.0	3.89	0.0
1.18	5.0	3.61	10.0
0.24	10.0	3.26	20.0
0.00	11.3	2.83	30.0
		2.29	40.0
		1.62	50.0
		0.78	60.0
		0.00	67.5

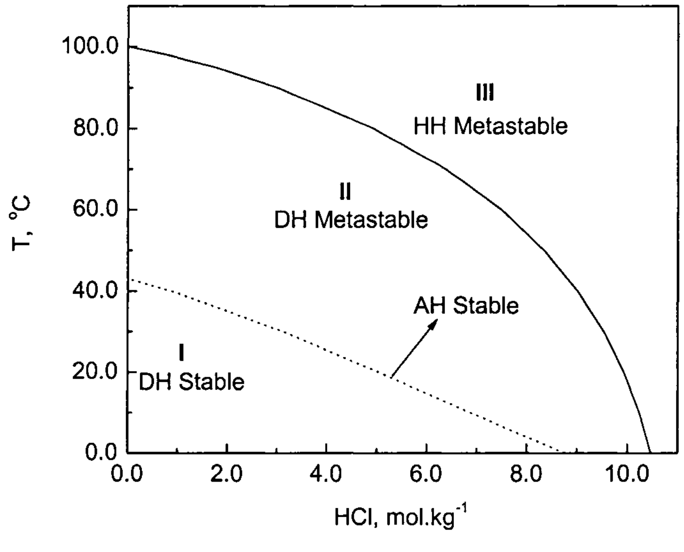

Figure 5.4. The $CaSO_4$ phase transition diagram in pure HCl solutions. Region I: DH stable; Region II: AH stable and DH metastable; Region III: AH stable and HH metastable.

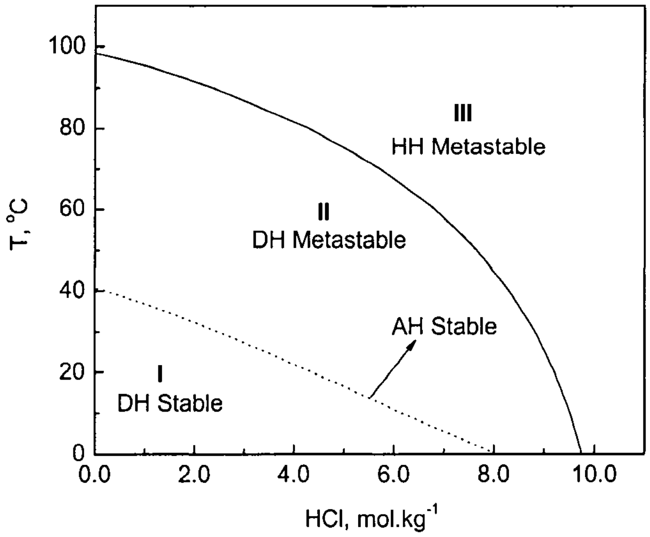

Figure 5.5. The CaSO4 phase transition diagram in pure HCl-0.5m $CaCl_2$ solutions.

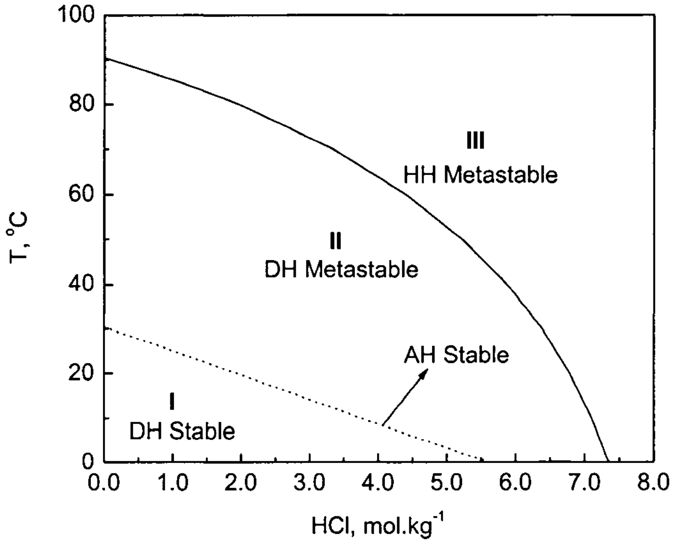

Figure 5.6. The CaSO4 phase transition diagram in pure HCl-2m $CaCl_2$ solutions.

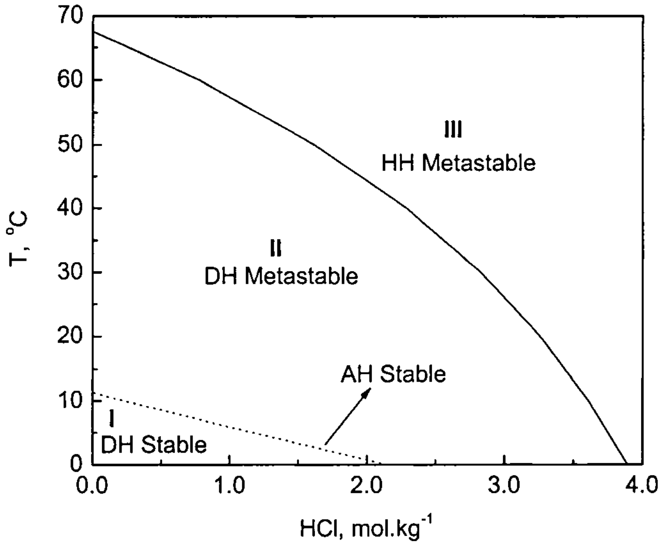

Figure 5.7. The $CaSO_4$ phase transition diagram in pure HCl-4m $CaCl_2$ solutions.

For instance, at 80 °C the transition DH-HH in pure HCl solutions corresponds to the concentration of 4.93 m (Figure 5.4). However, the concentration of HCl at the same transition point of DH-HH is lowered to 1.96 m when 2 m $CaCl_2$ is added to the system.

Similarly, the effect of $CaCl_2$ at fixed HCl concentration on the transition temperatures between DH-AH and DH-HH in mixed HCl- $CaCl_2$ media was investigated. The calculated results are presented in Table 5.2 and Figures 5.8-5.10. It can be seen that region I in which DH is the stable phase and region II where DH becomes metastable appear smaller when the HCl is introduced into $CaCl_2$ solutions, indicating that the transition temperatures between DH-AH and DH-HH decrease.

As discussed earlier (refer to Eqs. (5.9) and (5.10)) the effect of electrolyte (HCl and $CaCl_2$) concentration on the phase transition points, $T_{trans,\ DH/AH}$ and $T_{trans,\ DH/HH}$, may be explained on the basis of water activity changes. It was decided to examine this issue by comparing the effect of HCl and $CaCl_2$ on T_{trans}, and correlating this to water activity. This was done by looking first the effect of total Cl^- concentration for different electrolyte mixtures. On Figure 5.11 the phase diagram is constructed as a function of total chloride ion concentration for 3 systems: (a) pure HCl, (b) pure $CaCl_2$ and (c) mixed HCl-2m $CaCl_2$. It is clear that the nature of electrolyte in addition to (total) Cl^- concentration affects the respective transition temperatures. On a separate diagram (Figure 5.12) the variation of activity of water with $[Cl^-]_{total}$ is plotted for T = 25 °C for the respective 3 electrolyte systems, HCl, $CaCl_2$, and HCl-2m $CaCl_2$. The latter plot shows that the variation of activity of water with electrolyte concentration to follow the same trend although in absolute values HCl has stronger effect on water activity than $CaCl_2$. The effect of water activity on transition temperature is better seen in Figure 5.13. From the evaluation of Figures 5.11 and 5.13 it can be concluded that the observed lowering in transition temperature with increasing chloride electrolyte concentration is due to water activity. According to Figure 5.11 the phase transition temperature in the mixed HCl-$CaCl_2$ system (especially in the high concentration end) lies between those in pure HCl and $CaCl_2$.

Table 5.2. Transition Temperatures between DH-AH and DH-HH in Fixed HCl-$CaCl_2$ Solutions

DH-AH		DH-HH	
HCl = 0.0 m		HCl =0.0 m	
$CaCl_2$ (m)	T (°C)	$CaCl_2$ (m)	T (°C)
5.17	0.0	6.07	0.0
3.12	20.0	5.74	20.0
2.05	30.0	5.51	30.0
1.43	35.0	5.22	40.0
0.65	40.0	4.86	50.0
0.00	43.1	4.42	60.0
		3.85	70.0
		3.11	80.0
		2.06	90.0
		1.28	95.0
		0.61	98.0
		0.00	100.0
HCl = 1.0 m		HCl =1.0 m	

$CaCl_2$ (m)	T (°C)	$CaCl_2$ (m)	T (°C)
4.63	0.0	5.56	0.0
2.55	20.0	5.22	20.0
1.45	30.0	4.98	30.0
0.80	35.0	4.69	40.0
0.00	39.6	4.33	50.0
		3.89	60.0
		3.31	70.0
		2.55	80.0
		1.45	90.0
		0.59	95.0
		0.00	97.4
HCl = 3.0 m		HCl = 3.0 m	
$CaCl_2$ (m)	T (°C)	$CaCl_2$ (m)	T (°C)
3.52	0.0	4.49	0.0
1.37	20.0	4.15	20.0
0.80	25.0	3.91	30.0
0.42	28.0	3.62	40.0
0.00	30.7	3.25	50.0
		2.79	60.0
		2.20	70.0
		1.37	80.0
		0.01	90.0
		0.00	90.1
HCl = 6.0 m		HCl = 6.0 m	
$CaCl_2$ (m)	T (°C)	$CaCl_2$ (m)	T (°C)
1.78	0.0	2.80	0.0
		2.46	20.0
		2.22	30.0
		1.92	40.0
		1.54	50.0
		1.04	60.0
		0.72	65.0
		0.31	70.0
		0.00	72.9

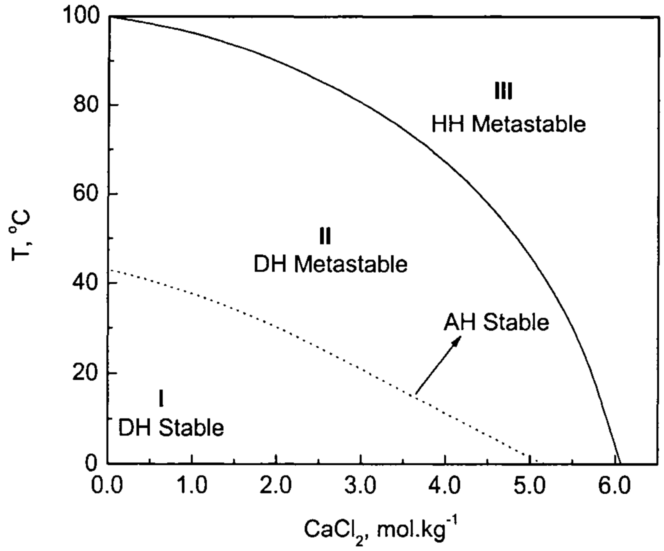

Figure 5.8. The CaSO4 phase transition diagram of DH-AH and DH-HH in pure $CaCl_2$ solutions. Region I: DH stable; Region II: AH stable and DH metastable; Region III: AH stable and HH metastable.

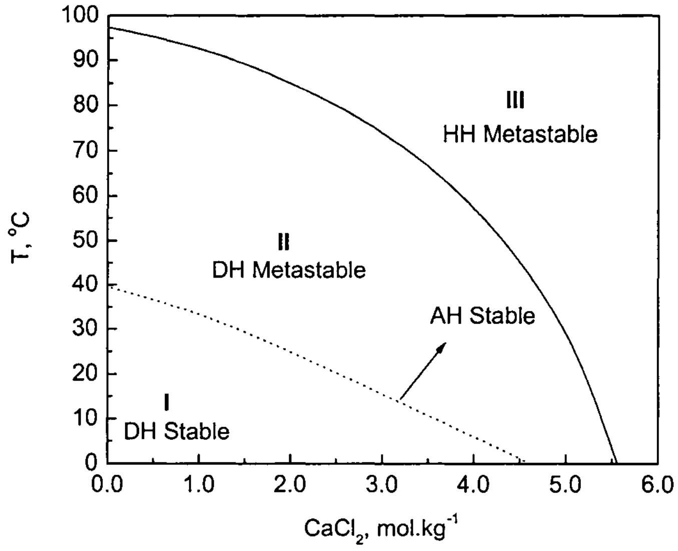

Figure 5.9. The $CaSO_4$ phase transition diagram in $CaCl_2$-1m HCl solutions.

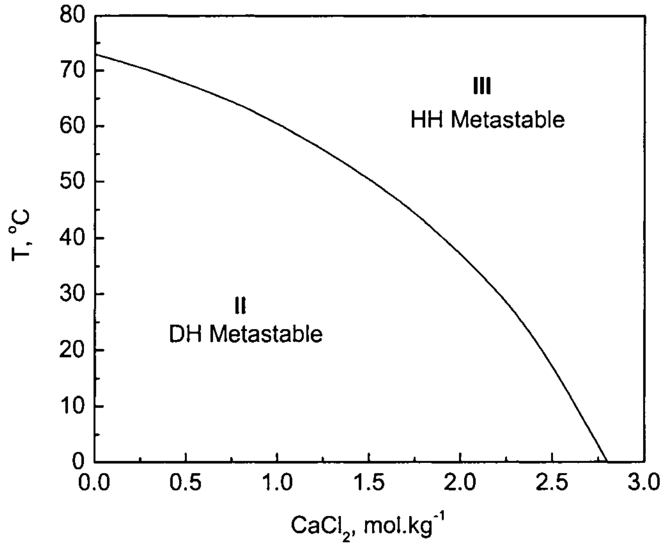

Figure 5.10. The $CaSO_4$ phase transition diagram in $CaCl_2$-6m HCl solutions.

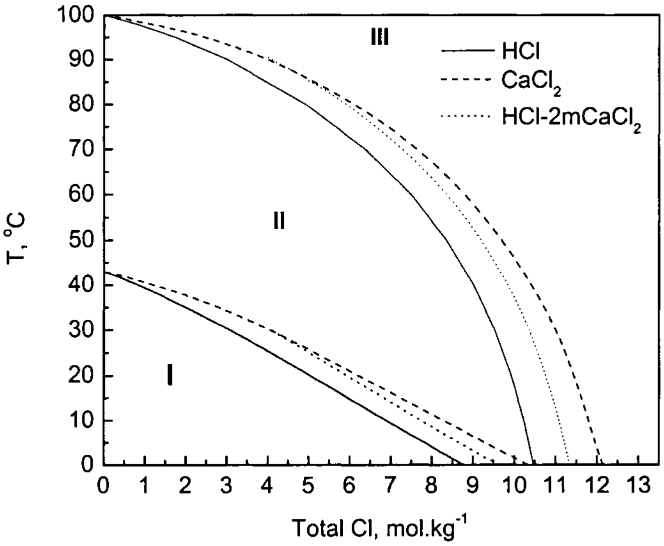

Figure 5.11. Comparison of $CaSO_4$ phase transition diagram in HCl, $CaCl_2$ and mixed HCl-2m $CaCl_2$ solutions.

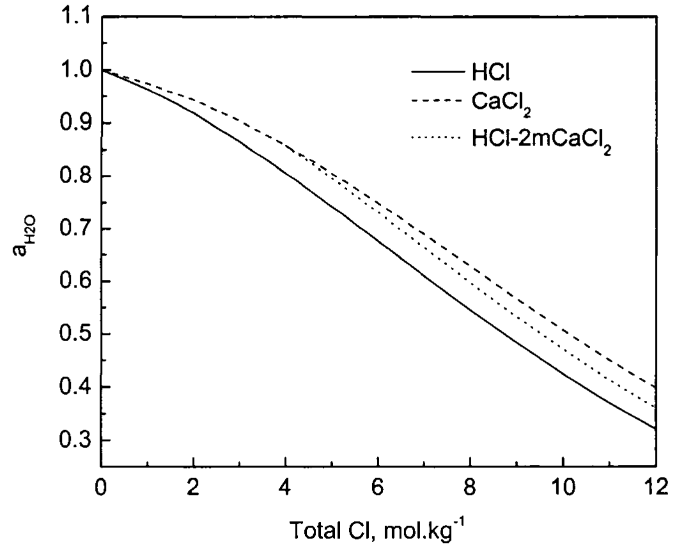

Figure 5.12. Activity of water as a function of total Cl concentration in HCl, $CaCl_2$ and mixed HCl-2m $CaCl_2$ solutions at 25 °C.

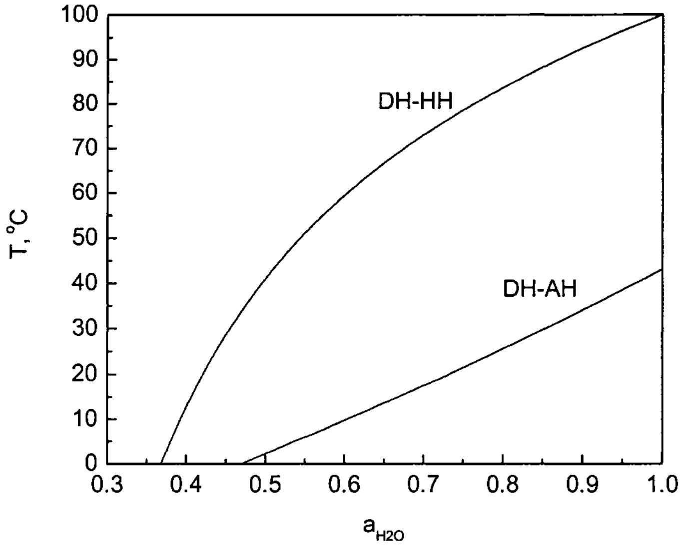

Figure 5.13. $CaSO_4$ phase transition temperature as function of the water activity in the HCl-$CaCl_2$-H_2O system.

Temperature Effects: Figures 5.14 and 5.15 illustrate the transition temperature lines between DH-AH and DH-HH at fixed temperatures as a function of $CaCl_2$ and HCl concentration. It can be seen the region of metastability of hemihydrate to increase at the expense of DH. In other words the production of hemihydrate becomes feasible at lower temperature with electrolyte concentration increase. This phenomenon is exploited in recently developed processes for the production of the high value α-$CaSO_4$ hemihydrate plaster material either via the transformation of dihydrate to α-hemihydrate in $CaCl_2$ solutions of at least 3 M concentration at 90 °C (22) (this is clearly predicted by Figure 5.8) or reaction of $CaCl_2$ solution with H_2SO_4 at 80 °C (23).

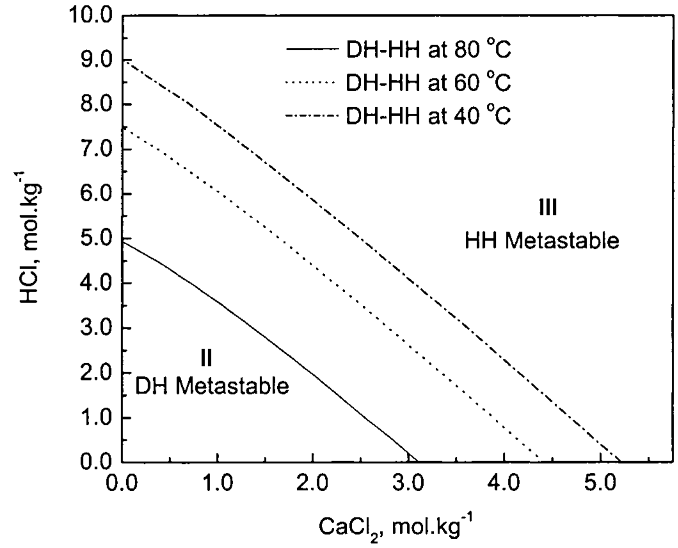

Figure 5.14. Region of metastability for DH and HH in $CaCl_2$-HCl Solutions at 40, 60, and 80 °C

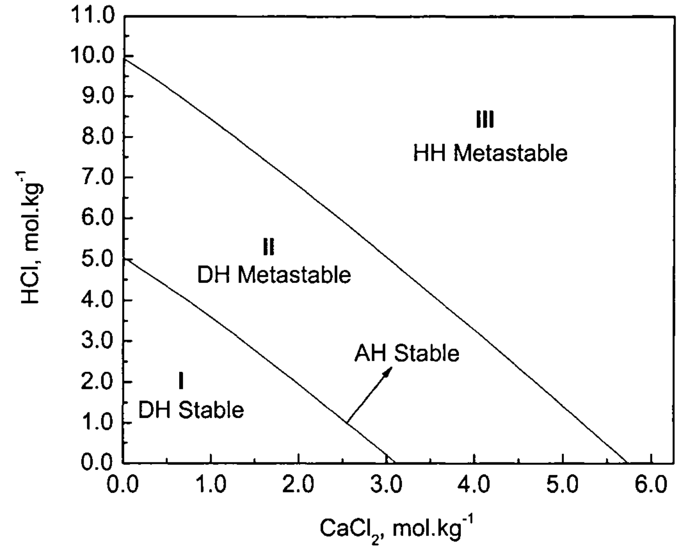

Figure 5.15. The $CaSO_4$ phase transition diagram of DH-AH and DH-HH in HCl-$CaCl_2$ solutions at 20 °C. Region I: DH stable; Region II: AH stable and DH metastable; Region III: AH stable and HH metastable.

5.4.3 Validation of Phase Transition Diagram

Reference has already been made to the fact that the presence of electrolytes such as HCl or $CaCl_2$ promotes the conversion of DH to hemihydrate by lowering transition temperature. The relevance and validity of the constructed phase diagram was further examined by conducting tests where DH or HH materials were equilibrated for 1 hour (or longer in certain cases) in various HCl-$CaCl_2$ mixed solutions or temperatures. The solids were characterized by XRD at the end of the equilibration period and the data is summarised in Table 5.3. In general very good agreement between experiment and model prediction was observed. In certain cases, like test nos 4, 7, 15, 16 and 19 the transition from DH to HH took longer than 1 hour but otherwise the predicted conversion from the model was obtained within maximum of 5 hours. The biggest discrepancy between the constructed phase diagram and the experimental results was observed with pure HCl solutions at 80 °C. Thus while the model predicted HH to be metastable in 5-6 M HCl at 80 °C in reality HH was found to be unstable independent if the starting material was HH or DH (refer to Test no 9). Finally experimentally determined regions of phase metastability are compared to those predicted by the phase diagram constructed in this work for the $CaSO_4$-HCl-$CaCl_2$-H_2O system at 80 °C (refer to Figure 5.16). The experimental data refers to equilibration time of 1 hour and were generated by Girgin (24). It can be appreciated from this diagram that the separation of one zone of metastability (say region II of DH metastability) from another one (say region III of HH metastability) is not sharp as the thermodynamic diagram predicts but there exists a transition zone between the two regions. This reflects of course the kinetics of phase transition. Otherwise the constructed diagrams are deemed satisfactory.

Table 5.3. Comparison of $CaSO_4$ Phase Transition in HCl-$CaCl_2$ Solutions between Model Prediction and Experiment (Equilibration Time: 1 Hour)

No	T/ °C	M	XRD (2)	XRD (24)	Model	Notes
			Starting: HH	Starting: DH		
1	298	8-14 HCl	HH		HH	
2	323	5-6 HCl	DH		DH	
3	323	7-12 HCl	HH		HH	
4	333	6 HCl-0.5$CaCl_2$	HH	DH*	HH	*100% HH in 5 hours
5	333	0.05-2.5 $CaCl_2$	DH		DH	
6	333	3 HCl-(0.5-1.5) $CaCl_2$	DH		DH	
7	343	6 HCl-0.5$CaCl_2$		HH(DH*)	HH	*100% HH in 2.5 hours
8	353	1-4 HCl	DH	DH	DH	
9	**353**	**5-6 HCl**	**AH**	**AH**	**HH**	
10		1 HCl-2.5$CaCl_2$		DH	DH	
11		2-3 HCl-1.5$CaCl_2$		DH(HH)	DH	
12		4-6 HCl-1.5$CaCl_2$		HH	HH	
13		1-1.5$CaCl_2$	DH	DH	DH	
14		2-2.5$CaCl_2$	DH(HH)	DH(HH)	DH	
15		3 $CaCl_2$	HH	DH(HH)*	DH/HH	*DH/HH in 5 hours
16		4 $CaCl_2$		DH(HH)*	HH	*100% HH in 5 hours
17		3HCl-(0.05-0.1)$CaCl_2$	HH(DH)		DH	
18		3HCl-(0.25-1)$CaCl_2$	HH(DH)	DH	DH	
19		3HCl-1.5$CaCl_2$	HH	DH(HH)*	DH/HH	*DH/HH in 2.5 Hours
20		3HCl-(2-3)$CaCl_2$	HH	HH	HH	

21	$6HCl-0.5CaCl_2$	HH	HH	HH

() signify minor component.

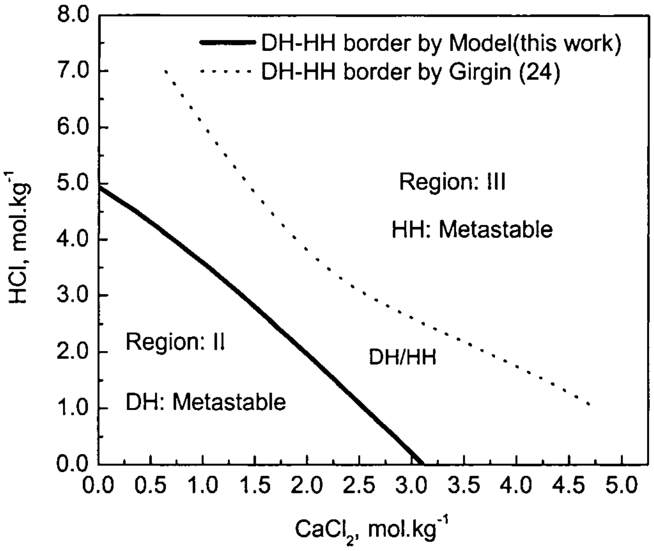

Figure 5.16. Comparison of DH-HH phase transition line between model prediction and experiment at 80 °C.

5.5 Conclusions

An OLI-based chemical model recently developed to calculate the solubility of $CaSO_4$ phases in chloride media has been successfully used to construct the phase transition diagrams in the $CaSO_4 - HCl - CaCl_2 - H_2O$ system between 0 and 100 °C. According to this model the $T_{trans.}$ for DH-AH and DH-HH in water was found to be respectively 43 °C and 100 °C. Upon increase of HCl and /or $CaCl_2$ concentration the corresponding transition temperatures decrease. Comparison of phase transition diagram predictions and experimental measurements showed good agreement in general for equilibrium times between 1 and 5 hours. The constructed phase diagram successfully determines the region of metastability of HH of interest to those seeking to produce the high value α-$CaSO_4 \cdot 0.5H_2O$ plaster material.

Acknowledgement

The support of Hatch, Noranda, Process Research Ortech, and NSERC (Natural Sciences and Engineering Research Council of Canada) is gratefully acknowledged.

5.6 Literature Cited

(1) Peek, E., Van Weert, G. *Chloride Metallurgy 2002: International Conference on Practice and Theory of Chloride/Metal Interaction*, CIM: Montreal, 2002, p561.

(2) Li, Z.; Demopoulos, G. P. Solubility of $CaSO_4$ Phases in Aqueous HCl + $CaCl_2$ Solutions from 283 K to 353 K. *J. Chem. Eng. Data* **2005**, 50, 1971.

(3) Li, Z.; Demopoulos, G. P. Development of an Improved Chemical Model for the Estimation of $CaSO_4$ Solubilities in the HCl - $CaCl_2$ - H_2O System up to 100 °C. *Ind. Eng. Chem. Res.* **2006**, in press.

(4) Ling, Yuanbing; Demopoulos, George P. Phase Transformation Relationships in the $CaSO_4$ - H_2SO_4 - H_2O System. *EPD Congress 2004*; Schlesinger, M. E. Ed.; TMS: Warrendale, Pa, 2004, p477.

(5) Van't Hoff, J. H.; Armstrong, E. F.; Hinrichsen, W.; Weigert, F.; Just, G. Gips und Anhydrit, *Z. Physik. Chem.* **1903**, 45, 257.

(6) Hardie, L. A. The Gypsum-Anhydrite Equilibrium at One Atmosphere Pressure. *Am. Mineral* **1967**, 52, 171.

(7) Raju, K. U. G.; Atkinson G. The Thermodynamics of "Scale" Mineral Solubilities. 3. Calcium Sulfate in Aqueous NaCl. *J. Chem. Eng. Data* **1990**, 35, 361.

(8) Hill, A. E. The Transition Temperature of Gypsum to Anhydrite. *J. Am. Chem. Soc.* **1937**, 59, 2242.

(9) Bock, E. On the Solubility of Anhydrous Calcium Sulphate and of Gypsum in Concentrated Solutions of Sodium Chloride at 25 °C, 30 °C, 40 °C, and 50 °C. *Can. J. Chem.* **1961**, 39, 1746.

(10) Power, W. H.; Fabuss B. M.; Satterfield, C. N. Transient Solubilities in the Calcium Sulfate – Water System. *J. Chem. Eng. Data* **1964**, 9, 437.

(11) Innorta, G.; Rabbi, E.; Tomadin, L. The Gypsum – Anhydrite Equilibrium by Solubility Measurements. *Geochim. Cosmochim. Acta* **1980**, 44, 1931.

(12) Partridge, E. P.; White, A. H. The Solubility of Calcium Sulfate from 0 to 200 ^{o}. *J. Am. Chem. Soc.* **1929**, 51, 360.

(13) Dahlgren, S. E. Calcium Sulfate Transitions in Superphosphate. *J. Agric. Food Chem.* **1960**, 8, 411.

(14) Martynowicz, E. T. M. J.; Witkamp G. J.; Rosmalen, G. M. The Effect of Aluminum Fluoride on the Formation of Calcium Sulfate Hydrates, *Hydrometallurgy* **1996**, 41, 171.

(15) Kruchenko, V. P.; Beremzhanov, V. A. The Solubilities of the Salts in the Calcium Sulphate-Hydrochloric Acid-Water System at 25 °C, *Russ. J. Inorg. Chem.* **1976**, 21, 281.

(16) Al-Othman, A.; Cheng, T. C.; Demopoulos, G. P. Regeneration of HCl and Production of Saleable Gypsum by Reaction of Spent $CaCl_2$ Leach Solutions with H_2SO_4. in *Proceedings of Fifth International Symposium on Waste Processing and Recycling in Mineral and Metallurgical Industries*; Rao, S. R. *et al.* Eds.; CIM: Montreal, Canada, 2004, p453.

(17) Dirksen, J. A.; Ring, T. A. Fundamentals of Crystallization: Kinetic Effects on Particle Size Distributions and Morphology, *Chem. Eng. Sci.* **1991**, 46, 2389.

(18) Sohnel, O.; Mullin, J. W. Expression of Supersaturation in Systems Containing Hydrates, Partially Dissociated Electrolytes and Mixtures of Electrolytes, *Chem. Eng. Sci.* **1978**, 33, 1535.

(19) *Aqueous System Modeling Course and Workshop*, OLI's manual, OLI System Inc. New Jersey, 2002.

(20) Jansz, J. J. C. Estimation of Ionic Activities in Chloride Systems at Ambient and Elevated Temperatures, *Hydrometallurgy* **1983**, 11, 13.

(21) Zemaitis, J. F.; Clark, D. M.; Rafal, M.; Scrivner, N. C. *Handbook of Aqueous Electrolyte Thermodynamics: Theory & Application*; AIChE: New York, 1986.

(22) Hina, A. Nancollas, G. H. Alpha Calcium Sulphate Hemihydrate and a Method of Making Alpha Calcium Sulphate Hemihydrate, *World Patent* No. WO0179116, 2001-10-25.

(23) Girgin, S.; Demopoulos, G. P. Production of the High Value Material, Alpha-$CaSO_4$ Hemihydrate out of Spent $CaCl_2$ Solutions by Reaction with H_2SO_4. in *EPD Congress 2004*; Schlesinger, M. E. Ed.; TMS: Warrendale, Pa, 2004, p627.

(24) Girgin, S. Ph.D. Thesis, in preparation, McGill University, Montreal, QC, Canada, 2006.

Chapter 6

The Effect of NaCl, $MgCl_2$, $FeCl_2$, $FeCl_3$ and $AlCl_3$ on Solubility of $CaSO_4$ Phases in Aqueous HCl or HCl + $CaCl_2$ Solutions at 298 to 353 K

6.1 Abstract

The effect of various chloride salts (NaCl, $MgCl_2$, $FeCl_2$, $FeCl_3$ and $AlCl_3$) on the solubility of three $CaSO_4$ modifications, namely calcium sulfate dihydrate, hemihydrate and anhydrite in aqueous HCl or HCl + $CaCl_2$ solutions up to 353 K was investigated. The concentration ranges (at ambient temperature) studied are up to 6 $mol{\cdot}dm^{-3}$ for HCl, 1.5 $mol{\cdot}dm^{-3}$ for $CaCl_2$, 3 $mol{\cdot}dm^{-3}$ for NaCl, $MgCl_2$ and $FeCl_2$, and 2 $mol{\cdot}dm^{-3}$ for $AlCl_3$ and $FeCl_3$. The solubility of $CaSO_4$ phases in all cases investigated was found to increase with temperature. In 0.5 $mol{\cdot}dm^{-3}$ HCl, the effect of metal chlorides on the solubility of dihydrate was a complex one with solubility increasing up to a certain metal chloride concentration and then decreasing in higher range of metal chloride concentration. On the other hand at higher HCl concentration (3 $mol{\cdot}dm^{-3}$) the solubility of dihydrate and anhydrite was found to consistently decrease with increasing metal chloride concentration. The only exception was NaCl which was found not to influence to a significant degree the solubility of dihydrate in HCl solutions. The solubility of dihydrate in pure $AlCl_3$ solution smoothly passes through a maximum value in (0 to 1.5) $mol{\cdot}dm^{-3}$ $AlCl_3$ concentration range. The presence of $CaCl_2$ causes the solubility of both dihydrate and hemihydrate to decrease due to common ion effect.

6.2 Introduction

Previously, we reported the solubility of three $CaSO_4$ modifications, namely dihydrate (DH), hemihydrate (HH) and anhydrite (AH) in aqueous HCl + $CaCl_2$ solutions at the temperature range of (283 to 353) K (1)[1]. These data are considered important both from the standpoint of developing chemical solution models (2)[2] as well as from the standpoint of designing a process for HCl regeneration and production of valuable gypsum materials, like α – $CaSO_4$ hemihydrate (3,4). In many industrial systems, however, there exist other metal chloride salts in addition to $CaCl_2$ in HCl media (5-9). It is indeed the object of this research to evaluate the effect various metal chlorides, such as NaCl, $MgCl_2$, $FeCl_2$, $FeCl_3$, and $AlCl_3$, have on the solubility of $CaSO_4$ phases in HCl or HCl + $CaCl_2$ solutions. There is currently limited work reported on the effect of metal chlorides on the solubility of $CaSO_4$ phases in particular in hot concentrated HCl solutions.

The solubility of calcium sulfate dihydrate at low temperature or anhydrite at elevated temperature in pure NaCl solutions was determined by many investigators. Raju and Atkinson (10) presented a comprehensive review of $CaSO_4$ solubility data in NaCl + H_2O system. Kruchenko (11) reported the solubility of gypsum (dihydrate) in aqueous solutions of $MgCl_2$ at (25, 40 and 50) °C. The results show that the solubility passes through a maximum at the concentration range of (0 to 35) % $MgCl_2$. Flint (12) investigated the effect of small additions of NaCl, $MgCl_2$, $AlCl_3$ and HCl on dihydrate solubility. According to Flint's work the uptake (solubility) of calcium sulfate by sea water brines increases from 0.8 % to (3 or 6) % by $AlCl_3$ or HCl respectively. Ostroff and

---

[1] See Chapter 3.

[2] See Chapter 4.

Metler (13) measured the solubility of dihydrate in mixed NaCl + $MgCl_2$ solutions with concentration range of (0.01 to 0.325) $mol{\cdot}kg^{-1}$ $MgCl_2$ up to 70 °C. Finally, the solubility of gypsum in aqueous electrolyte systems (such as NaCl and $MgCl_2$) of limited ionic strength at 25 °C was reported by Tanji (14) who also calculated these values with the aid of a computer program.

The above discussion suggests that there is still a requirement to systematically investigate the effects of various chloride salts on the solubility of calcium sulfate and its hydrates, especially in concentrated HCl – based solutions, this is done here for NaCl, $MgCl_2$, $FeCl_2$, $FeCl_3$, $AlCl_3$, $CaCl_2$ and their mixtures at over the temperature range (298 to 353) K.

6.3 Experimental Section

6.3.1 Chemicals

Analytically pure HCl, $CaCl_2{\cdot}2H_2O$, NaCl, $MgCl_2{\cdot}6H_2O$, $FeCl_2{\cdot}4H_2O$, $FeCl_3$ were supplied by Fisher with minimum purities of (36.5 to 38.0) %, 99.9 %, 99.9 %, 99.5 %, 99.9 % and 99.9 %, respectively. $AlCl_3$ (98.5 %) was supplied by Aldrich. All solutions were prepared by carefully weighing the appropriate quantities of acid or salts and de-ionized water into 1 L flasks. Three solid substances were employed as the saturating solid phase: Gypsum with 99 % purity that contained trace anhydrite ($CaSO_4$) was obtained from Alfa Aesar. Calcium sulfate hemihydrate (Plaster of Paris, also called beta-hemihydrate) was obtained from Fisher while anhydrite with 99 % purity was obtained from Alfa Aesar. De-ionized water with specific conductivity of 0.1 $\mu S{\cdot}cm^{-1}$ was used.

6.3.2 Procedure

The experimental technique used in the present work is the isothermal dissolution method that has been discussed in detail in an earlier report (1). To summarize: the method involves saturating aqueous electrolyte solutions with known composition with $CaSO_4$ solids in glass flasks thermostated at selected temperature with constant magnetic stirring. The temperature was controlled to ± 0.2 K. Five hours contact time was employed at 298 K to ensure the equilibration between calcium sulfate dihydrate or anhydrite and solution while 1 hour was used for hemihydrate saturation. At elevated temperatures, two hours instead of five hours was used since it was found to be adequate to ensure the attainment of equilibrium on one hand and on the other to minimize HCl and water vapor losses. After equilibration, the clear solution was sampled and filtered to determine the solution density at the temperature of the system. The measured densities were uncertain to ± 0.001 $g \cdot cm^{-3}$. Next, the filtered $CaSO_4$ saturated solution was diluted and its calcium or sulphur content was analyzed by ICP to determine the solubility. The triplicate determinations of dihydrate solubility in 1 $mol \cdot dm^{-3}$ HCl at ambient temperature were carried out. The uncertainty of the measured solubility values was within ± 0.111 $g \cdot dm^{-3}$ while the relative deviation was 0.77 %. The washed (with hot water and acetone) and dried solid phases were examined by XRD to determine whether the solid phase had been altered due to phase transformation during equilibration.

6.4 Results and Discussion

6.4.1 Solubility of $CaSO_4 \cdot 2H_2O$ in HCl + NaCl Solutions

Calcium sulfate dihydrate solubilities in mixed HCl (0.5 $mol \cdot dm^{-3}$) + NaCl solutions were measured at (323 and 353) K. The investigated concentration of NaCl is from (0.0 to 3) $mol \cdot dm^{-3}$ at ambient temperature. The results of experimentally determined solubilities are summarized in Table 6.1 and graphically in Figure 6.1. In Table 6.1 the concentration of HCl, NaCl and calcium sulfate ($CaSO_4$) is expressed both in concentration (c/mol·dm^{-3}) and molality (m/mol·kg^{-1}) for convenient practical and thermodynamic reference. However, the concentration of NaCl marked with c_3 is the initial concentration of the solution prepared at ambient temperature (24 ± 1 °C) before introducing calcium sulfate dihydrate. The other quantities of acid and salts in different units express the concentration at the conditions of the system. Figure 6.1 demonstrates that the solubility of dihydrate slightly increases with increasing NaCl concentration at 323 K while NaCl has limited effect on solubility of dihydrate in 0.5 mol·dm^{-3} HCl solutions at 353 K. For comparison the solubility of dihydrate in pure NaCl from Ostroff and Metler (12) is also included in Figure 6.1 (indicated with a dash line). It can be clearly seen that HCl causes a sharp increase of $CaSO_4$ (as DH) solubility.

Table 6.1. Solubility of $CaSO_4$ (1) as Dihydrate in 0.5 mol·dm^{-3} HCl (2) + NaCl (3) + H_2O (4)

solution parameters				solubility as $CaSO_4$ in different units		
c_3/ mol.dm^{-3a}	m_2/ mol·kg^{-1}	m_3/ mol·kg^{-1}	ρ_s / g·cm$^{-3\,b}$	γ_1/g·dm^{-3}	c_1/mol·dm^{-3}	m_1/ mol·kg^{-1}
			T = 323 K			
0.50	0.5089	0.5089	1.028	15.66	0.1150	0.1190
1.00	0.5137	1.0273	1.048	16.17	0.1187	0.1241
2.00	0.5236	2.0945	1.086	16.52	0.1213	0.1294
3.00	0.5369	3.2212	1.121	16.07	0.1180	0.1290
			T = 353 K			
0.50	0.5083	0.5083	1.114	21.24	0.1560	0.1496
1.00	0.5132	1.0265	1.169	21.32	0.1566	0.1471
2.00	0.5232	2.0928	1.225	21.81	0.1602	0.1519
3.00	0.5364	3.2186	1.277	21.36	0.1569	0.1508

[a] Initial concentration of solutions prepared at room temperature without calcium sulfate. [b] Experimental density of saturated solutions.

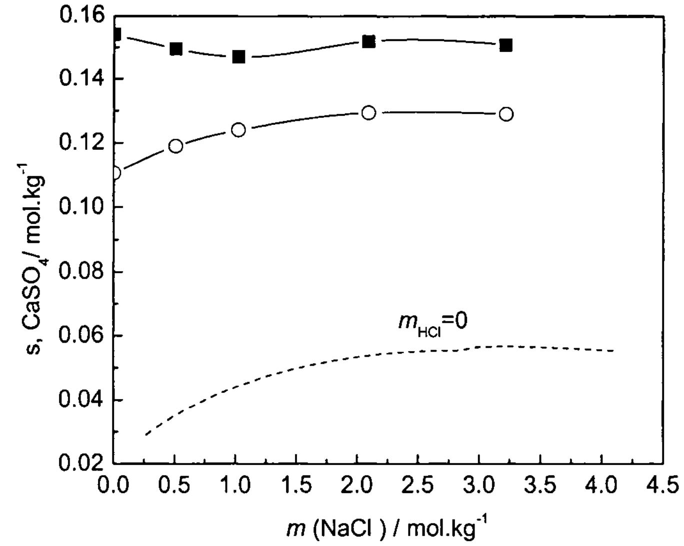

Figure 6.1. Solubility of calcium sulfate dihydrate in HCl (0.5 mol·dm^{-3}) + NaCl solutions: ○, 323 K; ■, 353 K; ----- , Ostroff and Metler[12] at 323 K.

6.4.2 Solubility of $CaSO_4{\cdot}2H_2O$ and $CaSO_4$ in HCl + $MgCl_2$ Solutions

The solubilities of calcium sulfate dihydrate and anhydrite in mixed HCl (0.5 and 3 mol·dm^{-3}) + $MgCl_2$ solutions are shown in Tables 6.2, 6.3 and 6.4, and also presented graphically in Figures 6.2, 6.3 and 6.4, respectively. The concentration of $MgCl_2$ investigated is in the range of (0 to 3) mol·dm^{-3}, and temperature range up to 353 K. As demonstrated in Figures 6.2 and 6.3 the solubility of dihydrate consistently increases with increasing temperature. It can be seen from Figure 6.2 that at low HCl concentration the solubility of dihydrate increases with increasing $MgCl_2$ concentration in the range of (0.0 to 0.5) mol·dm^{-3}. After passing a maximum, the solubility declines smoothly in the range of higher concentration of $MgCl_2$. However, addition of $MgCl_2$ in concentrated HCl solutions causes the solubility of dihydrate to decrease constantly as shown in Figure 6.3. These results show that the presence of $MgCl_2$ in HCl solutions markedly influences in a complex (unpredicted) fashion the dihydrate solubility. Similar trend is observed in the case of anhydrite solubility as illustrated in Figure 6.4.

Table 6.2. Solubility of $CaSO_4$ (1) as Dihydrate in 0.5 mol·dm^{-3} HCl (2) + $MgCl_2$ (3) + H_2O (4)

solution parameters				solubility as $CaSO_4$ in different units		
c_3/ mol.dm^{-3a}	m_2/ mol·kg^{-1}	m_3/ mol·kg^{-1}	ρ_s/ g·cm$^{-3\,b}$	γ_1/g·dm^{-3}	c_1/mol·dm^{-3}	m_1/ mol·kg^{-1}
			$T = 298$ K			
0.75	0.5128	0.7692	1.072	12.54	0.0921	0.0949
1.50	0.5222	1.5667	1.122	10.96	0.0805	0.0846
2.25	0.5340	2.4030	1.173	8.32	0.0611	0.0654
3.00	0.5459	3.2756	1.218	5.85	0.0430	0.0472
			$T = 323$ K			
0.75	0.5123	0.7685	1.065	15.99	0.1175	0.1222
1.50	0.5217	1.5651	1.117	14.51	0.1065	0.1129
2.25	0.5335	2.4009	1.167	11.41	0.0838	0.0905
3.00	0.5455	3.2730	1.212	8.50	0.0624	0.0690
			$T = 353$ K			
0.75	0.5115	0.7672	1.055	21.78	0.1600	0.1689
1.50	0.5209	1.5628	1.107	19.35	0.1421	0.1526
2.25	0.5327	2.3974	1.158	16.33	0.1199	0.1311
3.00	0.5449	3.2692	1.202	12.25	0.0900	0.1007

[a] Initial concentration of solutions prepared at room temperature without calcium sulfate. [b] Experimental density of saturated solutions.

Table 6.3. Solubility of $CaSO_4$ (1) as Dihydrate in 3 mol·dm^{-3} HCl (2) + $MgCl_2$ (3) + H_2O (4)

solution parameters				solubility as $CaSO_4$ in different units		
c_3/ mol.dm^{-3a}	m_2/ mol·kg^{-1}	m_3/ mol·kg^{-1}	ρ_s/ g·cm$^{-3\,b}$	γ_1/g·dm^{-3}	c_1/mol·dm^{-3}	m_1/ mol·kg^{-1}
			$T = 298$ K			
0.25	3.2034	0.2670	1.077	18.37	0.1349	0.1456
0.50	3.2255	0.5376	1.093	16.27	0.1195	0.1296
1.00	3.2683	1.0894	1.127	13.50	0.0992	0.1089
1.25	3.3009	1.3754	1.142	12.45	0.0914	0.1013
1.50	3.3232	1.6616	1.158	11.36	0.0834	0.0930
2.00	3.3790	2.2527	1.190	8.98	0.0659	0.0746
2.50	3.4419	2.8683	1.203	7.83	0.0575	0.0673
3.00	3.4932	3.4932	1.252	6.34	0.0466	0.0545

			$T = 323$ K			
0.25	3.1959	0.2663	1.074	26.23	0.1926	0.2099
0.50	3.2174	0.5362	1.090	24.79	0.1820	0.1996
1.00	3.2611	1.0870	1.123	20.83	0.1530	0.1697
1.25	3.2937	1.3724	1.136	19.65	0.1443	0.1616
1.50	3.3167	1.6584	1.154	17.76	0.1304	0.1468
2.00	3.3730	2.2487	1.186	14.83	0.1089	0.1243
2.50	3.4363	2.8636	1.213	13.18	0.0968	0.1128
3.00	3.4891	3.4891	1.243	10.01	0.0735	0.0870

[a] Initial concentration of solutions prepared at room temperature without calcium sulfate. [b] Experimental density of saturated solutions.

Table 6.4. Solubility of $CaSO_4$ (1) as Anhydrite in 3 mol·dm^{-3} HCl (2) + $MgCl_2$ (3) + H_2O (4)

solution parameters				solubility as $CaSO_4$ in different units		
c_3/ mol.dm^{-3a}	m_2/ mol·kg^{-1}	m_3/ mol·kg^{-1}	ρ_s / g·cm$^{-3\,b}$	γ_1/g·dm^{-3}	c_1/mol·dm^{-3}	m_1/ mol·kg^{-1}
			$T = 353$ K			
0.25	3.2203	0.2684	1.0586	24.81	0.1822	0.2015
0.50	3.2407	0.5401	1.0776	23.15	0.1700	0.1886
1.00	3.2812	1.0937	1.1059	18.77	0.1379	0.1552
1.25	3.3130	1.3804	1.1215	16.71	0.1228	0.1392
1.50	3.3344	1.6672	1.1377	14.89	0.1093	0.1247
2.00	3.3881	2.2588	1.1684	11.56	0.0849	0.0983
2.50	3.4503	2.8752	1.1980	9.41	0.0691	0.0814
3.00	3.5001	3.5001	1.2314	7.25	0.0533	0.0636

[a] Initial concentration of solutions prepared at room temperature without calcium sulfate. [b] Experimental density of saturated solutions.

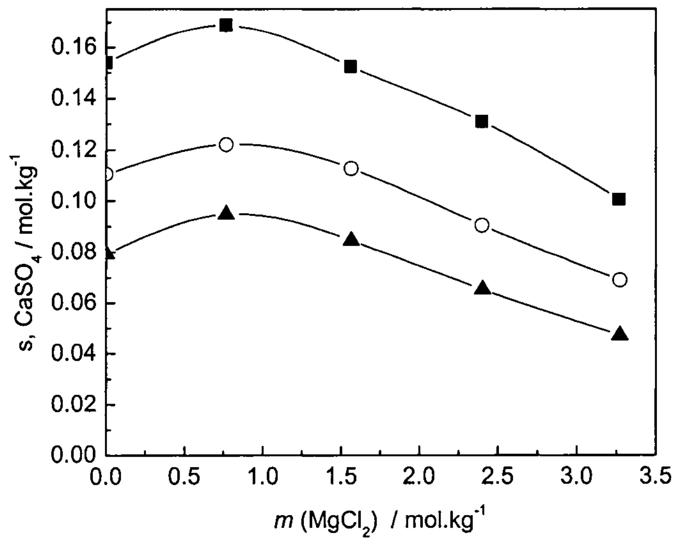

Figure 6.2. Solubility of calcium sulfate dihydrate in HCl (0.5 mol·dm^{-3}) + $MgCl_2$ solutions: ▲, 298 K; ○, 323 K; ■, 353 K.

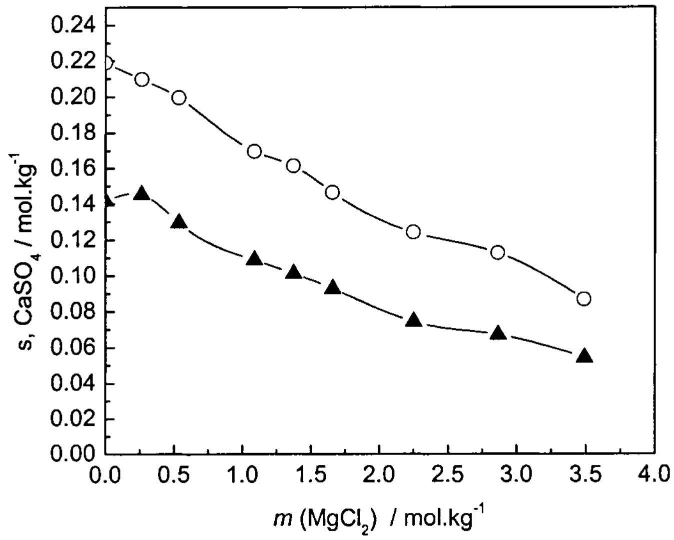

Figure 6.3. Solubility of calcium sulfate dihydrate in HCl (3 mol·dm^{-3}) + $MgCl_2$ solutions: ▲, 298 K; ○, 323 K.

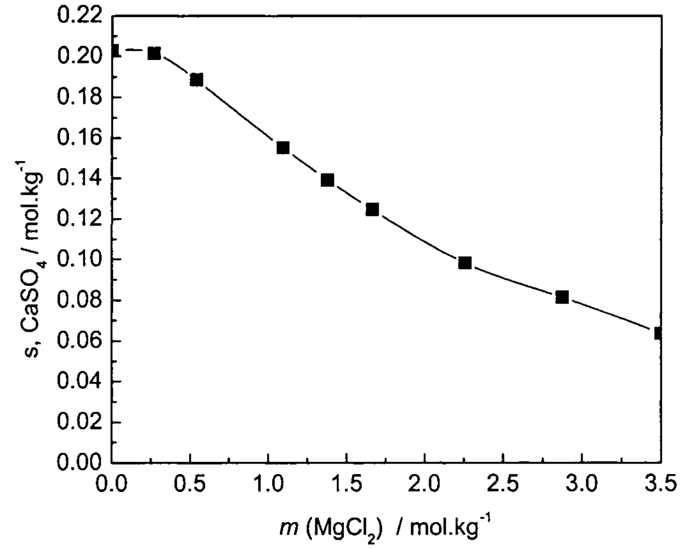

Figure 6.4. Solubility of calcium sulfate anhydrite in HCl (3 mol·dm^{-3}) + $MgCl_2$ solutions at 353 K.

6.4.3 Solubility of $CaSO_4 \cdot 2H_2O$ in $AlCl_3$ Solutions

The solubility data of calcium sulfate dihydrate in aqueous $AlCl_3$ solutions at (298, 323 and 353) K is shown in Table 6.5 and Figure 6.5. Figure 6.5 shows that an increase in temperature from (298 to 353) K leads to an increase in the solubility of dihydrate, but the position of the maximum on the diagram remains unchanged. A similar behavior was observed by Kruchenko (11) in the case of dihydrate solubility in $MgCl_2$ solutions. The two sets of data are compared in Figure 6.6. It can be seen that the dihydrate solubility in $AlCl_3$ solutions represented by solid lines is larger than that in $MgCl_2$ solutions. This may be due to partial hydrolysis of $AlCl_3$ that generates HCl hence the increase in solubility:

$$AlCl_{3(aq)} + H_2O \leftrightarrow AlOHCl_{2(aq)} + HCl \qquad (6.1)$$

Table 6.5. Solubility of $CaSO_4$ (1) as Dihydrate in $AlCl_3$(2) + H_2O(3)

solution parameters			solubility as $CaSO_4$ in different units		
c_2 /mol·dm^{-3} [a]	m_2/mol·kg^{-1}	ρ_s /g·cm^{-3} [b]	γ_l/g·dm^{-3}	c_l/mol·dm^{-3}	m_l/ mol·kg^{-1}
		$T = 298$ K			
0.25	0.2517	1.033	9.47	0.0695	0.0702
0.50	0.5080	1.065	10.95	0.0805	0.0815
1.00	1.0386	1.117	11.12	0.0817	0.0841
1.25	1.3144	1.140	10.33	0.0759	0.0789
1.50	1.5985	1.170	8.49	0.0624	0.0651
		$T = 323$ K			
0.25	0.2516	1.027	10.79	0.0792	0.0805
0.50	0.5077	1.057	13.01	0.0956	0.0977
1.00	1.0378	1.110	13.59	0.0998	0.1035
1.25	1.3137	1.137	12.21	0.0897	0.0936
1.50	1.5975	1.164	10.69	0.0785	0.0825
		$T = 353$ K			
0.25	0.2514	1.013	13.13	0.0965	0.0997
0.50	0.5071	1.045	16.82	0.1235	0.1282
1.00	1.0363	1.101	18.70	0.1373	0.1444
1.25	1.3115	1.128	17.90	0.1314	0.1390
1.50	1.5948	1.155	16.41	0.1206	0.1284

[a] Initial concentration of solutions prepared at room temperature without calcium sulfate. [b] Experimental density of saturated solutions.

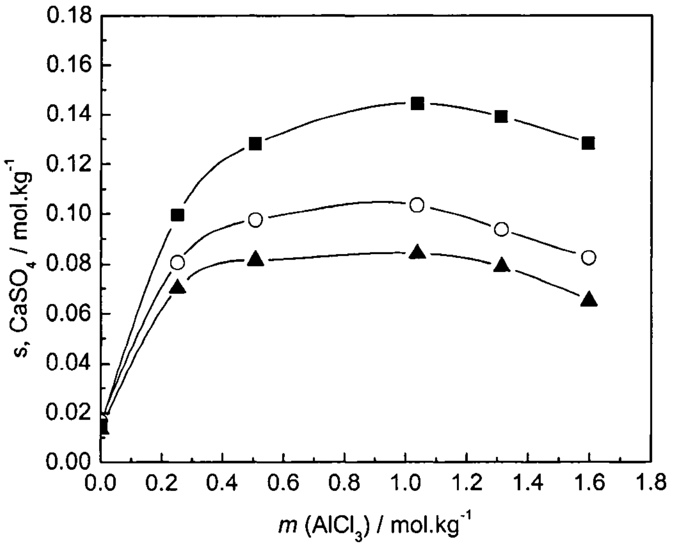

Figure 6.5. Solubility of calcium sulfate dihydrate in $AlCl_3$ solutions: ▲ , 298 K; ○ , 323 K; ■, 353 K.

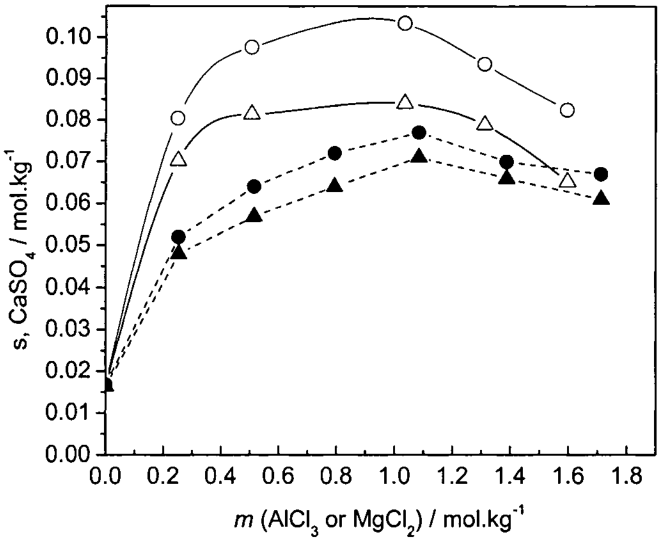

Figure 6.6. Comparison of dihydrate solubility in $MgCl_2$ and $AlCl_3$ solutions:▲ , $MgCl_2$ at 298 K;[11] ●, $MgCl_2$ at 323 K;[11] △, $AlCl_3$ at 298 K; ○, $AlCl_3$ at 323 K.

6.4.4 Solubility of $CaSO_4{\cdot}2H_2O$ in HCl + $AlCl_3$ Solutions

The solubility of calcium sulfate dihydrate in $AlCl_3$ + HCl solutions with two HCl concentration levels of (0.5 and 3) mol·dm^{-3} from (298 to 353) K was measured and listed in Tables 6.6 and 6.7 and Figures 6.7 and 6.8. Figure 6.7 shows that in 0.5 mol·dm^{-3} HCl the solubility of calcium sulfate dihydrate increases with increasing $AlCl_3$ concentration at first, passes through a maximum and then decreases with further addition of $AlCl_3$. However, at the higher HCl concentration (i.e. 3.0 mol·dm^{-3}) the presence of $AlCl_3$ causes the solubility of dihydrate monotonically to decrease as depicted in Figure 6.8.

Table 6.6. Solubility of $CaSO_4$ (1) as Dihydrate in 0.5 mol·dm^{-3} HCl (2) + $AlCl_3$ (3) + H_2O (4)

solution parameters				solubility as $CaSO_4$ in different units		
c_3/ mol.dm^{-3a}	m_2/ mol·kg^{-1}	m_3/ mol·kg^{-1}	ρ_s/ g·cm$^{-3\,b}$	γ_1/g·dm^{-3}	c_1/mol·dm^{-3}	m_1/ mol·kg^{-1}
			$T = 298$ K			
0.50	0.5085	0.5085	1.075	14.16	0.1040	0.1065
1.00	0.5162	1.0325	1.127	11.96	0.0879	0.0911
1.50	0.5187	1.5561	1.180	8.67	0.0637	0.0667
2.00	0.5323	2.1292	1.227	6.37	0.0468	0.0499
			$T = 323$ K			
0.50	0.5079	0.5079	1.069	18.81	0.1382	0.1428
1.00	0.5156	1.0312	1.124	16.43	0.1206	0.1259
1.50	0.5181	1.5543	1.172	12.69	0.0932	0.0986
2.00	0.5318	2.1271	1.221	9.72	0.0714	0.0768
			$T = 353$ K			
0.50	0.5069	0.5069	1.061	25.70	0.1888	0.1980
1.00	0.5145	1.0290	1.113	23.60	0.1734	0.1838
1.50	0.5170	1.5511	1.167	19.97	0.1467	0.1566
2.00	0.5307	2.1229	1.212	16.43	0.1207	0.1314

[a] Initial concentration of solutions prepared at room temperature without calcium sulfate. [b] Experimental density of saturated solutions.

Table 6.7. Solubility of $CaSO_4$ (1) as Dihydrate in 3 mol·dm^{-3} HCl (2) + $AlCl_3$ (3) + H_2O (4)

solution parameters				solubility as $CaSO_4$ in different units		
c_3/ mol.dm^{-3a}	m_2/ mol·kg^{-1}	m_3/ mol·kg^{-1}	ρ_s/ g·cm$^{-3\,b}$	γ_1/g·dm^{-3}	c_1/mol·dm^{-3}	m_1/ mol·kg^{-1}
			$T = 298$ K			
0.50	3.2228	0.5371	1.113	14.83	0.1089	0.1179
1.00	3.2625	1.0875	1.166	10.48	0.0770	0.0842
1.50	3.3197	1.6599	1.215	7.51	0.0551	0.0613
			$T = 323$ K			
0.50	3.2162	0.5360	1.109	21.68	0.1593	0.1741
1.00	3.2563	1.0854	1.161	16.96	0.1246	0.1376
1.50	3.3144	1.6572	1.208	12.86	0.0945	0.1060

[a] Initial concentration of solutions prepared at room temperature without calcium sulfate. [b] Experimental density of saturated solutions.

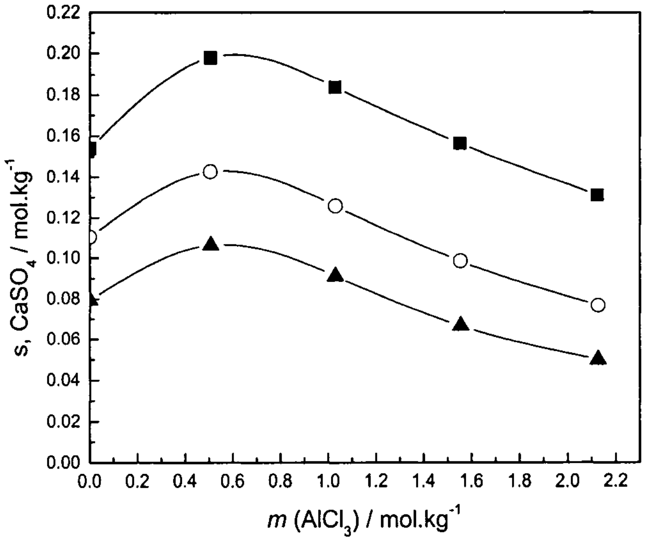

Figure 6.7. Solubility of calcium sulfate dihydrate in HCl (0.5 mol·dm^{-3}) + $AlCl_3$ solutions: ▲, 298 K; ○, 323 K; ■, 353 K.

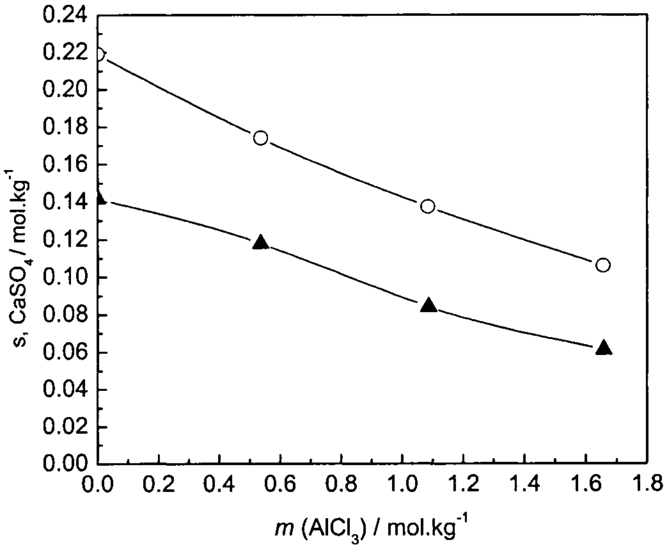

Figure 6.8. Solubility of calcium sulfate dihydrate in HCl (3 mol·dm^{-3}) + $AlCl_3$ solutions: ▲, 298 K; ○, 323 K.

6.4.5 Solubility of $CaSO_4 \cdot 2H_2O$ in HCl + $FeCl_2$ or $FeCl_3$ Solutions

The experimental data of solubility of dihydrate in aqueous solutions containing HCl (0.5 mol·dm^{-3}) + $FeCl_2$ at (323 and 353) K were determined and shown in Table 6.8 and Figure 6.9. Figure 6.9 shows the dihydrate solubility to increase with increasing concentration of $FeCl_2$ up to certain level and then to decrease with further increase in $FeCl_2$ concentration. In addition, the influence of $FeCl_3$ in HCl solutions from (0.5 or 3) mol·dm^{-3} on the solubility of dihydrate was investigated and the results are given in Tables 6.9 and 6.10 and Figures 6.10 and 6.11. Once more, upon an increase in $FeCl_3$ concentration the solubility of dihydrate in 0.5 mol·dm^{-3} HCl solutions increases up to a certain level and thereafter decreases while the solubility of dihydrate in 3 mol·dm^{-3} HCl constantly decreases with increasing $FeCl_3$ concentration.

Table 6.8. Solubility of $CaSO_4$ (1) as Dihydrate in 0.5 mol·dm^{-3} HCl (2) + $FeCl_2$ (3) + H_2O (4)

solution parameters				solubility as $CaSO_4$ in different units		
c_3/ mol.dm^{-3a}	m_2/ mol·kg^{-1}	m_3/ mol·kg^{-1}	ρ_s / g·cm$^{-3\,b}$	γ_1/g·dm^{-3}	c_1/mol·dm^{-3}	m_1/ mol·kg^{-1}
			$T = 323$ K			
1.00	0.5148	1.0297	1.117	16.46	0.1209	0.1261
1.50	0.5175	1.5525	1.166	15.21	0.1117	0.1180
2.00	0.5292	2.1166	1.212	13.31	0.0978	0.1050
3.00	0.5460	3.2760	1.306	9.88	0.0725	0.0803
			$T = 353$ K			
1.00	0.5140	1.0281	1.103	21.62	0.1588	0.1686
1.50	0.5167	1.5500	1.154	20.67	0.1518	0.1627
2.00	0.5283	2.1132	1.203	18.84	0.1384	0.1503
3.00	0.5451	3.2708	1.295	15.03	0.1104	0.1237

[a] Initial concentration of solutions prepared at room temperature without calcium sulfate. [b] Experimental density of saturated solutions.

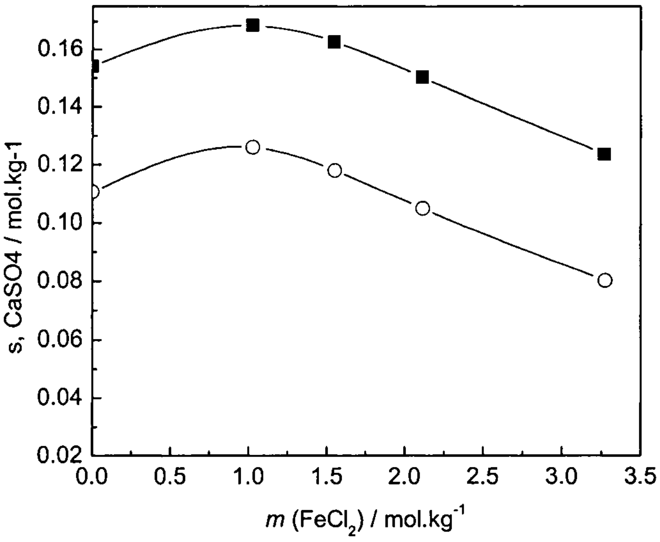

Figure 6.9. Solubility of calcium sulfate dihydrate in HCl (0.5 mol·dm^{-3}) + $FeCl_2$ solutions: ○, 323 K; ■, 353 K.

Table 6.9. Solubility of $CaSO_4$ (1) as Dihydrate in 0.5 mol·dm^{-3} HCl (2) + $FeCl_3$ (3) + H_2O (4)

solution parameters				solubility as $CaSO_4$ in different units		
c_3/ mol.dm^{-3a}	m_2/ mol·kg^{-1}	m_3/ mol·kg^{-1}	ρ_s / g·cm$^{-3\,b}$	γ_1/g·dm^{-3}	c_1/mol·dm^{-3}	m_1/ mol·kg^{-1}
			T = 323 K			
0.50	0.5125	0.5125	1.079	22.25	0.1635	0.1703
1.00	0.5222	1.0444	1.136	21.82	0.1602	0.1708
1.50	0.5368	1.6105	1.190	18.50	0.1359	0.1485
2.00	0.5455	2.1820	1.253	14.64	0.1075	0.1192
			T = 353 K			
0.50	0.5114	0.5114	1.068	29.29	0.2151	0.2282
1.00	0.5211	1.0422	1.125	28.77	0.2113	0.2289
1.50	0.5356	1.6067	1.180	26.18	0.1923	0.2133
2.00	0.5443	2.1772	1.239	21.69	0.1593	0.1796

[a] Initial concentration of solutions prepared at room temperature without calcium sulfate. [b] Experimental density of saturated solutions.

Table 6.10. Solubility of $CaSO_4$ (1) as Dihydrate in 3 mol·dm^{-3} HCl (2) + $FeCl_3$ (3) + H_2O (4)

solution parameters				solubility as $CaSO_4$ in different units		
c_3/ mol.dm^{-3a}	m_2/ mol·kg^{-1}	m_3/ mol·kg^{-1}	ρ_s / g·cm$^{-3\,b}$	γ_1/g·dm^{-3}	c_1/mol·dm^{-3}	m_1/ mol·kg^{-1}
			$T = 298$ K			
0.50	3.2541	0.5424	1.118	15.86	0.1165	0.1275
1.00	3.3377	1.1126	1.175	12.50	0.0918	0.1028
1.50	3.4253	1.7126	1.233	9.70	0.0713	0.0817
2.00	3.5130	2.3420	1.290	7.74	0.0569	0.0669
			$T = 323$ K			
0.50	3.2468	0.5411	1.114	23.37	0.1717	0.1899
1.00	3.3307	1.1102	1.169	19.37	0.1423	0.1610
1.50	3.4191	1.7096	1.225	15.46	0.1135	0.1315
2.00	3.5075	2.3383	1.277	12.57	0.0923	0.1100

[a] Initial concentration of solutions prepared at room temperature without calcium sulfate. [b] Experimental density of saturated solutions.

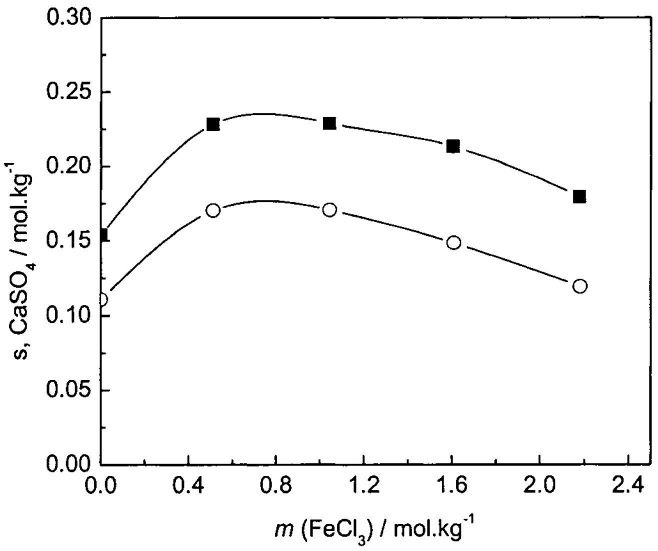

Figure 6.10. Solubility of calcium sulfate dihydrate in HCl (0.5 mol·dm^{-3}) + $FeCl_3$ solutions: ○, 323 K; ■, 353 K.

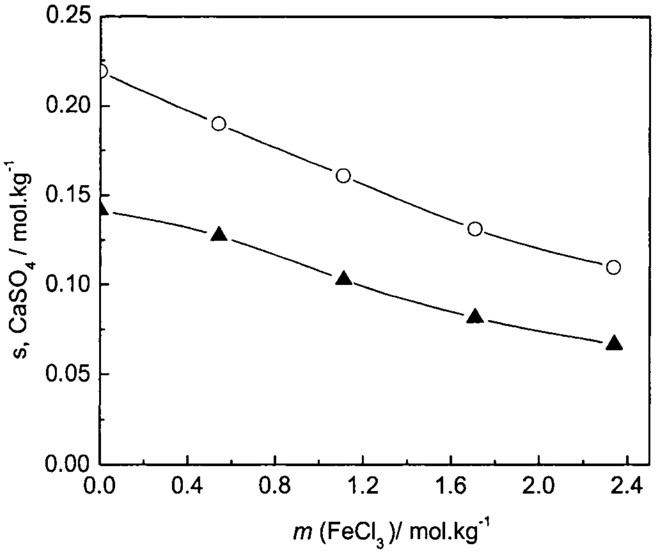

Figure 6.11. Solubility of calcium sulfate dihydrate in HCl (3 mol·dm^{-3}) + $FeCl_3$ solutions: ▲, 298 K; o, 323 K.

6.4.6 Comparison of Solubility Data

The effect of the various chloride salts at 323 K on the solubility of dihydrate in (0.5 and 3) mol·dm^{-3} HCl solutions is compared in Figures 6.12 to 6.15. Figure 6.12 depicts the influence of NaCl, $MgCl_2$, $FeCl_2$, $FeCl_3$ and $AlCl_3$ in 0.5 mol·dm^{-3} HCl solutions on dihydrate solubility as a function of chloride concentration. It is interesting to note that with the exception of largely $FeCl_3$ the effect of the other metal chlorides is proportional to their chloride content. In the case of $FeCl_3$, the solubility of dihydrate increases substantially greater than with the other salts although still it follows the shoulder – type dependency. Figure 6.13 provides a comparison of the same solubility data (as in Figure 6.12) but this time in terms of ionic strength[3]. This time the effect is somewhat magnified with $AlCl_3$ clearly separated from the divalent chloride salts. Similarly, Figures 6.14 and 6.15 show the respective data for dihydrate solubility in 3

---

[3] This is the nominal ionic strength; i.e. full dissociation of all electrolytes is assumed in calculating I. (Footnote added after publication of paper)

mol·dm^{-3} HCl as a function of total chloride concentration and ionic strength, respectively.

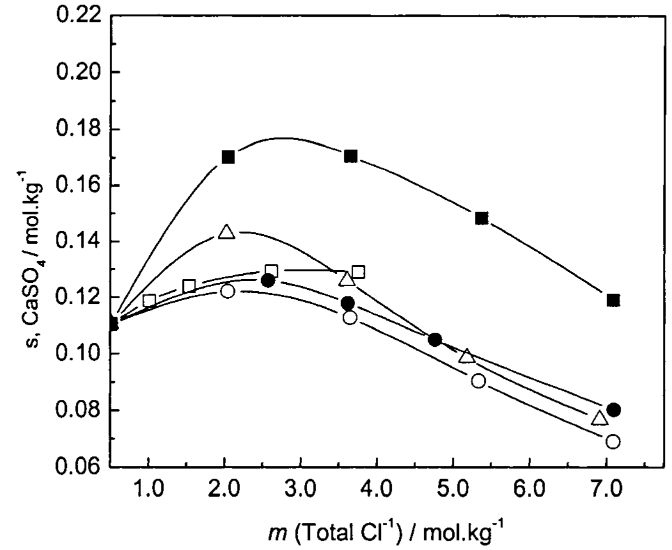

Figure 6.12. Comparison of dihydrate solubility in HCl (0.5 mol·dm^{-3}) + various chloride salts solutions versus total concentration of chloride at 323 K: □, NaCl; ○, MgCl$_2$; △, AlCl$_3$; ●, FeCl$_2$; ■, FeCl$_3$.

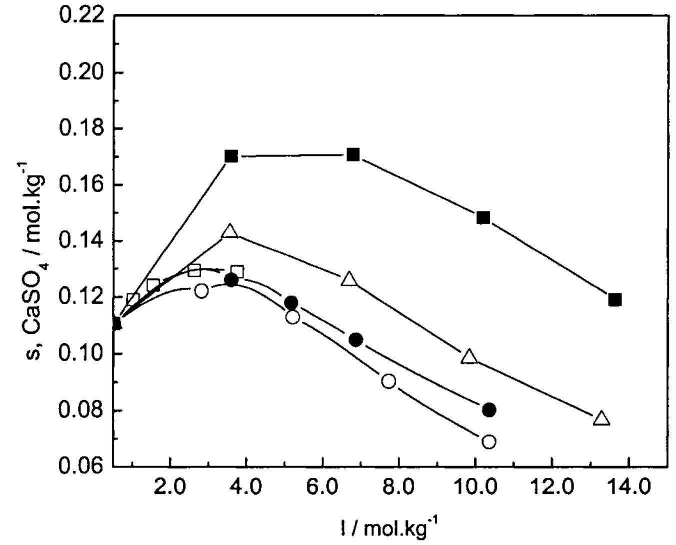

Figure 6.13. Comparison of dihydrate solubility in HCl (0.5 mol·dm^{-3}) + various chloride salts solutions versus nominal ionic strength at 323 K: □, NaCl; ○, MgCl$_2$; △, AlCl$_3$; ●, FeCl$_2$; ■, FeCl$_3$.

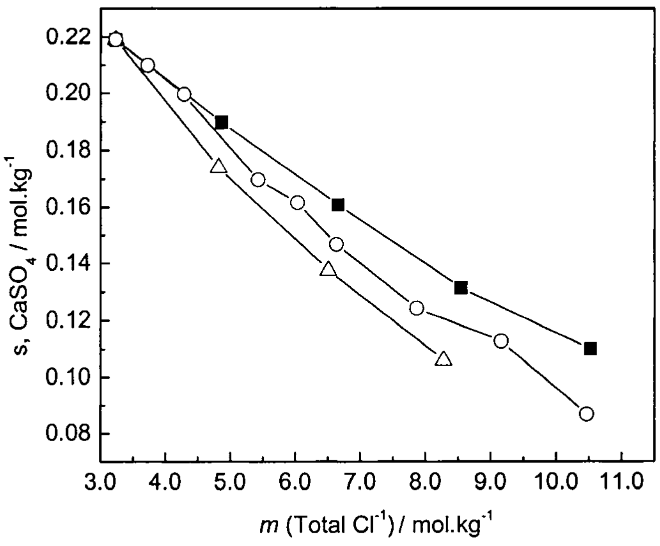

Figure 6.14. Comparison of dihydrate solubility in HCl (3 mol·dm^{-3}) + various chloride salts solutions versus total concentration of chloride at 323 K: ○, $MgCl_2$; △, $AlCl_3$; ■, $FeCl_3$.

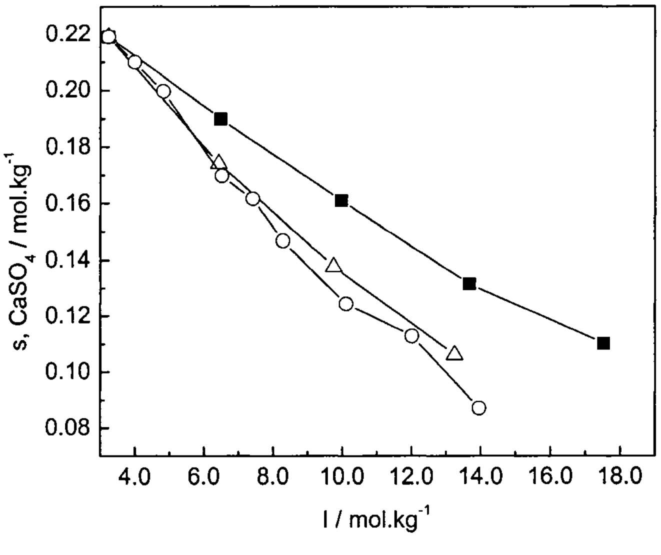

Figure 6.15. Comparison of dihydrate solubility in HCl (3 mol·dm^{-3}) + various chloride salts solutions versus ionic strength at 323 K: ○, $MgCl_2$; △, $AlCl_3$; ■, $FeCl_3$.

6.4.7 Solubility of $CaSO_4 \cdot 2H_2O$ in HCl + Chloride Salts + $CaCl_2$ Solutions

In this section the effect of $CaCl_2$ on the solubility of dihydrate in aqueous HCl (0.5 mol·dm^{-3}) + various chloride salt solutions was investigated at 323 K. The solubility of dihydrate in HCl (0.5 mol·dm^{-3}) + $MgCl_2$ (1 mol·dm^{-3}) + $CaCl_2$ at 323 K is listed in Table 6.11 and presented graphically in Figure 6.16. Figure 6.16 shows that the solubility of dihydrate consistently decreases with increasing concentration of $CaCl_2$ due to the common ion effect. In addition, the solubility of $CaSO_4$ as dihydrate in 0.5 mol·dm^{-3} HCl + chloride salts (NaCl, $MgCl_2$, $FeCl_2$, $FeCl_3$ and $AlCl_3$ with 0.5 mol·dm^{-3} concentration for each salt) + $CaCl_2$ solutions at 323 K was determined and given in Table 6.12. Similar trend with that of Figure 6.16 was observed, i.e. systematic decrease of solubility with increasing $CaCl_2$ concentration.

Table 6.11. Solubility of $CaSO_4$ (1) as Dihydrate in 0.5 mol·dm^{-3} HCl (2) + 1 mol·dm^{-3} $MgCl_2$ (3) + $CaCl_2$ (4) + H_2O (5) at 323 K

solution parameters				solubility as $CaSO_4$ in different units			
c_4/ mol.dm^{-3a}	m_2/ mol·kg^{-1}	m_3/ mol·kg^{-1}	m_4/ mol·kg^{-1}	ρ_s/ g·cm$^{-3\,b}$	γ_1/ g·dm^{-3}	c_1/ mol·dm^{-3}	m_1/ mol·kg^{-1}
0.25	0.5203	1.0406	0.2601	1.094	6.78	0.0498	0.0525
0.50	0.5210	1.0419	0.5210	1.115	3.54	0.0260	0.0275
1.00	0.5325	1.0649	1.0649	1.153	1.56	0.0115	0.0124
1.50	0.5440	1.0879	1.6319	1.190	0.86	0.0063	0.0069

[a] Initial concentration of solutions prepared at room temperature without calcium sulfate. [b] Experimental density of saturated solutions.

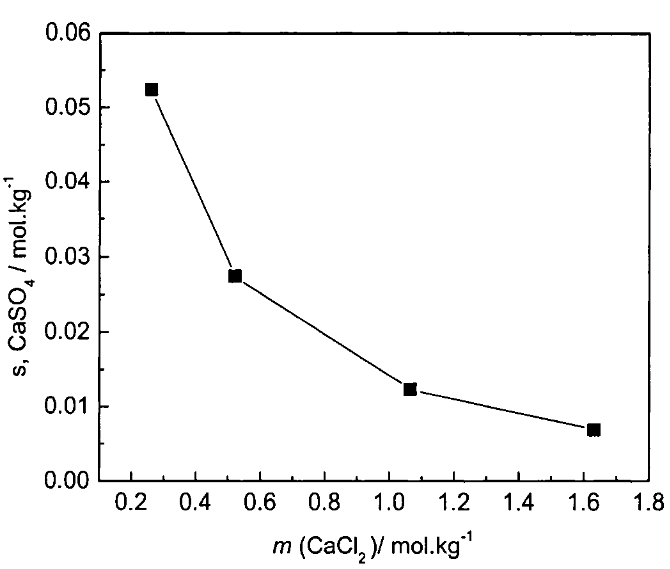

Figure 6.16. Solubility of calcium sulfate dihydrate in HCl (0.5 mol·dm^{-3}) + $MgCl_2$ (1 mol·dm^{-3}) + $CaCl_2$ solutions at 323 K.

Table 6.12. Solubility of $CaSO_4$ (1) as Dihydrate in 0.5 mol·dm^{-3} HCl (2) + 0.5 mol·dm^{-3} Chloride Salts (3) + $CaCl_2$ (4) + H_2O (5) at 323 K

solution parameters				solubility as $CaSO_4$ in different units			
c_4/ mol.dm^{-3a}	m_2/ mol·kg^{-1}	m_3/ mol·kg^{-1c}	m_4/ mol·kg^{-1}	ρ_s/ g·cm$^{-3\,b}$	γ_1/ g·dm^{-3}	c_1/ mol·dm^{-3}	m_1/ mol·kg^{-1}
0.25	0.5467	0.5467	0.2734	1.237	3.62	0.0266	0.0294
0.50	0.5499	0.5499	0.5499	1.251	1.75	0.0128	0.0144
1.00	0.5653	0.5653	1.1306	1.288	0.70	0.0052	0.0059
1.50	0.5779	0.5779	1.7336	1.326	0.39	0.0029	0.0033

[a] Initial concentration of solutions prepared at room temperature without calcium sulfate. [b] Experimental density of saturated solutions. [c] The concentration of individual salt (NaCl, $MgCl_2$, $FeCl_2$, $FeCl_3$ and $AlCl_3$).

6.4.8 Solubility of $CaSO_4$·$0.5H_2O$ in HCl + Chloride Salts + $CaCl_2$ Solutions

In this section the effect of $CaCl_2$ on the solubility of hemihydrate in aqueous HCl (6 mol·dm^{-3}) + various chloride salt solutions was determined at 333 K. The solubility of hemihydrate in HCl (6 mol·dm^{-3}) + $MgCl_2$ (1 mol·dm^{-3}) + $CaCl_2$ at 333 K is recorded in Table 6.13 and graphically illustrated in Figure 6.17. It can be seen from this Figure that the solubility of hemihydrate consistently decreases with increasing concentration of

$CaCl_2$ due to the common ion effect. Similar results were obtained in the case of solubility of hemihydrate in HCl (6 mol·dm^{-3}) + $FeCl_2$ (0.2 mol·dm^{-3}) + $CaCl_2$ at 333 K (data recorded in Table 6.14) and in 6mol·dm^{-3} HCl + chloride salts ($MgCl_2$, $FeCl_3$, $FeCl_2$ and $AlCl_3$ with 0.2 mol·dm^{-3} concentration for each salt) + $CaCl_2$ solutions at 333 K (data recorded in Table 6.15).

Table 6.13. Solubility of $CaSO_4$ (1) as Hemihydrate in 6 mol·dm^{-3} HCl (2) + 1 mol·dm^{-3} $MgCl_2$ (3) + $CaCl_2$ (4) + H_2O (5) at 333 K

solution parameters				solubility as $CaSO_4$ in different units			
c_4/ mol.dm^{-3}[a]	m_2/ mol·kg^{-1}	m_3/ mol·kg^{-1}	m_4/ mol·kg^{-1}	ρ_s/ g·cm^{-3}[b]	y_1/ g·dm^{-3}	c_1/ mol·dm^{-3}	m_1/ mol·kg^{-1}
0.25	7.1519	1.1920	0.2980	1.165	6.22	0.0457	0.0554
0.50	7.2324	1.2054	0.6027	1.181	3.04	0.0223	0.0274
1.00	7.3901	1.2317	1.2317	1.218	1.27	0.0093	0.0116
1.50	7.5826	1.2638	1.8956	1.253	0.72	0.0053	0.0068

[a] Initial concentration of solutions prepared at room temperature without calcium sulfate. [b] Experimental density of saturated solutions.

Table 6.14. Solubility of $CaSO_4$ (1) as Hemihydrate in 6 mol·dm^{-3} HCl (2) + 0.2 mol·dm^{-3} $FeCl_2$ (3) + $CaCl_2$ (4) + H_2O (5) at 333 K

solution parameters				solubility as $CaSO_4$ in different units			
c_4/ mol.dm^{-3}[a]	m_2/ mol·kg^{-1}	m_3/ mol·kg^{-1}	m_4/ mol·kg^{-1}	ρ_s/ g·cm^{-3}[b]	y_1/ g·dm^{-3}	c_1/ mol·dm^{-3}	m_1/ mol·kg^{-1}
0.25	6.9457	0.2315	0.2894	1.1254	11.38	0.0836	0.0987
0.50	6.9637	0.2321	0.5803	1.1380	6.12	0.0449	0.0535
1.00	7.1520	0.2384	1.1920	1.1763	2.33	0.0171	0.0207
1.50	7.3149	0.2438	1.8287	1.2097	1.23	0.0091	0.0112

[a] Initial concentration of solutions prepared at room temperature without calcium sulfate. [b] Experimental density of saturated solutions.

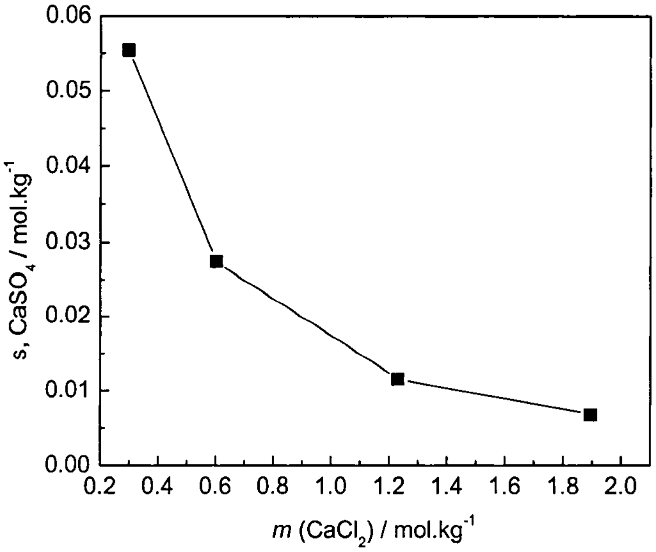

Figure 6.17. Solubility of calcium sulfate hemihydrate in HCl (6 mol·dm^{-3}) + MgCl$_2$ (1 mol·dm^{-3}) + CaCl$_2$ solutions at 333 K.

Table 6.15. Solubility of CaSO$_4$ (1) as Hemihydrate in 6 mol·dm^{-3} HCl (2) + 0.1 mol·dm^{-3} Chloride Salts (3) + CaCl$_2$ (4) + H$_2$O (5) at 333 K

solution parameters				solubility as CaSO$_4$ in different units			
c_4/ mol.dm^{-3a}	m_2/ mol·kg^{-1}	m_3/ mol·kg^{-1c}	m_4/ mol·kg^{-1}	ρ_s/ g·cm$^{-3\,b}$	γ_1/ g·dm^{-3}	c_1/ mol·dm^{-3}	m_1/ mol·kg^{-1}
0.25	7.0134	0.1169	0.2922	1.138	9.51	0.0699	0.0835
0.50	7.0329	0.1172	0.5861	1.149	5.01	0.0368	0.0445
1.00	7.2282	0.1205	1.2047	1.192	1.89	0.0139	0.0170
1.50	7.3788	0.1230	1.8447	1.225	1.01	0.0074	0.0094

[a] Initial concentration of solutions prepared at room temperature without calcium sulfate. [b] Experimental density of saturated solutions. [c] The concentration of individual salt (MgCl$_2$, FeCl$_2$, FeCl$_3$ and AlCl$_3$).

6.4.9 Identification of Equilibrated Solids

Partial results of solids characterization by XRD following the completion of the various solubility tests are tabulated in Table 6.16. The dihydrate in 3 mol·dm^{-3} HCl + 3 mol·dm^{-3} MgCl$_2$ solution at 323 K was converted to hemihydrate within the time of 5 hours while in 3 mol·dm^{-3} HCl + 2 mol·dm^{-3} MgCl$_2$ solution at 323 K no hemihydrate and anhydrite were detected in equilibrated solids. The solubility data presented in Tables 6.1 to 6.12, though, is for DH only, i.e. the data associated with conversion of DH to HH are excluded. It can be observed from Table 6.16 that the presence of $CaCl_2$ in HCl suppressed the transformation of hemihydrate to anhydrite, hence making possible the determination of its solubility by this isothermal dissolution method. The solubility data reported in Tables 6.13 to 6.15 refer to HH as the only equilibrated phase.

Table 6.16. XRD Characterization of the Equilibrated Solids with Equilibrium Time

T/K	c/mol·dm^{-3}	t/h	Equilibrated solid phase(s)[a]	Table
	Starting material is calcium sulfate dihydrate			
298	0.5(HCl) + 3($MgCl_2$)	5	DH	2
323	3(HCl) + 2($MgCl_2$)	5	DH	3
323	3(HCl) + 3($MgCl_2$)	5	HH	
323	3(HCl) + 3($MgCl_2$)	2	DH	3
353	1.5($AlCl_3$)	5	DH	5
323	3(HCl) +1.5($AlCl_3$)	5	DH	7
353	0.5(HCl) + 2($AlCl_3$)	2	DH	6
353	0.5(HCl) + 2($FeCl_3$)	2	DH	9
323	3(HCl) + 2($FeCl_3$)	5	DH	10
353	0.5(HCl) + 3($FeCl_2$)	2	DH	8
323	0.5(HCl) + 0.5 (NaCl, $MgCl_2$, $FeCl_2$, $FeCl_3$ and $AlCl_3$) + 1.5($CaCl_2$)	5	DH	12
	Starting material is β - calcium sulfate hemihydrate			
333	6(HCl) + 1($MgCl_2$) + 0.25($CaCl_2$)	1	HH	13
333	6(HCl) + 1($MgCl_2$) + 0.5($CaCl_2$)	1	HH	13
333	6(HCl) + 1($MgCl_2$) + 1($CaCl_2$)	1	HH	13
333	6(HCl) + 1($MgCl_2$) + 1.5($CaCl_2$)	1	HH	13

[a] DH - $CaSO_4 \cdot 2H_2O$; HH - $CaSO_4 \cdot 0.5H_2O$.

6.5 Conclusions

The effect of various chloride salts, such as NaCl, $CaCl_2$, $MgCl_2$, $FeCl_2$, $FeCl_3$ and $AlCl_3$ on the solubility of three $CaSO_4$ modifications, namely dihydrate, hemihydrate and anhydrite, in HCl solutions has been investigated. The solubility of dihydrate increases with increasing concentration of $MgCl_2$, $FeCl_2$, $FeCl_3$ and $AlCl_3$ up to a certain level thereafter decreasing with further increase of metal chloride concentration when the HCl concentration is 0.5 $mol{\cdot}dm^{-3}$. However, in the case of 3 $mol{\cdot}dm^{-3}$ HCl concentration the solubility of dihydrate consistently decreases with increasing metal chloride concentration. Comparing with divalent chloride salts ($MgCl_2$ and $FeCl_2$), the trivalent chloride salts $AlCl_3$ and $FeCl_3$ were found to have a larger influence on the solubility of dihydrate for same ionic strength. $CaCl_2$, owing to the common ion effect, causes the solubility of dihydrate and hemihydrate in the system HCl + various chloride salts + H_2O to decrease.

Acknowledgement

The support of Hatch, Noranda, Process Research Ortech and NSERC (Natural Sciences and Engineering Research Council of Canada) is gratefully acknowledged.

6.6 Literature Cited

(1) Li, Zhibao; Demopoulos, G. P. Solubility of $CaSO_4$ Phases in Aqueous HCl + $CaCl_2$ from 283 K to 353 K. *J. Chem. Eng. Data* **2005**, *50*, 1971 - 1982 .

(2) Li, Zhibao; Demopoulos, G. P. Development of an Improved Chemical Model for the Estimation of $CaSO_4$ Solubilities in the HCl + $CaCl_2$ + H_2O System up to 100 °C. *Ind. Eng. Chem. Res.* **2005**, in press.

(3) Girgin, S.; Demopoulos, G. P. Production of the High Value Material, Alpha-$CaSO_4$ Hemihydrate out of Spent $CaCl_2$ Solutions by Reaction with H_2SO_4. in *EPD Congress 2004*; Schlesinger, M. E. Ed.; TMS: Warrendale, Pa, 2004, 627-639.

(4) Al-Othman, A.; Cheng, T. C.; Demopoulos, G. P. Regeneration of HCl and Production of Saleable Gypsum by Reaction of Spent $CaCl_2$ Leach Solutions with H_2SO_4. in *Proceedings of Fifth International Symposium on Waste Processing and Recycling in Mineral and Metallurgical Industries*; Rao, S. R. *et al.* Eds.; CIM: Montreal, 2004, 453-467.

(5) Li, Zhibao; Demopoulos, G. P. $CaSO_4$ Solubilities in Concentrated Aqueous Chloride Solutions. In *Chloride Metallurgy 2002: International Conference on Practice and Theory of Chloride/Metal Interaction*; Peek, E., Van Weert, G. Eds; CIM: Montreal, 2002, 561-574.

(6) Dutrizac, J. E. Sulphate Control in Chloride Leaching Processes. *Hydrometallurgy* **1989**, *23*, 1-22.

(7) Borowiec, K.; Grau, A. E.; Gueguin, M.;Turgeon, J. F. Method to Upgrade Titania Slag and Resulting Product. *US Patent*, No. 5,830,420, Nov. 3, 1998.

(8) Ficara, P.; Chin, E.; Walker, T.; Laroche, D.; Palumbo, E.; Celik, C.; Avedesian, M. Magnola: A Novel Commercial Process for the Primary Production of Magnesium. *CIM Bulletin* **1998**, *91*, 75-80.

(9) McElroy, R. O.; Murray, W. Developments in the Terra Gaia Process for the Treatment of EAF Dust. *Iron Control in Hydrometallurgy*, Dutrizac, J. E.; Harris, G. B. Eds, CIM, Montreal, 1996, 505-517.

(10) Raju, K. U. G.; Atkinson G. The Thermodynamics of “Scale” Mineral Solubilities. 3. Calcium Sulfate in Aqueous NaCl. *J. Chem. Eng. Data* **1990**, *35*, 361-367.

(11) Kruchenko, V. P. The Solubilities of Gypsum in Aqueous Solutions of Magnesium Salts at 25, 40, and 50 °C. *Rus. J. Inorg. Chem.* **1985**, *30*, 892-895.

(12) Flint O. Increased Solubility of Calcium Sulphate in Sea Water Containing Hydrochloric Acid. *Desalination* **1968**, *4*, 328-335.

(13) Ostroff, A. G.; Metler, A. V. Solubility of Calcium Sulfate Dihydrate in the System NaCl-$MgCl_2$-H_2O from 28 ° to 70 °C. *J. Chem. Eng. Data* **1966**, *11*, 346-350.

(14) Tanji, K. K. Solubility of Gypsum in Aqueous Electrolytes as Affected by Ion Association and Ionic Strengths up to 0.15 M and at 25 °C. *Environ. Sci. Technol.* **1969**, 3, 656-661.

Chapter 7

A Speciation-Based Chemical Equilibrium Model of $CaSO_4$ Solubility in the H + Na + Ca + Mg + Al + Fe(II) + Cl + H_2O System

7.1 Abstract

This work describes a chemical model for calculating the solubility of $CaSO_4$ phases in the H + Na + Ca + Mg + Al + Fe(II) + Cl + H_2O system from low to high solution concentration within the temperature range of 298 K to 353 K. The model was built with the aid of OLI Systems platform via the regression of new solubility data of calcium sulfate dihydrate in HCl or HCl + $CaCl_2$ aqueous solutions containing various metal chloride salts, such as NaCl, $MgCl_2$, $FeCl_2$, and $AlCl_3$. Via this regression analysis new Bromley – Zemaitis activity coefficient model parameters and empirical dissociation constant parameters were determined for many ion pairs consisting of cations (Na^+, Mg^{2+}, Fe^{2+}, and Al^{3+}) and anions (SO_4^-, HSO_4^-, and $Al(SO_4)_2^-$), as well as for the species, $MgSO_4$(aq), $AlSO_4^+$, and $Al(SO_4)_2^-$. The new model was shown to successfully predict the solubility of calcium sulfate phases in multi-component systems not used in model parameterization. The new model helps to explain the complex effect metal chlorides have on the solubility of $CaSO_4$ phases on the basis of governing metal – sulfate speciation equilibria.

7.2 Introduction

The purpose of the present work is to develop with the aid of OLI software a chemical equilibrium model to describe the effect of various chloride salts on $CaSO_4$ solubility. The new model is built on a recently described model for the estimation of $CaSO_4$ solubilities in the $HCl - CaCl_2 - H_2O$ system (1)[1]. No similar model capable of simultaneously considering the effect of various metal chlorides on $CaSO_4$ solubility in HCl media exists. Before the new model is described a review of previous modeling studies of relevance to the system under investigation here is presented.

The modeling of the effect of chloride salts on calcium sulfate dihydrate (DH) solubility has been attempted by several authors with various degrees of success. Tanji (2) developed a computer program around a chemical model based on the formation of the ion pairs of $CaSO_4^0$, $MgSO_4^0$ and $NaSO_4^-$. This model proved useful in dealing with the solubility of gypsum in dilute aqueous electrolyte systems, such as NaCl, $MgCl_2$, $CaCl_2$, Na_2SO_4, $MgSO_4$ or their mixtures at 25 °C only. This model is not extendable to concentrated electrolyte solutions because it makes use of the Debye – Huckel limited ionic activity coefficient equation. Barba *et al.* (3) used successfully their thermodynamic model (4) to investigate the behavior of calcium sulfate dihydrate solubility in aqueous solution of Na_2SO_4 and $MgCl_2$ on the basis of experimental solubility values at 40 °C. The basis of their model was the NRTL equation applied to the ion-pairs of $CaSO_4^0$ and $MgSO_4^0$. Their model's applicability was not tested in HCl – containing multi-salt systems or at temperatures above 40 °C. Recent developments (5-7) in modeling the solubility of salts in electrolyte solutions reveals that a hybrid modeling approach that

---

[1] See Chapter 4.

combines ion – association and ion – interaction models may be the best one for strong complexing systems as is the case of metal sulfates. Thus Harvie and Weare (5) successfully modelled the solubilities of minerals in complex brine waters at 25 °C. More recently Casas *et al.* (7) have shown the chemical model on which OLI Systems software is based to be particularly suited for describing the high temperature solution chemistry of Al and Mg – containing sulfate solutions. The OLI Systems platform was used as well by the present authors to develop an improved chemical solution model for estimating $CaSO_4$ solubilities of all three modifications i.e. dihydrate, hemihydrate and anhydrite in HCl + $CaCl_2$ media (1). During the course of the latter work it was found that ion-ion interactions involving Ca^{2+} and SO_4^{2-} and in particular the bisulfate ion (HSO_4^-) to control the solubility of $CaSO_4$ in HCl media. Extension of the OLI Systems – based model into describing the effect of several metal chlorides on the solubility of $CaSO_4$ in HCl – containing media is done in this work. Both ion-ion interactions and speciation equilibria are considered.

The work described in this paper consists of the following: (1) testing of the commercially available OLI Systems software (package StreamAnalyzer version 1.3 (8)) against recently generated solubility data of the following systems (9)[2]: (a) $CaSO_4{\cdot}2H_2O$ (DH) + HCl + NaCl + H_2O, (b) $CaSO_4{\cdot}2H_2O$ (DH) + HCl + $MgCl_2$ + H_2O, (c) $CaSO_4{\cdot}2H_2O$ (DH) + HCl + $AlCl_3$ + H_2O, and (d) $CaSO_4{\cdot}2H_2O$ (DH) + HCl + $FeCl_2$ + H_2O; (2) determination of new model parameters, such as Bromley- Zemaitis parameters for ionic activity coefficients using OLI's regression module; (3) validation of the new model by comparing its predicted solubility against experimental solubility data for

---

[2] See Chapter 6.

$CaSO_4$ phases in several multi-component systems not used in model parameterization; (4) investigation of the effect of the various metal chlorides on the solubility of $CaSO_4$ in HCl media on the basis of governing speciation equilibria.

7.3 Chemical Equilibria

In $CaSO_4$ – saturated electrolyte aqueous systems, two types of reactions occur: partial dissolution of calcium sulfate and association (speciation) of ionic species. The solid – liquid – equilibria and speciation reaction equilibria involved in the H + Na + Ca + Mg + Al + Fe(II) + Cl + SO_4^{2-} + H_2O system are outlined below.

7.3.1 Dissolution Reaction of $CaSO_4$

$$CaSO_4 \cdot nH_2O \leftrightarrow Ca^{2+}(aq) + SO_4^{2-}(aq) + nH_2O(l) \tag{7.1}$$

where n is 0, 0.5 and 2 respectively for anhydrite (AH), hemihydrate (HH) and dihydrate (DH). The thermodynamic equilibrium constant, K_{SP}, for $CaSO_4$ solids is expressed as (1, 10)

$$K_{SP} = a_{Ca^{2+}} a_{SO_4^{2-}} a_{H_2O}^n = \left(m_{Ca^{2+}}\gamma_{Ca^{2+}}\right)\left(m_{SO_4^{2-}}\gamma_{SO_4^{2-}}\right)a_{H_2O}^n \tag{7.2}$$

where $m_{Ca^{2+}}$ and $m_{SO_4^{2-}}$ are the molal concentrations of cation Ca^{2+} and anion SO_4^{2-} in solution, $\gamma_{Ca^{2+}}$ and $\gamma_{SO_4^{2-}}$ are the ion activity coefficients, and a_{H_2O} is the activity of water. These thermodynamic equilibrium constants (K_{SP}) can be calculated from the standard Gibbs free energy of formation for all individual species in reaction (7.1). However, in OLI software (8) an empirical equation of the type shown below is used to improve the accuracy of solubility prediction.

$$Log_{10}K_{SP} = A + \frac{B}{T} + CT + DT^2 \tag{7.3}$$

where *A*, *B*, *C* and *D* are empirical parameters obtained via fitting to experimental solubility data. *T* is the temperature in Kelvin.

The $CaSO_4$ solubility, *s* (expressed in mol·kg) in pure water is simply $s = m_{Ca^{2+}} = m_{SO_4^{2-}}$, but in mixed HCl + $CaCl_2$ + chloride salt media the solubility becomes $s = \sum m_{"SO_4"}$, i.e. *s* is taken as the sum of all "SO_4"-containing species.

7.3.2 Speciation Reactions

Equations (7.4) to (7.9) represent the common dissociation equilibria for all systems considered in this work.

$$HSO_4^- \text{ (aq)} \leftrightarrow H^+\text{(aq)} + SO_4^{2-}\text{(aq)} \quad (7.4)$$

$$CaSO_4 \text{ (aq)} \leftrightarrow Ca^{2+}\text{(aq)} + SO_4^{2-}\text{(aq)} \quad (7.5)$$

$$CaCl_2 \text{ (aq)} \leftrightarrow Ca^{2+}\text{(aq)} + 2Cl^-\text{(aq)} \quad (7.6)$$

$$CaCl^+ \text{ (aq)} \leftrightarrow Ca^{2+}\text{(aq)} + Cl^-\text{(aq)} \quad (7.7)$$

$$CaOH^+ \text{ (aq)} \leftrightarrow Ca^{2+}\text{(aq)} + OH^-\text{(aq)} \quad (7.8)$$

$$H_2O \text{ (aq)} \leftrightarrow H^+\text{(aq)} + OH^-\text{(aq)} \quad (7.9)$$

Equations (7.10) to (7.21) represent the dissociation equilibria of the various metal complexes expected to occur in the present system.

$$NaSO_4^- \text{ (aq)} \leftrightarrow Na^+\text{(aq)} + SO_4^{2-}\text{(aq)} \quad (7.10)$$

$$MgOH^+ \text{ (aq)} \leftrightarrow Mg^{2+}\text{(aq)} + OH^-\text{(aq)} \quad (7.11)$$

$$MgSO_4 \text{ (aq)} \leftrightarrow Mg^{2+}\text{(aq)} + SO_4^{2-}\text{(aq)} \quad (7.12)$$

$$AlOH^{2+} \text{ (aq)} \leftrightarrow Al^{3+}\text{(aq)} + OH^-\text{(aq)} \quad (7.13)$$

$$Al(OH)_2^+ \text{ (aq)} \leftrightarrow AlOH^{2+} \text{ (aq)} + OH^-\text{(aq)} \quad (7.14)$$

$$AlOHCl^+ \text{ (aq)} \leftrightarrow Al^{3+}\text{(aq)} + OH^-\text{(aq)} + Cl^-\text{(aq)} \quad (7.15)$$

$$AlSO_4^{+}(aq) \leftrightarrow Al^{3+}(aq) + SO_4^{2-}(aq) \tag{7.16}$$

$$Al(SO_4)_2^{-}(aq) \leftrightarrow AlSO_4^{+}(aq) + SO_4^{2-}(aq) \tag{7.17}$$

$$FeOH^{+}(aq) \leftrightarrow Fe^{2+}(aq) + OH^{-}(aq) \tag{7.18}$$

$$Fe(OH)_2(aq) \leftrightarrow FeOH^{+}(aq) + OH^{-}(aq) \tag{7.19}$$

$$Fe(OH)_3^{-}(aq) \leftrightarrow Fe(OH)_2(aq) + OH^{-}(aq) \tag{7.20}$$

$$Fe(OH)_4^{-}(aq) \leftrightarrow Fe(OH)_3^{-}(aq) + OH^{-}(aq) \tag{7.21}$$

All cations with the exception of Fe(II), form sulfate-complexes (refer to reactions (7.5), (7.10), (7.12), (7.16), and (7.17)) hence are expected to influence the solubility (*s*) of $CaSO_4$ since $s = \sum m''SO_4''$. This means that we need to determine the concentration of the various sulfate-carrying chemical species, hence the adoption of a speciation-based modeling strategy.

As an example, the thermodynamic equilibrium constant for dissociation reaction (7.10) of $NaSO_4^-$ complex is expressed as

$$K_{NaSO_4^-} = \frac{(m_{Na^+}\gamma_{Na^+})(m_{SO_4^{2-}}\gamma_{SO_4^{2-}})}{m_{NaSO_4^-}\gamma_{NaSO_4^-}} \tag{7.22}$$

where m_{Na^+}, $m_{SO_4^{2-}}$ and $m_{NaSO_4^-}$ are the molal concentrations of cation Ca^{2+} and anions SO_4^{2-} and $NaSO_4^-$ in solution, γ_{Na^+}, $\gamma_{SO_4^{2-}}$ and $\gamma_{NaSO_4^-}$ are the ion activity coefficients.

In OLI software (8) the dissociation equilibrium constants are determined either by using the revised HKF equation originally developed by Helgeson and co-workers (11-15) to obtain the standard – state thermodynamic parameters of each aqueous species or by using empirical equations of the type of Eq. (7.3). The data used by OLI for all species involved in the chemical equilibria outlined in equations (7.1) and (7.4) to (7.21) are listed in the appendix (Tables A1 and A2). Some of these data are revised later in the present work with the aid of Eq. (7.3) to allow for more accurate description of the solubility equilibria. Finally, the ionic activity coefficients are calculated by the Bromley-Zemaitis activity coefficient model (8, 16) as follows:

$$Log\gamma_{\pm} = \frac{-A|Z_+Z_-|\sqrt{I}}{1+\sqrt{I}} + \frac{(0.06+0.6B)|Z_+Z_-|I}{(1+\frac{1.5}{|Z_+Z_-|I})^2} + BI + CI^2 + DI^3 \qquad (7.23)$$

where A is the Debye-Huckel parameter; I is the ionic strength of the solution; B, C, and D are temperature - dependent empirical coefficients; Z_+ and Z_- are the cation and anion charges, respectively; $B=B_1+B_2T+B_3T^2$ is the constant for ion interaction; C and D have the same form as B.

7.4 Results and Discussion

7.4.1 Solubility Evaluation with OLI's Existing Model

The effect of metal chlorides, namely NaCl, $MgCl_2$, $FeCl_2$, and $AlCl_3$ on $CaSO_4$ solubility in HCl or HCl + $CaCl_2$ media is evaluated first using OLI's existing model (software package StreamAnalyzer 1.3) by comparing model predictions to experimental measurements (9).

Monovalent Metal Chlorides (NaCl): Figure 7.1 compares the predicted $CaSO_4$ dihydrate (DH) solubility in aqueous 0.5 mol·dm^{-3} HCl + NaCl solutions at 323 and 353 K with experimental data (9). As it can be seen OLI gives reasonable prediction at low temperature (323 K), but it results in significant deviation from experiments at elevated temperature (353 K).

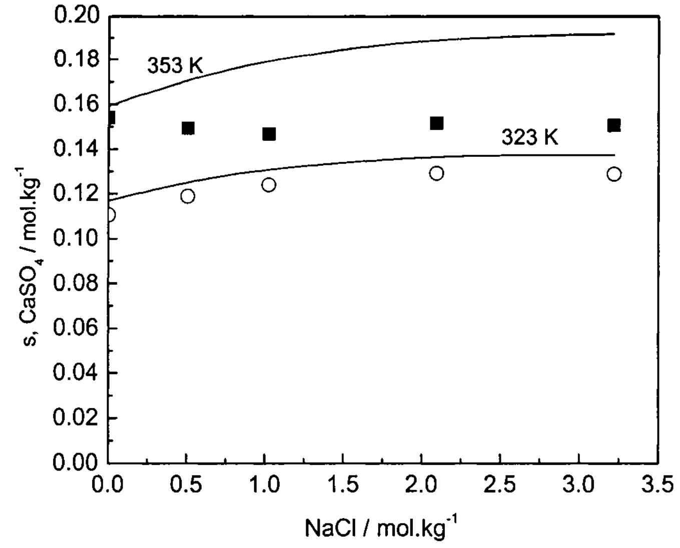

Figure 7.1. Comparison of OLI predicted (lines) and experimental (symbols) solubility of calcium sulfate dihydrate in 0.5 mol·dm^{-3} HCl + NaCl solutions at 323 and 353 K. ○, 323K; ■, 353K.

Divalent Metal Chlorides ($MgCl_2$ or $FeCl_2$): The solubility of dihydrate (DH) in 0.5 mol·dm^{-3} HCl + $MgCl_2$ or $FeCl_2$ solutions up to 353 K was calculated and compared with experimental data as shown in Figures 7.2 and 7.3. As it can be seen from Figure 7.2 OLI's existing model grossly overestimates solubility in the concentrated $MgCl_2$ range. For example, the average relative deviation at 298 K increases from 15% to 221% as the $MgCl_2$ concentration increases from 0.25 to 3 mol·dm^{-3}, respectively. The overestimation is further enhanced with temperature elevation. However, in the case of $FeCl_2$ (Figure 7.3) OLI's predictions are in good agreement with experimental data. The stark contrast between the effects of $MgCl_2$ and $FeCl_2$ on $CaSO_4 \cdot 2H_2O$ solubility as it will be explained later reflects the different extent of interaction of the cations (Mg^{2+} vs Fe^{2+}) with SO_4^{2-} or HSO_4^- anions.

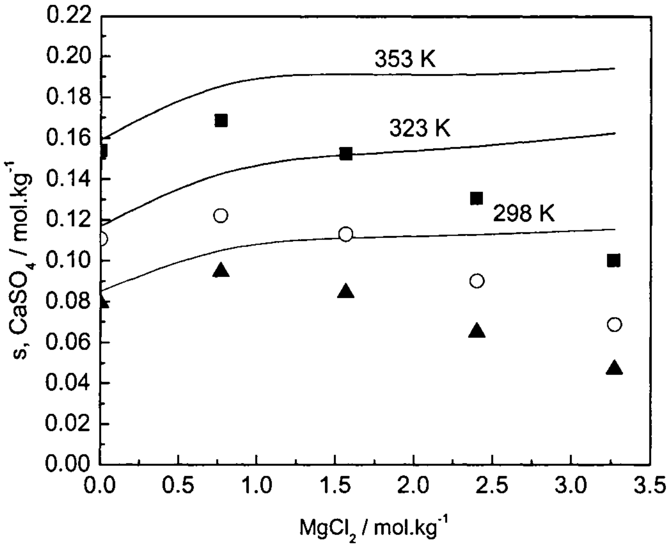

Figure 7.2. Comparison of OLI predicted (lines) and experimental (symbols) solubility of calcium sulfate dihydrate in 0.5 mol·dm^{-3} HCl + $MgCl_2$ solutions at various temperatures. ▲ , 298 K; ○, 323 K; ■, 353 K.

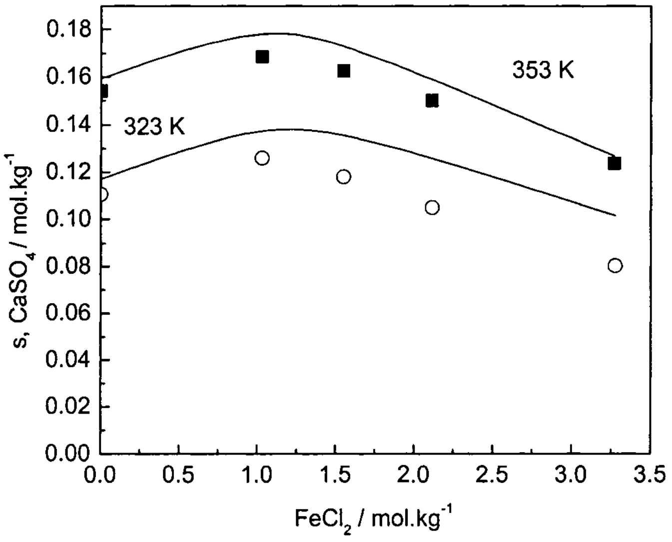

Figure 7.3. Comparison of OLI predicted (lines) and experimental (symbols) solubility of calcium sulfate dihydrate in 0.5 mol·dm^{-3} HCl + $FeCl_2$ solutions at 323 and 353 K. ○, 323 K; ■,353 K.

Trivalent Metal Chlorides ($AlCl_3$): The effect of $AlCl_3$ on $CaSO_4{\cdot}2H_2O$ solubility in the presence or not of HCl is evaluated in Figures 7.4 and 7.5. In the absence of acid (Figure 7.4) current OLI model gives reasonable predictions up to 0.5 mol·kg^{-1} $AlCl_3$ but completely fails in higher concentrations or in the presence of acid. This stark discrepancy between OLI's predicted values and measured solubilities is suspected to be linked to the Al(III) – SO_4^{2-} and Al(III) – HSO_4^- interactions and complexes. Apparently OLI overemphasizes the formation of aluminium- sulfate complexes (refer to reactions (7.16), and (7.17)).

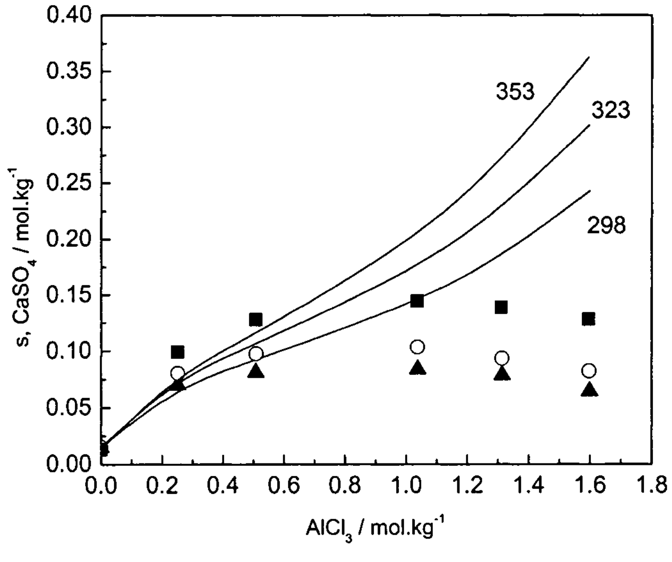

Figure 7.4. Comparison of OLI predicted (lines) and experimental (symbols) solubility of calcium sulfate dihydrate in $AlCl_3$ solutions at various temperatures. ▲, 298 K; o, 323 K; ■, 353 K.

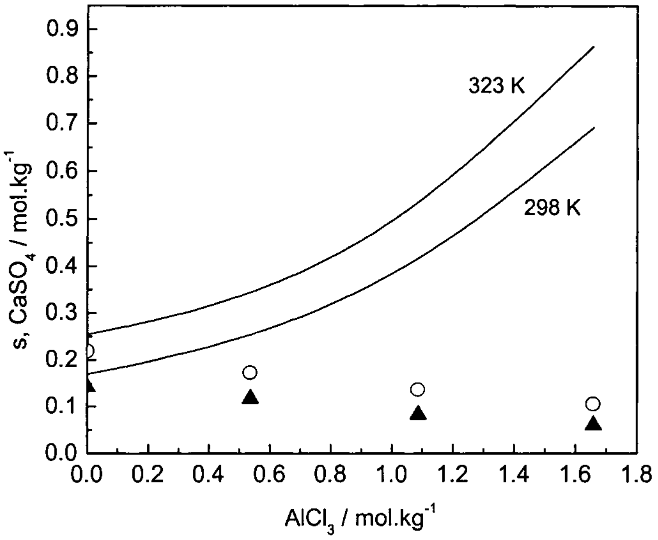

Figure 7.5. Comparison of OLI predicted (lines) and experimental (symbols) solubility of calcium sulfate dihydrate in 3 mol·dm^{-3} HCl + $AlCl_3$ solutions at 298 and 323 K. ▲, 298 K; ○ , 323 K.

7.4.2 Model Parameterization

With the view of improving OLI's prediction capacity new model parameters were evaluated via regression of recently reported experimental solubility data (9). The modeling methodology used in the present work is the same with the one followed for the HCl + $CaCl_2$ + H_2O system (1). In that work the solubilities of all $CaSO_4$ phases, i.e DH, HH and AH, were successfully modeled with a single set of model parameters that involved determination of new Bromley – Zemaitis interaction parameters (refer to Eq.(7.23)) for two ion – pairs, namely Ca^{2+} – SO_4^{2-} and Ca^{2+} – HSO_4^-, the empirical parameters in Eq. (7.3) for the solubility product constants of hemihydrate and anhydrite, as well as those of the dissociation constant of the HSO_4^- ion. All the model parameters determined previously (1) are retained (refer to Table 7.1) in the present work along the new ones determined here so to provide for a truly global model of $CaSO_4$ solubility in the the H + Na + Ca + Mg + Al + Fe(II) + Cl + SO_4 + H_2O system. This new model is called "OLI-McGill".

Table 7.1 Retained Model Parameters (Eqs. (7.3) and (7.23)) from Previous Work[1]

parameters	Species			
Eq. (7.3)	AH	HH	DH	HSO_4^-
A	-85.601	34.4739	40.11184	-66.6422
B	8775.05	-4939.1	-5481.185	7402.28
C	0.261521	-0.0870353	-0.115199	0.200352
D	-2.93598×10^{-4}	4.59692×10^{-5}	9.1384×10^{-5}	-2.20974×10^{-4}
Eq.(7.23)	Ca^{2-} - SO_4^{2-}		Ca^{2-} - HSO_4^-	
B_1	-0.246708		-0.0816875	
B_2	0.0035632		3.96067×10^{-4}	
B_3	-5.12319×10^{-5}		1.65505×10^{-5}	
C_1	0.0731743		0.00617896	
C_2	-0.00107027		6.64883×10^{-4}	
C_3	1.15506×10^{-5}		-1.07042×10^{-5}	
D_1	0.010482		0.00149402	
D_2	-2.91146×10^{-5}		-8.87896×10^{-5}	
D_3	1.28589×10^{-6}		1.05082×10^{-6}	

NaCl: As it was seen with the results of Figure 7.1 the current OLI model cannot predict well the effect of NaCl on the solubility of $CaSO_4$ in HCl-containing solutions. In order to improve OLI's prediction capacity we opted to determine new Bromley –Zemaitis interaction parameters for the Na^+–HSO_4^- ion pair via regression of experimental solubility data (9). The newly determined parameters are listed in Table 7.2. The results obtained with the new model, as shown in Figure 7.6, are in good agreement with experimental solubility values. The average relative deviation is 0.73 % at 323 K and 5.83 % at 353 K.

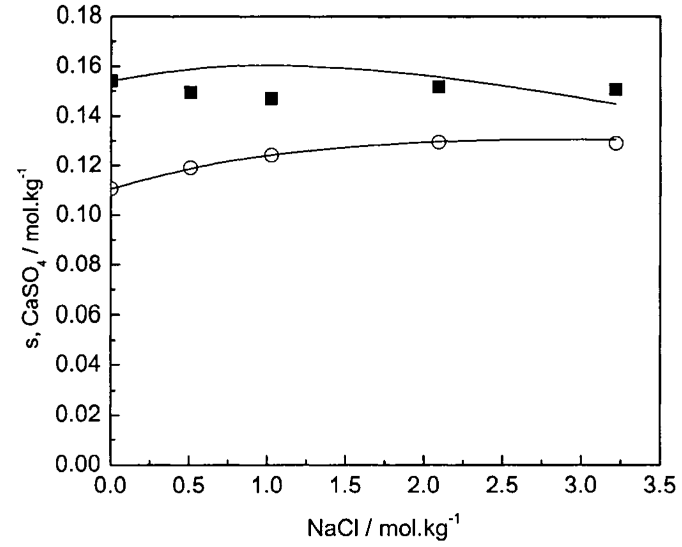

Figure 7.6. Comparison of new model's predictions (lines) with experimental (symbols) solubility data of calcium sulfate dihydrate in 0.5 mol·dm^{-3} HCl + NaCl solutions at 323 and 353 K. ○, 323K; ■, 353K.

$MgCl_2$ and $FeCl_2$: In the case of $MgCl_2$ the original model's poor prediction (refer to Figure 7.2) was corrected via the determination of new parameters for the dissociation constant of $MgSO_4$ (aq)(refer to Eq. (7.3)) and new Bromley – Zemaitis interaction parameters (refer to Eq. (7.23)) for the Mg^{2+} – HSO_4^- ion pair. The new model parameters are listed in Tables 7.2 and 7.3. Excellent fit was obtained between model and experimental data (compare Figure 7.7 to Figure 7.2). In the case of $FeCl_2$ new Bromley – Zemaitis interaction parameters were determined for the Fe^{2+}–HSO_4^- ion pair only and they are listed in Table 7.2. Figure 7.8 shows the good agreement between estimated solubilities with the new model parameters and experimental data (compare Figure 7.8 to Figure 7.3).

Table 7.2. New Bromley-Zemaitis Parameters (Eq. (7.23)) Determined in This Work

	Parameters		
Ion – pairs	B_1	B_2	B_3
$\mathrm{Na^+}$ – $\mathrm{HSO_4^-}$	-0.0411348	3.16081×10^{-5}	2.21523×10^{-5}
$\mathrm{Mg^{2+}}$ – $\mathrm{HSO_4^-}$	2.61643×10^{-3}	6.18387×10^{-5}	1.79359×10^{-5}
$\mathrm{Al^{3+}}$ – $\mathrm{HSO_4^-}$	0.10451	-1.24283×10^{-3}	3.81484×10^{-6}
$\mathrm{Al^{3+}}$ – $\mathrm{Al(SO_4)_2^-}$	-0.185343	-7.80230×10^{-3}	1.01848×10^{-4}
$\mathrm{Fe^{2+}}$ – $\mathrm{HSO_4^-}$	0.0883523	-2.81397×10^{-4}	9.16037×10^{-7}
	Parameters		
	C_1	C_2	C_3
$\mathrm{Na^+}$ – $\mathrm{HSO_4^-}$	-8.8400×10^{-4}	-2.613×10^{-6}	-3.800×10^{-8}
$\mathrm{Mg^{2+}}$ – $\mathrm{HSO_4^-}$	1.71060×10^{-2}	-2.55083×10^{-4}	-1.68969×10^{-6}
$\mathrm{Al^{3+}}$ – $\mathrm{HSO_4^-}$	-3.96191×10^{-2}	1.47872×10^{-3}	-9.22037×10^{-6}
$\mathrm{Al^{3+}}$ – $\mathrm{Al(SO_4)_2^-}$	2.82401×10^{-2}	1.85496×10^{-3}	-1.98538×10^{-5}
$\mathrm{Fe^{2+}}$ – $\mathrm{HSO_4^-}$	-1.21200×10^{-3}	-6.347×10^{-6}	-7.12×10^{-8}
	Parameters		
	D_1	D_2	D_3
$\mathrm{Na^+}$ – $\mathrm{HSO_4^-}$	5.5001×10^{-6}	6.0577×10^{-8}	5.4989×10^{-10}
$\mathrm{Mg^{2+}}$ – $\mathrm{HSO_4^-}$	-4.48639×10^{-6}	5.06316×10^{-6}	1.29337×10^{-7}
$\mathrm{Al^{3+}}$ – $\mathrm{HSO_4^-}$	6.32584×10^{-3}	-1.80374×10^{-4}	1.09527×10^{-6}
$\mathrm{Al^{3+}}$ – $\mathrm{Al(SO_4)_2^-}$	7.63313×10^{-5}	-1.11299×10^{-4}	1.1187×10^{-6}
$\mathrm{Fe^{2+}}$ – $\mathrm{HSO_4^-}$	1.6236×10^{-6}	1.1688×10^{-7}	1.037×10^{-9}

Table 7.3. New Eq. (7.3) Parameters Determined in This Work

Species	A	B	C	D
$\mathrm{MgSO_4(aq)}$	-44.0271	6173.37	0.0929154	-5.85151×10^{-5}
$\mathrm{AlSO_4^+}$	-28.2452	2545.53	0.137768	-1.81554×10^{-4}
$\mathrm{Al(SO_4)_2^-}$	-32.5402	900.581	0.127012	-1.81554×10^{-4}

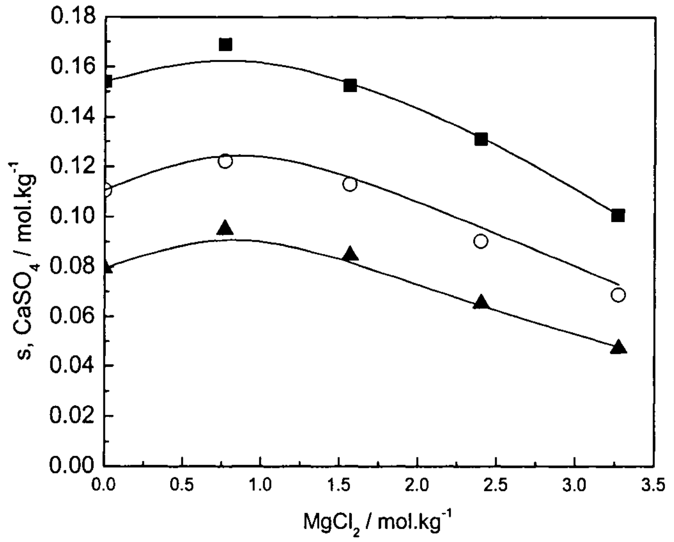

Figure 7.7. Comparison of new model's predictions (lines) with experimental (symbols) solubility data of calcium sulfate dihydrate in 0.5 mol·dm^{-3} HCl + $MgCl_2$ solutions at various temperatures. ▲, 298 K; ○, 323 K; ■, 353 K.

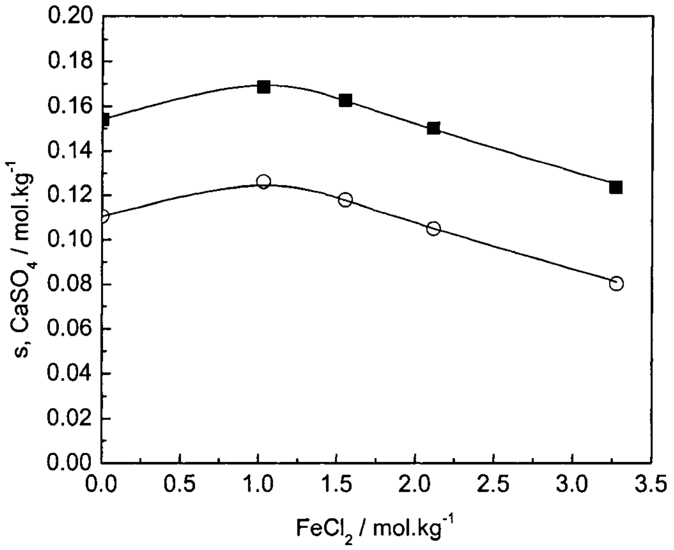

Figure 7.8. Comparison of new model's predictions (lines) with experimental (symbols) solubility data of calcium sulfate dihydrate in 0.5 mol·dm^{-3} HCl + $FeCl_2$ solutions at 323 and 353 K. ○, 323 K; ■,353 K.

$AlCl_3$: According to Ridley *et al.* (17) aluminium forms two Al-sulfate complexes, namely $AlSO_4^+$ and $Al(SO_4)_2^-$. In the original OLI model the dissociation constant of these two complexes is calculated with the HKF method. It was decided in this work to calculate instead the same constants using Eq. (7.3) (refer to Table 7.3). Best fit between model and experimental data (refer to Figure 7.9 and 7.10) was obtained when in addition the data of Table 7.3 new Bromley –Zemaitis interaction parameters were determined for the ion pairs Al^{3+}–HSO_4^- and Al^{3+}–$Al(SO_4)_2^-$(refer to Table 7.2).

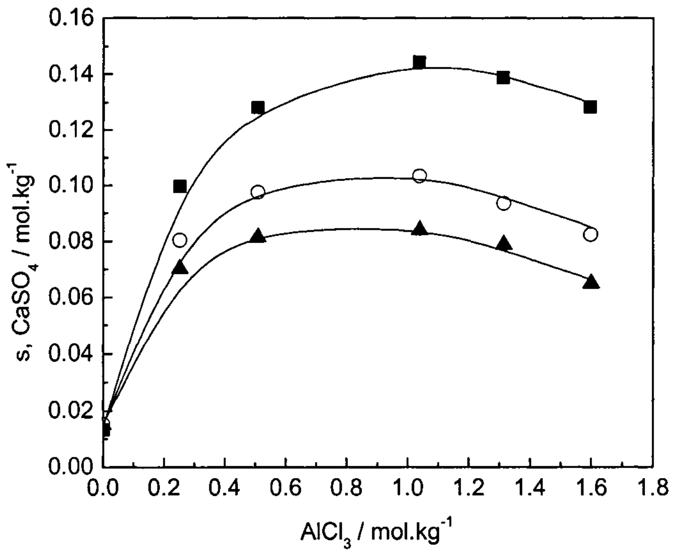

Figure 7.9. Comparison of new model's predictions (lines) with experimental (symbols) solubility data of calcium sulfate dihydrate in $AlCl_3$ solutions at various temperatures. ▲ , 298 K; o, 323 K; ■, 353 K.

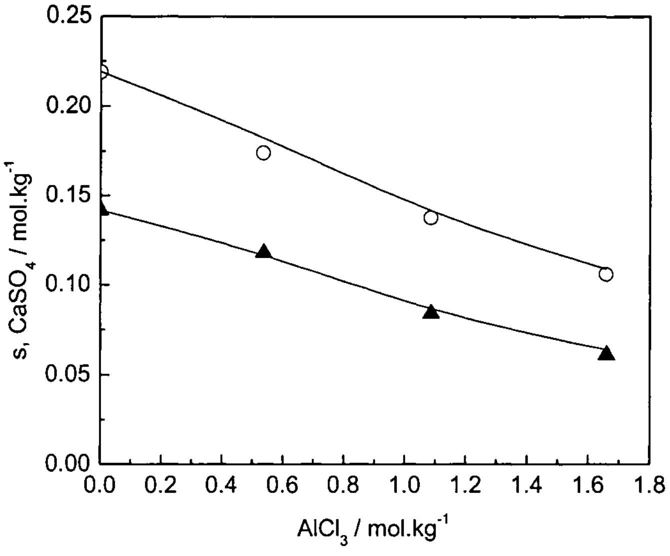

Figure 7.10. Comparison of new model's predictions (lines) with experimental (symbols) solubility data of calcium sulfate dihydrate in 3 mol·dm^{-3} HCl + $AlCl_3$ solutions at 298 and 323 K. ▲, 298 K; ○, 323 K.

7.4.3 Model Validation

Having successfully modeled the solubility data of calcium sulfate dihydrate in the H + Na + Ca + Mg + Al + Fe(II) + Cl + H_2O system, the model was subsequently validated by comparing model predictions with experimental solubility data not used in model parameterization. To accomplish this task a new databank with all new model parameters (summarized in Tables 7.1 to 7.3) was created. For the validation of the model not only the solubility of dihydrate was estimated but also that of anhydrite and hemihydrate. In Figures 7.11 to 7.13 the new model is evaluated against experimental solubility data for dihydrate, anhydrite and hemihydrate, respectively in HCl + $MgCl_2$ solutions. In Figures 7.11 and 7.12 model predictions of OLI's existing model are plotted as well for comparison purposes. Excellent agreement between new model's predictions and experimental data is observed for all three cases. It is noteworthy to point out that neither anhydrite, hemihydrate nor $CaCl_2$ were involved with the determination of the new model parameters (refer to Table 7.2 and 7.3) which makes remarkable the excellent predictions of the model plotted in Figures 7.12 and 7.13.

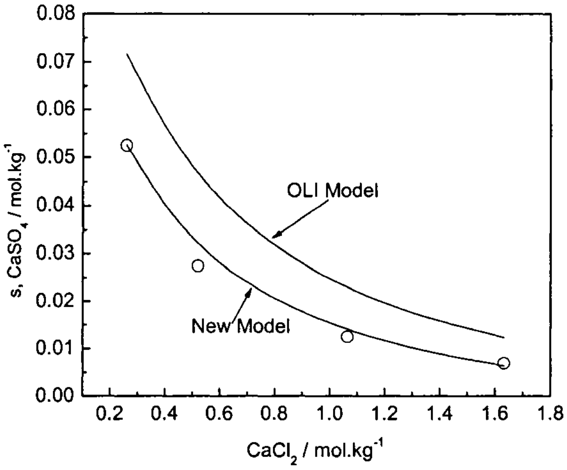

Figure 7.11. Comparison of OLI and new model's predictions with experimental (symbols) solubility data of calcium sulfate dihydrate in HCl (0.5 mol·dm^{-3}) + $MgCl_2$ (1 mol·dm^{-3}) + $CaCl_2$ solutions at 323 K.

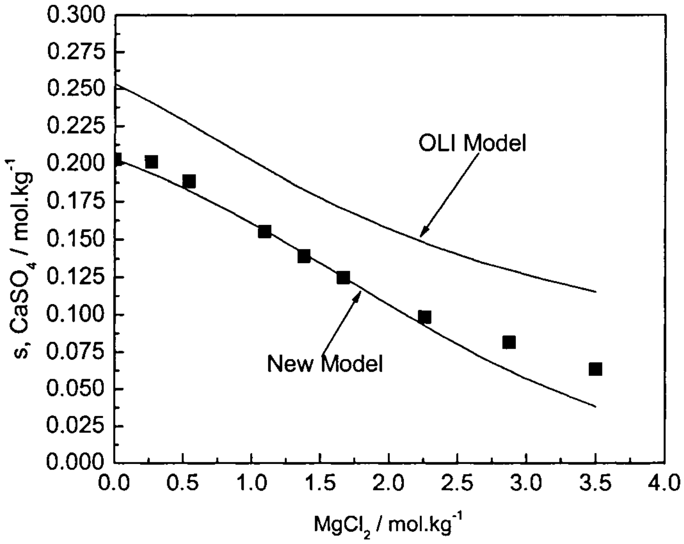

Figure 7.12. Comparison of OLI and new model's predictions with experimental (symbols) solubility data of calcium sulfate anhydrite in 3 mol·dm^{-3} HCl + $MgCl_2$ solutions at 353 K.

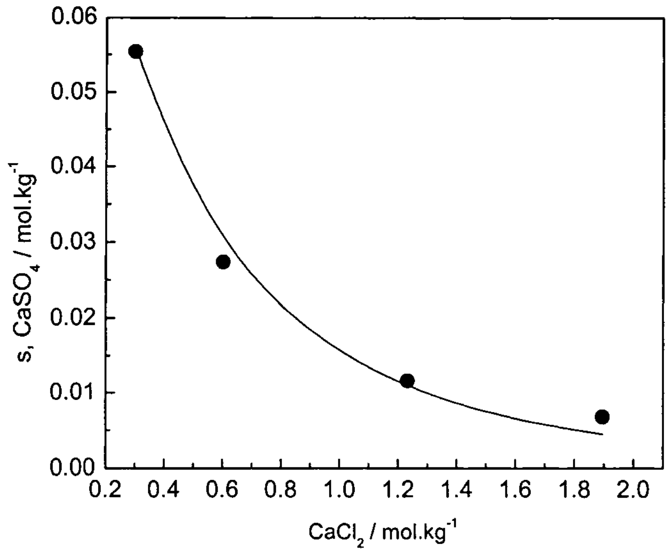

Figure 7.13. Comparison of new model's predictions (line) with experimental (symbols) solubility data of calcium sulfate hemihydrate in HCl (6 mol·dm^{-3}) + $MgCl_2$ (1 mol·dm^{-3}) + $CaCl_2$ solutions at 333 K.

7.4.4 Use of the Model

Following validation the new model was used to compare the effect of various chloride salts, such as NaCl, $MgCl_2$, $FeCl_2$, and $AlCl_3$ on the solubility of all three $CaSO_4$ phases, namely dihydrate, hemihydrate and anhydrite. The model's predicted solubility data is summarized in Figures 7.14 to 7.17. It can be noted the metal chlorides to impact the solubility of the three $CaSO_4$ phases in a complex way. The effect is seen to be stronger as the charge of the cation of the salt increases i.e as we move from NaCl to $MgCl_2$ or $FeCl_2$ to $AlCl_3$. In general the solubility of either of the three phases is modestly affected by NaCl but it is increasing with divalent and trivalent chloride salt molality in the low concentration range reaching a peak and then drastically decreasing in the higher concentration range end. Of all salts investigated $AlCl_3$ seems to suppress most the solubility of $CaSO_4$. A comparison of the data of Figures 7.14 to 7.17 reveals that in 1 mol·kg^{-3} HCl solution at 323 K independent of the type or concentration of chloride salt the relative order of stability of the three $CaSO_4$ phases is: AH > DH > HH. The new model can be used to construct phase transition diagrams depicting the relative stability of the three phases, i.e. AH, HH, and DH as a function of T and solution composition as done elsewhere (18).

In order to better appreciate the effect of the various metal chloride salts on $CaSO_4$ solubility the data of Figures 7.14 to 7.16 was re-plotted against ionic strength. It is clarified that in this case the true ionic strength was calculated considering the distribution of all chemical species. In contrast in Chapter 6 (see Figs. 6.13 and 6.15) the ionic strength used there was the nominal one that was calculated based on the assumption of full dissociation. This time the various metal chlorides gave equivalent effect. Figure 7.17 summarizes the data for dihydrate solubility. Similar trends were observed for hemihydrate and anhydrite solubilities. To explain the origin of the "S-shape" effect of ionic strength on solubility we have calculated the distribution of sulfate species for the $MgCl_2$ – HCl and $AlCl_3$ – HCl systems respectively as a function of ionic strength (Figure 7.18 and 7.19). On the_same graphs the solubility of dihydrate is plotted as well. As it can be seen in the case of $MgCl_2$ (Figure 7.18) the bisulfate ion (HSO_4^-) dominates the dihydrate solubility with_$MgSO_4$(aq) becoming modestly important at the high $MgCl_2$ concentration range. The relative abundance of $MgSO_4$(aq) increases from 1.8 % in 1mol·kg^{-1} $MgCl_2$ (I = 4.3 mol·kg^{-1}) to 17.7 % in 3 mol·kg^{-1} $MgCl_2$ (I = 10.2 mol·kg^{-1}). In the case of $AlCl_3$ (Figure 7.19) it can be seen that the solubility of dihydrate is controlled by the HSO_4^- ion again since the abundance of this ion parallels that of the solubility curve. It is reminded that_solubility, *s*, is the sum of all sulfate species. At the high concentration range (1.5 mol·kg^{-1} or I = 10 mol·kg^{-1}) the $Al(SO_4)_2^-$ species becomes the dominant "SO_4"-carrying species. Hence the observed similarity between $MgCl_2$ and $AlCl_3$ (when they are compared on the basis of ionic strength – refer to Figure 7.17) appears to be due predominantly to the bisulfate ion.

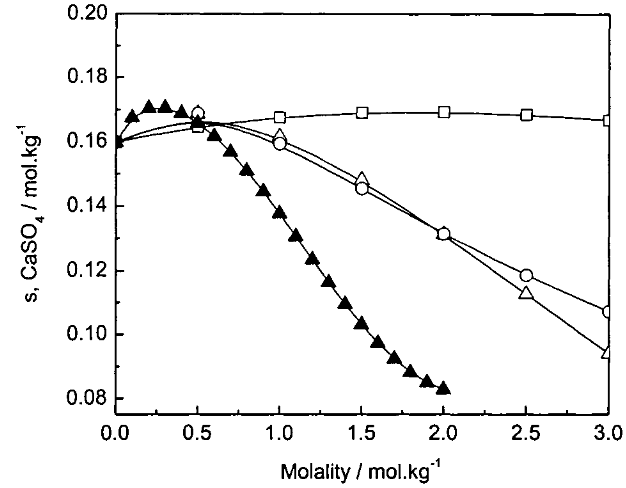

Figure 7.14. Effect of various chloride salts on the solubility of calcium sulfate dihydrate in 1 mol·dm^{-3} HCl solutions versus molal concentration at 323 K. □, NaCl; △, $MgCl_2$; ○, $FeCl_2$; ▲, $AlCl_3$.

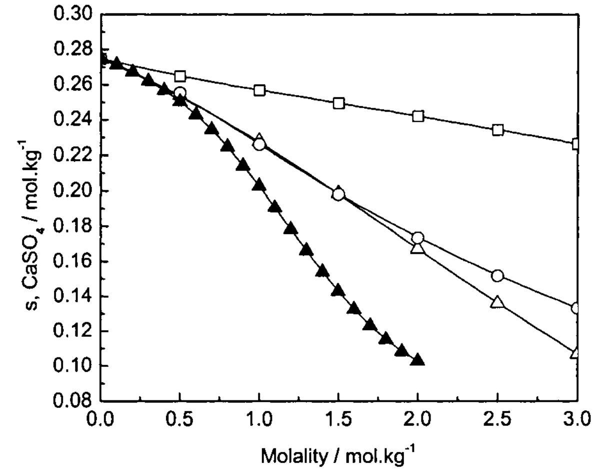

Figure 7.15. Effect of various chloride salts on the solubility of calcium sulfate hemihydrate in 1 mol·dm^{-3} HCl solutions versus molal concentration at 323 K. □, NaCl; △ $MgCl_2$; ○, $FeCl_2$; ▲, $AlCl_3$.

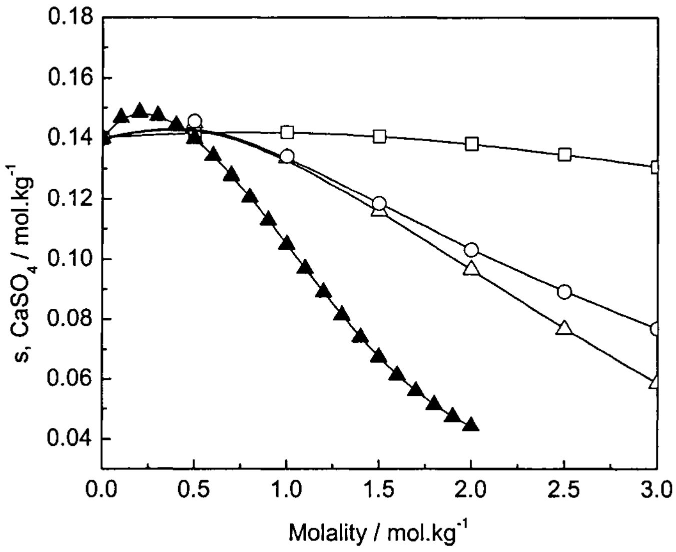

Figure 7.16. Effect of various chloride salts on the solubility of calcium sulfate anhydrite in 1 mol·dm^{-3} HCl solutions versus molal concentration at 323 K. □, NaCl; △, $MgCl_2$; ○, $FeCl_2$; ▲, $AlCl_3$.

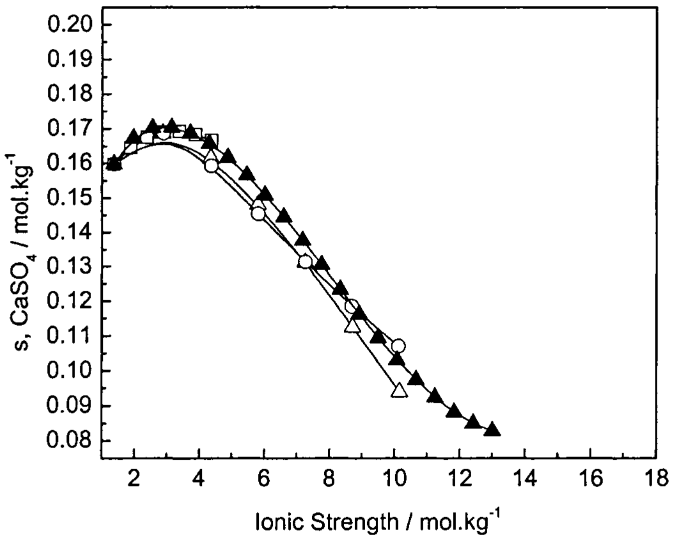

Figure 7.17. Effect of various chloride salts on the solubility of calcium sulfate dihydrate in 1 mol·dm^{-3} HCl solutions versus true ionic strength at 323 K.□ , NaCl; △ , $MgCl_2$; ○ , $FeCl_2$; ▲ , $AlCl_3$.

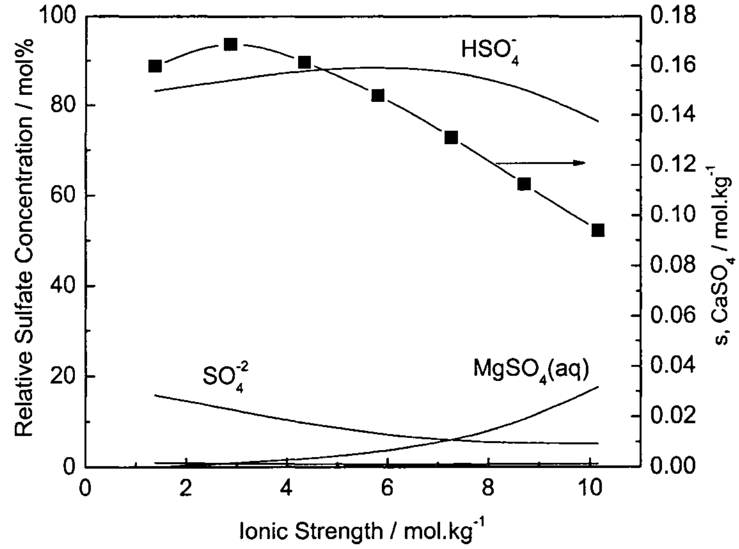

Figure 7.18. Sulfate speciation as a function of true ionic strength for dihydrate saturated solution containing 1m HCl + MgCl$_2$ at 323 K.

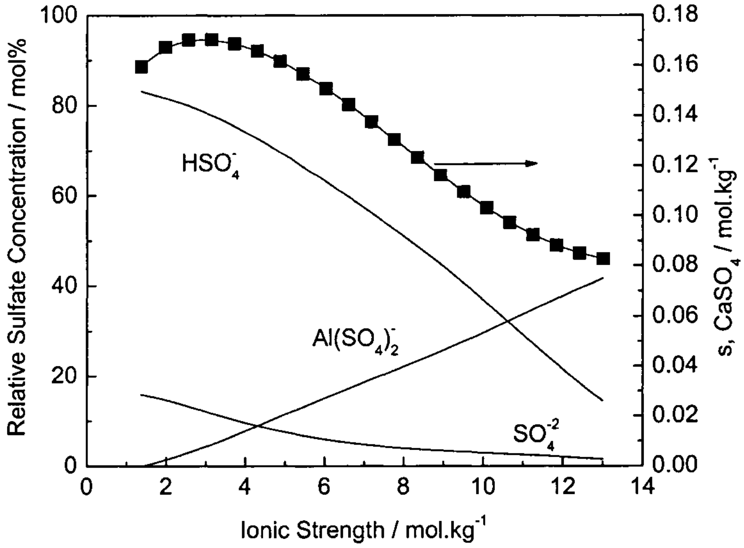

Figure 7.19. Sulfate speciation as a function of true ionic strength for dihydrate saturated solution containing 1m HCl + AlCl$_3$ at 323 K.

7.5 Conclusions

OLI Systems' Stream Analyzer software, when applied "as is" to the estimation of $CaSO_4$ solubility in HCl media containing various metal chloride salts such as NaCl, $FeCl_2$, $MgCl_2$, and $AlCl_3$ gave very poor results. The source of error was determined to be the Bromley – Zemaitis parameters for all cation – anion pairs and the dissociation constants of three metal-sulfate complexes, namely $MgSO_4$ (aq), $AlSO_4^+$, and $Al(SO_4)_2^-$. Upon regression of newly generated experimental data the above model parameters were corrected leading to the development of a new powerful model. The model was successfully validated by comparing its predictions against the solubility of all $CaSO_4$ phases under a wide range of conditions in terms of concentration, number of components and temperature. Finally it was shown with the aid of the new model that the solubility of all three $CaSO_4$ phases increases with increasing salt concentration up to 0.5 $mol{\cdot}dm^{-3}$ subsequently decreasing. $AlCl_3$ was found relatively to have the most depressing effect on $CaSO_4$ solubility. The effect of the various metal chlorides on $CaSO_4$ solubility was shown to be equivalent among them when their ionic strength is used as basis of comparison. The observed S-shape variation of solubility with ionic strength seems to be the outcome of the relative distribution of the various "SO_4" carrying species with HSO_4^- to be the main solubility –determining ion.

Acknowledgement

The support of Hatch, Noranda, Process Research Ortech, and NSERC (Natural Sciences and Engineering Research Council of Canada) is gratefully acknowledged.

7.6 Literature Cited

(1) Li, Zhibao; Demopoulos, G. P. Development of an Improved Chemical Model for the Estimation of $CaSO_4$ Solubilities in the $HCl-CaCl_2-H_2O$ System up to 100 °C. *Ind. Eng. Chem. Res.* **2006**, in press.

(2) Tanji, K. K. Solubility of Gypsum in Aqueous Electrolytes as Affected by Ion Association and Ionic Strengths up to 0.15 M and at 25 °C. *Environ. Sci. & Technol.* **1969**, 3, 656.

(3) Barba, D.; Brandani, V.; Giacomo G. D. Solubility of Calcium Sulfate Dihydrate in the System $Na_2SO_4-MgCl_2-H_2O$. *J. Chem. Eng. Data* **1984**, 29, 42.

(4) Barba, D.; Brandani, V.; Giacomo G. D. A Thermodynamic Model of $CaSO_4$ Solubility in Multicomponent Aqueous Solutions. *Chem. Eng. J.* **1982**, 24, 191.

(5) Harvie, C. E.; Weare, J. H. The Prediction of Mineral Solubilities in Natural Waters: the $Na-K-Mg-Ca-Cl-SO_4-H_2O$ System from Zero to High Concentration at 25 °C. *Geochim. Cosmochim. Acta* **1980**, 44, 981.

(6) Haghtalab, A.; Papangelakis, V. G.; Zhu, X. The Electrolyte NRTL Model and Speciation Approach as Applied to Multicomponent Aqueous Solutions of H_2SO_4, $Fe_2(SO4)_3$, $MgSO_4$ and $Al_2(SO4)_3$ at 230 – 270 °C. *Fluid Phase Equilibria* **2004**, 220, 199.

(7) Casas, J. M.; Papangelakis, V. G.; Liu, H. Performance of Three Chemical Models on the High – Temperature Aqueous $Al_2(SO4)_3$ - $MgSO_4$ - H_2SO_4 – H_2O System. *Ind. Eng. Chem. Res.* **2005**, 44, 2931.

(8) *Aqueous System Modeling Course and Workshop*, OLI's manual, OLI Systems Inc., NJ, 2002.

(9) Li, Zhibao; Demopoulos, G. P. The Effect of NaCl, $MgCl_2$, $FeCl_2$, $FeCl_3$ and $AlCl_3$ on Solubility of CaSO4 Phases in Aqueous HCl or HCl + $CaCl_2$ Solutions at 298 to 353 K. *J. Chem. Eng. Data* **2006**, in press.

(10) Anderson, G. M.; Crerar, D. A. *Thermodynamics in Geochemistry the Equilibrium Model*; Oxford University Press: New York, 1993.

(11) Helgeson, H. C.; Kirkham, D. H.; Flowers, G. C. Theoretical Prediction of the Thermodynamic Behavior of Aqueous Electrolytes at High Pressures and Temperatures: IV. Calculation of Activity Coefficients, Osmotic Coefficients, and Apparent Molal and Standard and Relative Partial Molal Properties to 600 °C and 5 kb. *Amer. J. Sci.* **1981**, 281, 1249.

(12) Tanger, J. C., IV; Helgeson, H. C. Calculation of the Thermodynamic and Transport Properties of Aqueous Species at High Pressures and Temperatures: Revised Equations of State for the Standard Partial Molal Properties of Ions and Electrolytes. *Amer. J. Sci.* **1988**, 288, 19.

(13) Shock, E. L.; Helgeson, H. C. Calculation of the Thermodynamic and Transport Properties of Aqueous Species at High Pressures and Temperatures: Correlation Algorithms for Ionic Species and Equation of State Predictions to 5 kb and 1000 °C. *Geochim. Cosmochim. Acta* **1988**, 52, 2009.

(14) Shock, E. L.; Helgeson, H. C.; Sverjensky D. A. Calculation of the Thermodynamic and Transport Properties of Aqueous Species at High Pressures and Temperatures: Standard Partial Molal Properties of Inorganic Neutral Species. *Geochim. Cosmochim. Acta* **1989**, 53, 2157.

(15) Shock, E. L.; Sassani, D. C.; Willis M.; Sverjensky D. A. Inorganic Species in Geologic Fluids: Correlations among Standard Molal Thermodynamic Properties of Aqueous Ions and Hydroxide Complexes. *Geochim. Cosmochim. Acta* **1997**, 61, 907.

(16) Rafal, M.; Berthold, J. W.; Scrivner, N. C.; Grise, S. L. Models for Electrolyte Solutions, in *Models for Thermodynamic and Phase Equilibria Calculations*, Sandler, S. I. (Ed.), Marcell Dekker: New York, 1994.

(17) Ridley, M. K.; Wesolowski, D. J.; Palmer, D. A.; Kettler, R. M. Association Quotients of Aluminum sulphate Complexes in NaCl Media from 50 to 125 °C: Results of a Potentiometric and Solubility Study. *Geochim. Cosmochim. Acta* **1999,** 63, 459–472.

(18) Li, Zhibao; Demopoulos, G. P. Model-Based Construction of Calcium Sulfate Phase Transition Diagrams in the HCl - $CaCl_2$ - H_2O System between 0 and 100 °C. *Ind. Eng. Chem. Res.* **2006**, submitted.

Chapter 8

Synopsis

8.1 Conclusions

The specific conclusions have already been summarized at the end of each chapter. Here, only the major global conclusions of present research are given.

1. The solubility of calcium sulfate dihydrate, hemihydrate and anhydrite in HCl and $CaCl_2$ or their mixed electrolyte solutions has been measured for a wide range of conditions up to 12 $mol{\cdot}dm^{-3}$ HCl, 3 $mol{\cdot}dm^{-3}$ $CaCl_2$ and (283 to 353) K. The solubility of dihydrate or anhydrite in HCl solution increases with the acid concentration up to around (2.5 to 3.0) $mol{\cdot}dm^{-3}$ HCl. It decreases gradually beyond this value. The solubility of calcium sulfate hemihydrate in HCl solution with more than 8 $mol{\cdot}dm^{-3}$ concentration decreases with increasing acid concentration. The addition of $CaCl_2$ in acid solution makes the solubility of all $CaSO_4$ modifications to decrease sharply due to the common ion effect.

2. The effect of various chloride salts, such as NaCl, $CaCl_2$, $MgCl_2$, $FeCl_2$, $FeCl_3$ and $AlCl_3$ on the solubility of three $CaSO_4$ modifications, namely dihydrate, hemihydrate and anhydrite, in HCl solutions has been investigated. The solubility of dihydrate increases with increasing concentration of $MgCl_2$, $FeCl_2$, $FeCl_3$ and $AlCl_3$ up to a certain level thereafter decreasing with further increase of metal chloride concentration when the HCl concentration is 0.5 $mol{\cdot}dm^{-3}$. However, in

the case of 3 $mol\cdot dm^{-3}$ HCl concentration the solubility of dihydrate consistently decreases with increasing metal chloride concentration.

3. Analysis of the experimental $CaSO_4$ solubility data in the $HCl-CaCl_2-H_2O$ system with OLI's StreamAnalyzer, a commercial available chemical equilibrium software revealed significant discrepancies. The source of deviation of OLI's prediction from experiment was traced to be the Bromley-Zemaitis model parameters for $Ca^{2+}-SO_4^{2-}$ and $Ca^{2+}-HSO_4^-$ ion pairs as well as the dissociation constant of HSO_4^-. A new set of model parameters was determined by fitting the experimental data for the system $CaSO_4\cdot 2H_2O-HCl-CaCl_2-H_2O$. The new model parameters yielded a highly improved model capable of predicting the solubility not only of dihydrate but also hemihydrate and anhydrite. The modeling results indicate that the speciation-based thermodynamic model forming the basis of OLI's StreamAnalyzer after the improvements made to it in this work is a good tool to describe $CaSO_4$ solubility behavior and calculate solution speciation. With the aid of the model the solubility curve for dihydrate (or anhydrite) as a function of HCl concentration (increasing solubility up to 3 m HCl and subsequent decrease) was successfully explained on the basis of the formation of HSO_4^- and ion activity coefficient changes.

4. The newly developed chemical model has been successfully used to construct the phase transition diagrams in the $CaSO_4 - HCl - CaCl_2 - H_2O$ system between 0 and 100 °C. According to this analysis the $T_{trans.}$ for DH-AH and DH-HH in water was found to be respectively 43 °C and 100 °C. Upon increase of HCl and /or

$CaCl_2$ concentration the corresponding transition temperatures decrease. Comparison of phase transition diagram predictions and experimental measurements showed good agreement in general for equilibrium times between 1 and 5 hours. The constructed phase diagram was shown to successfully determine the region of metastability of HH; this finding is of particular interest to those seeking to produce the high value α-$CaSO_4 \cdot 0.5H_2O$ plaster material.

5. OLI Systems' Stream Analyzer software, when applied "as is" to the estimation of $CaSO_4$ solubility in HCl media containing various metal chloride salts such as NaCl, $FeCl_2$, $MgCl_2$, and $AlCl_3$ gave very poor results. The source of error was attributed to the Bromley-Zemaitis parameters for all cation – anion pairs and the dissociation constants of three metal sulfate complexes, namely $MgSO_4$(aq), $AlSO_4^+$, and $Al(SO4)_2^-$. Upon regression of newly generated experimental data the above model parameters were corrected and thus a new powerful model making use of OLI System's platform was developed. $AlCl_3$ was found to have the most depressing effect on $CaSO_4$ solubility. The effect of the various metal chlorides on $CaSO_4$ solubility was shown to be equivalent among them when their ionic strength was used as basis of comparison.

8.2 Claims to Originality

1. The solubility of $CaSO_4$ modifications, namely dihydrate, hemihydrate and anhydrite in concentrated HCl, $CaCl_2$ and their mixed solutions up to 80 °C has been reported for the first time.

2. It is the first time that the effect of various chloride salts (NaCl, $MgCl_2$, $FeCl_2$, $FeCl_3$ and $AlCl_3$) on the solubility of three $CaSO_4$ modifications in aqueous HCl or HCl + $CaCl_2$ solutions up to 353 K was investigated.

3. It is the first time that a self – consistent chemical model based on a single set of model parameters for all $CaSO_4$ phases in the H + Na + Ca + Mg + Al + Fe(II) + Cl + H_2O system was developed with aid of OLI Systems software platform. With the aid of the newly developed model the bell – shaped solubility curves for dihydrate and anhydrite as a function of HCl or metal chloride concentration were successfully explained on the basis of the governing complexation equilibria and ion – activity coefficients.

4. It is the first time that phase transition diagrams for $CaSO_4$ phases in the HCl-$CaCl_2$-H_2O system are constructed.

8.3 Suggestions for Future work

1. The model should be expanded to include the effect of $FeCl_3$ on $CaSO_4$ solubilities.

2. The effect of various chloride salts (NaCl, $MgCl_2$, $FeCl_2$, $FeCl_3$ and $AlCl_3$) on $CaSO_4$ phase transition diagrams should be investigated by making use of the expanded OLI–based chemical model.

Appendix A:

Table A.1. Thermochemical Data for the Main Species in the H + Na + Ca + Mg + Al + Fe(II) + Cl + SO_4 + H_2O System**

Species	$\Delta\overline{G}^0_{f,25}$ (kJ/mol)	$\Delta\overline{H}^0_{f,25}$ (kJ/mol)	$\overline{S}^0_{f,25}$ (J/K/mol)	$C^0_{P,25}$ (J/K/mol)
H^+	0	0	0	0
OH^-	-157.29	-230.0	-10.7	-137.19
H_2O	-237.18	-285.85	69.95	75.35
SO_4^{2-}	-744.46	-909.6	18.83	-269.37
HSO_4^-	-755.76	-889.1	125.52	22.18
H_2SO_4(aq)	-683.07	-815.66	127.99	-279.9
Ca^{2+}	-552.79	-543.083	-56.48	-31.50
$CaSO_4$(aq)	-1309.28	-1447.27	20.92	-104.6
$CaCl_2$(aq)	-811.7	-883.08	25.104	129.537
$CaCl^+$	-682.41	-705.46	18.828	73.0945
$CaOH^-$	-717.138	-764.417	-14.4683	89.45
Cl^-	-131.29	-167.08	56.735	-123.177
HCl(aq)	-95.111	-116.42	105.28	-31.8
Na^+	-261.881	-240.30	58.4086	37.907
$NaSO_4^-$	-1011.8	-1153.4	83.571	-153.1
Mg^{2+}	-453.96	-465.97	-138.1	-22.34
$MgOH^+$	-623.897	-689.908	-86.1904	
$MgSO_4$(aq)	-1215.9	-1373.4	-53.6765	-82.5085
Al^{3+}	-483.7	-530.67	-325.1	-135.98
$AlOH^{2+}$	-692.35	-767.02	-176.6	55.229
$Al(OH)_2^+$	-899.06	-1000.0	-43.05	-50.21
$AlOHCl^+$	-826.585	-934.1	-118.3026	
$AlSO_4^+$	-1245.40	-1430.90	-217.0	1.9018
$Al(SO_4)^-$	-2000.7	-2338.9	-156.5	-44.95
Fe^{2+}	-91.5041	-92.2572	-105.855	-33.0536
$FeOH^+$	-274.47	-343.74	-37.22	50.802
$Fe(OH)_2$(aq)	-448.32	-554.88	5.4103	84.027
$Fe(OH)_3^-$	-626.14	-792.16	-26.1	193.87
$Fe(OH)_4^{2-}$	-777.72	-981.682	14.443	-207.7

*The data are from the "Public" Databank of OLI.

Table A.2. The Parameters for Species Whose Equilibrium Constant is Calculated with the Aid of Eq. (7.3) [a]

Species	*A*	*B*	*C*	*D*
$CaCl_2(aq)$	-46.242	14154.1	0.0408507	0.0
$CaCl^+$	2.40192	1871.39	-0.0136144	0.0
CaSO4(aq)	34.31792	-4403.012	-0.0884494	5.89741×10^{-5}
$H_2SO_4(aq)$	13.9312	-704.65	-0.002916	-3.24087×10^{-6}
HCl(aq)	32.1499	-1328.3	-0.10083	9.66894×10^{-5}
$NaSO_4^-$	-1.53099	627.892	-0.006295	1.44261×10^{-5}
$MgSO_4(aq)$	-44.2673	6128.7	0.091922	-6.20540×10^{-5}
$CaSO_4(s)$ (AH)	19.12274	-3066.119	-0.04785357	1.20537×10^{-5}
$CaSO_4\cdot2H_2O(s)$ (DH)	40.11184	-5481.185	-0.115199	9.1384×10^{-5}

[a] The data is from OLI's databank.